STUDIES ON THE PEDOLOGY OF FIVE SOILS ABOVE TERTIARY SEDIMENTS IN THE LOWER COAL RIVER VALLEY, SOUTH-EAST TASMANIA

By
KUSWARDIYANTO
(B.Sc. of Agriculture; Soil Science)

Submitted in fulfilment of
the requirement for the degree of
Master of Agricultural Science

DEPARTMENT OF AGRICULTURAL SCIENCE
THE UNIVERSITY OF TASMANIA
Hobart
November, 1996

THE STATEMENT OF ORIGINALITY

This thesis contains no material which has been accepted for the award of any other degree or diploma in any universities and to the best of my knowledge contains no copy or paraphrase of material previously published or written by any other person except where due reference is made in the text of the thesis.

Kuswardiyanto
University of Tasmania
Hobart
November, 1996.

ACKNOWLEDGMENTS

I wish to express my appreciation to my supervisor Dr. J.A. Beattie for his advice, encouragement and constructive criticism during the course of this study and in the preparation of this thesis. I also wish to thank to Mr. R.B. Doyle for his support and advice during the later part of this study.

Also I would like to particularly thank to Mr. D. Bradford for his friendliness and technical help, and to Mr. B. Peterson and Mrs. L. Dow for their technical assistance.

Special thanks to the Head of the Department of Agricultural Science, Professor R.J. Clark, for supporting and providing the excellent facilities and environment for my research.

I wish to express my gratitude to Dr. A. Ringrose-Voase and Mr. I. Salins of CSIRO Division of soils in Canberra for their tireless efforts in teaching me how to make soil thin sections and helping me to interpret them. Also thanks to Mr. R. Bottrill and Mr. R.N. Woolley in the Department of Energy and Resources, Tasmania for their help with X-ray diffraction analysis.

I would like to thanks also to the follow people at the University of Tasmania: to Mr. W. Jablonski in Central Science Laboratory for his help with microprobe analysis of thin sections; to Dr. Jocelyn McPhie and Dr. M.R. Banks for vital assistance with mineral identification; and to Mr. S. Stephens in the geology department for his friendliness and help in making thin sections.

Also I would like to thank AIDAB as my sponsor and the staff of the Research Office who have made my study in Australia possible.

I state my appreciation to my special friend and wife, Marian Kaye for her patience and enormous help in finishing my thesis and to my father and mother " Ibu Masru'ah dan ayah tercinta Kusnosuroto".

Finally I would like to dedicate my work to my son, Verto Ricky Kuswardiyanto.

TABLE OF CONTENTS

LIST OF FIGURES

LIST OF PLATES

LIST OF TABLES

ABSTRACT

A pedological study was made of five soils occupying a small relatively elevated (30-50 metres ASL) area of the University of Tasmania Farm, Cambridge, Tasmania.

The soils formed above unconsolidated Tertiary sediments. Examination and sample collection sites were chosen to represent areas of minimal erosion/deposition (UF1 and UF2) and a sequence on a straight uniform toeslope (UF3, UF4 and UF5) exposed to colluvial activity. Soil morphology was recorded at each site.

A major difference in primary profile form was noted as between a uniform, black cracking clay (UF1) and four duplex soils (UF2,UF3, UF4 and UF5) three of which (UF2, UF4 and UF5) were very strongly duplex.

Laboratory examination included physical, chemical and mineralogical analysis, viz, particle size analysis, bulk density measurement, soil reaction (pH 1:5 H_2O), electrical conductivity (EC 1:5 H_2O), cation exchange capacity and exchangeable cations (Ca, Mg, K, Na, Al and H), X-ray diffraction of oriented clay samples, micromorphology, and separation of light and heavy mineral fractions and magnetic minerals in selected sand separates.

All of the soils were shown to be slightly saline but strongly sodic and magnesic in the subsoil, increasing slightly in salinity but markedly in sodicity and magnesic character with depth with an apparent reversal of this trend deeper in the profile. The major source of salt was arguably atmospheric cyclic salt of marine origin.

The black cracking clay soil was shown to have formed by *in situ* weathering of a granular, base-rich, basalt glass sediment deposited on a Tertiary clay surface, now seen at 150 cm depth in the profile. Weathering and soil formation produced a mixed smectite, kaolinite material (80% clay) to 55 cm depth below which smectite was found to be dominant. The less weathered material below 74 cm depth contained only 25-30% clay above an abrupt lithologic discontinuity to dense, lenticular, Tertiary clay (up to 80% clay) at 150 cm depth.

The strong to very strong duplex form of the texture-contrast sodic soils was attributed to *in situ* weathering of clay-forming minerals and/or inheritance of clay from parent Tertiary sediments. No evidence in the form of depositional argillans was found to indicate an eluvial/illuvial process in the formation of the B2 horizons. The sandy A horizons were

considered to have formed in part by weathering and by wind sorting with a strong indication of aeolian sand accession from the sandy foreshore of Pitt Water, a shallow embayment receiving the flow of the Coal River, with extensive sandy flats exposed at low tide.

The UF2 soil, located on the broad summit of a gently domed and sloping spur, was considered to have formed within undisturbed Tertiary sediments apart from the effect of aeolian processes on the sandy A horizon. It contained secondary carbonate and manganese oxides in the lower B2 horizon.

The UF3, UF4 and UF5 soils, on a straight, 9% - 6% toeslope, were considered to have formed in colluvium of which Tertiary sediments were the dominant source. The parent material of the (uppermost) UF3 soil was strongly stratified with alternating sandy and clayey layers. A striking feature of this soil was the occurrence of a very large concretionary mass of iron oxides beginning at the base of the sandy A horizon and extending into the upper B2 horizon. Also notable was the occurrence of secondary carbonates just below the large glaebular mass of iron oxides. The sandy layers in the stratified sand-clay sequence below were marked by precipitation of iron oxides, disseminated or in small, soft glaebules. These features were considered to be the result of groundwater movement from a ridge of weathered Jurassic dolerite a few hundred metres to the west and directly connected with the study site via a backslope and footslope.

The UF4 and UF5 soils contained only small to medium, soft, iron-enriched glaebular segregations and no secondary carbonates were detected. However, the UF5 soil formed in fine sediment deposited above a basal channel deposit of well-rounded (water worn) coarse stones infilled by clay (a clast-supported deposit).

Physical and chemical characteristics and the clay mineralogy of the soils provided an explanation of management problems encountered in their use for agriculture. In the case of the black cracking clay (UF1) these include wide and deep cracking as the soil dries, a dispersed condition of the material within coarse structural units (peds) at shallow depth resulting in high bulk density and unfavourable pore-size distributions both of which were associated with sodicity. Together with the clay mineral composition this has resulted in a very narrow range of moisture content within which soil working and trafficking can be conducted with satisfactory results. The duplex soils have a moderately thick sandy topsoil

which has had the effect of reducing the rate of drying of the upper subsoil, with greatly reduced shrinkage and cracking. However, high bulk densities were measured for the sodic, dispersed, clay subsoils. The observed very slow internal drainage, poor aeration and poor root development may thus be explained.

Finally the soils have been classified in the new Australian soil classification (Isbell, 1996) in which it has been possible to place them precisely, providing an accurate summary of their properties.

I. INTRODUCTION

The word "soil" has different meanings for different people and interests. Geologists may regard soil as an epidermal unit of a geological body through which all material must pass in the erosion cycle from hard rock to sediments. Chemists may consider soil as a vessel or test tube into which mineral and biological matter has been placed by natural forces and agencies and into which fertilisers may be poured by man to supplement soil nutrient supply for plant growth. Physicists see soil as a particulate mass whose characteristics and behaviour change with moisture content and temperature. Ecologists consider soil as part of an environment conditioned by organisms. Agriculturists and industrialists may see soil as a system whose most obvious parts are aggregates and roots and which produces crops and livestock (Buol *et al*, 1980).

Soil scientists have suggested many definitions of soil and there is still no universally accepted definition. However, it is essential that the context of each soil study should be clear in terms of the definition adopted by the researcher. Hilgard (1914), cited by Jenny (1941) defined soils as "the more or less loose and friable material in which plants may find a foothold and nourishment by means of their roots". Rahman (1928), also cited by Jenny (1941) defined soil as "the upper weathering layer of the earth's solid crust". Joffe (1949) described soil as "a natural body, differentiated into horizons of mineral and organic constituents, usually unconsolidated and of variable depth, which differs from the parent material below". Nikiforoff (1959) regarded soil as "the excited skin of the subaerial part of the earths' crust". Soil Survey Staff (1975) defined soil as "the collection of natural bodies on the earths' surface, in places modified or even made by man of earthy materials, containing living matter and supporting or capable of supporting plants out of doors".

The morphogenetic concept of soil is generally attributed to Dokuchaev and his students working in Russia towards the end of the 19th century (Buol *et al*, 1980). Dokuchaev viewed soil as "a self-existent product of specific origin very distinct from parent rock" and proposed that soils were the products of the combined activity of five factors : living and dead plant and animal organisms, parent rock, climate, relief (topography), and time. Kellogg (1936) cited by Wilding *et al* (1983) stated the modern

concept of soil as a dynamic natural body, trending towards equilibrium with its environment, to which the principles of geography could be applied. He identified two kinds of activity during the genesis of a soil : destructural activities of physical and chemical weathering and constructural biological forces. Simonson (1959) summarised the processes of soil formation as : additions and losses of organic and mineral matter as solids, liquids and gases, translocation of materials from one point to another within the soil, and transformation of material and organic substances within the soil.

Butler (1958b) proposed a useful perspective on the diversity of concepts about soil, grouping the different kinds of interest as geographic, edaphic and pedologic. To these interests should be added the growing realisation of the role of soils as "environmental filters" (Doyle, personal communication).

The present study is concerned with the third of Butler's three areas of interest, pedology. This is the study of soil genesis, morphology and classification in order to understand the factors and processes of soil formation and principles of soil occurrence (Buol *et al*, 1980; Butler, 1959). Pedological studies are divided basically into two stages: field studies and laboratory studies. They involve descriptive, analytical, correlative and deductive techniques. Field studies may be parametric but are largely direct observations and interpretations and are concerned primarily with soil morphology, the stratigraphy of pedoderms, and principles of soil occurrence (Butler 1959, 1982). Field studies provide the basis and framework for quantitative laboratory studies (physical, chemical, mineralogical and biological) which, in conjunction with field data, can be developed into reliable knowledge of soil formation and environmental relationships for better soil classification (Northcote *et al*, 1975; Jenny 1941).

Marshall (1977) suggested that there are four main areas to be addressed in pedological studies :

(1) detailed study of processes of soil formation and development which is steadily becoming more quantitative and "biophysicochemical";

(2) comprehensive classification of soils as natural objects;

(3) isolation and individual study of agronomic factors in the use of soils for crop growth;

(4) connections between measurable properties and applications in engineering and construction.

The present study is concerned with the first two of these areas of soil study suggested by Marshall (1977). Accordingly the definition of soil adopted is that of Brewer (1964): "soil is the collection of natural bodies formed by alteration of sedimentary and/or igneous bodies due to exposure at the earth's surface and having an anisotropic arrangement of properties along an axis normal to the earth's surface".

The morphology, aspects of micromorphology, mineralogy, physical and chemical properties of five soils formed above unconsolidated Tertiary sediments have been studied in some detail. The soils fall into two broad groups of "primary profile forms" (Northcote, 1979), viz., duplex and uniform. The duplex soils are very strongly duplex with very slow to extremely slow subsoil permeability. The upper profile of the uniform soil is a black cracking clay. The data to be reported provide a basis for inferences concerning the genesis of the soils, including relationships with other landscape features, and their classification in the new scheme for Australian soils (Isbell, 1996).

II. LITERATURE REVIEW

2.1. Duplex Soils

Northcote (1979) defined duplex primary profile forms as "soil profiles dominated by the mineral fraction with a texture contrast of 1 1/2 texture groups or greater between the A and B horizons. Horizon boundaries are clear to sharp. The distance from the bottom of the A horizons to the top of the main B horizon occurs over a vertical interval of 10 cm or less; except for those profiles in which sesquioxidic layers (laterite) occur between the A and B horizons when the vertical interval between them may be as great as the thickness of the sesquioxidic layer. Examples of contrasting texture profiles include the following :

I sand over clay.

II sand over sandy clay loam.

III loam over clay.

IV loam or clay loam over medium or heavy clay".

The A horizons not only range widely in field texture but also in colour, from light to dark , red-brown, brown, yellow, grey, and they may also be continuously or sporadically bleached, especially in the lower part above the clayey subsoil. Further, they may have a thin surface crust, set hard seasonally, or remain soft. Pedality is usually weakly expressed.

The B2 horizons are usually at least light clays and most commonly they are medium to heavy clays ranging in colour from red through brown, yellow and grey in light to dark shades. In addition colour mottling is a common feature, especially below the upper B2 horizon. Macro-pedality also varies widely in expression from an apedal, massive condition through more or less strongly blocky, prismatic or columnar forms and from very coarse to very fine size. Pedality is often found to be strongly correlated with colour, the more mottled subsoils tending to massive or only weakly pedal structure. With increasingly strongly expressed pedality there is often the presence of more or less continuous depositional argillans (Brewer 1964) resulting in smooth and shiny ped surfaces.

Finally, the solum of duplex soils may range from thin to very thick and the profile reaction trend (pH) may be acid, neutral or alkaline.

Duplex soils account for about 20% of the Australian soil landscape (Northcote *et al*, 1975). They are probably the most extensive arable soils in Australia and they certainly present difficult management problems in most cases. They include a wide range of great soil groups, namely solonetz, solodized solonetz and solodic, soloth, red-brown earth, grey-brown, red, yellow and brown podzolic soils, desert loams and forms marginal to grey, brown and red clays (Stace *et al*, 1968). In Isbell's (1996) classification system for Australian soils, duplex soils are placed in the orders: chromosols (many), hydrosols (some), kurosols (many), and sodosols (many).

The duplex soils of the present study fall within the broad spectrum of soils with saline-sodic or sodic properties and further comment will be confined to these soils.

2.2. Saline-sodic and Sodic Duplex Soils

The pedogenesis of saline, saline-sodic and sodic soils was discussed many years ago by de Sigmond (1926). He discussed a sequence of development from solonchak (saline), to solonetz and solodized solonetz (saline-sodic), culminating in the soloth stage (sodic). Each stage was marked by distinctive macro-morphological features. However, further experience has shown that the correlation between soil morphology and soil chemistry is by no means universal (Northcote and Skene 1972; Rengasamy and Olsson 1991). Macro-morphological features once thought to be diagnostic are now seen to be capable of persisting long after change in chemical properties. In fact, the widely adopted classification of saline and alkali soils for management purposes (United States Salinity Laboratory Staff, 1954) is solely chemical, based on the electrical conductivity of the soil solution (saturation extract, EC sat 25^{o}C) and the exchangeable sodium percentage (ESP) with the commonly associated soil reaction (pH 1:5 water), viz., Table 1.

Table 1. The relationship of EC, ESP and pH to soil salinity and alkalinity *

soil condition	EC sat (25 °C) ($dS.m^{-1}$)	ESP ($m.mol^{+}Kg^{-1}$)	pH (1: 5 H_2O) (common)
saline	>4	<15	<8.5
saline-alkali	>4	>15	<8.5
nonsaline-alkali	<4	>15	8.5 - 10

* After United States Salinity Laboratory Staff (1954).

More recently, in recognition of the fact that salt-sensitive plants can be adversely affected in soils with EC sat. above 2 $dS.m^{-1}$ the Terminology Committee of the Soil Science Society of America (1987) has determined a lower critical level of 2 $dS.m^{-1}$ separating saline and nonsaline soils. The critical level of exchangeable sodium percentage has remained as ESP 15 for United States soils, although with growing recognition of sodic behaviour at much lower levels of ESP this may also be changed. This has already been proposed for Australian Soils by Northcote and Skene (1972). They reviewed the occurrence of saline, saline-sodic and sodic soils in Australia and their suggested critical level of ESP 6 has been adopted by most workers in this country, with the former ESP 15 level now separating classes of sodic (ESP 6 - 15) from strongly sodic (ESP >15) soils. Isbell (1996) has proposed a further class of hypernatric soils with ESP >25. Recent work has identified many soils showing properties associated with sodicity at even lower ESP values of 1.5 (Rengasamy and Olsson, 1991).

The correlation of sodicity with strongly alkaline soil reaction has also been shown not to be general (United States Salinity Laboratory Staff, 1954; Little, 1992; Beattie, 1995) with some sodic soils exhibiting strongly acid reaction and significant levels of exchangeable aluminium. There is increasing recognition that soils showing evidence of sodicity or sodic behaviour in varying degree are far more widespread in Australia than saline soils, on which much more attention has been focused in the past.

2.3. Saline-sodic and Sodic Duplex Soils in Australia

2.3.1. Origin

In Australia these soils are believed to have formed generally as a result of salt accession, dominantly of sodium chloride, in many cases to pre-existing soils of diverse

character (Isbell *et al*, 1983). These authors also considered it "unlikely that many of the present diverse and widespread varieties of sodic soils ever went through the complete classical sequence" of development. According to Chartres (1993) the process of salt accession has involved either or both of two processes :

(1) aeolian transport of salt of marine origin followed by inland deposition with rainfall, and

(2) aeolian transport of salt from interior playas or eroded soils in the arid and semi-arid zones.

The phenomenon of "cyclic salt" was recognised early by Teakle (1937) working in south-western Western Australia and later by Downes (1954) in south-eastern Australia. A detailed study of modern atmospheric salt accession was made by Hutton (1962) and it seems clear that much of the salt and exchangeable sodium found in soils of southern Australia may be attributed to an immediate atmospheric source (Peck, 1977).

Wind has been a major factor in soil formation over huge areas of the arid interior of Australia (Butler and Churchward, 1983). The siliceous sands of the desert sandhills form the single most extensive great soil group in Australia (Stace *et al*, 1968). A number of studies led by B.E.Butler in south-eastern Australia have shown the occurrence of large areas of windblown sand sheets and dunes to the west of the Riverine Plain (Butler, 1958a; Churchward, 1961) and source-bordering dunes extend along the courses of prior streams (Butler, 1950). Along some entrenched modern rivers, dunes occur well into the more easterly semi-arid to sub-humid zone. Beattie (1972) found extensive dune fields both north and south of the Murrumbidgee river between Wagga Wagga and Narrandera, east of the Riverine Plain and isolated dunes upstream of Wagga Wagga.

In addition to the evidence of wind action seen in the existence of sand dunes and sheets, very large areas of the Riverine Plain and of the Wagga Wagga region east of it have been mantled by parna, an aeolian clay, in which the modern soils have formed wholely or in part (Butler, 1956, 1958a; Van Dijk, 1958; Beattie, 1970, 1972). Parna is believed to have been a saline material originating in large part from wind-eroded soils and saline playas of the arid and semi-arid zones. Effects on pre-existing and modern soils may

be identified over a much greater area (Downes, 1954; Walker and Costin, 1971; Chartres *et al*, 1985). One of these effects may be the sodicity of a wide range of Australian soils which do not have obvious morphological properties associated with their condition. It seems that over large areas salinity and sodicity may indeed have been superimposed on pre-existing soil morphology in Australia.

Hutton and Leslie (1958), in a study of the accession of non-nitrogenous ions in rainwater to Victorian soils receiving more than 500 mm of annual rainfall, were able to relate decrease in chloride concentration to distance up to 300 km from an oceanic coast. None of the land mass of Tasmania would be excluded if, as is likely, a similar relationship held there. Indeed, the prevailing west to south-west winds are believed to carry atmospheric salt from the Southern Ocean across the island providing a major source of nutrients for west and south-west coastal and hinterland vegetation (Jackson, 1977; Bowman *et al*, 1986).

Some workers have pointed to a source of sodium and chlorine in the weathering of primary and secondary rocks (Gunn, 1967, 1985; Gunn and Richardson, 1979) and it would seem to be self-evident in consideration of the composition of terrestrial rocks (Johns and Huang, 1966). However, as pointed out by Isbell *et al* (1983) the distribution of sodic duplex soils is not confined to any particular parent material, topography, or rainfall zone in southern Australia. This suggests a net gain of salt such as suggested by Chartres (1993), whatever the primary source may have been, to soil landscapes that have been essentially stable for very long periods of time. At the present time the mean annual rainfall, averaged over the whole of Australia, is 420 mm, of which 87% is lost to the atmosphere by evapotranspiration (Australian Water Resources Council, 1975). There is much evidence to support the belief that this relationship has persisted at least during most of the Quaternary (Bowler, 1976). Thus the accumulation of salt in old soils and weathered zones in Australia can be understood in broad outline.

2.3.2. Morphology

Morphological descriptions of representative saline-sodic and sodic duplex soils have been given by Stace *et al* (1968) and classified as solonetz, solodized solonetz and solodic soils, and soloths. However a wide range of other Australian great soil groups includes many soils that are either saline-sodic or sodic at some depth in the profile, usually the subsoil, but do not show the macromorphological characteristics of solonetz, solodized solonetz and solodic, or soloth soils (Stace *et al,* 1968; Rengasamy and Olsson, 1991). They include : solonchak; grey-brown and red calcareous soils; desert loams; grey, brown and red clays; black earths; solonized brown soils; red-brown earths; calcareous red earths; red earths; and yellow earths. General descriptions of only solonetz, solodized solonetz and solodic, and soloth soils are summarized below after Stace *et al*, 1968. Black cracking clays (black earth) are given detailed attention in a later section of this review.

2.3.2.1. Solonetz

The essential features of solonetz are prominent texture differentiation with an abrupt boundary between loamy A horizons and clay B2 horizons, neutral to alkaline surface soil and strongly alkaline subsoil with pH (H_2O, 1:5) rising above 9.0 and sodium and magnesium dominance of the exchange complex in the lower horizons. True solonetz with neutral to alkaline A horizons are rare. These soils have thin A horizons, generally less than 10 cm thick, of brownish grey to brown loamy sand to clay loam. The A1 and A2 horizons are weakly differentiated and are massive to weak platy or blocky, compact, and brittle to pulverulent when dry.

The clay content usually increases by one to two-fold in the B2 horizons. In the upper part these are grey-brown, yellow-brown, red-brown or variously mottled sandy clays to light medium clays, dense, and characteristically of moderate medium prismatic to columnar pedality. Consistence is extremely hard when dry and tough when moist. The soil colour in the lower B horizons may be grey-brown or yellow-brown, and the pedality may be weak to strong, fine polyhedral or blocky. The lower B horizons usually contain

secondary carbonate as nodules or soft patches. The subsoils are moderately saline and the sola usually less than 60 cm thick.

These soils are widely distributed in NE Queensland, SE Queensland, northern New South Wales, South Australia and central Western Australia as small slight rises in terrain of medium-textured alluvial and colluvial deposits where annual rainfall is 500 mm to 600 mm on average.

2.3.2.2. Solodized solonetz and solodic soils

The important feature of these soils is again strong texture differentiation but with a very abrupt wavy boundary between A and B2 horizons. They have well developed, bleached A2 horizons and strongly pedal, coarse columnar or blocky B2 horizons. The A and upper B2 horizons are moderately acid above strongly alkaline lower subsoils where the pH may exceed 9. The solodized solonetz may be distinguished from the solodic soils by their domed columnar macropeds in contrast to the medium to coarse blocky to prismatic peds of the solodics, although as pointed out above morphology may persist after chemistry has changed.

The A horizons range from loose, coarse sands to massive or weak platy loams and clay loams but the coarser field textures are more common. The A1 is typically brownish grey to light grey brown, weakly differentiated from the A2, and low in organic content. The A2 is generally bleached white and varies from a thin capping of a centimetre or two above the clay subsoil to as much as 30 to 45 cm, with often a few to many ferromanganiferous nodules in the lower part.

The B2 horizons generally range from grey, grey-brown, yellow-brown or red-brown sandy clays to medium clays and are often mottled. The surfaces of the blocky peds and columns in the uppermost B2 horizon are often stained dark brownish grey by organic matter and some black manganiferous spots may occur near the top of the B2 horizon. The peds are very dense (bulk density may exceed 2) with very slow permeability. The B2 horizon grades into strongly alkaline B-C horizons which are commonly grey to yellow-brown, often of lower clay content, weak to moderate fine blocky or massive, less dense

than the B2, neither so hard nor tough and may contain a few nodules or soft segregations of secondary carbonate. The B-C horizons are often moderately saline.

These soils occur on extensive plains, valley floors and slopes above a wide range of substrates from igneous and sedimentary rocks to unconsolidated sediments where annual rainfalls are 400 to 1000 mm.

2.3.2.3. Soloths

The soloths also generally have a strong texture contrast and abrupt boundary between A and B2 horizons with a strongly bleached A2 horizon. Pedality and consistence are similar to those of solodized solonetz. The essential difference is that the soloths are acid throughout the solum. Soloths are widespread in the moister subhumid lands of south-western Australia and throughout eastern Australia.

The A horizons are usually thick, but their depth varies with field texture which ranges from loamy sand to clay loam and sandy clay. The A1 is often relatively thin and pale, varying from light brownish grey to light brown and reddish brown and is usually massive with brittle to hard consistence and weak platy or fine blocky pedality. The A2 is commonly thicker than the A1, almost white, massive, and brittle and pulverulent when dry.

The B2 horizon is usually somewhat mottled and variously coloured brownish grey, yellow-grey, grey -brown, yellow-brown and reddish brown. The texture ranges from sandy clay to heavy clay with either moderate to strong medium blocky or columnar compound peds separating to medium blocky. The dominant exchangeable cations are magnesium and aluminium. The lower part of the B horizon often contains significant to moderate amounts of soluble salts and is moderately to strongly sodic although the dominant exchangeable cation is still magnesium. Soloths occur on plains and slopes in low hilly lands, mainly in areas of 500 to 1300 mm annual rainfall, on medium-textured parent materials ranging from weathered acid igneous rocks to unconsolidated sediments.

2.3.3. Physical characteristics

Most saline-sodic and sodic soils of the subhumid to semi-arid cropping and grazing areas of southern Australia are of duplex primary profile form (Northcote, 1979; Northcote and Skene, 1972). This means that the subsoil has a relatively high clay content with field textures in the range from sandy clay loam to heavy clay while the topsoils may range from sand to clay loam. The topsoils and subsoil are abruptly to sharply separated and this may be further emphasised by cultivation. Except for the sandy topsoils, most tend to crust or set-hard on drying ("hardsetting", Northcote, 1979). Sandy clay loams are strongly hardsetting.

Butler and Hubble (1977) have generalised the features of duplex soils of the temperate semi-arid zone: the sandy loam topsoil passes abruptly to a dense, sandy clay at about 20 cm depth, the topsoil has weak pedality, is hard and brittle when dry with high pulverescence (Butler, 1955) and tends to crust or set hard after rain; the subsoil is a dense sandy clay or clay, extremely hard when dry, very firm with high coalescence when moist, and with either coarse pedality or massive structure.

Probably the most important physical behaviour of these soils is in relation to water because of a number of other associated adverse characteristics. These include instability of primary and compound peds and associated voids due to slaking, swelling and dispersion; high bulk density and penetrometer resistance of coarsely pedal or massive subsoils; slow to extremely slow permeability of subsoils when moist or wet, leading to intermittent topsoil waterlogging, together with poor aeration and high 15-bar water retention in the subsoil, so that available water capacity is low in both topsoil and subsoil and much subsoil water is physically inaccessible to roots.

The stability of small (3-5 mm) air-dry or sheared and remoulded moistened specimens of soils in contact with an excess of water has been correlated by Emerson (1977) with field characteristics and behaviour of the associated soil material in bulk, with practical applications in the construction of farm dams and soil conservation structures. Clay subsoils that are sodic and either massive or of weak, very coarse pedality often remain in a dispersed state on drying. At least in the temperate zone the depth of drying out

and cracking is restricted and subsoils remain moist below depths of 40 - 50 cm even through prolonged drought (Beattie, personal communication). The degree of cracking is closely associated with the mineralogy of the clay fraction but the cracks do not open laterally by more than a few millimetres and in the vertical plane are usually terminated upwards at the subsoil/topsoil boundary and downwards at 40-50 cm depth.

This behaviour is associated with very high bulk density (1.8 - 2.0 g, cm^{-3}) (Stace *et al.*, 1968; Emerson, 1967; 1977; Beattie, personal communication) and in this situation the slow to extremely slow permeability of the subsoil (< 10 to < 0.1 mm, day^{-1}) following closure of any upper subsoil cracks is understandable, as is its extension to very slow vapour and gas transfer. Effective rooting depth is limited in such conditions to depths of 40 - 50 cm of which up to 20 cm is the sandy topsoil in the case of University of Tasmania farm soils (Beattie, personal communication).

There has been a considerable increase in published work on saline-sodic and sodic soils in Australia in the last twenty years and particularly in the last ten years, of which a sample is reviewed below.

Emerson and Bakker (1973) showed that the saturated hydraulic conductivity of a sodic red-brown earth B2 horizon declined dramatically with colloid dispersion and linked this to the periodic saturation of A and upper B2 horizons of similar sodic soils in the New South Wales Riverina and Goulburn Valley of Victoria. Many Australian duplex soils have extremely slowly permeable B2 horizons due to sodicity (Mc Cown *et al,* 1976; Loveday *et al,* 1978) and this is seen to have the consequence of a small profile water store, largely provided by the depth and field texture of the A horizon (Mc Cown *et al,* 1976; Shaw *et al,* 1994) so that effective soil depth is correspondingly shallow. Runoff and soil erosion are related to these soil characteristics and Williams (1983) has explained the extremely large peak discharge of the Burdekin River, North Queensland, in terms of high intensity rainfall on large areas of shallow solodics in the upper catchment. Williams concluded that for duplex soils the water entry properties of horizons rather than their water holding properties determined the size of the profile water store.

So and Aylmore (1993) pointed out that surface waterlogging gave rise to high initial rates of evaporation and that rapid drying of the surface soil could be accompanied by hardsetting or surface crusting depending on field texture. For a given soil, exchangeable sodium percentage (ESP) may be a good indicator of its hardsetting behaviour. However, ESP alone was not a very good indicator of such physical behaviour over a range of soils because of large differences in " sodium sensitivity" of hardsetting soils. Decreased seedling emergence was well correlated with modulus of rupture (MOR, kPa) of the hardsetting surface soil.

The behaviour of soil aggregates under field moisture regimes has been correlated with the results of laboratory experiments using pure homoionic clay mineral suspensions (recognising that the soil clay fraction usually contains more than one clay mineral, that carbonates and sesquioxides may be present, and that contents of clay and coarser particles are also variable) in order to deduce the nature of inter-particle bonding and management implications (Emerson, 1983). Thus it has been recognised that aggregate and voids stability depends very much on the attractive and repulsive forces associated with intermolecular and electrostatic interactions between the soil solution and solid phases. It has long been known that the heat of wetting of soil arises from a decrease in the free energy of water, particularly in associating with the soil colloidal fraction. Rengasamy (1990) summarized factors responsible for this decrease in energy of interacting water molecules. Rengasamy and Olsson (1991) have discussed sodicity and soil structure in this context, presenting a five-stage model of changes in particle arrangement in clay aggregates with wetting and drying of contrasting sodic and calcic systems. Thus physical behaviour of sodic soil is closely related to chemical and mineralogical properties which are discussed in following sections of this review.

Shaw *et al* (1994) found that high sodicity in surface soils caused increased crusting and decreased water entry. Reduced soil water storage, poor aeration and increased soil strength resulted from high levels of subsoil sodicity. Earlier, Rengasamy and Olsson (1991) pointed out that sodic soils are subject to severe structural degradation and restrict plant performance through poor soil-water and soil air relations. So and Cook (1993)

found that cultivation generally leads to decreasing structural stability which is manifested as slaking and dispersion. The hydraulic conductivity of slaked and dispersed clay soils is strongly dependent on the amount of dispersed clay. They also stated that the amount of dispersed clay can be predicted from the clay content and the amount of exchangeable sodium. Emerson and Bakker (1973) suggested that the spontaneous dispersion of clay from a wet aggregate of low ESP immersed in water depended on the gradient of the soluble salt concentration at the boundary of the intact portion of the aggregate, as well as the actual salt concentration. So and Cook (1993) found that dispersion, as measured by end-over-end shaking had greater relevance to hydraulic conductivity than did aggregate stability as assessed by wet sieving and that the amount of dispersed material as a proportion of the bulk soil was a more appropriate index of dispersion than dispersion ratios. Aragues and Amezketa (1991) suggested that exchangeable sodium content of soil expressed as cmol (+) kg^{-1} was a better predictor of both amounts of dispersed material and dispersion ratios than ESP but that spontaneously dispersible clay was strongly correlated with clay content and ESP. Emerson and Bakker (1973) found that the permeability of aggregate beds washed with Ca or Mg solutions showed only a negligible decrease with time. The rate of decrease for a given ESP was faster the greater the initial flow rate and also for smaller-sized aggregates. The ESP required to produce a given decrease in flow rate was reduced when Mg was the complementary cation rather than Ca. Mg-saturated aggregates were more easily dispersed by mechanical action than calcium-saturated aggregates. Once sufficient sodium was present to cause dispersion, the rate of flow of water depended on the rate of dispersion. Sumner (1993) concluded that at high ESP levels and when the soil solution concentration exceeded 5 $mmolc^{+}L^{-1}$, swelling was the dominant mechanism for reduced hydraulic conductivity. At lower ESP values, clay dispersion was the main mechanism for reduced permeability, the effect being enhanced by reduced threshold electrolyte concentration.

2.3.4. Chemical characteristics

Soil reaction trend (Northcote, 1979) in most profiles identified as solonetz (Stace *et al* , 1968) is alkaline with near neutral 1: 5 water pH in the surface, values above 9 within about 60 cm depth and a strong dilution effect. Although most solodized solonetz and solodic soils have been found to have an alkaline reaction trend, the surface pH is usually strongly acid (at or near pH 5.0) and the deep subsoil between 8 and 9. However, some of these soils have a neutral reaction trend and in some others the deep subsoil pH has been recorded as exceeding 9. Soloths appear to be more variable, usually with an acid trend but some showing a neutral trend and, more rarely, an alkaline trend. Thus, for the solodized solonetz and solodic soils and soloths, soil reaction is not reliably associated with profile morphology.

The level of soluble salts is low in the upper profile of all of these soils but is always high in the deep subsoil of solonetz with total soluble salts in the range 0.3 - 0.5% by 100 cm depth, of which at least half and more commonly more than 80% is recorded as NaCl. The salt levels in solodized solonetz and solodic, and soloth soils are much more variable in total amount and also in the ratio of NaCl to total soluble salts. In many cases both total soluble salt and chlorides are low throughout, even to depths in excess of 200 cm, while in others levels above 1.5% for total soluble salts and 0.5% for chlorides have been recorded within 100 cm depth. More commonly levels are 0.2 - 0.3% and 0.05 - 0.1% for total soluble salts and chlorides respectively. However, in the majority of these soils the levels are below these values while lower ratios of chlorides to total soluble salts are found in the presence of secondary gypsum and carbonates.

In accord with the apparent age and highly weathered condition of the soil materials (Rengasamy and Olsson, 1991) the levels of nitrogen, phosphorus and sulphur in the surface horizons are usually low to very low even by comparison with other Australian soils. Levels of P and S of 0.03% or less are not uncommon. Perhaps surprisingly in view of their apparent weathering status, levels exceeding 0.05% for P and S have been recorded for soloths and in excess of 0.5% for N.

Although it has been emphasised above that soil chemistry and morphology appear not to be well correlated within these soil classes, the exchange complex is distinguished by relatively high levels of exchangeable sodium and magnesium, particularly in the subsoil and deep subsoil. Thus high to very high exchangeable sodium percentages (ESP) are common and, conversely, low to very low ratios of calcium to magnesium. None of the representative profiles described by Stace *et al* , (1968) has an ESP below 1 in the surface. Only the soloths have an ESP less than 2 while some solonetz and solodized solonetz have a surface ESP near 10.

The subsoil and deep subsoil ESP values may be highly variable but have been recorded as high to extremely high for all classes (range 26 to 62) bringing them within the hypernatric range of Isbell (1996). Most deep subsoils have an ESP above 15% but some have been recorded as low as 2% to 4% from 60 cm to 120 cm depth.

Although in earlier work (eg., Loveday, 1974b) a satisfactory correlation of response to added gypsum with ESP was obtained, the modifying effect of field texture was recognised. More recently (Rengasamy and Olsson, 1991; Sumner, 1993) the use of ESP alone has been found to be unsatisfactory in explaining and/or predicting dispersive behaviour over a wide range of soils. Sumner pointed out that there is now no generally accepted definition of a sodic soil, particularly in the aftermath of attempts to relate sodicity and dispersive behaviour on a more quantitative predictive basis. Recent experience shows that soils may be dispersive with ESP's of 1 or even in the absence of exchangeable sodium. Thus other criteria: sodium adsorption ratio of the soil solution (SAR), the total electrolyte concentration (TEC) at which dispersion occurred and the point at which attractive and repulsive forces in colloidal clay systems were in balance (critical flocculation concentration, CFC) have been proposed as offering a better means both of predicting soil dispersivity, which is after all the main physical problem of so-called sodic soils, and devising technology for their better management. Unfortunately few such data are yet available for Australian soils.

Rengasamy and Olsson (1991) used SAR, electrical conductivity (EC) and threshold electrolyte concentration (TEC) and pH, measured in a 1: 5 (w/v) soil : water suspension to

classify sodic soils. When threshold electrolyte conductivity (TEC) is less than EC and SAR > 3 the predicted soil behaviour is saline-sodic. Sodic soils are those with SAR > 3 and EC < TEC. Soil reaction (pH) of acidic sodic soils is < 6, neutral sodic soils, 6 - 8, and alkaline sodic soils > 8. While the ESP of a soil may be only approximately twice the SAR of a 1:5 (w/v) soil : water extract (Rengasamy *et al.*, 1984) the practical difficulties in measurement of ESP are such that SAR 1:5 is now the preferred index.

Other factors are also involved, notably the level of exchangeable Mg, the Ca/Mg ratio, presence of sesquioxide cements and the type and amount of organic matter. Dispersion of clay in soil with SAR 1 : 5 > 3 increased as the Ca/Mg ratio fell below 1, but significant reduction of hydraulic conductivity occurred only when both SAR was > 3 and total cation concentration (TCC) was less than flocculation levels (Rengasamy *et al.*, 1984). Earlier, Bakker *et al* (1973) found that dispersion of Mg-saturated subsoil material from a Shepparton red-brown earth occurred at about half the water content at which it dispersed when Ca - saturated.

While organic matter may not be a significant factor in relation to stability/dispersity below the upper subsoil, its role in maintenance of topsoil aggregation has long been known and good soil management practices take account of this. However the effects of organic matter can be complex. Organic matter present in small amounts and containing high concentrations of low molecular weight acids has been shown to have dispersive effects in the presence of exchangeable sodium and as the labile constituents effective in particle bonding (eg., polysaccharides) decrease in amount (Churchman *et al*, 1993). As pointed out by Sumner (1993) the remaining organic matter contributes mainly to negative charge, tending to promote dispersion.

Red soils in which sesquioxides are significant in maintaining aggregate stability have been found to be more stable with increasing sodicity than other soils in laboratory experiments (McNeal *et al*, 1968). Nevertheless many irrigated sodic red-brown earths show little evidence of this effect and this appears also to be the case with certain acid sodic soils in which aluminium is a major exchangeable cation (Beattie, personal communication). In both cases permeability is very slow. On the other hand the strongly

aggregated subsoils of other sodic red-brown earths formed in parna deposits (Butler, 1956; Butler and Hutton, 1956; Van Dijk, 1958; and Beattie, 1970) are so resistant to disaggregation as to have required a specific descriptive term, "subplastic" (Butler, 1955). Although the subject of intense study, the basis of subplasticity has defied explanation .

It is clearly difficult to generalise in the face of such an evidently very complex set of interacting factors. Sumner (1993) has provided a thorough review of present knowledge. In doing so he has suggested a number of specific topics for research.

2.3.5. Clay mineralogy

There are few direct data recording the clay mineralogy of Tasmanian soils. However, there is a much larger file of data for cation exchange capacity and exchangeable cations. Together with field morphological observations, including structure, consistence and shrink/swell behaviour, these data allow inferences to be made about the nature of the clay fraction of a number of representative Tasmanian soils, including some that are saline sodic or sodic. Although few of these data have been published they are now accessible via the computer data bank of the CSIRO Division of Soils, Adelaide, South Australia. A computer file of original field descriptions and laboratory data for nearly three hundred type profiles of Tasmanian soils is held in the soils section of the Department of Agricultural Science, University of Tasmania. The original data were recorded by officers of the Tasmania Region, CSIRO Division of Soils, Hobart, under the supervision of K.D. Nicolls (Beattie, personal communication).

Data from two solonetz, four solodized solonetz, five soloth and five red-brown earth soils selected to represent these great soil groups have been included in the Handbook of Australian soils (Stace *et al*, 1968). Kaolinite is recorded in all sixteen B2 horizons, co-dominant with illite in twelve, and with randomly interstratified material or montmorillonite in four (one solodized solonetz and three soloths in which illite was not identified). It is interesting that the approximate amount of kaolinite in the clay fraction of two of the three soloths, in which it occurs with randomly interstratified material (10 - 20%), is 65 - 80%. The most common range for illite is 40 - 50% with a low of 3 - 10% (one soloth) and a

high of 65 - 80% (two red-brown earths) while the soloths as a group vary more widely in illite content (3 - 10% to 50 - 65%). The solodized solonetz (20 - 30% to 65 - 80%) and red-brown earths (30 - 40% to 65 - 80%) are less variable.

Although selected as representative the sample of these three great soil groups described by Stace *et al* (1968) is small and generalizations are risky. Nevertheless, Rengasamy and Olsson (1991) have reported that the acidic sodic soils (soloths) are highly weathered with generally low cation exchange capacity. In the case of the soloths described by Stace *et al* (1968) this may be seen to be supported by the dominance of kaolinite (40 - 50% to 65 - 80%) in the clay fractions. However, this is not reflected in the data for cation exchange capacity (CEC). The rounded mean CEC for the soloths is 32 $cmol^{+} kg^{-1}$ (clay basis) in the upper B2 horizon, the same as for the red-brown earths and only marginally lower than for the solonetz (34) and solodized solonetz (36). These CEC's are all well within the range recorded for soil illites and far higher than that of kaolinites, viz, 10 - 40 and 0 - 8 $cmol^{+}kg^{-1}$ respectively (Churchman *et al*, 1993).

Sodicity is usually associated with reduced permeability of soil to water which can be slow to extremely slow in medium and heavy textured soils (Churchman *et al*, 1993). However, it is being recognised increasingly that all soils do not respond to the presence of sodium ions in the same way or to the same extent (Shainberg and Letey, 1984) and soil behaviour such as gypsum responsiveness (Loveday, 1974b) cannot be predicted accurately in relation to any particular critical level of exchangeable sodium percentage (ESP) (Sumner, 1993).

Volume changes with swelling are most marked in the case of smectitic soils and the swelling of illitic and kaolinitic soils is much less. Although swelling can result in reduced permeability, the main factor in severely reduced permeability is dispersion, particularly in illitic and kaolinitic soils (Churchman *et al*, 1993). It has been shown that clay dispersion can occur at low values of ESP (Shainberg and Letey, 1984) with consequent degradation of soil structure and loss of conducting voids. Moreover, illites are now known to be more dispersive than montmorillonites (Oster *et al*, 1980; Shainberg and Letey, 1984) and to disperse in contact with soil solutions of higher electrical conductivity (EC) in which

montmorillonites remain flocculated. Very fine-grained Na - and Ca - illites, on the other hand, have been shown to flocculate at EC's similar to those required for Na - and Ca - montmorillonites (Emerson, 1983).

Finally, the critical coagulation concentration (CCC) values for soils and their relation with soil reaction (pH) are often different from those of the dominant clay mineral present (Goldberg and Forster, 1990). Thus, while inferences may be drawn about swelling and/or dispersive behaviour of field soils from their clay mineralogy and the compositions of the exchange complex and saturation extract, field heterogeneity remains a barrier to specific extrapolation of laboratory data.

2.3.6. Soil classification

In Soil Taxonomy (Soil Survey Staff, 1975) each of the orders Aridisol, Mollisol, and Inceptisol includes salt-affected and/or sodic soils with the presence of diagnostic sub-surface horizons: argillic, natric, calcic and salic, providing the basis for further classification.

Isbell (1996) classified sodic soils into the order Sodosols. He defined these soils as having clear or abrupt textural separation of A and B horizons with ESP more than 6 in the major part of the upper 0.2 m of the B2 horizon and pH (1:5 H_2O) above 5.5. Solodized solonetz and solodic soils, some soloths, and many red-brown earths and desert loams are classified within this order.

2.3.7. Soil management

Rengasamy and Olsson (1993) stated that because of sodicity in the rootzone and associated soil physical and chemical constraints the productivity of irrigated agriculture in Australia is low for most crops. Over 80% of Australian irrigated soils are sodic and have degraded structure limiting water and gas transport and root growth. Irrigation without appropriate drainage leads to the formation of perched water tables and build up of salts in soil solutions with increased SAR exacerbating sodicity, dispersivity and very slow permeability.

Greene and Ford (1985) reported the application of gypsum at rates up to 15 $t.ha^{-1}$ to the surface of two red duplex soils. At both sites, approximately five years after application they found that only when 15 $t.ha^{-1}$ of gypsum was applied was sodium in the upper 25 cm significantly decreased. Exchangeable Mg was not decreased below 15 cm.

Scotter (1985) studied the effects of infiltrating dissolved gypsum, sodium chloride and distilled water on the hydraulic conductivity of a sodic heavy clay at matric potentials between -0.5 and -8 kPa. He suggested that percolation of one pore volume of gypsum solution (concentration 29 me/l) induced an approximately fourfold increase in hydraulic conductivity relative to that with distilled water. This enhanced conductivity did not change when the permeating solution was changed to sodium chloride solution (30 me/l). However when distilled water was substituted for either the gypsum or sodium chloride solutions the hydraulic conductivity declined rapidly. Akram *et al* , (1989) found that the application of gypsum and H_2SO_4 reduced ESP and pH and increased dry matter yield. Tiwary *et al* (1989) found that application of gypsum and of pyrite resulted in decreased pH, electrical conductivity and exchangeable sodium content and increased crop yield. The application of the amendments to 10 cm depth produced better crop yield than when applied to 20 cm depth. Omar *et al* (1990) stated that pore size distribution has a major direct and indirect effect on the basic infiltration rate. The exchangeable sodium percentage and organic matter content only indirectly affect the basic infiltration rate.

2.4. Secondary Iron and Manganese Deposits in soils

The distribution and forms of iron and manganese in soils due to pedogenesis are often amongst the most visible soil morphological characteristics and may be especially prominent in terms of soil colour and as pedological features (Brewer, 1964). Thus they have been interpreted as indicators of the kind and intensity of pedological processes determining the nature of soils (Taylor *et al*, 1983). The amounts and forms of iron oxides, in particular, have been adopted as diagnostic characteristics of soil horizons (Soil Survey Staff, 1975), the weathering stage of soil materials (Jackson and Sherman, 1953) and in soil classification (Soil Survey Staff, 1975; Isbell, 1996).

Glaebular and cutanic (Brewer, 1964) concentrations of iron and manganese may occur together in the same feature. However, McKenzie (1975) found that although iron could deposit on manganese oxides, manganese favoured sites where both manganese and iron already existed and that the association was one of interlayering rather than co-deposition.

While both iron and manganese are important plant micronutrients, the mobility of manganese in the common pH range of soils is such that manganese toxicity is far more common and the accumulation of secondary Mn relative to Fe reflects soil hydrology (McDaniel *et al*, 1992). Increased levels of soil solution manganese can occur readily with waterlogging and this may follow an annual cycle, for example, in some soils of the eastern Riverina near Wagga Wagga, New South Wales (Beattie, personal communication). Furthermore, manganese oxides identified in soils (Taylor *et al,* 1964) are much more complex in chemical composition than iron oxides. Because of their negative charge in the desirable pH range of agricultural soils, small particle size and large surface area, manganese oxides accumulate heavy metals (Taylor and McKenzie, 1966; Taylor, 1968) and this can result in cobalt deficiency in pastures and stock grazing them (Adams *et al,* 1969). Iron oxides, particularly when dispersed as very fine, colloidal, particles in acidic soils, are known to form very stable complexes with phosphate, arsenate, silicate and organic anions. So stable is the complexing in the case of added fertiliser phosphorus that the phosphorus is quickly rendered unavailable to plant roots and is said to be "fixed" (Wild, 1958; Smith, 1965). Thus the presence of secondary or residual accumulations of both iron and manganese in the root zone or upper soil profile can be an indication of particular soil management hazards.

2.4.1. Iron

As the fourth most abundant element, the level of iron in the crustal rocks of the earth is about 5 %, after oxygen (46%), silicon (28%) and aluminium (8%). However, iron may be accumulated or depleted during weathering and soil formation so that the levels of iron in soils vary widely. In Australian soils the common range is from less than 0.1% to 15%

(Table 2) but iron may comprise more than 35% of the mineral fraction of iron-rich laterites (Taylor *et al,* 1983). A north Queensland krasnozem subsurface material contained about 50% goethite plus haematite (Gillman and Bell, 1976).

Table 2.Approximate % Fe in surface horizons of major Australian great soil groups

Podzol	< 0.1
Solodized solonetz and solodic	1.3
Soloth	1.2
Red-brown earth	3.6
Black earth	4.0
Red earth	5.0
Krasnozem	16.0

(After Stace *et al,* 1968)

The amounts, forms and depth functions of iron in soil profiles have long been objects of study in pedology (soil formation), soil chemistry and mineralogy, as well as in soil fertility and plant nutrition. In pedological studies they may be interpreted for degree and kind of weathering and oxidation/reduction conditions of soil environments (Schwertmann, 1985) processes of translocation, concentration and reorganisation of soil constituents in the formation of pedological features and soil fabrics (Brewer, 1964; Brewer and Sleeman, 1988) and trends of soil development such as podzolisation and lateritization (Beattie, personal communication).

Pedogenic concentrations of iron oxides, described by Brewer (1964), may be identified as cutans, glaebules or pedotubules. These iron-containing pedological features are normally studied in thin section and their composition and orientation determine their optical properties. Thus ferrans (cutans of iron oxides coating the surfaces of voids) are translucent to opaque and usually isotropic because of their very fine grain size. Glaebules (nodules, concretions) may vary in size from microscopic to macroscopic (up to many centimeters) and are translucent to opaque in thin section and usually red or yellow in reflected light depending on degree of hydration. Sesquioxidic pedotubules are usually relatively large infillings of tubular voids and are distinguished by their colour.

The oxidation state of iron and the distribution, dispersal and particle size of iron oxides are major determining factors of soil colour. Although the redness of soils is not

always well correlated with the amount of iron present it is indicative of mineralogical differences (Brewer, 1964; Schwertmann, 1985). A small amount of iron in highly oxidised and dispersed state on the surfaces of the soil mineral fraction can produce a dominant effect, masking that of the humus fraction, while a larger amount of iron concentrated in secondary glaebules (Brewer, 1964) may contribute little to soil colour.

In soil fertility, iron oxides, especially when colloidal, dispersed or microcrystalline, play important roles in relation to the availability of several essential plant nutrients, including P, Cu, Zn, Co, and Mn. The retention of applied soluble phosphates by soils such as the krasnozems with high levels of "free iron" is well known (Norrish and Rosser, 1983). In relation to soil physical fertility, the state, distribution and forms of iron oxides present may often be reliable guides to important soil qualities of drainage and aeration. However, a direct contribution by even very finely divided, X-ray amorphous iron oxides to soil structural stability remains uncertain (Emerson, 1983) and recorded positive effects have been attributed to interaction of iron and organic matter (McIntyre, 1956).

The common iron oxides in soils are goethite (alpha FeOOH), hematite (alpha Fe_2O_3), lepidocrocite (gamma FeOOH), ferrihydrite ($HFe_5O_8.4H_2O$), maghemite (gamma Fe_2O_3) and magnetite (Fe_3O_4). All have been identified in different Australian soils which often contain more than one form (Taylor *et al*, 1983). All except magnetite owe their occurrence to soil forming processes acting on primary sources or on earlier pedogenic forms with change in environmental factors. Magnetite occurs commonly in small amounts as a resistant primary mineral.

Goethite (yellow brown) is most common, being found in most soils and in most climates. Hematite (red) is also very common, more particularly in aridic and tropical soils where the inhibiting effect of organic matter is much less due to its rapid oxidation, but also occurs in association with goethite in other environments. Although in lesser amount than goethite it may dominate in conferring a red colour such as in red-brown earths. Both goethite and hematite may occur as major components of iron-rich glaebules (Brewer, 1964).

Lepidocrocite occurs commonly in hydromorphic soils under humid temperate conditions, often associated with goethite (Taylor *et al*, 1983). The mineral may be recognised by its distinctive orange colour (Schwertmann, 1985).

Ferrihydrite in varying proportion with goethite has been identified in placic horizons (Soil Survey Staff, 1975; Campbell and Schwertmann, 1984), bog iron ores (Evans *et al*, 1978) and ochreous deposits in drainage ditches, pipes and boreholes. Previously regarded as amorphous its crystalline nature was recognised relatively recently.

Maghemite has been found frequently in subtropical and tropical soils low in soluble aluminium (Taylor and Schwertmann, 1974; Coventry *et al*, 1983) and occasionally in humid temperate zone soils. In the latter occurrences the maghemite was concentrated in the surface soil which also contained charcoal suggesting its formation as a result of fire since it is known that heating any pedogenic iron oxide to 300 - 500 ^{o}C in the presence of organic matter will produce maghemite (Schwertmann and Taylor, 1977).

In spite of much in vitro experimentation which has yielded a degree of understanding of the formation of the common iron oxides in simple chemical systems, processes of formation in the much more complex soil environment remain speculative.

When the amount present is high enough, ie., 10% or more, both X-ray diffraction and infra-red spectroscopy can be used to identify iron oxides in soil materials (Taylor *et al*, 1983). Differential thermal analysis can be useful in providing added confirmation of the occurrence of minerals whose presence is known or suspected from other data. Mossbauer spectroscopy is a relatively new technique of great promise in the identification of iron minerals in soils with much lower limits of detection than X-ray diffraction (Kodama *et al*, 1977).

A number of techniques have evolved for the chemical removal of "free iron oxides" from soil materials by differential dissolution and each of these may be regarded as efficient for the soils for which they were developed. Indeed this is a common state of affairs in soil chemistry generally.

McKeague *et al* (1971) and Weber *et al* (1974) proposed differential dissolution procedures for estimation of the iron present as crystalline oxides, ferrihydrite and

amorphous iron-organic complexes. The latter are removed first using 0.1 M sodium pyrophosphate. This is followed by acid ammonium oxalate extraction (pH 3) in the dark to remove an "amorphous inorganic fraction" supposed to be poorly crystalline ferrihydrite. Finally the crystalline Fe (III) oxides are removed by dithionite-citrate-bicarbonate extraction (Mehra and Jackson, 1958). However the term "free iron oxide" does not have precise meaning in terms of composition.

However determined, the iron content of a soil profile can vary markedly with depth, together with relative amounts of iron-bearing minerals. Such depth functions although based on empirical extraction procedures, are nevertheless of great interest in studies of pedogenesis.

2.4.2 Manganese

Although far less abundant than iron, averaging only 0.1% (1,000 ppm) of the earth's crust, manganese is widely distributed in at least trace amounts in most rocks and in larger amounts in ferromagnesian minerals. Manganese, like iron, may accumulate or be depleted during pedogenesis and soil Mn content may range from the smallest trace to as much as 0.3% or 3,000 ppm. It is also found in much higher concentration in the form of glaebules and surface films or cutans, ie., mangans (Brewer, 1964) where it may constitute up to 30% or so of the particular pedological feature.

Manganiferous pedological features include deposits in planar and cylindrical voids (cracks and channels) as mangans (manganiferous cutans) and glaebules (nodules, concretions) (Brewer, 1964; Sullivan and Koppi, 1992). Mangans are very dark brown to black in reflected light and opaque in thin section. Glaebules rich in manganese oxides are also very dark brown to black in reflected light and opaque in thin section and range in size from microscopic up to a few centimeters in diameter. The microscopic accumulations may be well dispersed. Manganiferous glaebules usually include a considerable amount of iron. They also occur both in greater size and frequency in soil horizons subject to seasonal waterlogging and of restricted drainage.

Manganese oxides do not influence soil colour as generally as do iron oxides. However, mangans are usually relatively limited in extent but may be numerous, thus conferring a fine mottling effect.

As an essential element manganese is the only micronutrient that may be deficient or toxic over large areas. Below pH 6 manganese may be toxic but never deficient. Above pH 7 manganese may be deficient but never toxic (Leeper, 1970). Manganese glaebules are effective in adsorbing and occluding cobalt. In some soils this may render useless attempts to control cobalt availability via cobalt application as fertiliser (Adams *et al,* 1969; McKenzie, 1975). Lead is also accumulated by manganese oxides (Norrish, 1975) and addition of manganese dioxide to lead-contaminated soils has reduced the uptake of lead by plants (McKenzie, 1978).

Taylor *et al* (1983) listed thirteen of the more important crystalline oxides of manganese amongst the large number of mineral forms identified in geological studies (Hewett and Fleischer, 1960). Of these only two, birnessite and lithiophorite, have been identified frequently in soil materials. The others, identified once or a few times, are hollandite, todorokite, pyrolusite, psilomelane and manganite. Generally, manganese oxides in soils are very fine grained, of low crystallinity, of variable composition and are often reported as amorphous.

Birnessite occurs in both acid and alkaline soil materials but is more common in materials of alkaline reaction. Lithiophorite occurs most commonly in acidic subsurface horizons (Taylor *et al*, 1964).

As with the iron oxides the formation of manganese oxides in field soils is imperfectly understood on the basis of <u>in vitro</u> studies of transformations of synthetic compounds (McKenzie, 1971). These studies indicate that the presence of small or large amounts of foreign ions inhibits the formation of pyrolusite and nsutite repectively and such conditions are the norm in soils. Hausmannite and manganite too are not likely to be stable in soils (Eswaran and Raghu Mohan, 1973). According to Taylor *et al* (1983) either MnO_2 or birnessite is formed first, followed by recrystallization to lithiophorite, or less frequently to todorokite. A mechanism for the accumulation of interlayered manganese and

iron oxides, whose structure has been shown using the electron probe microanalyser, has been proposed by Burns and Burns (1975). Briefly, structural similarity of ferrihydrite and δ–MnO_2 favour epitaxial intergrowth of these minerals. Thus the nucleation and growth of manganese glaebules may begin with a deposit of ferrihydrite followed by epitaxial growth of δ-MnO_2 and ferryhydrite alternately with fluctuating Eh and pH.

The mineralogy of manganese oxides in soils may be determined by X-ray diffraction only where sufficiently concentrated such as in glaebules or planar void and channel infills but even so further concentration may be required (Taylor *et al*, 1964). Because of their mixing with iron oxides and other soil constituents the chemical composition of manganese oxides cannot be determined directly (Taylor *et al*, 1964). A further complication is the variable concentration of constituent elements so that chemical analysis is not very helpful in identification of manganese minerals.

2.5. BLACK CRACKING CLAY SOILS

2.5.1. Nomenclature

Black cracking clay soils are known throughout the world by different names. In South Africa they are called black cotton or black turf soils, black earth in Australia, melanites in Ghana. Other names have been taken from the local language, such as regurs in India, tirs in Morocco, smonitzas in Yugoslavia, badobes in Sudan,sols de paluds in France. Still other names have been used, such as grumusols in USA, margallitic soils in Indonesia (Oakes and Thorp, 1950; Dudal, 1963).

2.5.2. Occurrence, topography and climate

These soils occur in all five continents from 45^{o} South to 45^{o} north, but mainly in tropical and subtropical areas. The major areas of occurrence are in Africa and Asia but they also occur extensively in Australia, North America and South America (Dudal, 1963). The full extent of black cracking clay soils worldwide is well over 100 million acres (Templin *et al*, 1956). In Africa, black cracking clay soils are widely distributed south of the Sahara with the largest occurrences in Niger, Chad, Sudan and South Africa (Oakes

and Thorp, 1950). In Asia, the largest area of these soils is in India. They are also relatively extensive in Java, Madura and other small islands in Indonesia including Lombok (Dudal, 1963). Of the 20 - 30 million acres of these soils in the United States, about half are in Texas, with sizable areas in California, Alabama and Mississippi (Templin *et al,* 1956). Extensive areas of well-drained brown grumusols developed from weathered ultrabasic volcanic rocks exist in north-central and eastern Arizona (Johnson *et al*, 1962). The types of parent materials associated with grumusols over a wide range of rainfall regimes are marl, coralline limestone, calcareous sandstone, indurated limestone, non-calcareous sandstone and chalk mainly in humid climates with rainfall from 1000 to 1500 mm per annum (Ahmad and Jones, 1969).

Generally, black cracking clay soils occupy plains or gentle slopes of undulating to level landscapes with slopes of 5% or less although a few are on steeper slopes (Ahmad and Jones, 1996; Northcote *et al*, 1975; Dudal, 1963; Soil Survey Staff, 1975; Wilding *et al*, 1983).

They occur most extensively in regions with moderate to high mean annual temperatures ranging from 16 to 29 ^{o}C and medium to low mean annual rainfall from 500 to 900 mm. They also occur in cool regions where mean annual rainfall is less than 1270 mm (Oakes and Thorp, 1950). Regur soils occur in landscapes with mean annual rainfall ranging from 430 to 1400 mm and average annual temperatures near 24 ^{o}C (Simonson, 1954). Caribbean grumusols occur under a humid climate with rainfall ranging from 1000 to 1500 mm per annum (Ahmad and Jones, 1969). In Western United States, black cracking clays are found at altitudes ranging from about 100 to 2,500 m ASL, mean annual rainfall from 254 to 1000 mm and mean annual temperatures from 4 to 18 ^{o}C (Buol *et al*, 1980). In Arizona, they occur at elevations less than 650 m under rainfall of about 635 mm per year. Other occurrences in the northern hemisphere are in humid zones with 1000 mm or more mean annual precipitation and elevations above 2,500 m (Johnson *et al.*, 1962). According to Templin *et al* (1956) the Houston black clay soils of southern Texas classified earlier as grumusol receive a mean annual precipitation from 700 to 900 mm. In

the higher rainfall areas they tend to occur on undulating upland. Mean annual temperatures range from 18 to 21 °C.

Black cracking clays are widely distributed in Eastern Australia from Southern Tasmania to the base of Cape York Peninsula in regions of 500 - 1,000 mm annual rainfall. The largest areas are those of the Liverpool Plains in New South Wales and the Darling Downs and Central Highlands in Queensland (Stephens, 1962; Northcote *et al.*, 1975). They may be directly derived from basalt by weathering and soil formation. They are also found in association with calcareous mudstones and clayey sandstones, lithic and feldspathic sandstones, diorite and andesite and high-clay alluvium (Northcote *et al,* 1975). Isbell (1996) has classified these soils in the order Vertosol.

2.5.3. Morphology

Black cracking clay soils have unique morphology. Horizonation is often only weakly expressed. This is attributed to convection and the self-mixing that results from shrinking and swelling of the clay with drying and wetting (Wilding *et al,* 1983). The profile is often deep with dark-coloured surface and subsurface horizons (Stephens, 1962). There is commonly a transitional horizon with gradual to diffuse upper and lower boundaries and properties intermediate between the A and C horizon consisting of dark greyish brown clay with diffuse olive-brown mottles and very coarse prismatic or blocky structure (Young, 1976). Soil consistence is hard when dry, very firm when moist and very plastic and very sticky when wet (Northcote *et al*, 1975; Young, 1976). Bulk densities of peds are extremely high, ranging from 1.74 to 1.98. Values below 1.8 are always associated with a weakly granular or "self-mulching" material forming a thin surface horizon. In the middle and lower parts of the profiles, bulk densities are uniformly high (Johnson *et al*, 1962; Young, 1976). The dark clay horizons have strong, medium, sub-angular blocky peds becoming polyhedral with depth (Northcote *et al*, 1975). Permeability is very low, remaining uniform throughout the A horizon or decreasing to a minimum value in its lowest part (Young, 1976).

Templin *et al* (1956) have described the profile of Houston black clay, perhaps the best known of these soils. It consists of a thick uneluviated upper horizon of black or very dark clay, the moist colour of the surface soil ranging from very dark grey (10YR 3/1) to dark greyish brown (2.5Y 3/1). In the undisturbed, moist state, the structure of the upper horizon is moderate, medium, granular becoming gradually weaker and coarser with depth to weak, coarse, irregular blocky about 45 cm below the surface. The structure varies greatly with moisture content. When wet the soil is an apedal mass of sticky clay. When dry the surface condition is a mulch of very hard granules. Soft masses of segregated $CaCO_3$ occur from 1 to 1.8 m below the surface to depths ranging from 2 to 3 m. According to Johnson *et al* (1962) typical colours of the brown grumusols of Arizona range from brown (10YR 4/2 to 4.5/2, dry) to dark brown (10YR 3/2, when moist). Field texture is clay or silty clay. The upper layer from 2 to 5 cm thick has strong very fine granular structure while the lower horizons have very coarse parallelipipedal or lenticular aggregates. Wide, vertical cracks are present in the dry soil. Below the granular surface horizon the soil has high bulk density and low porosity. However, plant roots usually extend down to the bed rock via planar voids. Ahmad and Jones (1969) have described Caribbean grumusols as generally clay in texture with a tendency to increase in clay content with depth. They have a very weak medium blocky structure in the surface and are massive in the lower horizons. The colours range from grey to very dark grey or very dark brown (between 10YR 7/2 and 10YR 4/3). Plant roots are abundant in the upper profile and decrease with depth. Soils derived from calcareous parent materials have free calcium carbonate in the profile, the amount increasing with depth. The regur soils of India (Simonson, 1954) are dark yellowish brown to very dark greyish brown (from 10YR 4/4 to 10YR 3/2) in colour. Field texture ranges from loam to clay. The upper horizons have a moderate medium granular structure. The lower horizons have weak fine blocky peds and a few very coarse concretions of secondary carbonate. Plant roots are found down to the bed rock.

2.5.4. Physical Properties

2.5.4.1. Swelling and shrinking characteristics

The soils crack significantly with drying, commonly forming cracks at least 6 mm wide in a polygonal surface pattern. The depth of the cracks may be from 25 cm to more than 2 m (Abedine and Robinson, 1971; Northcote *et al*, 1975; Young, 1976). Although the cracks are normally open to the surface, they may not always be apparent at the surface. The average depth of cracks is inversely related to the amount of precipitation or irrigation (Johnson *et al*, 1962).

The degree of cracking is affected by the length of the drying period, the kind of soil, clay content, clay mineralogy, CEC, exchangeable cations and organic matter and iron content. Also the frequency of occurrence of cracks and crack depth are affected to a considerable extent by the kind and density of vegetation (Abedine and Robinson, 1971; Yaalon and Kalmar, 1972; Davidson and Page, 1956; Franzmeier and Ross, 1968; Bronswijk and Evers-Vermeer, 1990). Davidson and Page (1956) reported that the removal of iron was followed by increased swelling of the clay. Removal of organic matter had a similar effect, while soil saturated with sodium swelled more, dispersed, and was more impermeable than soil saturated with other cations. Franzmeier and Ross (1968) found that kaolinite or mica dominant soils have coefficient of linear extensibility (COLE) values <0.03 whereas those dominated by montmorillonite have COLE values >0.03. Anderson *et al* (1973) found that variations of COLE in vertisols are highly correlated with the percentage of fine clay and ESP. Bronswijk and Evers-Vermeer (1990) reported that in all aggregates, shrinkage started immediately with the first water extraction from saturated soil. Light clay soils had percentage of length extensibility (PLE) values of about 13 whereas the PLE values of heavier clay soils were about 17 and were regarded as strongly swelling and shrinking soils. Volume decreases on drying varied from 13 % to 42 % with COLE values of 0.05 and 0.20 respectively. The majority of Dutch clay soils have COLE values between 0.11 and 0.15.

Several ways are used to determine swelling and shrinkage phenomena of cracking clay soils. Commonly, however, they come up with different results. Stirk

(1954) found that there were four shrinkage phases accompanying progressive water withdrawal from natural soil aggregates, namely:

(1) structural shrinkage, dependent upon the degree of structural development, where the change in the soil volume is less than the volume of water removed;

(2) normal shrinkage characterized by a volume change ratio value of about 1.0;

(3) residual shrinkage, with a volume change ratio between 0 and 1, dependent upon both structure and texture (aggregates and particle size) and commencing generally at pF levels drier than the wilting point (about pF 4.2);

(4) no shrinkage, with a volume change ratio of zero, the commencement of this phase is dependent upon particle size distribution and is reached at a variable pF up to 6.5.

Fox (1964) discussed five assumptions regarding the character of the change in soil volume in the field:

(a) Contraction and expansion of the soil with change in water content in a defined moisture range around 46 % moisture content is three-dimensional and equidimensional. At moisture contents above the defined range, contraction and expansion will be unidimensional.

(b) Within or above the defined moisture range air does not enter horizontal interstices to replace water withdrawn.

(c) Contraction and expansion of the soil , within and above the defined water range, will be normal.

(d) Shrinkage and expansion characteristics are identical as the measurements are made in a drying cycle and the effect of hysteresis is ignored.

(e) The density of the soil water is assumed to be unity.

Unidimensional swelling is swelling in the vertical direction only. Three-dimensional or equidimensional swelling is swelling such that air does not enter the horizontal voids. Normal swelling is the swelling that is equal to the change in soil volume.

Berndt and Coughlan (1976) examined a Waco black earth on the Darling Downs, Queensland. Unsupported cores were used to measure volume and water changes by removing the cores from their supporting tubes and placing them on rigid bases. They

were then allowed to dry slowly by restricted exposure to the atmosphere. The dimensions of unsupported cores did not change immediately after being removed from their supporting tubes. The samples were physically stable and water was not redistributed when the support was removed. The subsequent shrinkage of unsupported cores was approximately equal in the vertical and horizontal dimensions. Shrinkage during drying to 0.47 $g.g^{-1}$ water content was three dimensional. Swelling was approximately three-dimensional at water contents less than 0.31 $g.g^{-1}$, then unidimensional up to water contents of 0.41 - 0.45 $g.g^{-1}$. Swelling during subsequent wetting tended to be initially greater than three-dimensional and less than three-dimensional at the highest water contents. Fox (1964a,b) reported that there was no visible soil cracking of Houston black clay in the field at more than 45% moisture content, at moisture contents between 40% and 45% cracking was clearly visible at 20% of the sites and below 40% moisture content cracking occurred at 100% of the sites.

Holmes (1955) pointed out that the change in volume of the pore space by swelling or shrinkage in high clay soils was more important than filling or emptying of the pore space by water. The moisture tension versus water content relationship in the case of such soils was determined by the swelling properties of the clay rather than by pore size distribution. A study conducted by George and Bridge (1973) showed that in an unconfined sample of black earth, swelling aggregates deformed into inter-aggregate pore space during water absorption reducing the size of the inter-aggregate pores and that swelling into the inter-aggregate pore space occurred at lower negative water pressures with increasing height in the sample. Three-dimensional shrinkage was found in the cores from the 10 to 20 cm depth. From 30 - 50 cm depth one-dimensional shrinkage occurred. Chan (1981) also concluded that expansion and contraction in the horizontal dimension of vertisols is internally accommodated by the vertical interstices of the soils. However the 7.5 by 7.5 cm cores used by Chan were sufficiently large to obtain representative samples for only the top 20 cm. To reflect the field situation, the soil cores have to be large enough to include a representative specimen of the field structure. Larger core sample holders have to be used for the deeper layers.

The extent of swelling can vary considerably in different soils or at different depths in the same soil. The variations range from normal swelling in extensively swelling soils to less than normal swelling in moderately swelling soils as found for a transitional red-brown earth (Jayawardane and Greacen, 1987). De Vos and Virgo (1969) pointed out that desiccation of the upper profile during the dry season usually results in shrinkage and the formation of deep vertical cracks with rough cleavage faces. In a study by Virgo (1981) on a Somalia vertisol during the drying period, surface cracking commenced at a soil moisture content of 35%. Significant deep cracking extending to 500 mm below surface cracks exceeding 10 mm in width developed only at moisture contents below 27%. Bronswijk (1989) found that the magnitude and the frequency of swelling and shrinkage decreased strongly with increasing depth in a Dutch clay soil. In the top soil, swelling and shrinkage were mainly determined by evapotranspiration whereas volume changes in the subsoils were determined by drainage.

2.5.4.2. Bulk density characteristics

Determination of field bulk density-water content relationships from in situ swelling measurements is likely to be more accurate than measurements on core samples, especially in cracking soils (Jayawardane and Greacen, 1987). Berndt and Coughlan (1976) suggested that it was not possible to ensure a constant relationship between bulk density and moisture content in the field. However at moisture contents between 35% and 55% there was quite good concordance with bulk density values. Fox (1964) found that the accuracy of bulk density determination fell with decreasing moisture content, particularly at moisture contents below 35%, due to increasing hardness of the soil. Chan (1981) found that bulk density increased with decreasing moisture content at all depths. For the 10 to 20 cm layer, bulk density was much lower than that of the deeper layers over the whole range of moisture content. Bulk density values were found to increase much more rapidly with decreasing moisture content in the 30 - 50 cm depth.

Yule and Ritchie (1980) suggested that to describe pore size distribution, bulk density and potential vertical movement of vertisols, soil shrinkage and water content relationships

were needed. The shrinkage curves were described in terms of structure, shrinkage and residual water loss phases. Structural water loss increased with depth due to increasing matric potential and the volumetric soil water content at the swelling limit (intersection point of structural and shrinkage water loss phases) was about 5%. All shrinkage was assumed to be normal and equidimensional and was included in a shrinkage water loss phase. The water loss was not replaced by air in the intrapedal pores, rather cracks formed. Also Gumbs and Warkentin (1972) reported that bulk density of clay soils increased sharply over the range 1.10 to 1.25 $g.cm^{-3}$ with decreasing rate of water movement. Vertical water movement was more affected by a change in bulk density in confined than in unconfined specimens. The effect of a change in bulk density on horizontal movement of water in confined specimens increased with an increase in initial water content. Also there was an exponential relationship between increase in bulk density and decrease in infiltration rate. The rate of infiltration depended to a large extent on the diffusivity near the surface. Because of swelling that decreased porosity and hydraulic conductivity at the surface, infiltration into confined samples was lower than into unconfined. George and Bridge (1973) found that during water absorption bulk density decreased with depth in a clay soil until pore water pressures were from -20 to -10 cm H_2O. During desorption bulk density increased at all depths as the pore water pressures decreased from 0 to - 8 cm H_2O. In unconfined samples, no differences in the pore water pressure versus moisture content relationship occurred with depth during absorption or desorption and bulk density remained constant. Jayawardane (1984) reported that in the horizon of a clay soil where swelling was less, the dry bulk density decreased relatively with increasing soil moisture content. Conversely the wet bulk density decreased markedly with decreasing moisture content. On the other hand, in horizons showing greater swelling, high moisture content was associated with decreased dry bulk density. McKenzie *et al* (1988) found that bulk density of a self-mulching grey clay did not change during the measurement period in any of their treatments (fallow,wheat and safflower) indicating that drying was accompanied by structural shrinkage. Parameters derived from clod shrinkage curves showed that there was a tendency toward improved structure in the

soil under wheat and safflower at depths of 0.15 m and 0.25 m and not for fallow treatment below 0.05 m and 0.25 m.

2.5.4.3. Soil structure

Brewer (1964) defined soil structure as "the physical constitution of a soil material as expressed by the size, shape and arrangement of the solid particles and voids, including both the primary particles to form compound particles and the primary particles themselves". Soil Survey Staff (1975) defined soil structure as "the aggregation of primary particles into compound particles or clusters of primary particles which are separated from adjoining aggregates by surfaces of weakness". Closely following Brewer's definition, Wilding and Hallmark (1984) defined soil structure as "the physical constitution of soil material as expressed by size, shape and arrangement of the solid particles and voids into secondary polyhedral units of primary particles". Letey (1991) defined soil structure from the viewpoint of the soil physicist as "the size, shape and arrangement of the solid particles and voids which are highly variable and associated with a complex set of interactions between mineralogical, chemical and biological factors". He also noted that the study of soil structure is not directly related to soil structure itself but rather the functionality of soil structure in relation to how soil structure affects water flow, root development, plant growth and aeration. Earlier, Taylor and Ashcroft (1972) described soil structure as "the arrangement of primary particles such as sand, silt and clay into compound particles or clusters that are separated from adjoining clusters". They also pointed out that soil structure does not affect plants directly but operates through several factors such as aeration, compaction, water relations and temperature. These factors do not only influence plant growth individually but also interact with each other. Baver *et al* (1972) defined soil structure as "the arrangement of sand,silt and clay into aggregates and the arrangement of these aggregates into a composite pattern".

Wilding and Hallmark (1984) suggested that there are three major processes in the formation of aggregates in soils, as follows :

(1) desiccation or dewatering that causes fabrics to become denser and more compact.,

(2) shear failure in unconfined surface horizons with relief of vertical stresses by upward movement (overburden pressures confine vertical movement in subsoil).,
(3) the biological activity of soil fauna such as arthropods and annelids, together with the mix of organic and mineral constituents in the formation of granular aggregates. They also stated that in cracking clay soils, granular, angular blocky or subangular blocky aggregates were commonly found in surface horizons. In subsoils, prismatic, angular blocky, wedge-shaped aggregates, or compound prismatic-blocky structure were usual.

2.5.4.4. Aggregate stability

According to Wilding and Hallmark (1984) the stability of aggregates is a function of the relative degree of cohesion within aggregates and adhesion between aggregates. Cohesion is caused by water/particle interactions and cementation by organic matter, sesquioxides, silica, carbonate and clay. Adhesive forces are dependent on the presence or absence of surfaces of weakness and the degree of surface accommodation between peds. Rengasamy *et al* (1988) categorized aggregate stability in several kinds of soils in which smectites are dominant including black earths. They concluded that sodium adsorption ratio (SAR) and total cation concentration (TCC) controlled internal repulsive forces of clay crystallites that were responsible for slaking and dispersion. The interactive forces between water molecules and counter-ions resulted in aggregate breakdown due to slaking. There was a positive correlation between SAR values of the soil solution and the electrolyte concentration at which dispersion occurred, the higher SAR values tending to increase dispersion. Aggregates from low sodic heavy clay soils (SAR < 3) were strongly slaking with formation of micro-aggregates because of the interaction of water molecules with their highly charged surfaces. Letey (1991) stated that an aggregate stability test was highly dependent upon the chemical composition of the water used, the initial moisture content of the aggregates, the sieve aperture and the time factor. Prebble (1987) measured aggregate stability of vertisols by wet sieving and correlated the result with Walkley-Black organic carbon. He noted that aggregate stability decreased with increasing clay content due to greater swelling pressure. The aggregate stability of soil after many years under grass was

much greater compared to its condition under forest. This may be due to the presence of grass roots physically binding aggregates, together with fungal hyphae or a different type of organic carbon. The C/N ratio generally decreases with increasing years of cultivation. Pojasok and Kay (1990) found that there was a significant correlation between dispersible clay soil and wet aggregate stability. Bromegrass exudate treatments were associated with greater stability than corn exudate treatments. The stability of aggregates increased with increasing solution concentrations of Ca and Mg. Harte (1988) pointed out that water stable aggregation was a one-dimensional determination of soil structure that ignored soil porosity and its form. There was a tendency for no-till management to improve aggregate stability. Root fissures and cracks were observed accompanying no tillage treatments. Bulk density, a function of soil porosity, provided a rough measure of soil structure. He suggested that a simple way to measure the tendency of soil aggregates to slake was by applying an arbitrary energy input in the form of a stream of water. Perfect *et al* (1990) concluded that on average, frozen and thawed clay soils had a significantly higher wet-aggregate stability and less dispersible clay than unfrozen soils. Dispersible clay decreased with increasing $CaCl_2$ concentration, indicating an electrical double layer effect. Wet-aggregate stability increased with decreasing water content for frozen aggregates but not for unfrozen. There was some indication that the slower the rate of freezing, the greater the increase in stability.

2.5.4.5.Water movement

Prathapar *et al* (1989) reported that the unsaturated hydraulic conductivity of a moderately swelling black cracking clay decreased with depth but in only the surface soil under a wheat crop was it significantly greater than in the deeper layers. Compaction at 0.4 m depth was attributed to cultivation. The mean root length density under pasture was higher than that under wheat. Blake *et al* (1973) reported that the hydraulic conductivity of a cracking clay soil remained fairly high in the surface horizon but fell to very low values in the lower B and C horizons. Maximum tritium concentration was found in the surface and at 70 to 80 cm depth. Hoogmoed and Bouma (1980) reported that vertical infiltration

decreased with time, particularly in initially dry soil. Horizontal absorption was low and increased slightly over a 5-hour period. Ritchie *et al* (1972) reported that the hydraulic gradient of a clay soil did not vary appreciably from unity throughout the profile down to the water table depth of about 175 cm. The water table did not rise appreciably, indicating lateral movement of water through the porous material of the C horizon. In field plots hydraulic conductivity values were between 2.0 and 3.5 cm/day. Hydraulic conductivity values for undisturbed cores varied between 0.5 and 0.4 cm/day approximately and for repacked soil cores the value was about 0.1 cm/day. Hydraulic conductivity of 21 cm diameter cores of various lengths ranged from 0.07 to 0.45 cm/day and the values for 60 cm diameter cores between 0.12 and 0.42 cm/day. It was concluded that core diameter should be much greater than core length to minimize the wall effect.

Lal *et al* (1970) pointed out that the diameter of the soil column significantly affected the rate of advance of the wetting front, the cumulative infiltration and the amount of swelling. The rate of advance of the wetting front in 100 minutes of infiltration was 0.00, 0.04, 0.057, 0.093, 0.1 and 0.142 cm. sec^{-1} for 1.25, 2.54, 4.44, 6.95, 9.52 and 14.62 cm diameter columns. Column diameter was the most important factor controlling the depth of wetting front and the rate of infiltration. Both column diameter and aggregate size were important contributing factors to swelling in the initial stage of infiltration. However, at longer times and deeper penetration of wetting fronts column diameter was the only factor affecting swelling. The greater the tube diameter, the greater was the swelling. In a field study McIntyre *et al* (1982) found that the infiltration rate of a 379 day plot was constant at 0.9 mm/day from day 10 to day 70. It then again decreased until about day 270. Cumulative infiltration rate was constant at 3.5 mm/day by day 15. The measurement after day 110 gave a value close to 3.5 mm/day and the infiltration rate remained constant at close to 3.5 mm/day from day 15 to day 145.

2.5.5. Chemical properties

Soil reaction of black cracking clay soils is generally in the neutral to alkaline range associated with a high percentage of calcium and magnesium; some non-calcareous soils

range from 5.2 to 6.8; most are above 6.0 (Johnson *et al*, 1962; Ahmad and Jones, 1969; Northcote *et al*, 1975). Typically pH ranges from 6.0 to 7.5 in the A horizon, rising slightly with depth (Young 1976). Electrical conductivity is about 2 - 6 $dS.m^{-1}$ in the surface horizons. Soluble salts increase in the lower horizons and there is a tendency to a downward increase of sodium on the exchange complex. Charles *et al* (1964) found that CEC of both clay and organic matter increased linearly with pH. CEC increased at a relatively constant rate from pH 2.5 to 5.0 with a somewhat smaller increase from pH 5.0 to 6.0 and a particularly marked rise between pH 7.0 and 8.0. Carbonate nodules or concretions also appear as a surface scatter on some gilgai mounds. Soft carbonate segregations and hard nodules or concretions, generally less than 1 cm in diameter, may occur in the subsoils (Northcote *et al* , 1975). Organic carbon is highest in the surface horizon, ranging from 0.80 to 2.11 % in grumusols, decreasing sharply from the upper to the second horizon and then very gradually with depth (Johnson *et al* , 1962).

The dominant cation in all profiles studied by Johnson *et al.* (1962) was calcium, ranging from 16 to 39 me/100 g. Magnesium levels have also been found to be relatively high particularly in the transitional layer above rock (Ahmad and Jones, 1969). In profiles from cooler, more humid areas, magnesium is relatively more abundant, and potassium and sodium are low (Johnson *et al* , 1962). The presence of exchangeable Mg increased the dissolution of $CaCO_3$ in calcareous soils and the electrolytes prevented the dispersion of the clay (Alperovitch *et al*, 1981). Also calcium and magnesium constitute the dominant exchangeable cations in calcareous grumusols over volcanic ash (Ahmad and Jones, 1969). In Australian black cracking clay soils, cation exchange capacities range from 20 to 80 cmol (+) kg^{-1}, varying with both clay content (ranging from 40 - 80%) and clay minerals. Calcium is usually the dominant exchangeable cation in the upper horizons and magnesium in the deep subsoils (Hubble et al, 1983).

2.5.6. Classification

In " The Australian Soil Classification" Isbell (1996) included black cracking clay soils in the order "Vertosols". He described them as having a clay field texture with more

than 35 % clay throughout the solum except for thin surface horizons less than 3 cm thick. Open cracks occur with drying that are at least 5 mm wide and extend upward to the surface or to the base of any plough layer. There are slickensides and lenticular peds at some depth in the profile.

Soil Survey Staff (1975) classified black cracking clays as Vertisols: mineral soils that do not have a lithic or paralithic contact or petrocalcic horizon or duripan within 50 cm of the soil surface. They have more than 30% clay in all horizons down to a depth of 50 cm or more after the upper soil to a depth of 18 cm has been mixed. They also have cracks open to the surface or to the base of a plough layer or a thin surface crust that are at least 1 cm wide at a depth of 50 cm unless the soil is irrigated. They have one or more of the following characteristics: gilgai (micro relief), slickensides at some depth between 25 cm and 1 m that are close enough to intersect and wedge-shaped aggregates with long axes tilted 10^{o} to 60^{o} between 25 cm and 1 m depth. They are divided into suborders in relation to frequency and duration of cracking and temperature regime.

2.5.7. Soil management

Implications for agricultural management of black cracking clays follow from consideration of their physical and chemical properties outlined above. Although the chemical fertility of these soils in often relatively high, eg., those of the Darling Downs and Lockyer Valley in South-East Queensland and of the Liverpool Plains in North-Western New South Wales, physical limitations can reduce their productivity.

These limitations arise from high clay contents, the general dominance of the clay fraction by smectite, and sodicity. Thus plant/soil/water relationships may be difficult to optimise consistently. Rainfall and irrigation water may move rapidly down cracks at first but permeability may be extremely slow after crack closure. The high density of peds and very fine pores within peds lead to very slow entry of water and much of this water may be held within peds at tensions beyond the wilting point and thus be unavailable for plant uptake. These conditions are associated with poor aeration. Below the immediate surface (self-mulching) plant roots are often confined to cracks separating large to very large peds

and severe root damage may occur due to adhesion of roots to surfaces as these separate with drying and shrinkage.

Black cracking clays are often extremely sticky when wet and in this condition also lose much of their bearing strength. Accessibility for cultural operations may be reduced so that either their timeliness may be seriously affected or, if operations are carried out under adverse conditions, severe structural damage to the upper profile may occur. Most of the soils are sodic and their tendency to be dispersive, coupled with loss of humified organic matter under cropping, makes such problems much worse. Management aimed at maintaining a high level of humus in the upper profile is important for reduction of these effects.

On sloping lands, severe erosion may occur due to overland flow in storm conditions after infiltration rate has been reduced by surface dispersion and sealing. Humus is important here too, together with management to provide a protective cover of vegetation during the period of high probability of occurrence of high intensity storm rainfall.

III. STUDY AREA

3.1. Location

The study area comprises part of the University of Tasmania farm located between Cambridge and Richmond in the lower Coal River Valley with a frontage to Pitt Water (Figure 1). Investigations were carried out on five soil profiles including a black cracking clay soil (UF1) in "Davis" paddock, and duplex soils (UF2, UF3, UF4 and UF5) in "Wattle" paddock (Figures 2a and 2b).

3.2. Climate

The climate of the Coal River Valley is essentially mild and dry (Nye, 1924) characterised by winters that are cool inland but milder near the coast and by warm to very warm summers. The prevailing winds are westerly but most of the rainfall comes from depressions held stationary in the western Tasman sea (Baillie and Leaman, 1989). Mean annual rainfall is low to moderate (483 - 584 mm). Rainfall is fairly evenly distributed throughout the year but December and October are the wettest months. Variation in rainfall is caused predominantly by rain shadow and elevation effects. The rainfall is relatively low from January to March generally higher from April to December but lowest in June, the driest month (Table 3).

Table 3. Average monthly rainfall and rain days at Hobart airport (1958 - 1993). /*

Period	Jan	Feb	Mar	Apr	May	Jun	Jul	Aug	Sept	Oct	Nov	Dec	year
monthly (mm)	38	35	37	44	39	29	49	49	41	50	45	59	515
rain days	9	8	10	11	13	13	13	14	13	14	13	13	144

/* cited from Bureau of meteorology Tasmania.

Evaporation (Table 4) is relatively high from October to March but decreases in late April and is low from May to August before steadily increasing again in the spring period (September to November) .

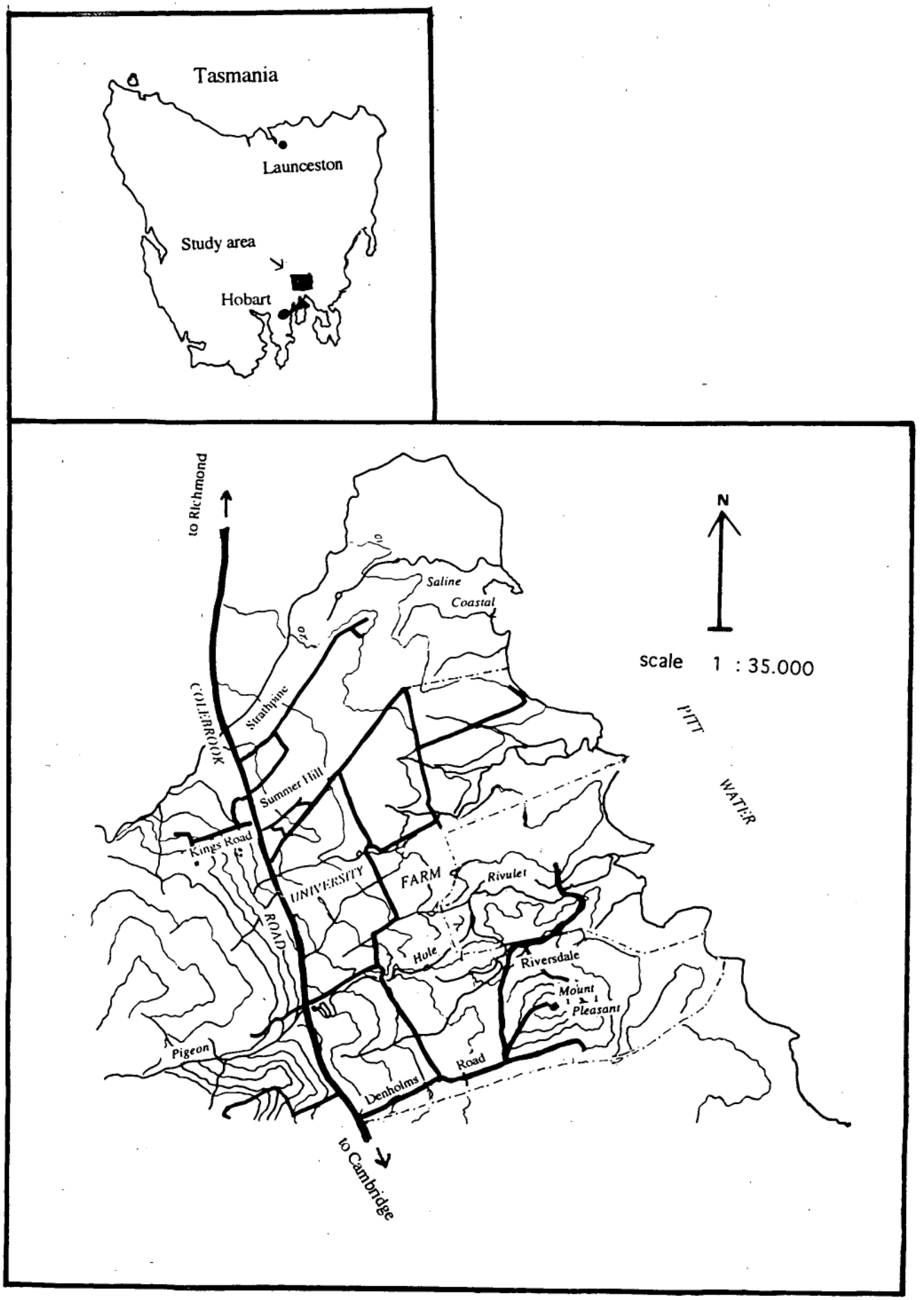

Figure 1. Location map of study area.

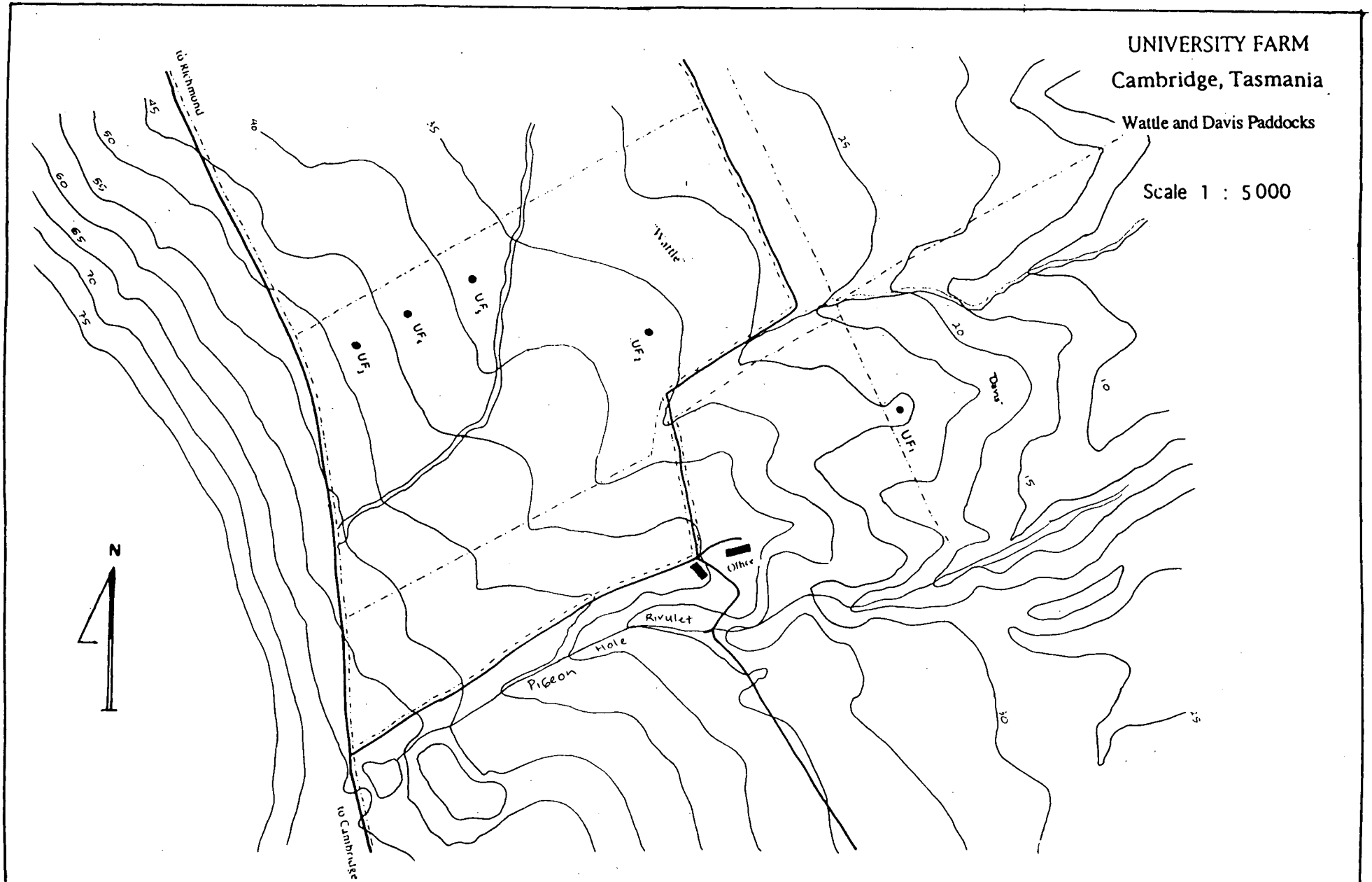

Figure 2a. Study area showing sampling site, contour interval 5 m.

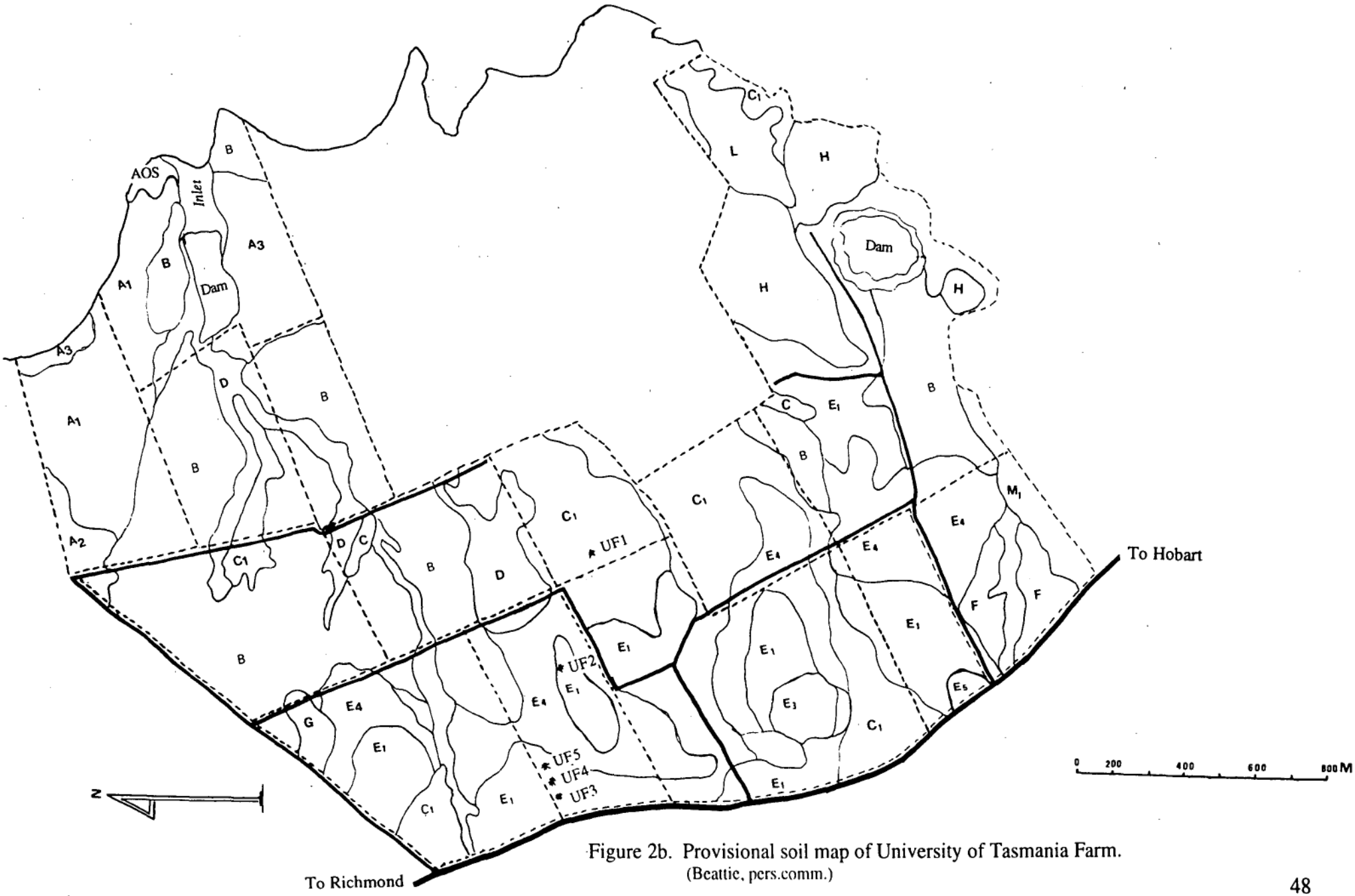

Figure 2b. Provisional soil map of University of Tasmania Farm.
(Beattie, pers.comm.)

Soil Reference

SERIES A Very strongly duplex soils on broad, gently domed interfluves and gentle to moderate sideslopes;
Type A1: .Light grey-brown, deep, sand above medium clay at 30-70cm depth.
Type A2: Light grey-brown, loamy sand above coarse columnar, clay at about 15 cm depth.
Type A3: Light grey-brown, sandy loam above coarse columnar, clay at about 15 cm depth.

SERIES B Very strongly duplex soils on slight (2 - 3%) uniform slope. Grey-brown, loam to sandy loam above gravelly loamy sand, above gravelly coarse columnar heavy clay at 15 to 30 cm depth, very hard and tough when dry, very sticky and plastic when wet. Some carbonate glaebules occur erratically in the lower subsoil.

SERIES C Uniform to gradational on soils floodplains (C1), gentle to short and steep erosional slope (C2, C3), and flat floors of incisions (C4), black, well structured, deeply cracking clay with self-mulching surface; fine earth and nodular secondary carbonate at shallow depth; on some steep slopes large hard carbonate glaebules are scattered on the surface; area mapped C3 has a few cm of clay loam grading to clay with cracking to surface.

SERIES D Moderately strongly duplex soils on gentle sideslopes of shallow incisions enclosing broad, saline flats toward Pitt Water; variably stony, grey-brown loam to sandy clay loam above medium clay at about 15 cm depth; may have fine earth and glaebular secondary carbonate lower in profile.

SERIES E Strongly duplex soils on gently domed summits and moderate to gentle slopes.
Type E1: Grey-brown loam to sandy loam to about 15 cm above sandy medium clay grading to heavy clay and back to sandy clay , above Tertiary clays or Triassic sandstone (E1(s)).
Type E2: As above but with loamy sand topsoil.
Type E3: Deep sand with many iron-indurated, angular, sandstone and rounded, hardened, iron oxide fragments in the sand matrix.
Type E4: Topsoil as for Type E1 but subsoil is friable, heavy clay, continuous to at least 150 cm depth; this soil occurs on gently sloping to very gently sloping toeslopes below Type E1 and above series B.
Type E5: As for Type E1 but a heavier textured topsoil due to admixture of dolerite-derived colluvium.

SERIES F Weakly duplex to gradational soils on gently sloping footslopes; dark grey-brown sandy clay loam to clay loam to about 15 cm depth above medium to heavy clay above coarse, rounded dolerite gravel at 50 cm; some fine earth and glaebular carbonate in subsoil.

SERIES G Gradational soils of broad, flat, shallow drainageway between Type E4 and series B; grey-brown loam grading to medium clay by about 15 cm depth.

SERIES H Gradational soil on flat summits and moderate to steep sideslopes of dolerite knolls; stony brown clay loam grading to reddish brown stony medium clay above dolerite bedrock at shallow depth (15-50 cm). ("Brown soils on dolerite")

SERIES L Gradational soil on moderate to gentle footslopes/toeslopes of dolerite knolls; dark grey-brown to black clay loam grading to medium clay above weathered dolerite rock. (Black soils on dolerite).

SERIES M Uniform soils on alluvium.
Type M1: Grey-brown, clay loam.
Type M2: As above but slightly heavier field texture and very tough, on floodplain step or terrace above M1.

SM Saline marsh.

AOS Aboriginal occupation site.

Table 4. Average pan evaporation at Hobart airport (1986 - 1993)./*

Period	Jan	Feb	Mar	Apr	May	Jun	Jul	Aug	Sept	Oct	Nov	Dec	year
daily (mm)	6.4	5.8	4.2	3.0	1.8	1.4	1.4	2.0	2.9	4.2	4.9	5.6	43.6

/* Bureau of Meteorology Tasmania.

Average monthly maximum and minimum temperatures at Hobart airport are given below (Table 5). Frost may occur at any time between April and November but frost has been recorded in every month of the year. Snow falls only very occasionally during the winter months, but does not accumulate to a thickness of more than a few centimetres and does not remain on the ground for any length of time.

Table 5. Average maximum and minimum temperatures at Hobart airport (1944 -1989)./*

Period	Jan	Feb	Mar	Apr	May	Jun	Jul	Aug	Sept	Oct	Nov	Dec	year
mean max (^{o}C)	22.3	22.2	20.6	18.1	15.0	12.7	12.2	13.2	15.2	17.2	18.8	20.3	17.3
mean min (^{o}C)	11.8	11.8	10.6	8.8	6.4	4.4	3.9	4.5	5.9	7.3	9.0	10.6	7.9

/* Bureau of Meteorology Tasmania.

The predominant winds are north-westerly with 67% of observations at 9.00 am from this sector. South-easterlies are common in the afternoon with 42% of observations at 3.00 pm in this quadrant (Bureau of meteorology Tasmania, 1992).

3.3. Vegetation and Land Use

Most of the original vegetation of the study area has long been cleared to make way for farming. However, the area was probably a woodland or open woodland (Walker and Hopkins, 1990) with *Eucalyptus amygdalina*, *E. Viminalis*, *Acacia dealbata* and *A. mearnsii* as the major species (Jackson, 1965; Davies, 1988).

The Coal River Valley and the Sorell District east of Pitt Water became important agriculturally soon after the early settlement of Hobart Town and for a time were the main cereal growing areas supplying the colonies of New South Wales. However, although

dependence on this region for wheat production was short-lived it has remained important for oats and high-quality malting barley. Oats is now the main cereal crop and wheat is grown to a much lesser extent. Root crops, such as potatoes, swedes and carrots are only grown in small quantities. Apples, pears, apricots and quinces are grown in moderate quantities for local consumption (Gatehouse, 1967). A number of new high-value horticultural crops have been introduced following installation of stages I and II of the South-East Irrigation scheme (Davies, 1988).

Since 1980 the University farm soils have been cultivated more intensively for various grain (buckwheat, wheat, oats, triticale, barley), vegetable (broad beans, navy beans, field peas) and horticultural (fennel, canola, poppies) crops. Supplementary irrigation has been used at first from farm dams and subsequently from stage II of the South-East Irrigation Scheme.

3.4. Geology and Geomorphology

The geology of the Coal River Valley has been studied by Leaman (1971), Figure 2c, Table 6.

The Coal River Valley is the topographic expression of a pair of parallel faults of Jurassic age (Leaman, 1971). Subsequent movement along the western fault, named the Coal River fault, occurred in Tertiary times (Gatehouse, 1967). Subsidence occurred generally along the valley in the Tertiary and fine-grained sediments (Tertiary clay formation) were deposited in the graben thus formed (Baillie and Leaman, 1989). These have remained as unconsolidated clays with intercalated sands. Fossil evidence suggests a fresh water lacustrine depositional environment (Nye, 1924).

The oldest rocks in the area are mudstones with minor interbedded sandstones of Permian age. Triassic sediments also occur as sandstones and subsidiary mudstone. These formations were intruded during the Jurassic period by basic magma to form a dolerite sill

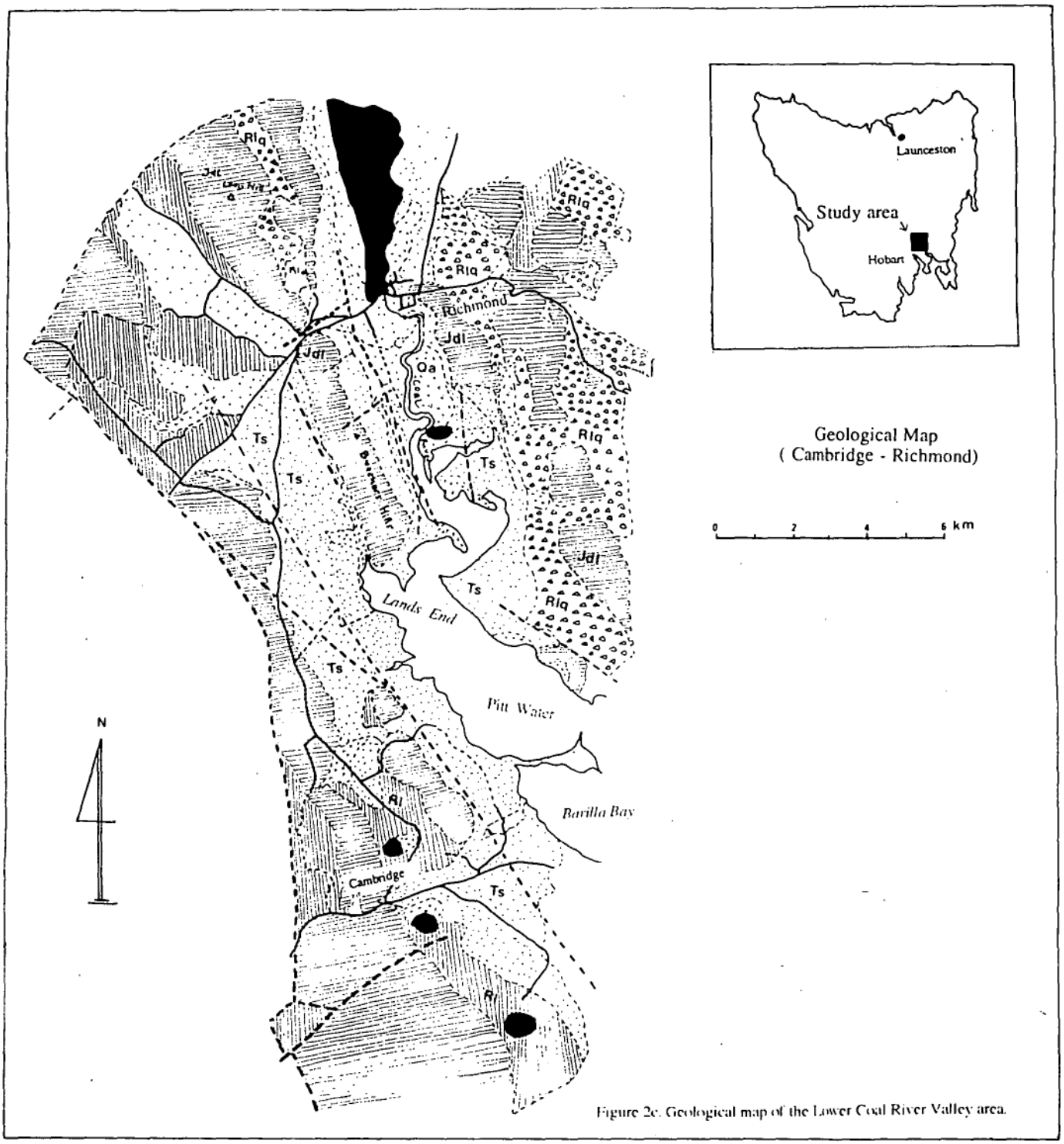

Figure 2c. Geological map of the Lower Coal River Valley area.

After : Symons (1975).

Qa — Alluvial deposits including younger gravels and swamp deposits.

Ts — Tertiary sediments predominantly sub-basalt silt and fine sand with lignite material stippled.

Tertiary basalt

Ri — Triassic sediments lithic arkose and lutite.

Rlq — Triassic sediments dominantly medium-coarse Quartz sandstone with minor mudstone.

Jdl — Jurassic dolerite.

with accompanying formation of chert and quartzite (Leaman, 1971). This basic igneous intrusive event was very extensive in Tasmania and Jurassic dolerite is the most extensive rock exposed within the State. Dolerite is a medium-grained igneous rock which is chemically and mineralogically similar to basalt. The essential minerals being basic feldspars (plagioclase), pyroxene and olivine with magnetite and ilmenite as accesory minerals. Chemically dolerite is relatively low silica (quartz < 5%) and high in magnesium, calcium and iron. Sodium and potassium are very low (Milner, 1962).

All of these rock types are represented in hills and ridges forming the upper slopes bounding the Coal River Valley (Holz, 1994).

Tertiary sediments occur along the southern boundary of both the Richmond and Sorell geological maps (1:50,000) with deposits extending north of Richmond in the

Table 6. Geological formations represented in the Coal River Valley *

System	Formation and rock type	Maximum thickness (m)
Quarternary	Alluvium, river gravels, and beach deposits; aeolian sands	>3
Tertiary	Basalt, clay and sand, coal	>200
Jurassic	Tholeiitic dolerite	
Triassic	Felspathic sandstone, mudstone, coal, quartz sandstone, mudstone and shale	>150 >300
	disconformity or unconformity	
Permian	Cygnet coal measures Carbonaceous shale and felspathic sandstone	60
	disconformity or unconformity	
Permian	Ferntree mudstone, siliceous pebbly, siltstone	170-185
Permian	Risdon sandstone, pebbly quartz sandstone	5
Permian	Malbina formation, siliceous siltstone and sandstone	>40
Permian	Cascades group, fossiliferous mudstone and limestone	>30

* Cited after Leaman, (1971).

valleys. The graben formation was initiated prior to the injection of dolerite (Leaman, 1971). Tertiary pale grey clays and sands are exposed in cliffs along the Coal River. The

clays are plastic when wet. These clays and sands were apparently derived from the dolerite and sedimentary rocks (Triassic sandstones and Permian mudstone) by weathering in the catchment area of streams feeding into the ancient lakes (Gatehouse, 1967). Thus these sediments have a mixed mineralogy. Volcanic activity during the Tertiary is represented in the Coal River Valley by valley basalt flows which overlie and interfinger with the Tertiary sediments and several centres of volcanic activity have been identified within a few kilometres of the site of the present study (Baillie and Leaman, 1989).

The low lying gently undulating surfaces south of Campania and in the Pitt Water area are underlain by Tertiary sediment with dolerite forming the high ridges and many individual hills (Leaman, 1971). However, some exposures of Triassic sandstone occur beneath the dolerite cap.

At some localities the clays are thinly bedded and the sands and sandy clays are impregnated with iron oxides forming ironstone (Nye, 1924). An interesting feature is the occurrence of laminar ironstone following bedding planes and joints within the Tertiary deposits. The occurrence of ferricretes, silcretes and calcretes has been reported by Holz (1994). A thin veneer of Quaternary sediment is found in depositional environments (Leaman, 1971; Hólz, 1994).

The local topography of the University of Tasmania Farm is cut in mainly Tertiary sediments, in part overlain by Quaternary alluvial fan and debris flow deposits (Holz, 1994) with minor outcrops of Triassic sandstone and Jurassic dolerite (Figure 2c).

The UF1 site is located on a flat to gently domed, knoll or summit at an elevation of 25 m above sea level (asl). The surface drainage pattern is radial away from the site. The UF2 site lies on the axis of a broad flat-topped ridge at an elevation of 35 m ASL and an easterly slope of 7%.

Profiles UF3, UF4 and UF5 in order from highest to lowest form a short transect on a valley-side toeslope (9% - 6% easterly slope). Above UF3, a short distance above the Richmond Road, is a steeper footslope below a very steep, rocky backslope cut in Jurassic dolerite. The upper footslope above the road is cut in Triassic sandstone. UF3 is at an elevation of 47m, UF4 at 43 m, UF5 at 38 m ASL.

3.5. Soils

The University of Tasmania Farm is sited in the south-east quarter of the Hobart sheet of the Reconnaissance Soil Map of Tasmania (Loveday, 1955). The farm soils are mapped as dominantly "Soils of Alluvial Deposits" with a small area of "Brown soils on Dolerite". An intensive survey (field scale 1: 3,000) in the summer of 1980 - 81 by Dr. J.A. Beattie (pers. comm.) assisted by several final year agricultural science students, allowed preparation of a provisional soil map and reference (Figure 2b). This shows that most of the area is occupied by strongly to very strongly duplex soils. Other soils include uniform to gradational black cracking clays, weakly duplex to gradational loams, sandy clay, loams and clay loams over medium clay, and deep uniform sands on elevated sites.

More recently, Holz (1994) has shown that a large part of the area is a pediment toeslope and alluvial toeslope mantled by debris flow deposits, sourced in the catchments of Belbin and Pigeonhole Creeks, in which the series A and B soils have formed while large areas of E series soils have formed either within Tertiary sediments *in situ* or within colluvial and/or aeolian materials derived chiefly from Tertiary sediments.

IV. MATERIALS AND METHODS

4.1. Location, description and collection of soil specimens.

Investigations were carried out on five soil profiles including a black cracking clay (UF1), (Stace *et al*, 1968), and duplex soils (UF2, UF3, UF4 and UF5), (Northcote *et al*, 1975) located in the area of "Davis" and "Wattle" paddocks at the University farm, Richmond, (Figure. 2a).

Soil profiles were exposed in pits and described generally in accordance with the protocol of McDonald *et al* (1990). Data recorded included depth of horizons, soil colour, field texture, soil structure, voids, soil water status, consistency, stickiness, type of plasticity, degree of plasticity, segregations of pedogenic origin, roots, slickensides, and boundaries between horizons. Soil colour was recorded as described by Munsell colour (1994).

4.2. Physical, chemical and mineralogical analysis

Air-dried samples of fine earth (< 2 mm) were used for laboratory analysis. Physical characteristics measured in this study included particle size distribution by the hydrometer method and bulk density using the clod method (Loveday, 1974a). Chemical characteristics measured included soil reaction (pH 1:5, water and 0.01M $CaCl_2$), electrical conductivity (EC 1:5 water), organic carbon by Walkley-Black method (Rayment and Higginson, 1992), cation exchange capacity and exchangeable cations by ammonium chloride extraction (Rayment and Higginson, 1992), and exchangeable Al^{3+} and H^+ by 1 M KCl extraction and titration (McLean, 1965). Exchangeable Na^+ and K^+ in the NH_4Cl extract were determined by means of an Eel flame photometer. Exchangeable Ca^{2+} and Mg^{2+} were measured using a 902 GBC double beam atomic absorption spectrophotometer. Cation exchange capacity was determined by the sum of exchangeable Na^+, K^+, Ca^{2+}, Mg^{2+}, Al^{3+} and H^+, see Appendix 1.

Clay mineralogy was determined semi-quantitatively by X-ray diffraction. A clay -rich solution was treated with 30% H_2O_2 to remove organic matter and iron and aluminium oxides were removed by dithionite-citrate extraction (Mehra and Jackson, 1958). The clay suspension was then split in two with one portion saturated with 1M $CaCl_2$ and the other with 1M KCl. Two glass slides were then smeared with calcium-saturated clay and a further two slides with potassium-saturated clay. Two glass slides, one smeared with calcium and the other with potassium-saturated clay were air dried. A slide of potassium saturated clay was heated in the furnace for two hours at a temperature of 500-550 ^{o}C. The other slide of calcium-saturated clay was solvated with glycerol in a closed weighing box in the oven for at least an hour at 70 ^{o}C. The clay minerals were identified by the various basal spacings measured in Angstrom units on traces after running on a Phillips X-ray diffraction apparatus at the Department of Resources and Energy, Rosny, Tasmania. Semi-quantitative analysis was estimated by measuring the width in degrees 2 θ at half peak height of each peak on trace and then calibrating with data from mixtures of samples of known composition (Woolley, personal communication, Department of Resources and Energy of Tasmania).

The sand fraction was separated by sieving between 0.50 and 0.037 mm (all sand passed the 0.5 mm sieve). The sand fraction retained on the 0.125 mm sieve was further separated using bromoform with a specific gravity of 2.84 g/cc to produce "light" and "heavy "mineral fractions.

To obtain magnetic and non-magnetic minerals, the "heavy minerals" were separated by means of magnetic separation. Finally the minerals were identified and counted on glass slides using a Leitz ortholux petrographic microscope.

To determine quartz, plagioclase and K feldspar, the "light mineral" grains were mounted on a glass slide, stained with sodium cobaltinitrate and malachite green after treatment with hydrogen fluoride and counted using the petrographic microscope: yellow colours indicate K-feldspar, green for plagioclase and a clear colour for quartz (Graham, 1955; Bailey and Stevens, 1960).

4.3. Micromorphological analysis.

Undisturbed soil samples were collected from each soil pit in tin boxes (20 x 10 x 8 cm). Prior to impregnation soil water was removed by oven drying at 60^{0}C. The samples were then impregnated with CR64 polyester resin. The impregnated samples were cut to small blocks by diamond saw and polished by grinding with aluminium oxide and kerosene. The samples then were bonded to glass slides with UV glue. Finally the samples were ground and polished before they were covered with a plastic coverslip. Further details can be found in Murphy (1986). Scanning electron microprobe analysis was used to confirm and quantify identification of iron, manganese and silicon glaebules and tubules. Thin sections were examined under petrographical microscope to describe micromorphological features according to Brewer (1964) and Brewer and Sleeman (1988).

V. RESULTS AND DISCUSSION

5.1. Black cracking clay soil (UF1)

5.1.1. Field-observed soil morphology

Profile UF1 is described below (plate 1). The description includes soil colour, field texture, structure, moist soil strength, stickiness, type of plasticity, degree of plasticity, root distribution and horizon boundaries.

The profile to 74 cm depth is a medium clay, very dark coloured to 30 cm depth below which the colour changes gradually to brownish hues and then to light olive brown. Dark mottles and crack fillings in lower materials represent addition of surface material and dark clay was traced down cracks and channels to at least 74 cm depth. Cracking observed is due to shrinking of the clay on drying. Vertic character is further evidenced by the presence of stress cutans to 74 cm depth.

A light-coloured, porous, crumbly, granular material was observed below 74 cm, continuing to 150 cm depth. The field texture was sandy clay loam. There was little change in this material below the gradual irregular upper boundary to the cracking clay upper profile. The lower boundary was abrupt and wavy to olive grey heavy clay at 150 cm depth. However, secondary carbonate in the form of isolated, vertically orientated crack or channel fillings was observed in small amount below 140 cm depth and transgressing the boundary at 150 cm depth.

The basal clay was very strongly cutanic, parting to fine, lenticular primary structural units.

Depth (cm)	Description (UF1)
0 - 5	Black (10 YR 2/1 moist); medium clay; moderate fine (2-5 mm) granular structure; moderate moist strength; moderately sticky; moderately plastic, normal plastic; abundant fine roots; many cracks; self mulching; gradual irregular boundary,
5 - 18	Black (10 YR 2/1 moist); medium clay; moderate medium (5-10 mm) prismatic and angular blocky structure; moderately firm moist strength; moderately sticky; moderately plastic, normal plastic; abundant fine roots; many cracks; gradual irregular boundary,
18 - 30	Black (10 YR 2/1 moist); medium clay; moderate medium (5-10 mm) angular blocky and prismatic structure; moderately firm moist strength; moderately sticky; moderately plastic normal plastic; common fine roots; many cracks; stress cutans; gradual irregular boundary,
30 - 55	Brown (10 YR 4/3 moist); common medium distinct brown (10 YR 4/4) and common medium distinct brownish black (10 YR 3/2) mottles; medium clay; moderate coarse (10-20 mm) angular blocky structure; moderately firm moist strength; moderately sticky; moderately plastic, normal plastic; few fine roots; many cracks; gradual irregular boundary,
55 - 74	Light olive brown (2.5 Y 5/6 moist); few medium distinct brownish black (10 YR 3/2) mottles, medium clay, moderate coarse (10-20 mm) angular blocky structure; moderately firm moist strength; moderately sticky; moderately plastic, normal plastic; few fine roots; gradual irregular boundary,
74 - 150	Pale yellow (5 Y 7/4 moist); few medium distinct brownish black (10 YR 3/2) and few medium distinct olive black (5 Y 3/2) mottles; fine sandy clay loam; moderate medium (2 - 5 mm) granular structure; moderately weak moist strength; slightly sticky; slightly plastic, normal plastic; very few to few, fine to coarse crack fillings of soft secondary carbonate below 140 cm depth; abrupt wavy boundary,
150 - 175	Greyish olive (5 Y 5/3 moist); heavy clay; moderate coarse (10-20 mm) parting easily to fine and very fine lenticular structure; very firm moist strength; moderately sticky; very plastic, normal plastic; carbonate as above; stress cutans; few medium iron oxide soft segregations.

Plate 1. Profile UF1

5.1.2. Physical characteristics

Detailed physical data are given in Appendix 1 (Table 22).

Figure 3 shows the variation in coarse sand, fine sand, silt and clay with depth. There are two marked discontinuities in the depth functions of clay and fine sand near 74 and 150 cm depth and these show complementary trends. After increasing from 65 % to 81% in the upper profile clay decreases sharply to 32.5% near 74 cm and increases again from 37% to 76% near 150 cm depth. Fine sand increases from 7.6% to 38% and decreases from 29.1% to 8.3 % at the same depths and then to 7.7% near 160 cm depth. The depth functions of silt and coarse sand have broadly similar form and also show discontinuities near 74 and 150 cm depth. Further, the coarse sand / fine sand ratio varies between 0.5 and 1.1 in the upper profile (to 74 cm depth), falls sharply to between 0.2 and 0.4 between 74 and 150 cm depth and remains at 0.4 in the first 20 cm depth of the olive clay substrate.

Figure 4 shows the relationship between bulk density (clod method, Loveday 1974) and % clay with depth. There is a broad tendency for bulk density and % clay to have similar trends down the profile. Bulk density is relatively high to a depth of 74 cm. The immediate surface material, which is self-mulching, has a bulk density of 1.41 g/cm^3. Bulk density increases sharply to 1.55 g/cm^3 at 5 cm depth. The relatively high bulk density in the upper profile to 74 cm depth is associated with organisation of this material in compact and dense peds.

Bulk density then falls sharply in the crumbly layer, between 74 cm and 150 cm depth, ranging from 1.25 to 0.93 g/cm^3. This is in harmony with the vesicular and porous nature of this light crumbly material. Bulk density again increases sharply in the olive heavy clay (1.31 and 1.49 g/cm^3) This increase in density is again associated with a much higher clay content and much denser packing of this material.

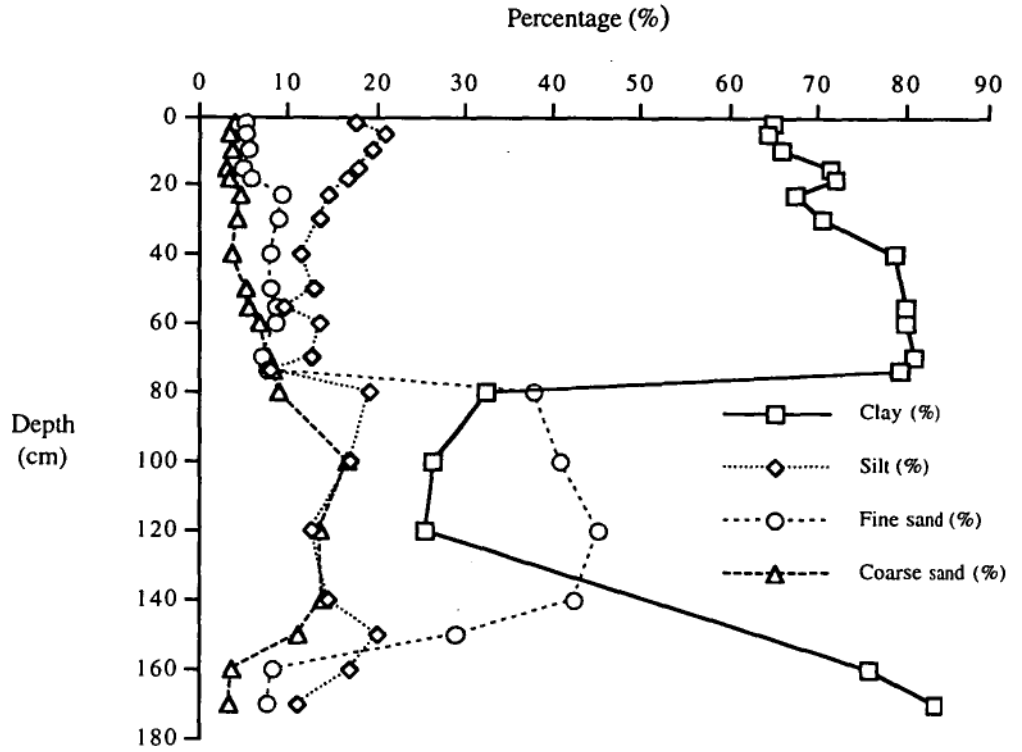

Figure 3. Depth functions of clay, silt, fine sand and coarse sand, UF1

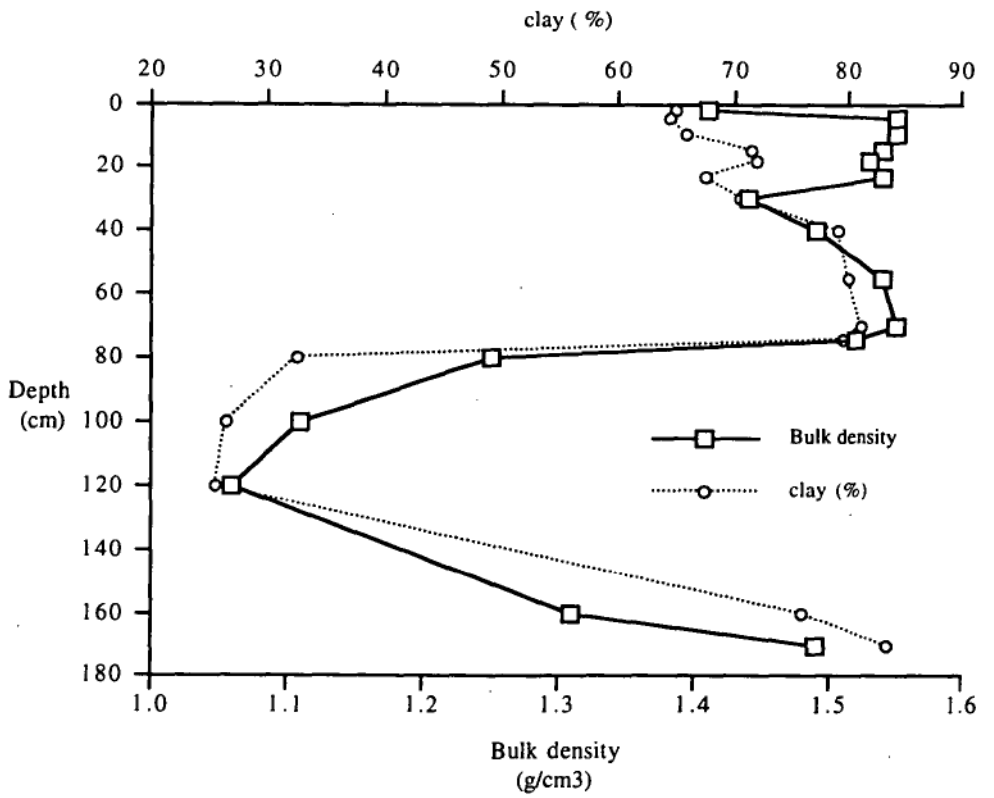

Figure 4. Depth functions of clay content and bulk density, UF1

5.1.3. Chemical characteristics

Detailed chemical data are given in Appendix 1 (Table 22).

Soil reaction (pH 1: 5 H_2O) is in the neutral range (Northcote, 1979) in the upper 40 cm of the profile (Figure 5), ranging from 6.5 to 7.0, but increases between 40 and 74 cm from 7.0 to 8.7 and the soil remains strongly alkaline (pH >8.5) to the maximum depth sampled (170 cm). The sharp increase in pH is associated with increased exchangeable sodium, exchangeable sodium percentages approaching 30 from 80 cm to 150 cm depth (Figure 6). Exchangeable magnesium is also much higher from 80 cm to 150 cm depth.

The upper profile is non saline and the lower profile is slightly saline (Doyle, 1993). The electrical conductivity ranges from 0.14 to 0.25 dS/m in the upper 40 cm of the profile (Figure 5). Below 50 cm it is fairly constant at 0.46 - 0.59 dS/m. This is probably due to the greater amount of water movement through the vertically orientated planar voids of the upper profile resulting in some leaching and consequent accumulation lower in the profile.

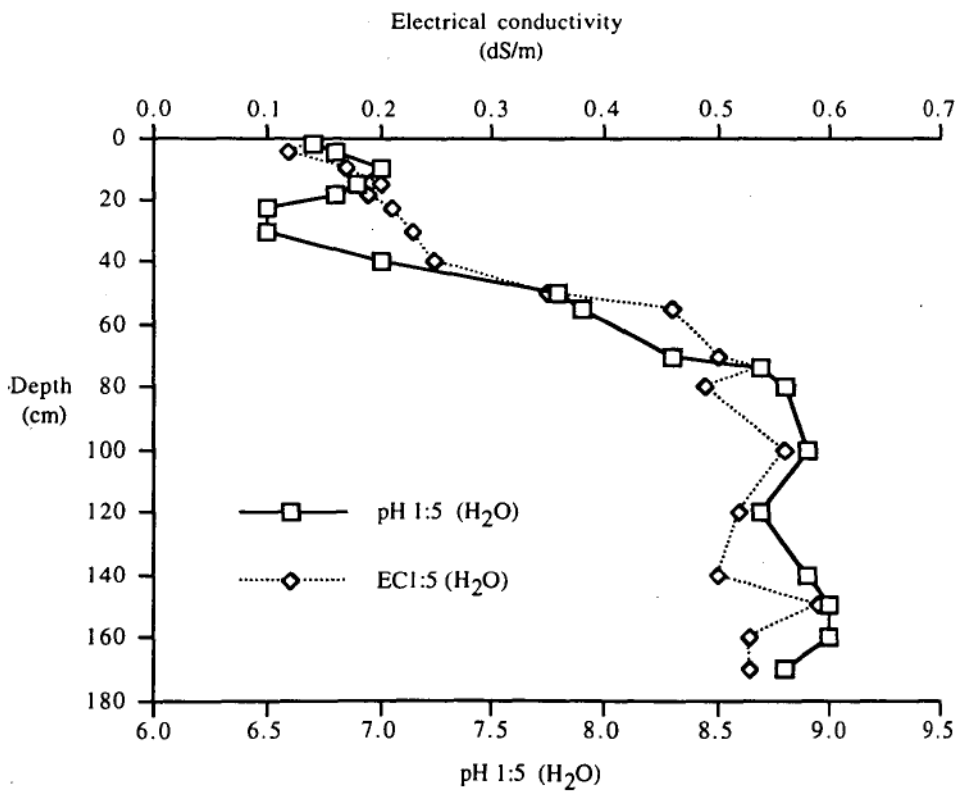

Figure 5. Depth functions of pH (1:5 H_2O) and electrical conductivity (EC 1:5 H_2O), UF1

Figure 6 shows the depth functions of exchangeable cations (Ca^{2+}, Mg^{2+}, Na^{+}). The general trend shows exchangeable Mg^{2+} and Na^{+} increasing to a depth of 74 cm, while Ca^{2+} decreases. The lower profile, below 74 cm, is dominated by exchangeable Mg^{2+} and Na^{+}.

Exchangeable Na^{+} increases steadily from 2.7 to 8.3 cmol(+)/kg with depth to 74 cm below which it increases sharply to 13.6 cmol(+)/kg and a maximum of 14 cmol(+)/kg at 140 cm depth in the crumbly layer before falling back to 11 and 10 cmol(+)/kg in the olive clay. The high exchangeable Na levels result in ESP values above 10 in the upper 40 cm and 20 or more below.

Exchangeable Mg^{2+} is present in higher amounts than exchangeable Ca^{2+} and Na^{+} throughout the profile. Exchangeable magnesium shows a general trend to increase with depth but rises sharply below 74 cm depth. Magnesium, along with sodium, has been implicated in poor soil physical conditions, namely toughness when dry to moist and dispersivity when wet (Rengasamy and Olsson, 1991).

Exchangeable Ca^{2+} decreases significantly from the surface to 74 cm depth (from 9.7 to 6.7 cmol(+)/kg) then dramatically increases in the light crumbly layer to from 10.2 to 12.3 cmol(+)/kg. In the olive clay calcium again decreases to 8.9 cmol(+)/kg.

Exchangeable K^{+} is high at the surface (1.81 cmol(+)/kg) in conformity with other black cracking clays (Stace *et al*, 1968) then decreases with depth to 0.04 cmol(+)/kg (Table 22, Appendix 1).

The cation exchange capacity (CEC) decreases very slightly in the upper 30 cm despite the gradual increase in clay content, probably reflecting the decreasing level of organic matter (Figure 7) Between 30 cm and 74 cm the CEC is relatively stable as is the clay content and clay mineralogy (Table 7). Below 74 cm there is a dramatic increase in CEC.

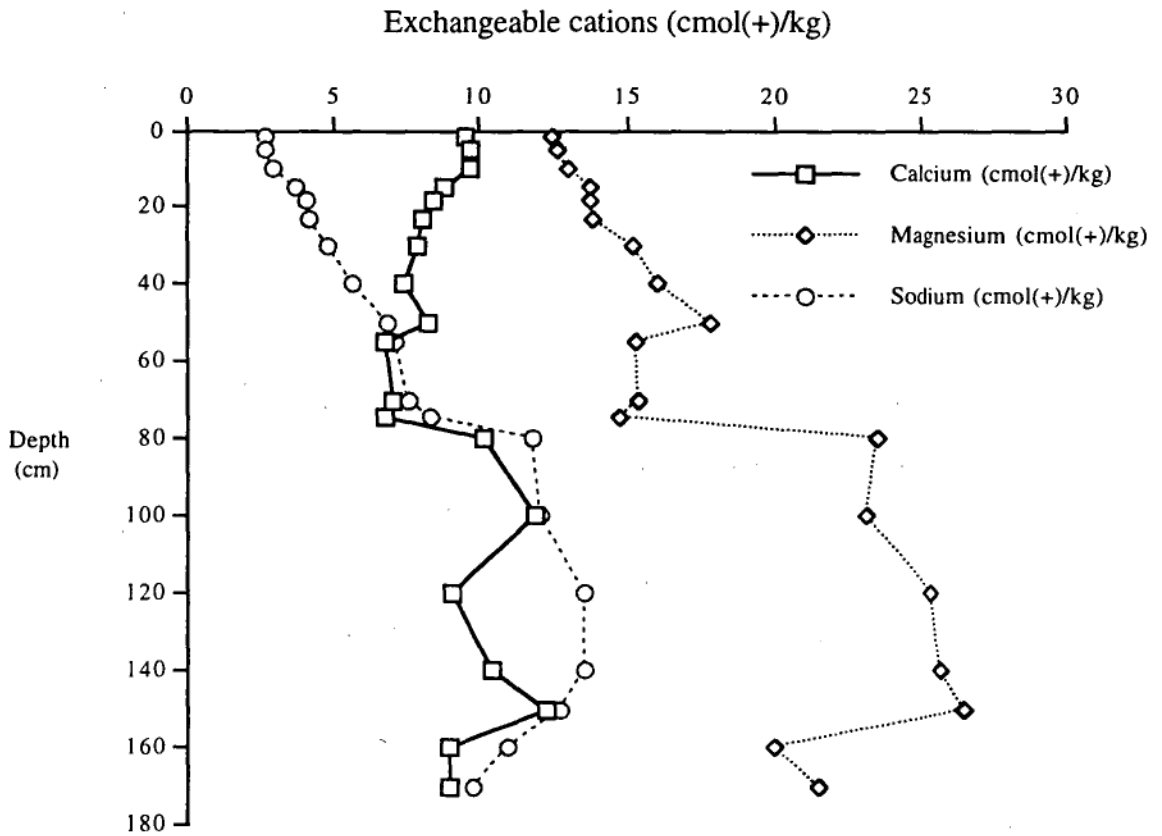

Figure 6. Depth functions of exchangeable Ca, Mg and Na, UF1

Figure 7 shows the relationship between clay content and CEC with depth. In the upper 20 cm the clay content increases from 65 to 72% while the organic carbon content decreases from 3.2% to 2%. As a consequence the CEC remains relatively stable. Below 20 cm, to about 50 cm, both clay content and CEC increase slightly. From 50 cm to about 74 cm both remain static at 79 - 81%. Below 74 cm there is a dramatic decrease in clay content (25.5 - 27%) and a dramatic increase in CEC (42 - 52 cmol(+)/kg). This can only be explained by a change in the nature of the exchange complex. In the upper profile there is a mixture of kaolinite and smectite while in the zone between 74-150 cm smectite is dominant (Table 7). It is also suspected that allophane may be present in the light crumbly layer (74 - 150 cm depth) as the material returned a positive NaF field test although this is not conclusive. The presence of moderate amounts of kaolinite suggests a greater degree of

weathering in the upper horizons. In the olive clay layer, below 150 cm, the clay content is again very high (80%) while the CEC is somewhat lower, perhaps partly due to the absence of allophane (negative NaF field test).

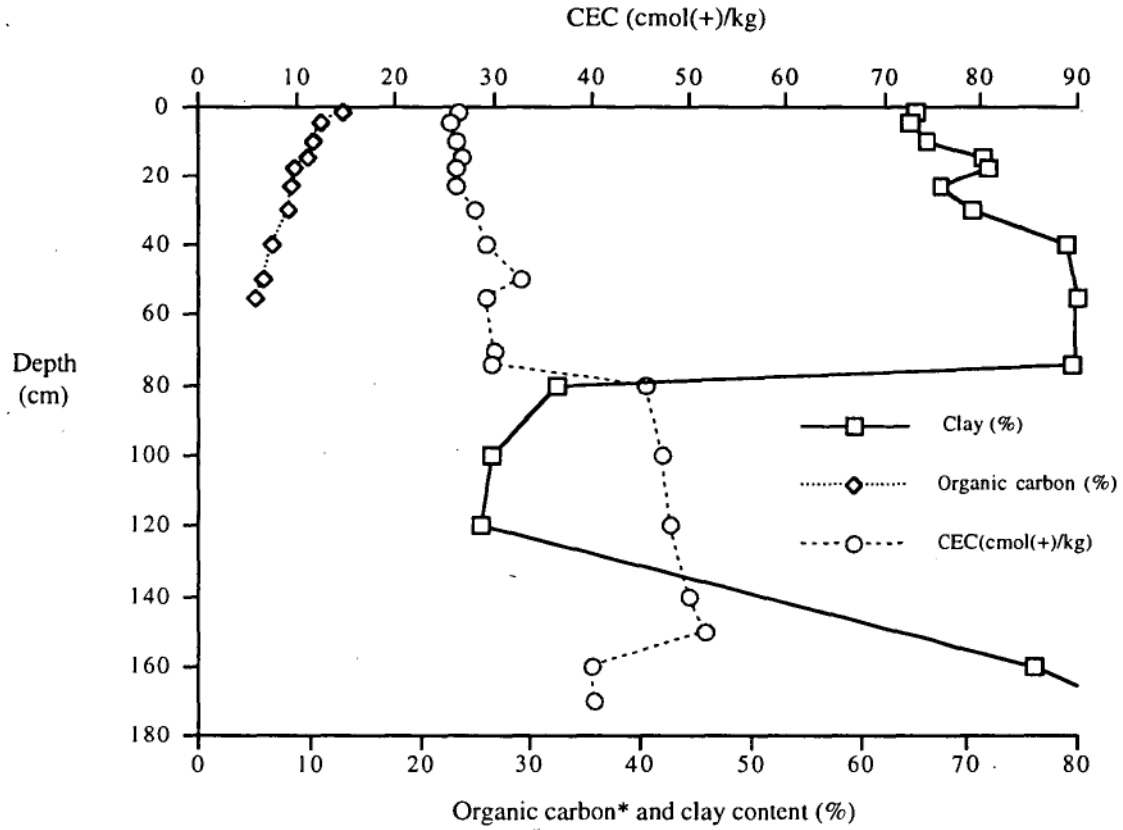

Figure 7. Depth functions of CEC, organic carbon and clay content, UF1
*organic carbon data are x 4

CEC was determined by summation of exchangeable cations so that the presence of free secondary calcium carbonate, which may contain some magnesium , is very likely to result in overestimation of exchangeable calcium and, to a lesser degree, magnesium. Maxima of both calcium and magnesium were measured in the 140 -150 cm depth sample. The calcium maximum was more strongly marked both absolutely and relatively. However, discounting the summation of exchangeable cations for these increases in calcium and magnesium still leaves a high CEC in excess of 48 cmol (+) kg^{-1} for the whole material and some 132 cmol (+) kg^{-1} on a clay basis. Of this total exchangeable sodium contributes about 34 cmol (+) kg^{-1} (ie, an ESP of 26), exchangeable calcium 28 cmol (+) kg^{-1} and exchangeable magnesium 70 cmol (+) kg^{-1} . A CEC in excess of 120 cmol (+) kg^{-1} is indicative of an exchanger with a much higher capacity than any smectite. Vermiculite

may reach 150 cmol (+) kg^{-1} but was not detected in this material. The presence is indicated of a component or components of very high CEC in the mineralogy of the exchange complex of the material from 74 to 150 cm depth.

The granular material has been identified as a basalt glass (Dr. Jocelyn McPhie, personal communication, see also section 5.1.7. below). Basalt glass, particularly in a sandy or granular form, rapidly undergoes hydration accompanied by significant changes in cations (especially alkalis and alkaline earths) with only slight weathering. These cations are exchangeable. Also, a few zeolite grains were seen in the 200 - 177 μM sand fraction. The presence of zeolites in a slightly weathered basalt glass is normal and would add further to the cation exchange capacity. Finally, as earlier stated, the material gave a positive NaF field test. Although considered unreliable in itself the test may well be indicative in this case of allophane in the clay fraction. Thus the high CEC may be explained by contributions from hydrated basalt glass particles, zeolites and possibly allophane over and above that due to smectite (section 5.1.4).

5.1.4. X-ray diffraction analysis of clay fractions

Smectite and kaolinite are in similar proportions in the upper profile while smectite is dominant in the lower layers (Table 7). The presence of smectite in the profile can be associated with the strong shrinking and swelling behaviour of the soil with change in moisture content. The decrease in kaolinite with depth may be an indication of greater intensity of clay mineral weathering near the soil surface. Smectite was dominant in the granular material below 74 cm depth and in the basal Tertiary clay (150 - 160 cm depth).

Table 7. Semi quantitative X-ray diffraction analysis, (UF1)
l - little(11-25%) ; md - moderate(26-50%); m - much(>50%)

Depth (cm)	Smectite	Kaolinite
30 - 40	md	md
50 - 55	md	md
70 - 74	m	l
120-140	m	l
140-150	m	l
>160	m	l

5.1.5. Micromorphology

Micromorphological features of the profile have been identified from a number of thin sections using the petrographic microscope and the composition of several pedological features (including relict features) has been determined by electron microprobe analysis (Plates 6 to 18). Detailed analytical data are given in Appendix 2, Tables 27 to 33.

Plate 6 shows the micromorphological features of the soil at 20 cm depth in thin section. The features marked (A) have been shown to be quartz by microprobe analysis (89% SiO_2), while features marked (B) appear to be clay nodules coated with iron oxide (13.6% FeO). Features marked (C) show iron oxide accumulation (58% FeO) and are interpreted as iron oxide glaebules. The quartz grains are moderately well rounded and may reflect input via a surficial aeolian or colluvial process. They may have been derived originally from Triassic sandstone or more recent sandy beach deposits of Pitt Water.

In plate 7 the features marked (A) are silica bodies (96.5 % SiO_2) which may be seen to be almost perfectly circular in cross-section in most cases. Some of these bodies appear to be solid or to have only a small central void while most are empty within an orientated chalcedonic rim whose extinction behaviour simulates a uniaxial interference figure (i.e, pseudouniaxial). This effect is visible in plate 9 and 11 and especially in plate 14.

Plate 8 shows the fabric of discrete granular bodies making up the crumbly material. The fabric is aporic and more specifically: quartzic ferraric fragmoidic porphyric (Brewer and Sleeman, 1988).

Plate 9 hows the micromorphological features of the soil at 40 cm depth in thin section. The feature marked (A) shows the silica bodies, circular in cross-section.

Plate 10 from 40 cm depth indicates a channelled and fissured structure, more specifically: intergrade quartzic ferraric fragmoidic porphyric (Brewer and Sleeman, 1988).

Plate 11 shows the micromorphological features of the lower density crumbly material at 90 cm depth. Features marked A are circular bodies of silica (SiO_2 95%) with a central void. In some cases the siliceous rim has been fractured and displaced slightly emphasising its eggshell-like form. Whole, more solid, individuals have been examined in

the light fraction of sand grades (passing 200 μM and retained on 177 μM mesh) isolated by disaggregation of the enclosing material. They were seen to be spherical or elliptical in form, in harmony with their circular cross section. The features marked B are iron oxide-cemented glaebules (FeO 17.7%) while features marked (C) are dark- coloured bodies (round in thin section) that contain titanium (TiO_2 1.9%).

A sequence of plates shows some details of the features of the light crumbly layer (90 cm depth). Plate 12 shows an electron micrograph of a chalcedonic feature while Plate 13 shows the distribution of silica, iron and titanium in this feature. Plate 14 shows the micromorphological features of a thin section at 90 cm depth. The features marked (A) are chalcedony (SiO_2, 95.1%) and the features marked (B) appear to be iron oxide glaebules (FeO 17.7%). The fabric is aporic; more specifically ferraric chalcedic porphyric (Brewer and Sleeman, 1988).

Plate 15 shows the micromorphological features of a thin section at 90 cm depth. The features marked (A) show strongly orientated clay minerals (argillans) coating matrix material in the crumbly layer. Electron microprobe analysis data for the clay coatings indicate high Al levels (Al_2O_3 22.1%). As the clay coatings are orientated in relation to cracks and other voids it is likely that they indicate translocation of fine colloidal clay suspensions. The development of voids and particularly cracks is assisted by the shrinking of the smectitic clays on drying. The features marked (B) have been identified as feldspar grains (K_2O 1.1%, Al_2O_3 15.2% and SiO_2 49.8%).

Plate 16 shows the micromorphological features of a thin section at 150 cm depth. The features marked (A) are iron oxide accumulations (FeO 13.3%). Features marked (B) are probably feldspar grains as they are high in potassium, silica and aluminium and have the cleavage and interference colour of feldspars (K_2O 12.9%, Al_2O_3 18.2% and SiO_2 56%).

Plate 17 is a photomicrograph of the olive clay material at 150 cm depth in thin section. The micromorphological description is fissured fabric, more specifically quartzic chlamydic porphyric (Brewer and Sleeman 1988).

5.1.6. Mineralogy of sand fraction

Table 8 shows that ilmenite, iron oxides and pyroxene occur in greater amount throughout the profile while zircon, rutile, leucoxene and carbonate are minor minerals. There is a tendency for slight decrease in zircon and rutile with depth. This may indicate a greater degree of weathering of the upper soil layers. Levels of leucoxene are low through the profile. The occurrence of ilmenite closely follows the separation of the three major horizons: moderate amounts to 74 cm, trace from 74 - 150 cm and moderate amounts again below 150 cm depth. Carbonate crystals were found only in the light, crumbly layer (74 - 150 cm) and in the upper 10 cm depth of the olive clay.

Table 9 shows that the diagnostic minerals, sideromelane and tachylite, were found in the 80 cm - 100 cm depth specimen representing the least-altered basalt glass. Quartz is common in all specimens except that from 80 cm - 100 cm depth. Calcic plagioclase is relatively common in amount to 74 cm depth in contrast to K-feldspar which is present in moderate amount only in the surface specimen.

The mineralogical data thus support the idea that the profile contains at least two, possibly three materials of distinctly different origin.

Table 8. Heavy mineral analysis of sand fraction (177 micron),UF1

Depth (cm)	(0-5)	(10 -15)	(23-30)	(60-70)	(80 -100)	(150-160)	(> 160)
Ilmenite	moderate	moderate	moderate	moderate	trace	trace	moderate
Leucoxene	trace	trace	trace	trace		trace	trace
Zircon	trace	trace	trace	trace	trace	trace	n.d
Rutile	trace	trace	trace	trace	trace	n.d	n.d
Carbonate	n.d	n.d	n.d	n.d	little	trace	n.d
Iron oxide	moderate	moderate	moderate	moderate	moderate	much	little
Pyroxene	moderate	little	little	little	moderate	little	much

n.d = not detected

Table 9. Light mineral analysis of sand fraction (177 micron),UF1

Depth (cm)	(0-5)	(10 -15)	(23-30)	(60-70)	(80 -100)	(150-160)	(> 160)
K-Feldspar	moderate	little	trace	little	n.d	n.d	trace
Plagioclase	little	moderate	moderate	little	n.d	little	trace
Quartz	much	much	much	much	trace	much	much
Sideromelan	n.d	n.d	n.d	n.d	moderate	n.d	n.d
Tachylite	n.d	n.d	n.d	n.d	moderate	n.d	n.d

n.d = not detected

5.1.7. Origin of materials and soil formation

The low density, granular material from 74 cm - 150 cm depth is of considerable interest. At first, the silica bodies were considered to be droplet structures indicative of a volcanic, pyroclastic airfall sediment (Dr. M.R. Banks, personal communication). Subsequently the material has been examined by Dr. Jocelyn McPhie, a specialist volcanologist now working in the Department of Geology, University of Tasmania. She has identified the granular material as a little-weathered basaltic glass. The silica (chalcedonic) bodies are amygdules, that is, vesicles, infilled by chalcedony deposited from siliceous fluids.

The chalcedony forms cutan-like linings of the vesicle walls and, less commonly, solid void fillings. The basaltic glass particles include both transparent sideromelane and inclusion-rich tachylite. Both indicate quenching of a basalt lava, the former usually indicative of water as the quenching agent. Tachylite occurs both in subaerially and subaqueously quenched lavas. Eruption of basalt into a swampy environment could produce the observed results. The material is also quite finely fragmented, relatively well sorted and only poorly vesicular, suggesting an explosive origin involving interaction of basalt lava with groundwater or surface water, i.e, phreatomagmatic. Sub-rounding of the basalt glass granules and inclusion of a small fraction of sub-rounded foreign mineral grains suggests some mixing and minor terrestrial transport. However the transport process must have involved very little abrasion to permit survival of the fragile glass particles and siliceous bodies. The orientation of the siliceous bodies suggests little or no disruption following their formation. This also suggests stability of the study site. Finally,

four volcanic vents have been located within a few kilometres of the study site (Figure 2c) within the Pitt Water tract of the Coal Valley graben (Leaman, 1972) and Banks identified others in the Derwent Valley many years ago (Banks, 1962).

The near-surface stratigraphy of the study site is shown in figure 7a and 7b along two transects at right angles, one generally north-south, the other generally east-west. It is notable that the granular basalt glass material is bevelled to non-existence on the north and south-facing sideslopes within a few tens of metres of the pit site (0 on the transect lines). To the west a shallow saddle separates the low knoll, on which the study site was located, from an ascending slope. Granular basalt glass was not found under the saddle nor under the surface of the ascending slope beyond it. However, increasing numbers of dolerite and sandstone clasts did appear on this slope. To the east the granular material was terminated at an infilled channel with basal lag concentrate of dominantly dolerite (5-10 cm) clasts from 55 cm depth. There is evidence that the granular basalt glass deposit occurs to the east of this channel as a subsurface strip on the broad, transversely almost flat, summit of the spur descending towards Pigeon Hole Rivulet (Figure: 2a). Detailed study of this aspect must await a future opportunity. To the north and south the levelling of the basaltic glass deposit has occurred by slope retreat with no evidence of a lag concentrate or stoneline. In this regard it would be anticipated that the basalt glass had a much wider occurrence initially and that the study site represents one of its, perhaps very few, relict occurrences. Its importance in relation to a detailed history of development of the terrain in which it occurs may therefore be considerable. Much of the surficial mantle of materials resting above Tertiary sediments within the area of the University of Tasmania Farm was transported from local catchments to the west as debris flow and alluvial fan sediments (Holz, 1994).

There is good evidence for the continuity of the basalt glass from 150 cm depth to the modern surface. Silica bodies have been identified in the material at 20 cm depth although the material at this depth is now quite strongly weathered on the whole. No rock fragments of Jurassic dolerite, Triassic sandstone or Permian mudstone were found in the 200 - 177 μM fraction and evidence of Jurassic dolerite and Triassic sandstone, at least, would be expected had much colluvial (erosional / depositional) mixing occurred. Very few larger

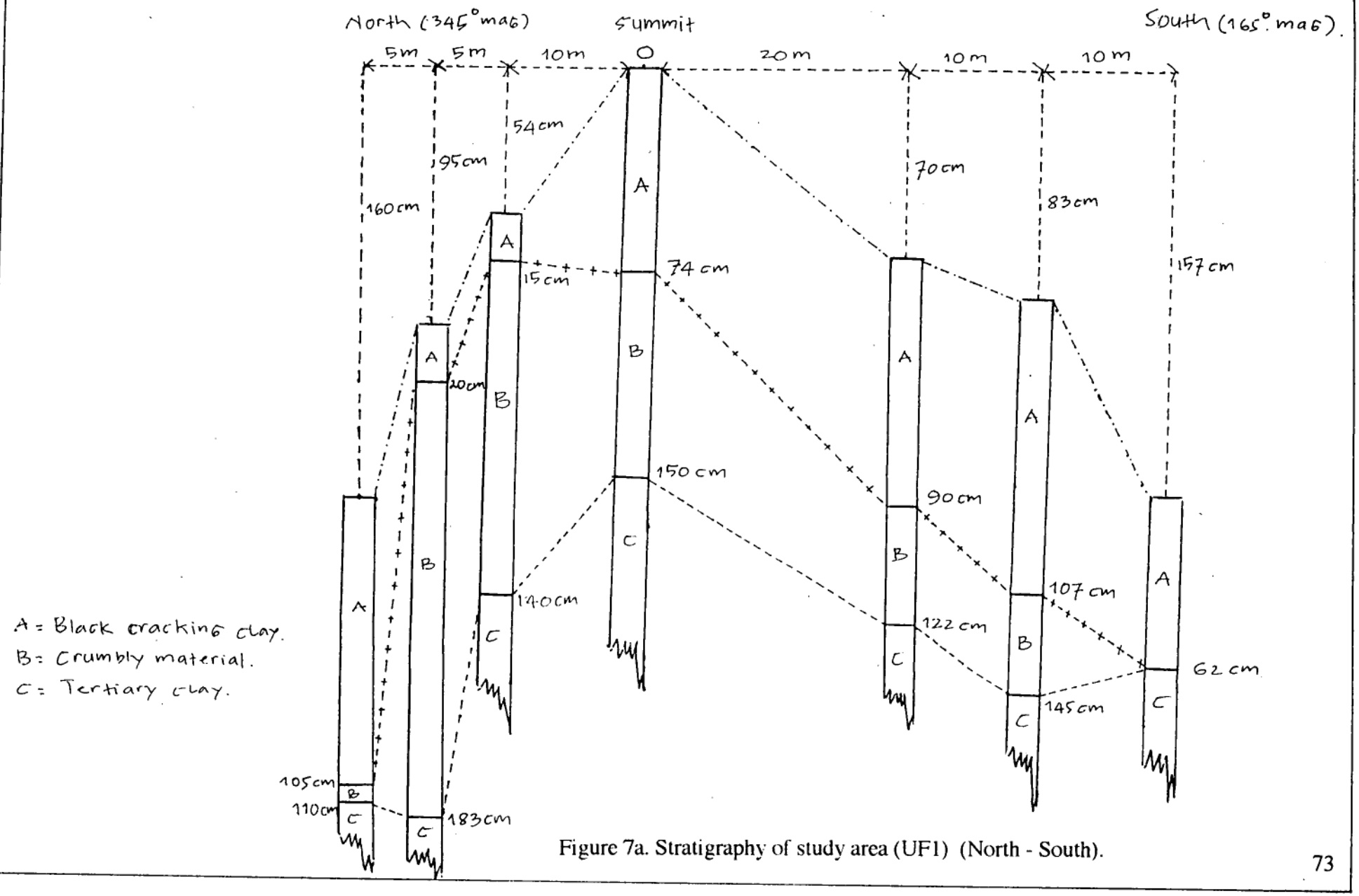

Figure 7a. Stratigraphy of study area (UF1) (North - South).

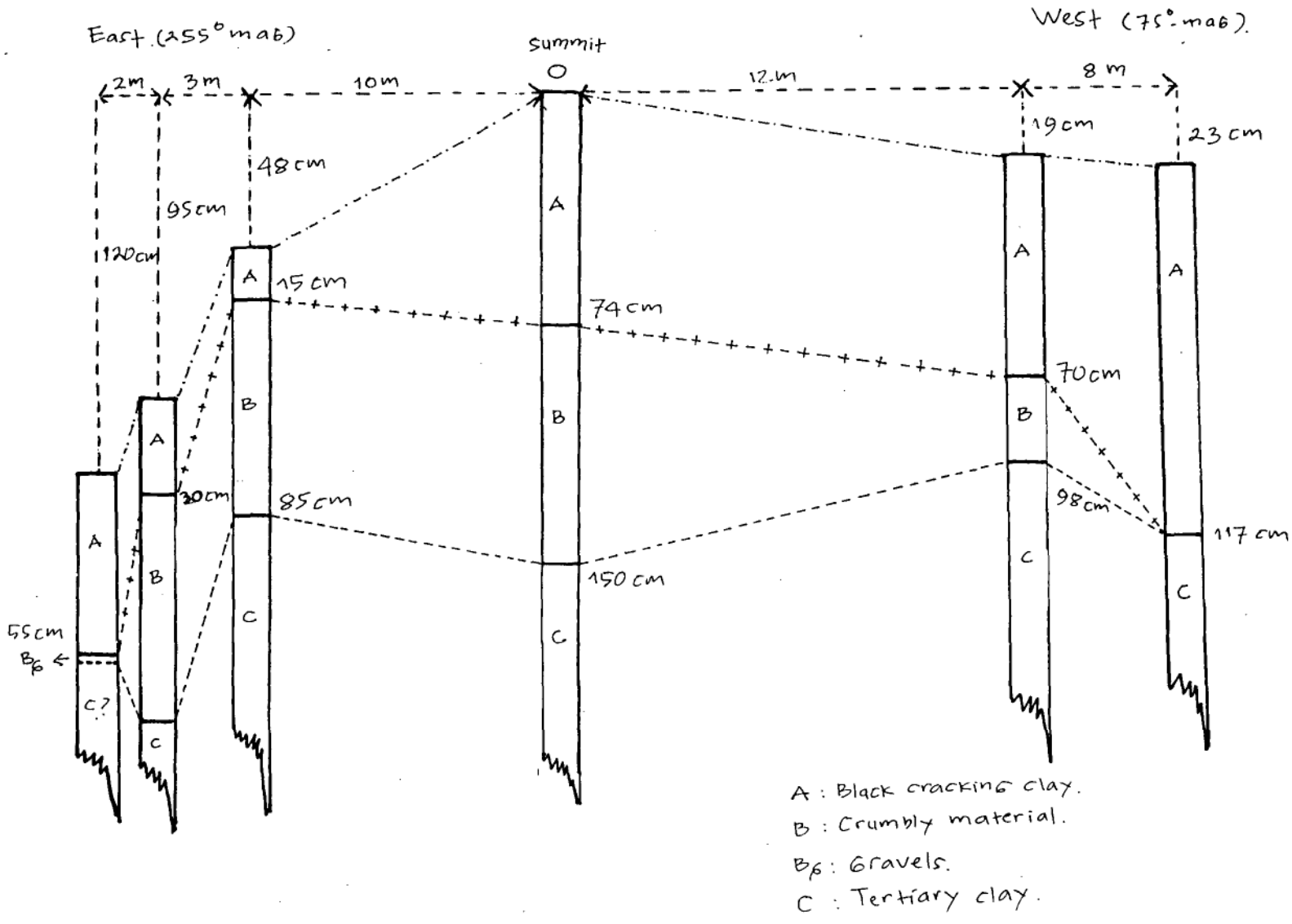

Figure 7b. Stratigraphy of study area (UF1) (East - West).

dolerite and sandstone clasts were seen on nearby summit to upper slope surfaces, i.e, within a radius of 20 metres. None were found in the pit walls or the material excavated in preparing the profile for study. The presence of the few nearby surficial clasts may therefore be due to accidental delivery by agricultural implements (cultivators, harrows).

Two kinds of materials of very different origin comprise the section exposed at the study site, viz., a basal Tertiary clay clearly predating an overlying, particulate basalt glass. The time frame of the disconformity is not known and must await the application of modern dating methods.

The basalt glass has been modified by soil forming processes as the "parent rock" of the modern black cracking clay soil. Its characteristics on deposition are most nearly approached by those of the material from 74 to 150cm depth.

Modification of the material above 150 cm depth by soil forming processes has been most marked to a depth of 74 cm. This is shown by colour, pedality, consistence (including bulk density and clay content) as well as depth functions of clay mineralogy, organic matter, exchangeable cations and cation exchange capacity.

It is a common feature of Australian soils particularly those of high clay content, that magnesium and sodium are increasingly dominant over calcium on the exchange complex with depth. This is a feature of the present profile which becomes both strongly magnesic and strongly sodic with depth. One source of these ions may have been as cyclic salt from the Southern Ocean. Another may have been a more alkalic rather than calcic character of the parent sediment. Leaching has been far from complete. The pH ranges from neutral in the surface few centimetres to strongly alkaline at depth and the exchange complex is virtually saturated throughout. Nevertheless, effects of leaching may be seen in the increases in exchangeable magnesium and sodium to 150 cm depth, with decreases in the basal clay explained by its very slow permeability other than via major planar voids (where secondary carbonate occurs). On the other hand, exchangeable calcium decreases to 74 cm depth, increases in the less-weathered material from 74 to 150 cm depth and decreases again in the basal clay.

While both smectite and kaolinite have been identified throughout the modern soil profile above 74 cm depth, the weathering effect is evident in increase of kaolinite and decrease of smectite above 74 cm depth. The markedly lower clay content below 74 cm may also indicate the lower limit of stronger weathering effects, and the persistence of material much closer in its properties to those of the original parent sediment.

Secondary carbonate deposits transgress the abrupt discontinuity at 150 cm depth. Their origin is considered to be via release of calcium by weathering of the basaltic glass deposit, its combination with carbon dioxide in the soil solution and translocation downwards to observed sites of accumulation.

The soil profile to 74 cm depth has been identified as a sodic, black cracking clay. Continuing pedogenetic changes in a dispersed, high-clay material of high bulk density and extremely slow permeability are likely to be slow. This may account for the relatively thin upper profile and slight pedogenic alteration of the substrate from 74 cm to 150 cm depth in view of the apparent long-term stability of the specific study site. The local landform is an isolated knoll, very gently domed, with radial dispersion of any rainfall-induced overland flow and protection from run-on. Thus the solum may be quite old although probably very much younger than the late Eocene to early Miocene age assigned to the Coal River Valley basalts, perhaps with implications for more recent volcanism.

5.1.8. Soil classification

According to a new classification system for Australian soils (Isbell, 1996) this profile may be classified as "Episodic-Endocalcareous, Self-mulching, Black Vertosol". This classification represents the key features of the overall profile well ie, its high clay content, swell-shrink behaviour, high ESP and the presence of secondary carbonate at depth. The US Soil Taxonomy (Soil Survey Staff, 1975) classification is "Sodic Haplustert". This classification emphasises the sodic nature of the soil, the ustic moisture regime, the high clay content and swell-shrink behaviour of the soil, but does not represent its self-mulching surface or the presence of secondary carbonate.

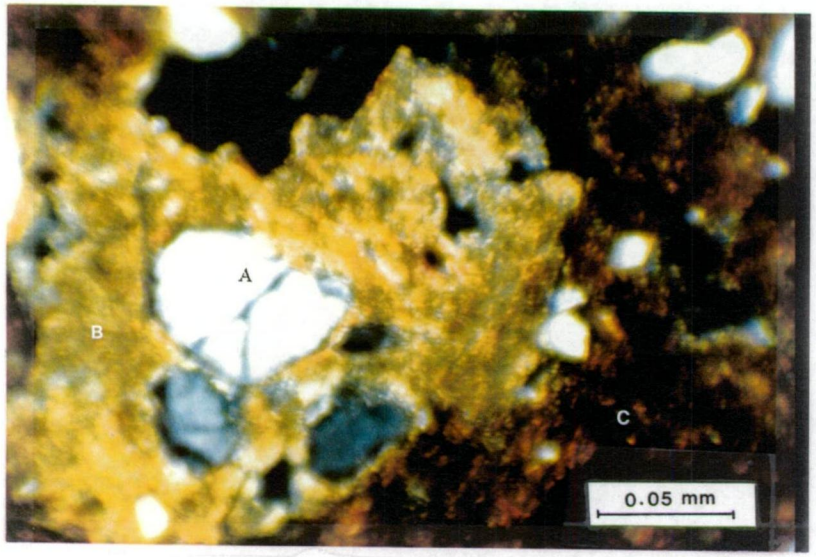

Plate 6. Fabric, UF1, 20 cm depth, (A). Quartz grain (SiO_2, 89%); (B). Clay micro-ped with iron oxide coating (FeO, 13.6%); (C). embedded, sharply separated sesquioxidic nodule (FeO, 58%). (X 50 crossed polarizers)

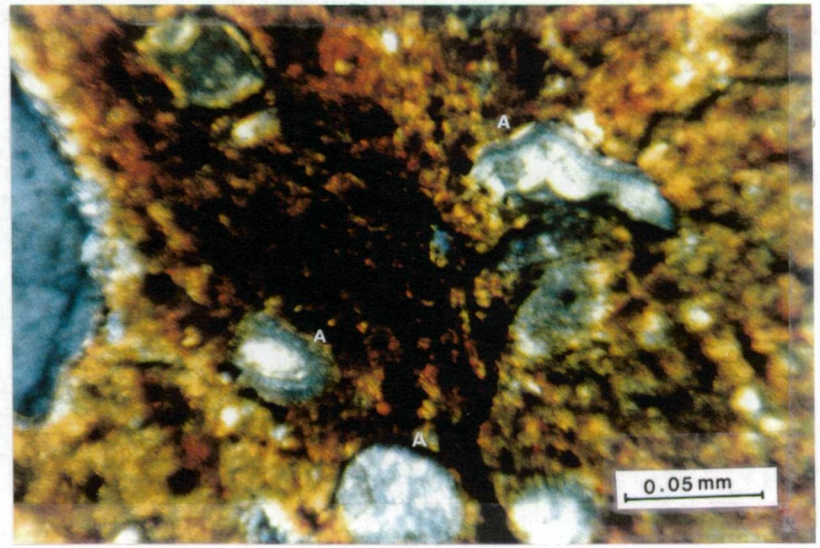

Plate 7. Fabric, UF1, 20 cm depth. (A) Silica bodies, circular in cross-section, identified as granular basalt glass structures (x 50 crossed polarizers).

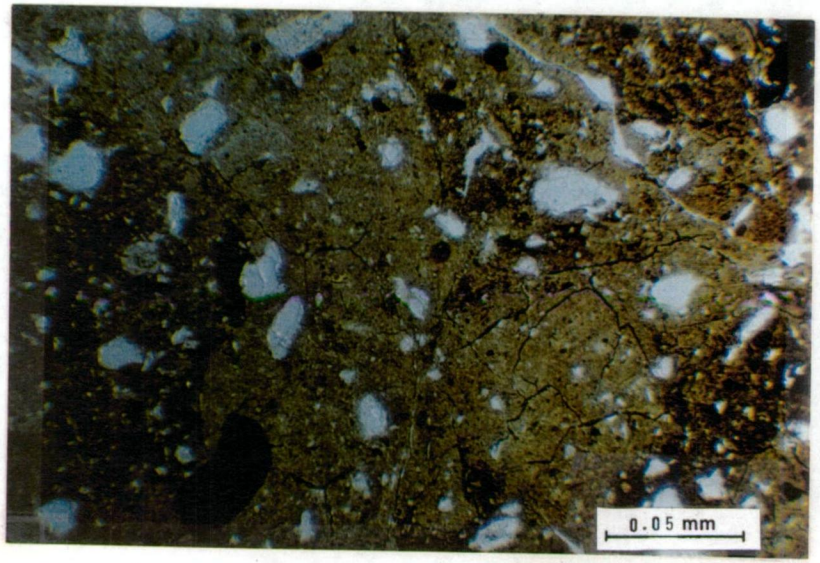

Plate 8. Thin section from UF1 at 20 cm depth.Aporic fabric; more particularly Quartzic Ferraric Fragmoidic Porphyric., (X 50 plain light)

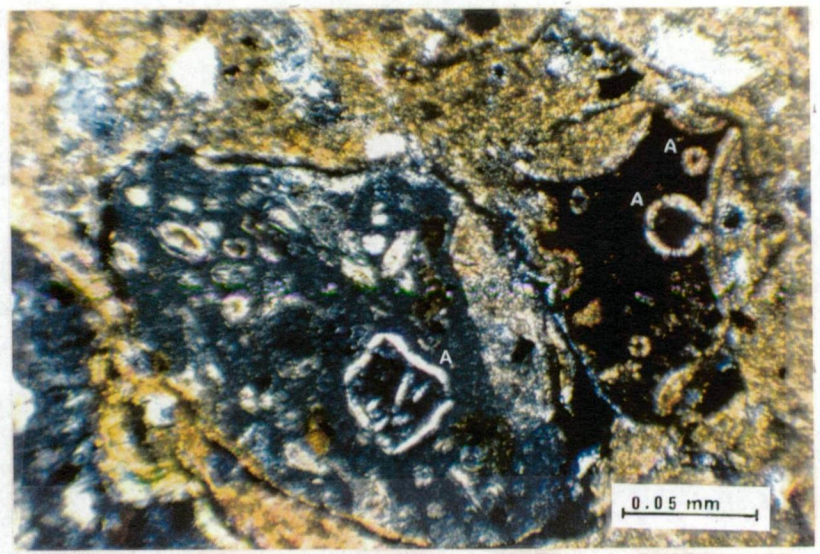

Plate 9. Fabric, UF1, 40 cm depth. (A) Silica bodies, circular in cross-section, identified as granular basalt glass structures (x 50 crossed polarizers).

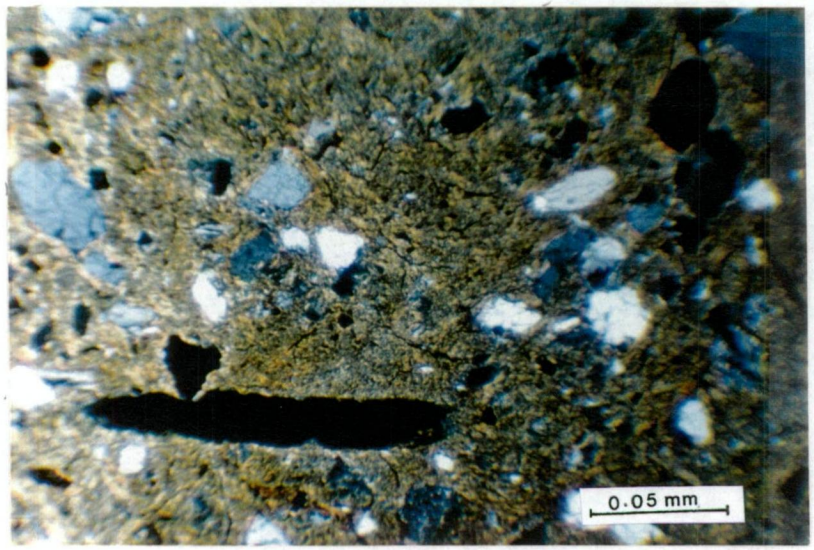

Plate 10.Fabric, UF1, 40 cm depth, Chanelled and fissured structure; more particularly : Intergrade Quartzic-Ferraric Fragmoidic Porphyric.(X 50 crossed polarizers)

Plate11. Hand specimen, UF1, 90 cm depth. (A) Silica bodies, circular in cross-section, identified as granular basalt glass structures (SiO_2, 95%), (B) Iron oxide nodules, orange (FeO, 17.7%), and (C) Titanum accumulation, black spots (TiO_2, 1.9%) (x 40).

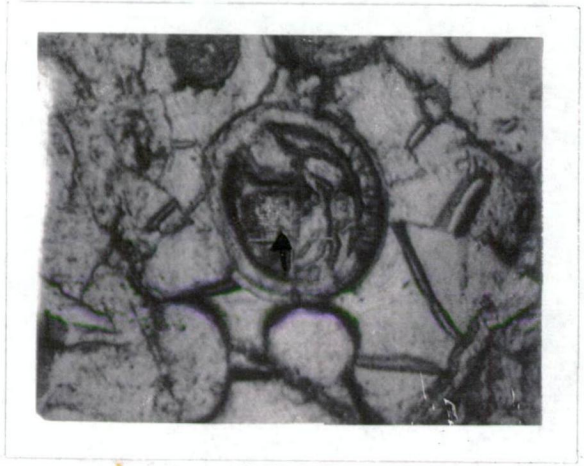

Plate 12.Fabric, UF1, 90 cm depth. Electron micrograph showing a chalcedonic feature indicated by the arrow (x 400).

Plate 13.Fabric, UF1, 90 cm depth. Electron micrograph showing the distribution of Si, Fe and Ti from plate 12 (x 1800).

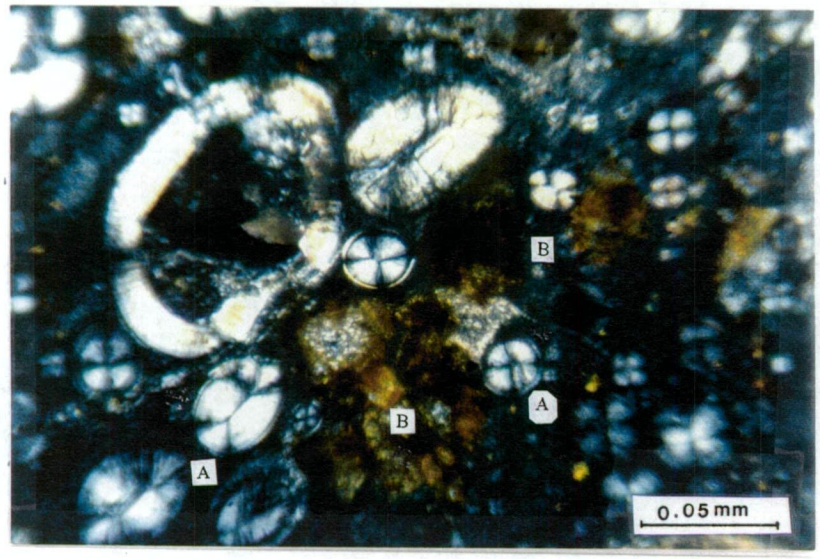

Plate 14.Fabric, UF1, 90 cm depth. (A) Chalcedony (SiO_2, 95.1%), (B) iron oxide glaebules (FeO, 17.7%). Aporic fabric; more particularly Ferraric Chalcedic Porphyric. (X 50, crossed polarizers)

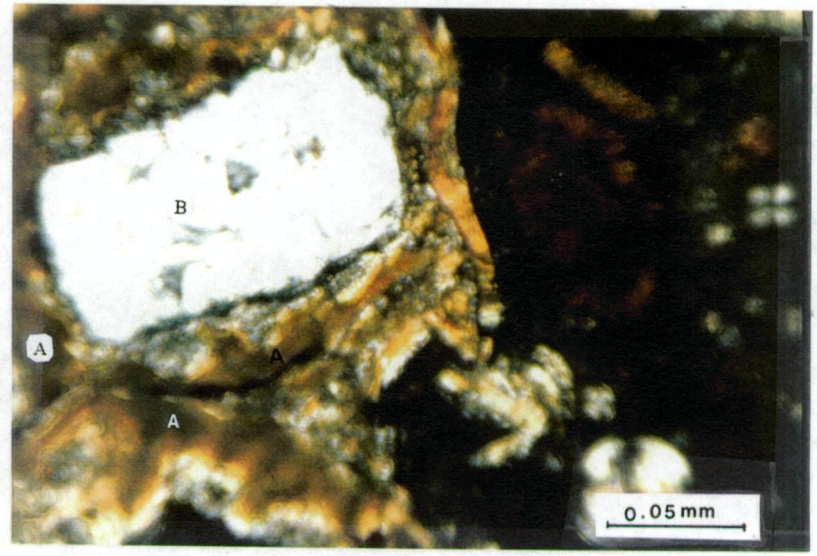

Plate 15.Fabric, UF1, 90 cm depth. (A) Coatings of orientated clays (Al_2O_3 18% and SiO_2 54%) (Argillans). (B) weathered feldspar grain (K_2O 1.1%, Al_2O_3 15.2% and SiO_2 49.8%). (X 50, crossed polarizers)

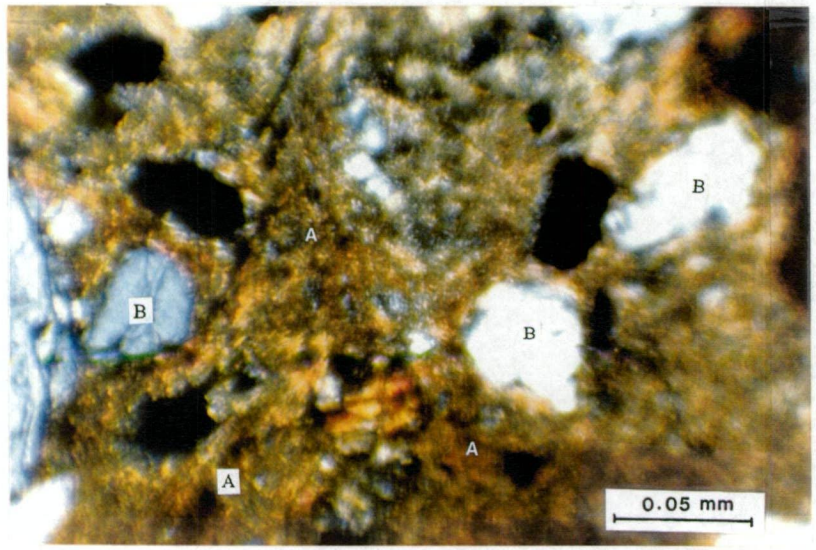

Plate 16.Fabric, UF1, 150 cm depth. (A) iron oxide glaebule(FeO 13.3%), (B) Feldspar grains (K_2O 12.9%, Al_2O_3 18.2% and SiO_2 56%). (X 50, crossed polarizers).

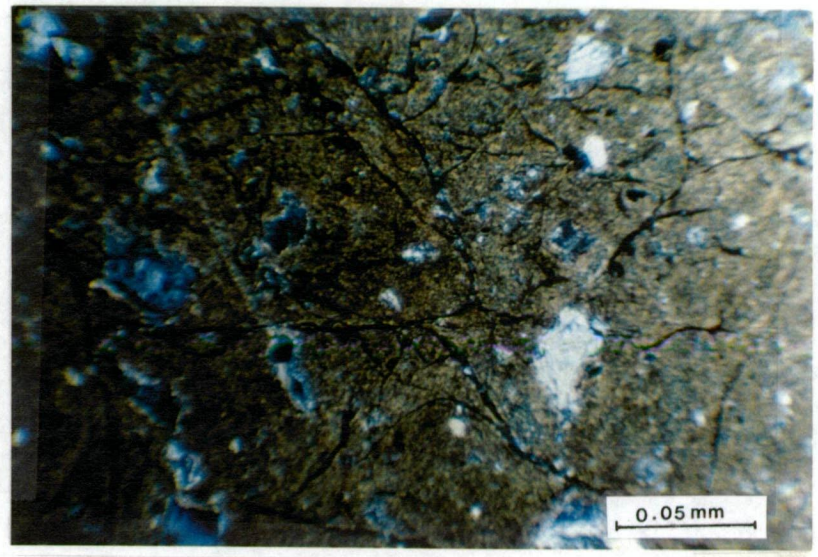

Plate 17.Fabric, UF1, 150 cm depth, .Fissured fabric; more particularly Quartzic Chlamydic Porphyric.(X 50 crossed polarizers).

5.2 Duplex soils (UF2, UF3, UF4, UF5)

The UF2, UF4 and UF5 profiles are strongly duplex and are representative of the soils of this upper slope study area of the University Farm, below the Cambridge - Richmond Road north of Pigeon hole Rivulet (Figure 2). They have a number of common features as well as some others that differentiate them one from another (see below).

While also duplex the UF3 soil is not so strongly duplex as UF2, UF4 or UF5. It is a variant containing a heavy local accumulation of secondary iron oxides. The iron oxides have evidently precipitated from iron-rich groundwaters moving downslope, eastwards, from the steep Jurassic dolerite ridge west of the road (Beattie, personal communication).

Groundwater movement occurs, particularly, through the sandy loam topsoil above the impermeable clay subsoil. The iron oxides precipitated in this past of the profile are in the form of concretions, some of which have become very large, somewhat irregular, broadly rounded, tabular. They have been known to cause serious damage to cultivation machinery.

At greater depths, thinner laminar forms occurs along angled joint planes or more permeable strata in the underlying sediment. Nye (1924) described laminar ironstones following bedding planes and joints within the Tertiary clay deposits.

5.2.0. UF2 Duplex Soil

5.2.1. Field-observed soil morphology

A detailed profile description and photograph (plate 2) of the duplex UF2 soil are given on page 72. The profile has a sandy loam surface horizon from 0 cm to 19 cm depth with a clear irregular boundary. Below 19 cm depth, the profile is dominated by clay with weak to very weak, coarse columnar pedality, parting to coarse prismatic and blocky and a high content of smectite (Table 7). Internal drainage is extremely slow and the soil normally remains moist below 50 cm depth.

The moist topsoil colour is dark brown (10YR 3/3), but is much lighter on drying (10YR 5/2 and 10YR 5/1) in a thin (1 - 2 cm) layer above the clay subsoil. Reddish brown

Depth (cm	Description UF2
0 - 19	Dark brown (10YR 3/3 moist); sandy loam; weak medium (5-10 mm) granular structure; very weak moist structure; non sticky; slightly plastic, normal plastic; many fine roots; clear irregular boundary
19 - 46	Brown (10YR 4/3 moist); few medium distinct yellowish brown (10YR 5/6) mottles; medium clay; moderate medium (5-10 mm) prismatic and angular blocky structure; moderately firm moist strength; very sticky; very plastic, normal plastic; common fine roots; many cracks; clear smooth boundary,
46 - 62	Yellowish brown (10YR 5/4 moist); few medium distinct strong brown (7.5YR 5/6) and dark reddish brown (5YR 3/2) mottles; medium clay; moderate medium (5-10 mm) columnar and angular blocky structure; very firm moist strength; very sticky; very plastic, normal plastic; few fine roots; gradual smooth boundary,
62 - 75	Dark yellowish Brown (10YR 4/4 moist); few medium distinct yellowish red (5YR 5/6) and dark reddish brown (5 YR 3/2) mottles; medium clay; moderate medium (5-10 mm) angular blocky structure; very firm moist strength; very sticky; very plastic, normal plastic; few fine roots; gradual smooth boundary,
75 - 89	Yellowish brown (10YR 5/6 moist); few medium distinct brown (10YR 5/3) mottles; medium clay; moderate medium (5-10 mm) prismatic; very firm moist strength; very sticky; very plastic, normal plastic; few fine roots; clear smooth boundary,
89 - 100	Yellowish brown (10YR5/4 moist); many coarse distinct black (7.5YR 2.5/1) manganese nodules (distinct layer); medium clay; moderate coarse (10-20 mm) angular blocky structure; moderately firm moist strength; very sticky; very plastic, normal plastic; few fine roots; clear smooth boundary,
100 - 120	Light olive brown (2.5Y 5/4 moist); common coarse distinct black (7.5YR 2.5/1) and strong brown (7.5 YR 5/6) mottles; light clay; moderate medium (5-10 mm) prismatic structure; very firm moist strength; very sticky; very plastic, normal plastic; few fine roots; clear smooth boundary,
120 - 138	Light olive brown (2.5Y 5/6 moist); sandy light clay; moderate medium (5-10 mm) angular blocky structure; moderately firm moist strength; slightly sticky; slightly plastic, normal plastic; common medium carbonate nodules and few medium manganese nodules; gradual smooth boundary,
138 - 156	Light olive brown (2.5Y 5/4 moist); sandy light clay; moderate medium (5-10 mm) prismatic structure; moderately firm moist strength; slightly sticky; slightly plastic, normal plastic; few medium manganese nodules, gradual smooth. boundary.

Plate 2. Profile UF2

mottles in the clay subsoil indicate oxidation-reduction processes due to very low hydraulic conductivity. The coarse columnar and prismatic peds below 19 cm depth indicate a sodic soil type.

A black glaebule-rich layer is found from 89 cm to 100 cm depth. The glaebules have been shown to contain much manganese by microprobe analysis (Appendix 2, Table 38). These manganese glaebules decrease in abundance with depth from 100 to 156 cm depth. Carbonate glaebules are found between 120 and 138 cm depth associated with both vertical and horizontal planar voids.

5.2.2. Physical characteristics

Detailed physical data are given in Appendix 1, Table 23.

As shown in Figure 8, clay content is low in the surface horizons (0-20 cm) ranging from 14 to 17.5%. Below 20 cm clay content increases abruptly to reach 46.5 % by 46 cm depth. Below 46 cm clay content gradually decreases to 33 % (89 - 110 cm depth) and 23% by 160 cm depth. The sand fraction is dominated by fine sand, approaching 60% in the surface horizon, dropping sharply to 30% in the upper subsoil, increasing gradually to 45% by 90 cm depth, followed by a more rapid decrease to 35% at 110 cm depth before increasing below 120 cm to exceed 50% by 160 cm depth. The opposite trends of clay and fine sand are in accord with the field textures below 19 cm and 89 cm depth and indicate initial stratification of the materials comprising the subsoil of this profile. The coarse sand fraction (all less than 0.5 cm) also falls sharply in the upper subsoil, increasing again below 89 cm to a peak at 110 cm before decreasing again. The coarse sand/fine sand ratio values also indicate stratification. The silt content changes little.

Figure 9 shows the relationship between clay content and bulk density with soil depth. Clay content and bulk density co-vary from 0 - 50 cm and from 100 cm to 160 cm depth but from 50 - 100 cm depth bulk density increases or is steady while clay content decreases. In the soil surface both clay and bulk density are relatively low ranging from 14 to 17.5 % and from 1.36 to 1.41 g/cm^3 respectively. Infills of sandy material occur from

19 cm to 46 cm depth and appear to be due to cracking and swelling of clay soil as described by Holz (1994). Bulk density exceeds 1.60 g/cm^3 by 30 cm depth, reaching a high of 1.89 g/cm^3 at 110 and 120 cm depth. Such high bulk densities indicate a dispersed condition of the soil material with low porosity and very fine voids, explaining both poor root development into the subsoil and the very to extremely slow subsoil permeability observed by Beattie (personal communication). The zone of maximum manganese oxide precipitation is coincident with the higher bulk density values.

5.2.3. Chemical characteristics

Detailed chemical data are given in Appendix 1, Table 23.

The profile is moderately to strongly acid above 75 cm depth, pH decreasing from pH 5.8 at 5 cm to pH 5.5 at 45 cm and pH 5.6 at 75 cm depth (Figure 10). The pH rises steeply below 75 cm to exceed pH 9.0 at 130 cm depth, indicating increasing sodicity in the lower subsoil below an acid upper profile, typical of soloths, in Australia (Stace, et al, 1968; Beattie, 1995). Although this rapid increase in alkalinity does not appear at first sight to be well correlated with increases in exchangeable sodium or exchangeable sodium percentage (ESP) a factor of significance in similar soils of the University Farm is the presence of exchangeable aluminium in the upper subsoil (Beattie, 1995).

After decreasing slightly from the surface to 19 cm depth electrical conductivity increases steadily to 0.38 dS/m by 100 cm depth (Figure 10). Thus the upper profile is non-saline but the lower profile tends to increasing salinity with depth (Doyle, 1993).

Figure 11 shows the depth functions of basic exchangeable cations (Ca^{2+}, Mg^{2+} and Na^{+}). Magnesium is the dominant exchangeable cation in the subsoil although decreasing in amount below 100 cm depth. Exchangeable sodium also increases from 19 cm to 100 cm depth, decreasing slightly below this depth before increasing again at 160 cm depth.

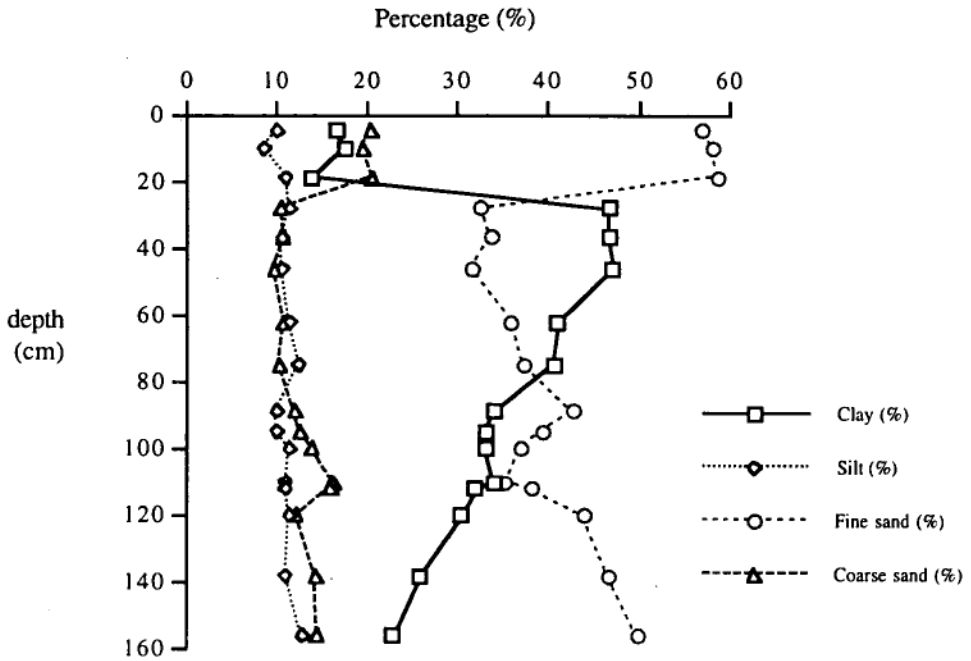

Figure 8. Depth functions of clay, silt, fine sand and coarse sand, UF2

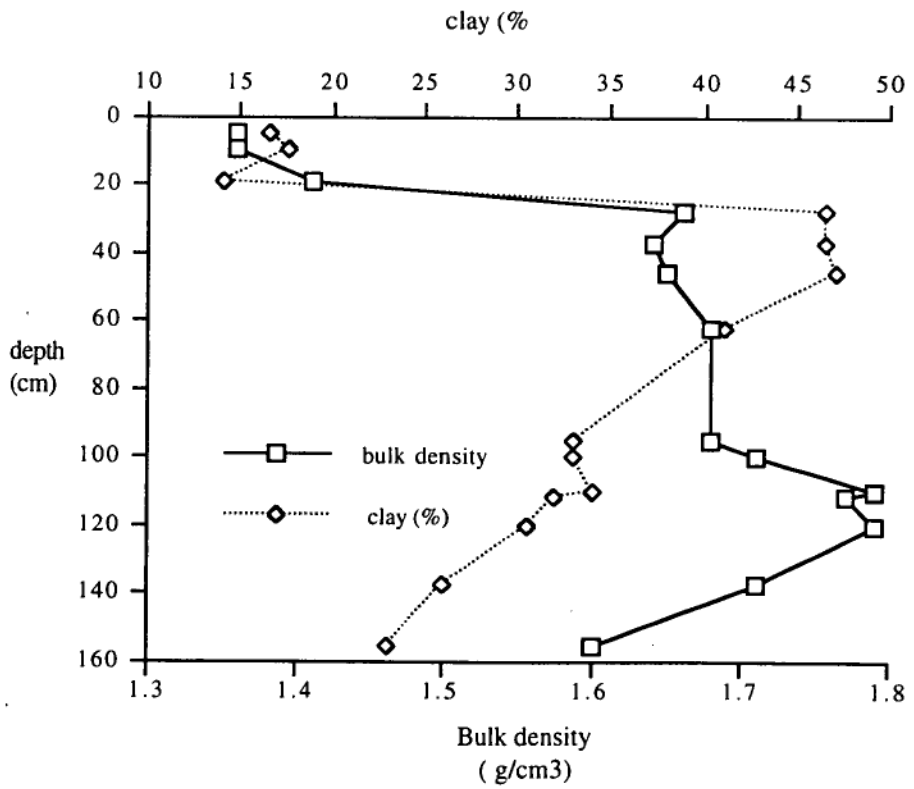

Figure 9. Depth functions of clay content and bulk density, UF2

Although co-dominant with exchangeable Mg^{2+} above 19 cm depth, exchangeable Ca^{2+} increases relatively little in the upper subsoil to 28 cm depth, below which it decreases before increasing slightly at 89-100 cm depth, co-incident with rises in both exchangeable Mg^{2+} and Na^{+}. Fluctuations are more marked below 120 cm and exchangeable Ca^{2+} reaches a maximum at 160 cm depth co-incident with the occurrence of carbonate glaebules. While especially marked in soloths, dominance of Mg^{2+} over Ca^{2+} in clay subsoils is a common feature of many Australian soils (Stace *et al,* 1968; Northcote and Skene, 1972).

High Mg^{2+} and Na^{+} have been implicated in poor physical condition due to dispersivity, such as tough to hard consistence when moderately moist to dry, low to extremely low hydraulic conductivity and poor aeration (Rengasamy and Olsson, 1991).

Exchangeable K^{+} (not graphed) tends to increase with depth, ranging from 0.11 to 0.51 cmol(+)/kg (Table 23, Appendix 1).

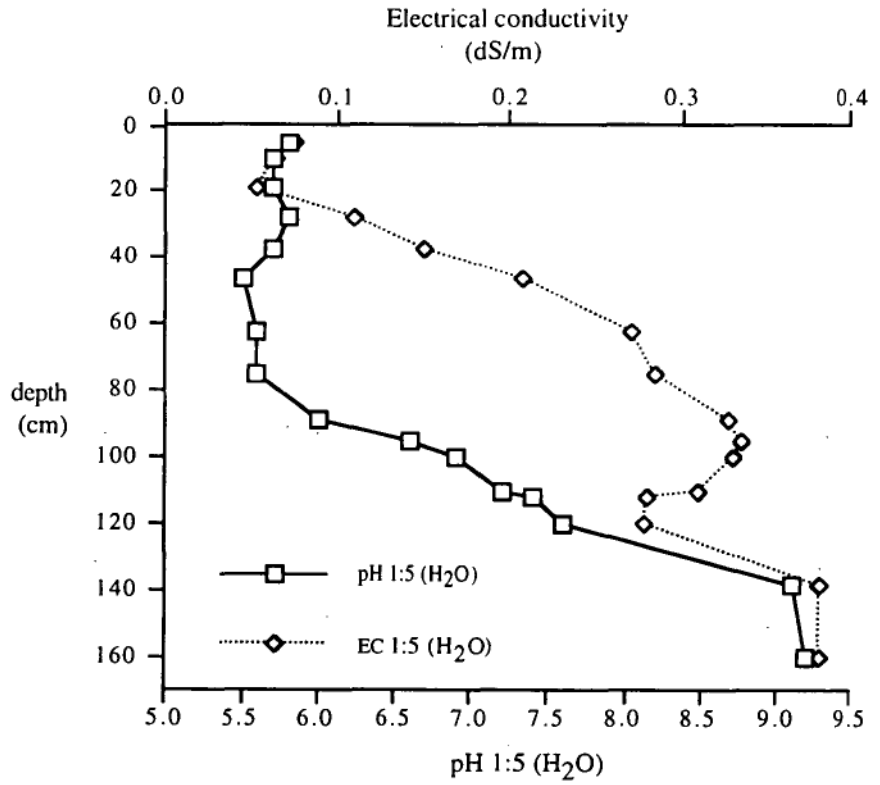

Figure 10. Depth functions of pH (1:5 H_2O) and electrical conductivity EC (1:5 H_2O), UF2

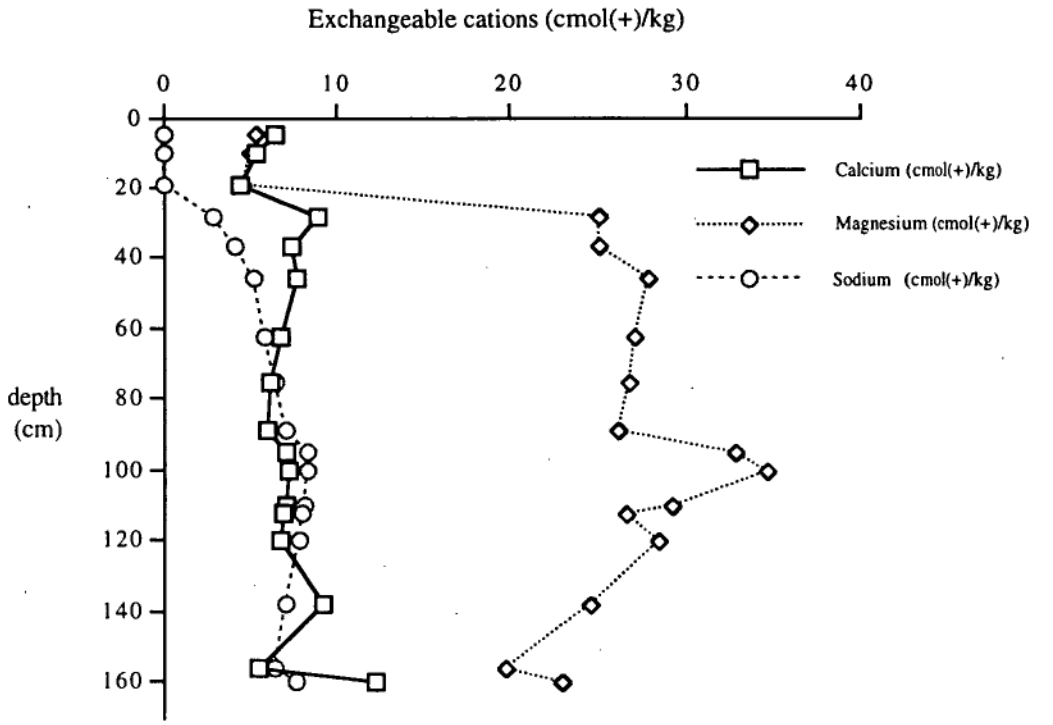

Figure 11. Depth functions of exchangeable Ca^{2+}, Mg^{2+}, and Na^{+}, UF2

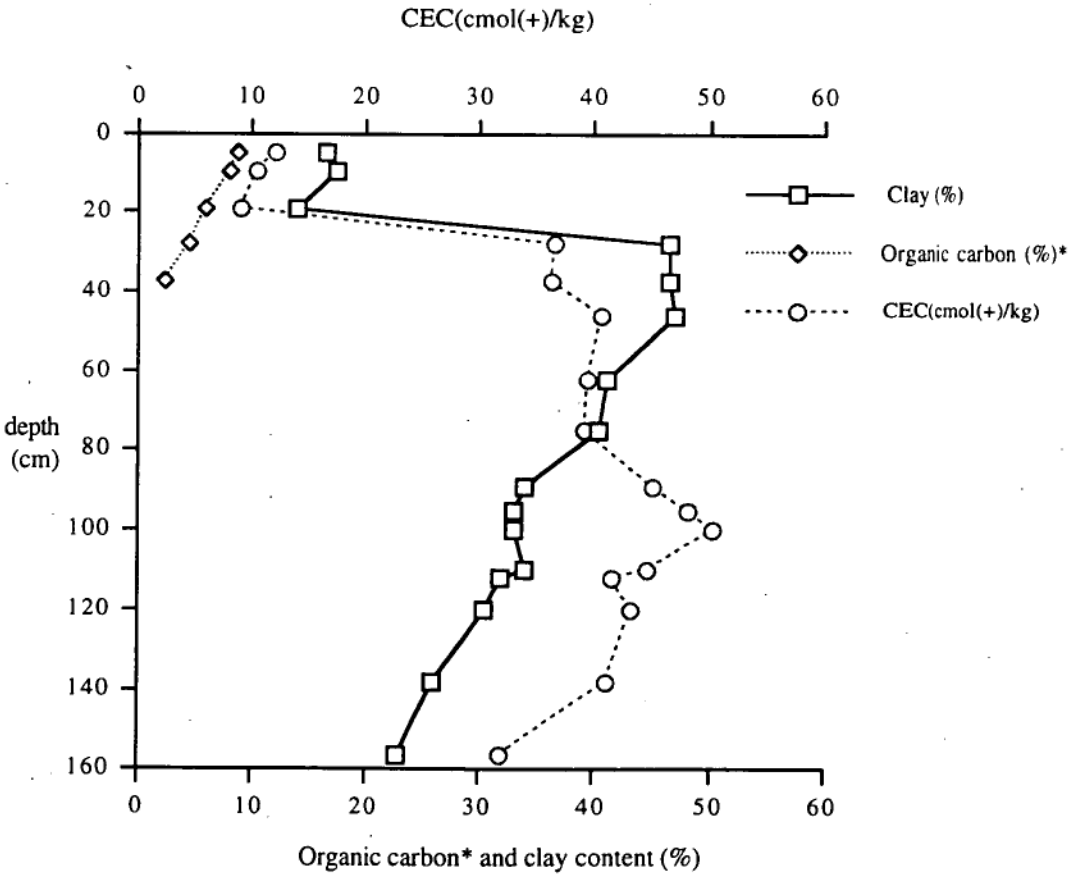

Figure 12. Depth functions of CEC, organic carbon and clay content, UF2

* Organic carbon data are x 4

Figure 12 shows depth functions of clay, organic carbon and cation exchange capacity (CEC). Clay content changes little in the sandy topsoil, increasing sharply below 20 cm while organic carbon content decreases from 2.22 to 0.59% from the surface to 37 cm depth. As a result the CEC decreases with depth in the topsoil before increasing markedly in the clay subsoil due to both its high clay content and the mineralogy of the clay fraction (Table 10). CEC is lower relative to clay content to 80 cm depth, the trend reflecting a decreasing proportion of kaolinite. The reverse is true, i.e., high CEC with lower clay content, below this depth as smectite becomes more dominant. The depth functions of clay and CEC are roughly parallel below 100 cm depth.

5.2.4. X-ray diffraction analysis of clay fractions

Table 10. Semi quantitative X ray diffraction analysis, UF2
t - trace (<10%); l - little(11-25%) ; md - moderate(26-50%); m - much(>50%)

profile	depth (cm)	Smectite	Kaolinite	Illite
UF2	37 - 46	m	md	-
	95 - 100	m	t	t
	> 156	m	t	t

Table 10 shows the dominance of smectite throughout the subsoil with kaolinite increasing towards the surface probably due to weathering effects. The dominance of smectite in this subsoil is not associated with strong shrink/swell behaviour as it is in the black cracking clay (UF1) described above. Two reasons may be suggested for this difference. First, the presence of the sandy loam topsoil to 19 cm depth reduces drying of the subsoil and second, there is a much greater amount of kaolinite in the upper subsoil, below which the profile rarely, if ever, dries (Beattie, personal communication).

5.2.5. Micromorphology

Detailed analytical microprobe data are given in Tables 34 to 38 (Appendix 2).

Plate 18 shows photomicrograph of a typical field from a thin section at 12 cm depth in the UF2 soil. Features marked (A) have been shown to be quartz (95.5% SiO_2) while features marked (B) are iron oxide concretions (37.1% FeO) using microprobe analysis.

Plate 19 is also a photomicrograph of the material at 12 cm depth showing chambered fabric with coarse quartz grains coated with fine grained iron oxides, viz., quartzic ferraric plectic porphyric fabric (Brewer and Sleeman, 1988).

Plate 20 shows a photomicrograph from a thin section at 98 cm depth. The features marked (A) are quartz (96.1% SiO_2). Features marked (B) are iron oxide concretions (39.2% FeO). Features marked (C) are manganese-enriched nodules (5.1% MnO).

Plate 21 is also a photomicrograph from a thin section of the material at 98 cm depth. The fabric is aporic, i.e, the matrix is relatively dense-packed with embedded quartz grains, and with skew planes, viz., quartzic porphyric fabric according to Brewer and Sleeman (1988).

5.2.6. Mineralogy of sand fraction

Table 11 shows that the minerals ilmenite, pyroxene and iron oxides are relatively high throughout the profile while minerals such as leucoxene, zircon, tourmaline and rutile are relatively minor minerals. Levels of leucoxene are less than those of ilmenite throughout the profile. Leucoxene is alteration product of ilmenite. Zircon is present throughout the profile, while rutile is relatively higher in the surface horizon. The distribution of pyroxene and iron oxide suggests a facies change in the Tertiary sediments between 120 and 138 cm depth roughly co-incident with sharply divergent curves for % clay and % fine sand and a marked change in coarse sand/fine sand ratio.

Table 11. Heavy mineral analysis of sand fraction (177 micron),UF2.

Depth (cm)	(0 - 5)	(10 - 16)	(46 - 62)	(112 - 120)	(138 - 156)	(> 156)
Minerals						
Ilmenite	moderate	much	moderate	moderate	moderate	little
Leucoxene	trace	little	trace	little	trace	trace
Zircon	trace	trace	trace	trace	trace	trace
Tourmaline	trace	trace	trace	n.d	n.d	trace
Rutile	little	trace	little	trace	trace	trace
Iron oxide	little	trace	little	little	moderate	moderate
Pyroxene	moderate	trace	little	little	moderate	moderate

n.d = not detected

Table 12. Light mineral analysis of sand fraction (177 micron),UF2

Depth (cm)	(0 - 5)	(10 - 16)	(46 - 62)	(112 - 120)	(138 - 156)	(> 156)
Minerals						
K-Feldspar	n d	little	trace	n d	n d	n d
Plagioclase	n d	n d	n d	moderate	moderate	moderate
Quartz	much	much	much	much	much	much

n.d = not detected

Quartz is relatively high throughout the profile (Table 12). Calcic plagioclase is absent from the sandy topsoil but high in the deep clay subsoil. The relative absence of K-feldspar suggests no very recent contributions of sediment from either Triassic sandstone or Permian mudstone sources (Gatehouse, 1967).

The presence of readily weatherable pyroxene and calcic plagioclase is indicative of a recent Jurassic dolerite source while zircon, tourmaline and rutile grains, many of which were seen to be well-rounded, indicate more ancient Triassic sandstone and/or Permian mudstone sources. Each of these sources is known to have contributed to the Tertiary sediments formation with the added possibility of the sandy topsoil being comprised of largely windblown sand (Leaman, 1971; Holz, 1994).

5.2.7. Origin of materials and soil formation

The UF2 soil profile was located on the axis of a broad spur descending in a north-easterly direction at a low angle (7%). The site was chosen in order to reduce the possibility of run-on and sediment deposition.

The profile to a depth of 156 cm is believed to be comprised of two distinct kinds of material distinguished by marked differences in macro morphological (colour, pedality, consistence), physical, chemical and mineralogical characteristics. The boundary is clear between the sandy surface horizon and the clay-rich subsoil. The clay content in the profile decreases progressively from the upper clayey subsoil (below 20 cm) to the base of the profile. The regular decrease in clay and increase in fine sand, below 20 cm, suggests that there is a major discontinuity in the subsoil of this profile above 120 cm depth which is in contrast to profiles UF3 and UF5 and supports the idea that the solum has developed *in situ* within Tertiary sedments. No evidence was noted that would suggest that the material is colluvium. The fine sand component shows a gradual overall increase from 30 cm to the maximum depth exposed at 160 cm except for a slight decrease between 90 and 110 cm with an increase in coarse sand/fine sand ratio.

The high clay content in the upper subsoil may be due to one of three processes or some combination of these. These are: 1) more intense weathering of primary and secondary minerals near the soil surface, 2) clay translocation from the topsoil due to high dispersivity, or 3) clay inheritance from the apparent parent material, Tertiary sediments. The higher proportion of kaolinite and the amounts of pyroxene and plagioclase, in the upper profile, support the first-mentioned process. The absence of depositional argillans suggests that clay translocation within the subsoil cannot have been a very significant process and the dispersed, very slowly permeable clay would also seem to preclude its occurrence.

Black manganese glaebules occur at 100 cm depth and decrease in abundance to 156 cm. Their presence is associated with increased bulk density and also suggests anaerobic conditions. In contrast to this, carbonate glaebules found between 120 and 138 cm depth associated with vertical planar voids may indicate drier conditions in this depth interval.

There is a further possible mechanism that may have contributed to the strongly duplex character of the solum, i.e., much of the sand of the topsoil may represent aeolian sorting

and/or deposition. The numerous occurrences of low dunes, sheets and pillows of windblown sand within the boundaries of the University Farm (Beattie, pers. comm.) provide evidence of previously active aeolian processes. Also in the course of present agricultural use the sandy surface horizons are subject to wind erosion when exposed and dry.

A gradual increase in exchangeable sodium and ESP was evident from 19 cm to 100 cm and a slight decrease below 120 cm depth. Magnesium was the dominant exchangeable cation, its trend being similar to that of exchangeable sodium but more pronounced. These properties and the acidity of the profile to 80 cm depth below which pH rises steadily to exceed pH 9.0 by 140 cm indicate a profile condition in accord with that described as a soloth, at least for the profile to 90 cm depth. The relatively high clay content together with high levels of exchangeable Na^+ and Mg^{2+} in the subsoil is a common feature of Australian sodic soils. These soils exhibit poor physical conditions ie. tough and compact pedality, poor aeration and plant root environment and both swelling and dispersivity on wetting.

Salinity, although increasing to nearly a metre depth, is never more than slight. However the source of the salt may be accepted provisionally as atmospheric cyclic salt of marine origin as for the UF1 soil.

5.2.8. Soil classification

According to a new classification system for Australian soils (Isbell, 1996) this profile may be classified as "Manganic endocalcareous subnatric brown sodosol". This classification explains the key features of the overall profile: strong texture contrast between sandy topsoil and clay subsoil, high ESP, the presence of secondary carbonate and manganese.

The US Soil Taxonomy (Soil Survey Staff, 1975) classification is Typic Natrustalf. This classification emphasises the sodic nature of the soil, the ustic moisture regime and the texture contrast but it does not highlight the manganese-enriched horizon or the secondary carbonate.

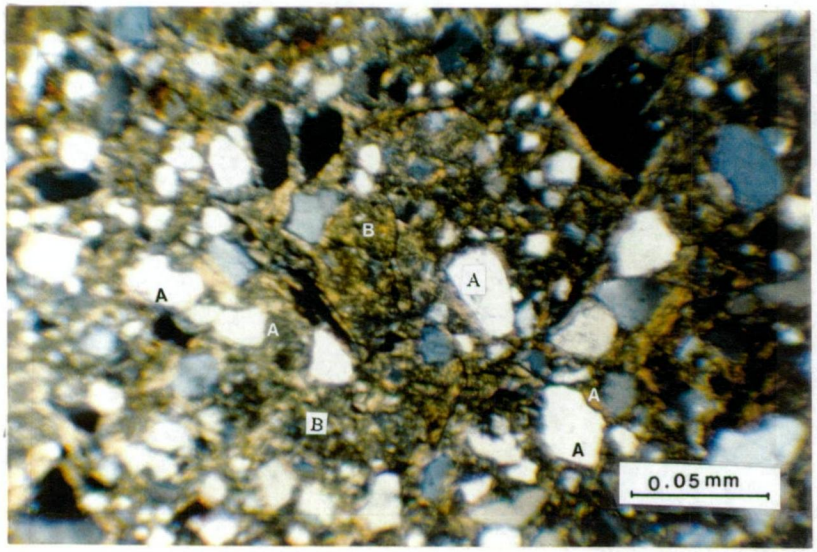

Plate 18.Fabric, UF2, 12 cm depth, (A.) Quartz grain (SiO_2 95.5%); (B).Iron oxide (FeO 37.1%). (X 50 crossed polarizers).

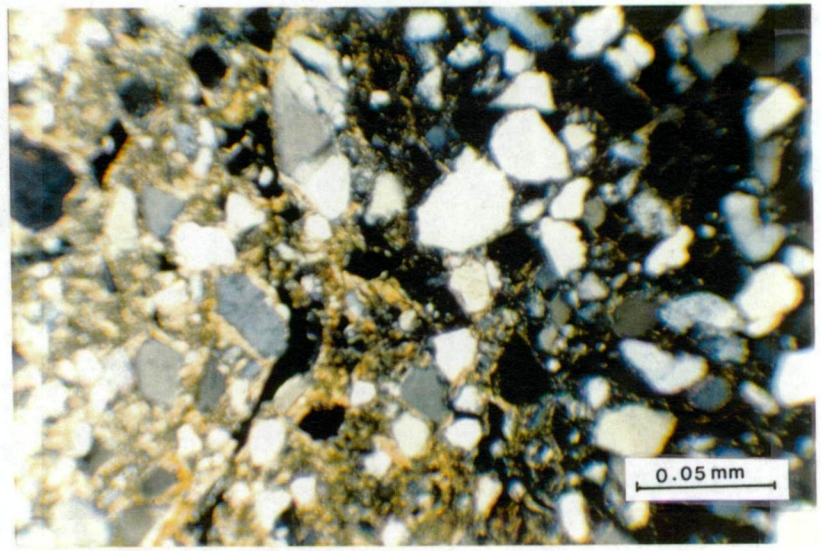

Plate 19.Fabric, UF2, 12 cm depth. Chambered structure; more specifically Quartzic Ferraric Plectic Porphyric(X 50 crossed polarizers).

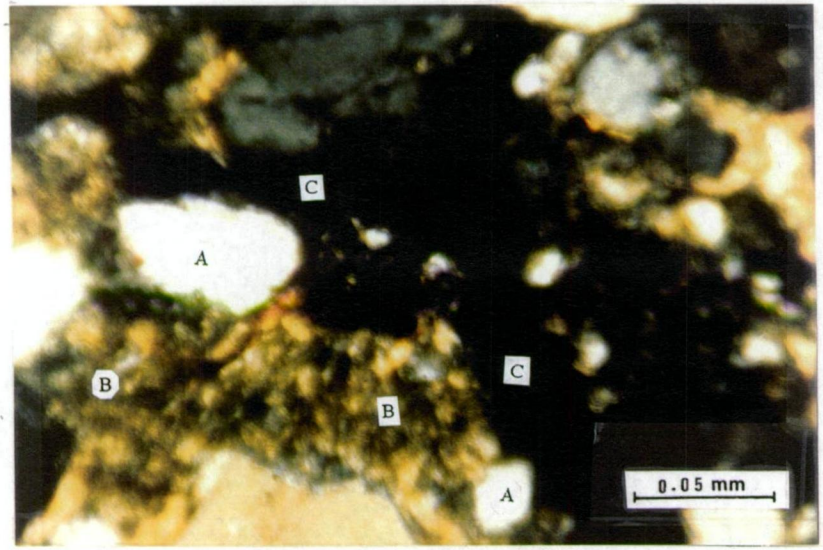

Plate 20.Fabric, UF2, 98 cm depth, (A.) Quartz (SiO_2 96.1%); (B). Iron oxide accumulation (FeO 39.2%); (C). Manganese nodules (MnO 5.1%). (X 50 crossed polarizers).

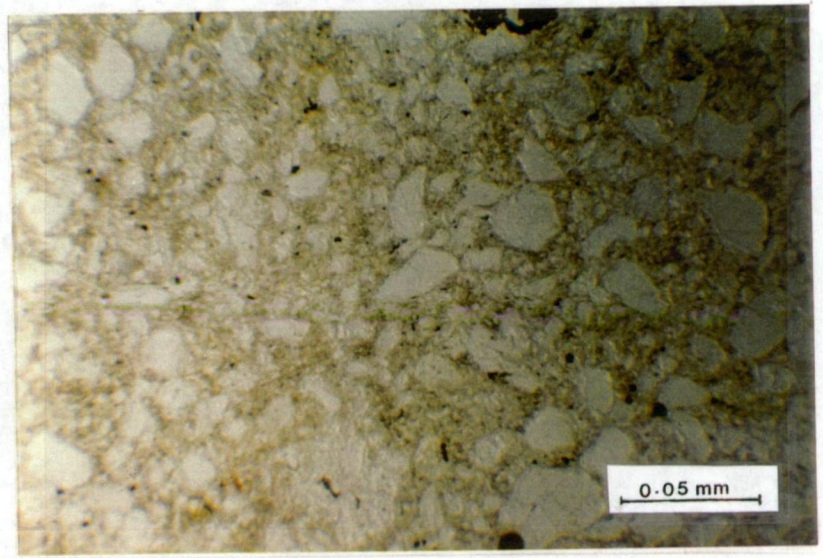

Plate 21.Fabric, UF2 98 cm depth Mangans; more specifically Quartzic Porphyric Fabric. (X 50 plain light).

5.3. UF3 (Duplex soil)

5.3.1. Field-observed soil morphology

A detailed profile description and photograph (plate 3) of the duplex soil UF3 is given on page 94. The profile is sandy loam on the surface horizon (0 - 15 cm) with a clear boundary. Clay content increases below 15 cm depth.

The soil colour is greyish brown (10YR 5/2) on the surface to 12 cm, then changes to brown (10YR 4/3) with common coarse yellowish brown (5YR 5/8) mottles between 12 and 59 cm depth. Reddish brown (2.5YR 5/4) mottles occur between 15 and 52 cm depth due to iron oxide accumulation. The colour changes below 66 cm depth to greyish olive (5Y 6/4) probably due to reducing conditions. Common coarse iron oxide nodules are found between below 5 cm and 52 cm depth.

The field texture is sandy loam from the surface to 15 cm depth with very weak angular blocky peds. Below 15 cm a sharp change to light clay occurs. Below 66 cm depth the soil is still light clay but contains an anastomosing series of iron pans. The texture changes to light medium clay from 74 to 112 cm depth with a prismatic structure and a few iron nodules occur. Below 112 cm depth the soil is light clay. Some secondary carbonate accumulations are found at about 20 cm and 86 cm depth.

5.3.2. Physical characteristics

Detailed physical data are given in Appendix 1 (Table 24).

Figure 13 shows clay content and fine sand content have inverse trends with depth. The clay content decreases from 16.5% at the surface to 11.5% at 32 cm depth. Clay then increases steadily from 32 to 95 cm depth increasing from 11.5 to 49.0%. Below 95 cm depth clay content decreases, dropping from 49.0 to 22.0% by 140 cm depth.

Thus the clay depth function shows both a strong duplex soil and a "clay bulge" in the region below 20 to cm. This may be due to either clay translocation or preferential weathering in the subsoil (discussed in section 5.3.7).

Fine sand decreases fairly steadily from the surface to 95 cm depth dropping from 57.3% in the surface horizons to about 11.0% at 95 cm depth. Below 95 cm depth the fine

sand content begins to increase sharply reaching greater than 53.0% by 130 cm. The gradual decline in fine sand with depth supports field evidence of sand infills seen down cracks. These infills are likely due to swelling and shrinking in the subsoil as described by Holz (1994). The clay dispersivity observed is probably due to high exchangeable Na^+ (Figure 18).

The silt fraction decreases from the surface to 32 cm depth from 15% to 20% then decreases from 32 cm to 59 cm depth to 9% and increases again from 59 cm to 95 cm depth to 36.5%. Below 95 cm depth the silt decreases to 15%.

Clearly the irregular patterns of the various particle size fractions suggests the profile has developed in a stratified deposit.

Figure 14 shows the depth functions of clay and bulk density. There is no clear relationship between bulk density and clay content with soil depth. Bulk density is 1.78 g/cm^3 in the surface, then decreases slowly to 1.4 g/cm^3 at 20 cm depth and increases to 2.16 at 32 cm depth probably due to the presence of many iron nodules. The bulk density decreases again to 1.77 g/cm^3 at 88 cm depth possibly due to a decrease in iron oxide content. Due to the presence of iron oxide nodules the bulk density increases again below 88 cm depth ranging from 1.77 to 2.16 g/cm^3.

Depth (cm)	Description UF3
0 - 6	Greyish brown (10 YR 5/2 moist); sandy loam, very weak; medium (5-10 mm) angular blocky structure; moderately firm moist strength, slightly sticky; slightly plastic, normal plastic; many fine roots, clear smooth boundary,
6 - 12	Greyish brown (10 YR 5/2 moist); few medium distinct yellowish brown (10 YR 5/8) mottles; sandy loam; weak coarse (10-20 mm) angular blocky structure; moderately firm moist strength; slightly sticky; slightly plastic, normal plastic; common iron nodules; fine common roots; gradually smooth boundary,
12 - 42	Brown (10 YR 4/3 moist) common coarse distinct yellowish red (5 YR 5/8) and faint red (2.5 YR 5/4) mottles; light clay; strong coarse (10-20 mm) prismatic structure; very firm moist strength; very sticky; very plastic, normal plastic; many iron nodules; few coarse sporadic pockets of soft secondary carbonate; few fine roots; gradually smooth boundary,
42 - 59	Brown (10 YR 4/3 moist); common coarse distinct yellowish brown (10 YR 5/6) mottles; light clay; strong coarse (10-20 mm) prismatic structure; very firm mist strength; very sticky; very plastic, normal plastic; discontinuous iron pan; few fine roots; gradual wavy boundary,
59 - 75	Pale olive (5 Y 6/4 moist); few medium distinct yellowish brown (10 YR 5/6) mottles; light clay; strong coarse (10-20 mm) angular blocky structure; very firm moist strength; very sticky; very plastic, normal plastic; continuous iron pan; few fine roots; abrupt wavy boundary,
75 - 95	Pale olive (5 Y 6/4 moist); common coarse distinct yellowish brown (10 YR 5/6) and dark grey (10 YR 4/1) mottles; light medium clay; strong coarse (10-20 mm) prismatic and platy structures; very firm moist strength; very sticky; very plastic, normal plastic; discontinuous iron pan; few fine roots; many free carbonate soft segregations; clear wavy boundary,
95 - 114	Light olive grey (5 Y 6/2 moist) few medium distinct yellowish brown (10 YR 5/6) and brownish grey (10 YR 4/1) mottles; light medium clay; strong coarse (10-20 mm) subangular blocky structure; very firm moist strength; very sticky; very plastic, normal plastic; few iron nodules; gradual smooth boundary,
114 - 135	Light grey (5 Y 7/2 moist); few medium distinct yellowish brown (10 YR 5/6) mottles; light clay; strong coarse (10-20 mm) subangular blocky structure; very firm moist strength; very sticky; very plastic, normal plastic; max cont.

Plate 3. Profile UF3

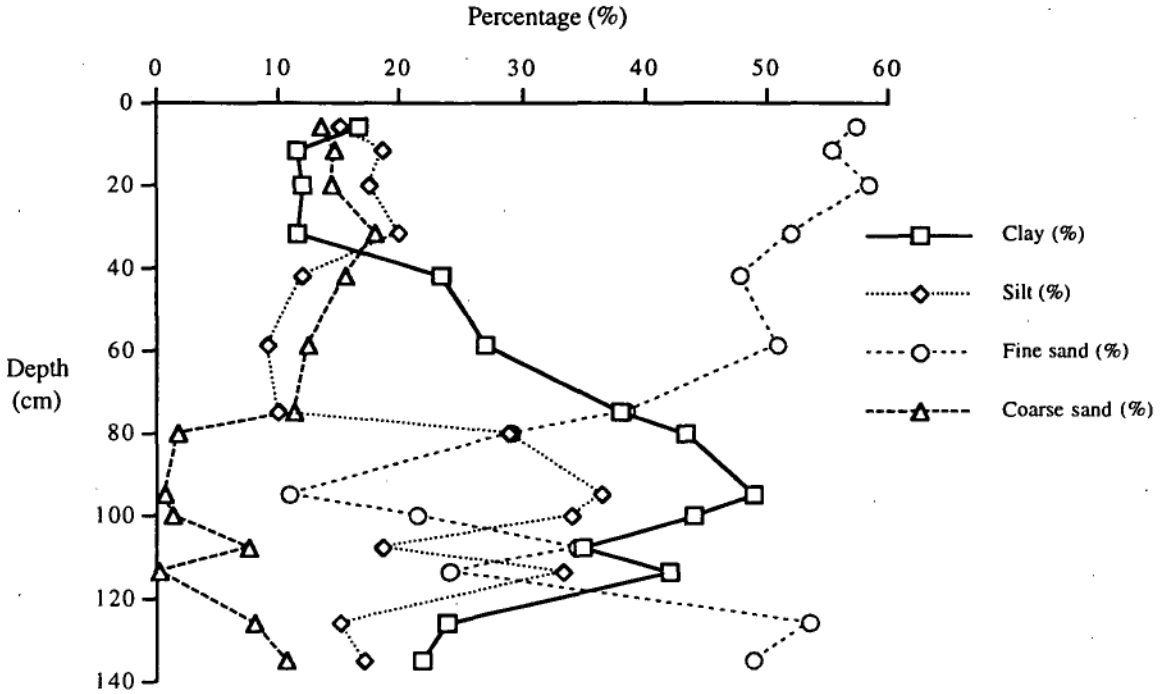

Figure 13. Depth functions of clay, silt, fine sand and coarse sand, UF3

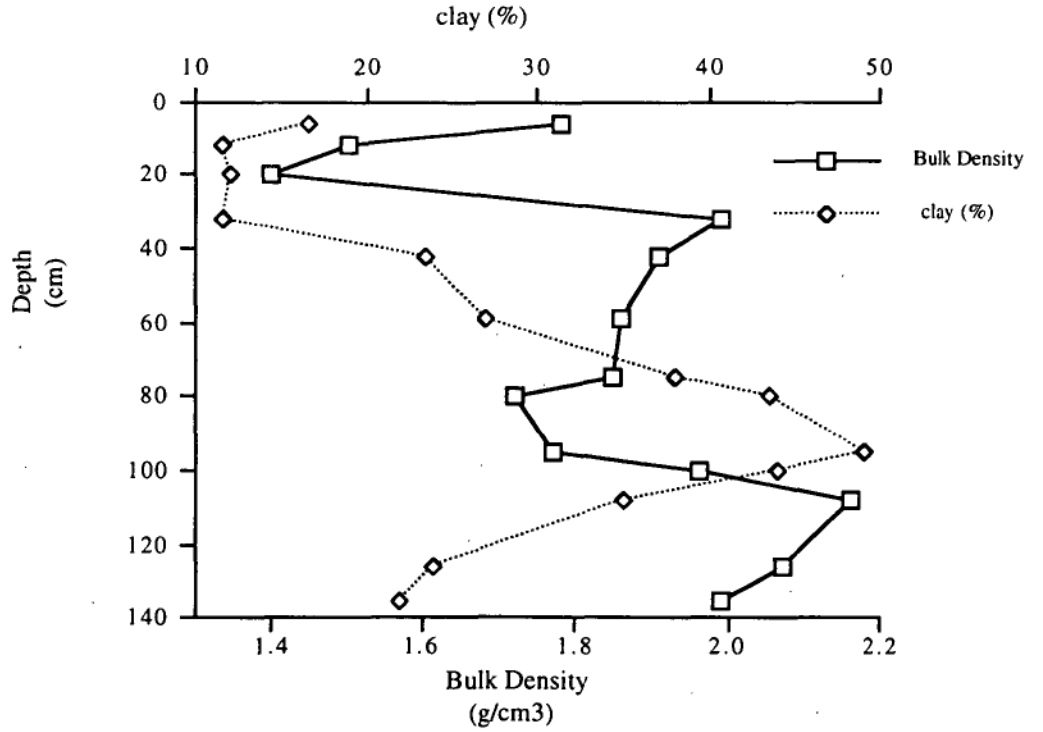

Figure 14. Depth functions of clay content and bulk density , UF3

5.3.3. Chemical characteristics

Detailed data are given in appendix 1, Table 24.

Figure 15 shows depth functions of pH (H_2O 1:5) and electrical conductivity (H_2O 1:5). Both pH and electrical conductivity have a somewhat similar trend with soil depth. The profile is neutral at the surface, slightly acid in the lower topsoil and alkaline in the subsoil. The pH is 6.6 on the surface then decreases slowly to pH 5.8 at 20 cm depth and increases gradually from 20 to 95 cm depth from pH 5.8 to pH 8.3. Below 95 cm depth pH remains at 8.0 or higher. It is likely the increase in pH is due to the increase in exchangeable Na^+ (Figure 16).

The electrical conductivity trend is very similar to that of the clay content (Figure 14 and 15). Electrical conductivity is 0.11 dS/m in the surface, then decreases to 0.05 dS/m at 20 cm depth. This is probably due to slight surface concentration of salts by evaporation. Electrical conductivity then gradually increases to 0.43 dS/m to the depth of the "clay bulge" at about 75-95 cm. Below 95 cm depth electrical conductivity decreases to 0.26 dS/m following the decrease in clay content. This close relationship between clay content and electrical conductivity may be due to fine micro-pores retaining saline soil solutions which are not readily leached during soil formation (Talsma, 1967). On the surface layer the soil is considered non saline while the subsoil would be classified as slightly saline (Doyle, 1993).

Figure 16 shows depth functions for three basic exchangeable cations: Ca^{2+}, Mg^{2+} and Na^+. Exchangeable Mg^{2+} is clearly the dominant cation in the subsoil with moderate amounts of Ca^{2+} in the topsoil. Both exchangeable Na^+ and Mg^{2+} increase markedly with depth. Exchangeable Na^+ is 0.38 cmol(+)/kg from the surface to 32 cm then increases to 0.93 cmol(+)/kg at 42 cm depth. Exchangeable Na^+ then increases rapidly to 6.72 cmol(+)/kg at 95 cm depth, and decreases again below 95 cm depth to 2.31 cmol(+)/kg. Exchangeable sodium percentage (ESP) is below 10 from the surface to 59 cm then slightly increases below 59 cm changing from 10 to 13, see Table 24.

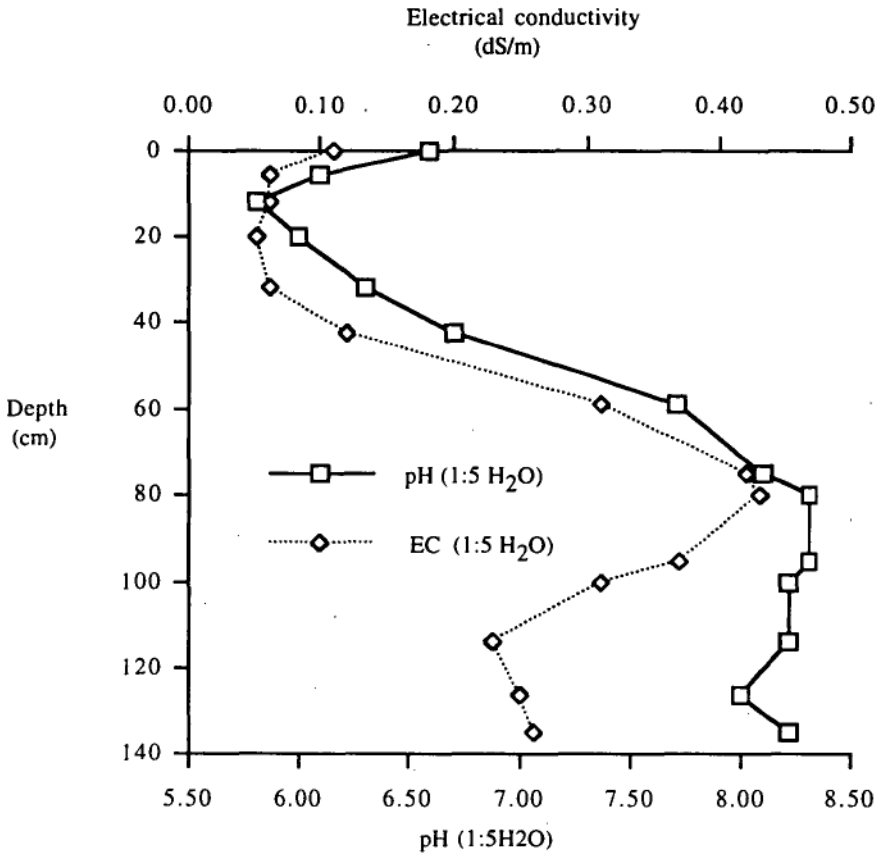

Figure 15. Depth functions of pH(1: 5 H_2O) and electrical conductivity (EC 1: 5 H_2O), UF3

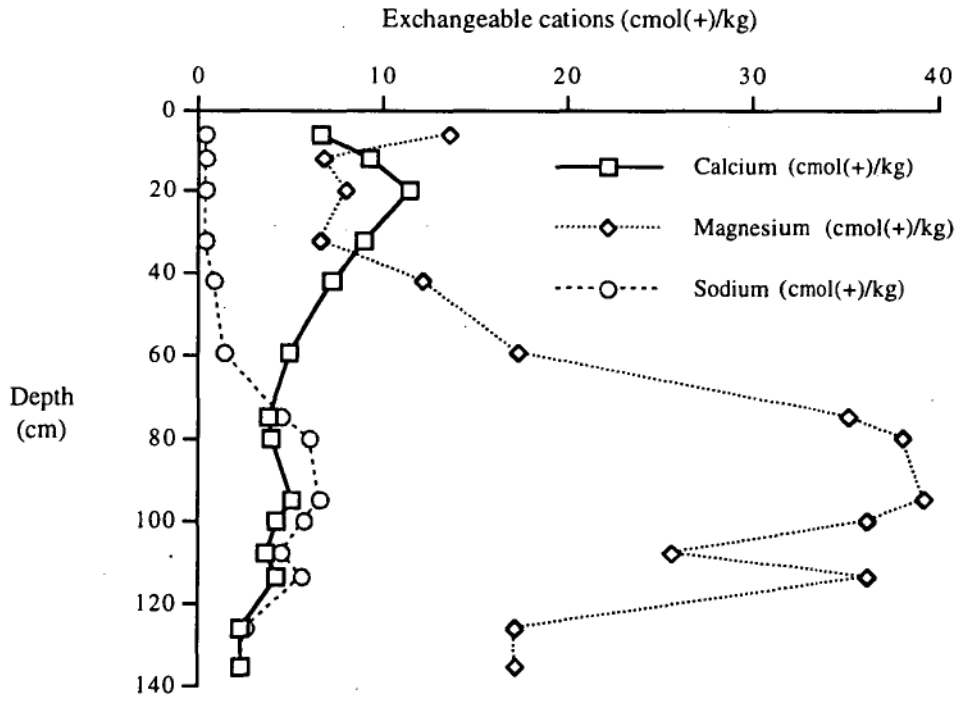

Figure 16. Depth functions of exchangeable Ca, Mg and Na, UF3

Levels of exchangeable Mg^{2+} are relatively high throughout the profile. Exchangeable Mg^{2+} decreases sharply from the surface to 32 cm dropping from 13.72 to 6.71 cmol(+)/kg. Exchangeable Mg^{2+} then increases rapidly to 39.33 cmol(+)/kg at 95 cm depth due to the increase in clay content. Below 95 cm depth exchangeable Mg^{2+} decreases again to 17.2 cmol(+)/kg. High levels of exchangeable Mg^{2+} and Na^{+} have been implicated in poor soil physical conditions such as high soil strength when dry and dispersivity and swelling when wet (Rengasamy and Olsson, 1993). This is confirmed by the field properties of this soil and result in poor aeration and low permeability in the subsoil.

Exchangeable Ca^{2+} is 6.7 cmol(+)/kg on the surface then increases to 11.6 cmol(+)/kg at 20 cm depth. This increase may be due to the presence of free carbonate glaebules which are present at about 20 cm. Exchangeable Ca^{2+} decreases gradually below 20 cm to 3.74 cmol(+)kg^{-1} at 75 cm depth. From 75 cm to 95 cm depth exchangeable Ca^{2+} increases to 5.1 cmol(+)/kg and this may be related to the presence of free carbonate. Below 95 cm depth exchangeable Ca^{2+} decreases again to 2.3 cmol(+)/kg. K^{+} is relatively low ranging from 0.04 to 0.49 cmol(+)/kg throughout the profile and is not graphed (Table 24, appendix 1).

Figure 17 shows depth functions for clay content, organic carbon and CEC. Clay content and CEC have a similar trend with depth, while organic carbon tends to decrease steadily from the surface. Organic carbon decreases from 2.3 to 0.5 % between the surface and 42 cm depth.

CEC decreases from the surface to 32 cm, from 21 to 16 cmol(+)/kg. CEC then increases steadily to 51.5 cmol(+)/kg at 95 cm. From 95 to 108 cm depth CEC decreases again, ranging from 51.1 to 34 cmol(+)/kg, then increases slightly to 46 cmol(+)/kg at 114 cm depth. Below 114 cm CEC decreases to 22 cmol(+)/kg.

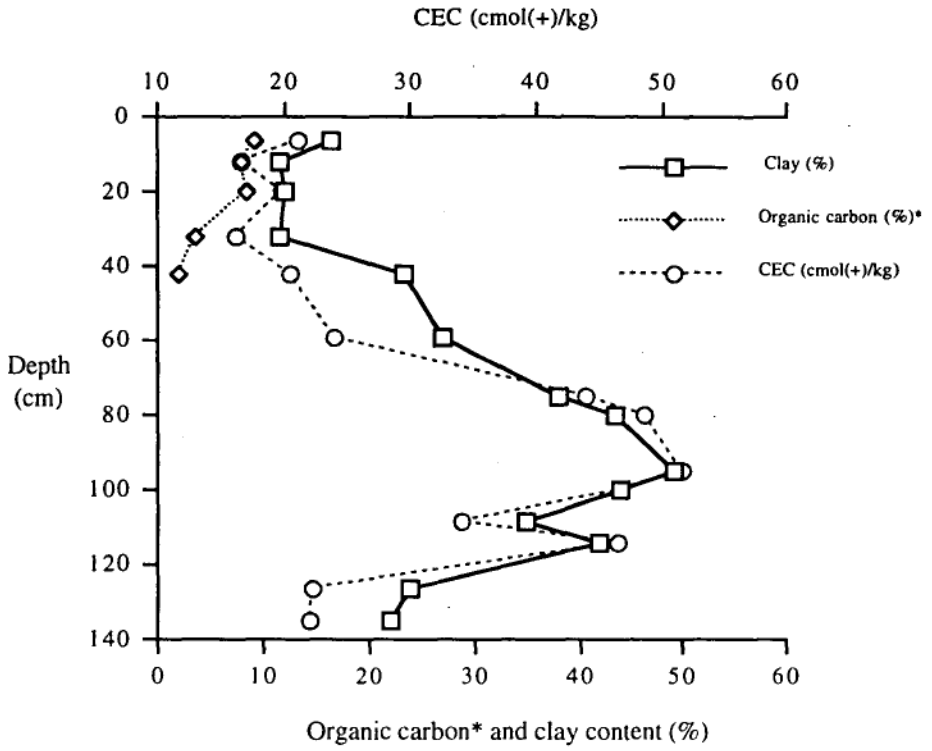

Figure 17. Depth functions of CEC, organic carbon and clay content, UF3
* Organic carbon data are x 4.

The slight decrease in CEC values in the upper profile (0 - 32 cm) is likely to be due to the decrease of organic matter and clay content to a depth of 32 cm. The increase in CEC in the upper subsoil (32 - 95 cm) is clearly due to the large increase in clay content. It is somewhat surprising that the influence of clay mineralogy has not affected the CEC as the smectite content increases to a moderate level in the 125 - 135 cm depth material.

5.3.4. X ray diffraction analysis of clay fractions

Table 13 shows that kaolinite is more dominant in the upper layers while smectite and illite are minor clay minerals. The domination of kaolinite and low levels of smectite in the upper layers is an indication of greater intensity of weathering near the soil surface. In the lower horizons smectite increases to moderate levels. The presence of high levels of magnesium in the subsoil may reduce any tendency for alteration of smectite to kaolinite.

Table 13. Semi quantitative X ray diffraction analysis, UF3
t - trace (<10%); l - little(11-25%) ; md - moderate(26-50%); m - much(>50%)

profile	depth (cm)	Smectite	Kaolinite	Illite
UF3	52 - 66	t	m	t
	74 - 88	l	m	t
	104- 112	t	m	t
	125-135	md	m	t

5.3.5. Micromorphology

Detailed analytical data are given in Tables 39 to 47 (see Appendix 2).

Plate 22 shows a photomicrograph from a thin section at 15 cm depth. Features marked (A) have been proven by both electron microprobe and petrographic examination to be iron oxide rich accumulations (82% FeO). This is coupled with the presence of iron nodules observed in the field soil (plate 3). Features marked (B) have been identified as quartz (95.9% SiO_2). Features marked (C) have been identified as feldspar (12.5% K_2O, 30.6% Al_2O_3, 67.2 % SiO_2) by both microprobe analysis and petrographic identification.

Plate 23 is a photomicrograph of a thin section of material at 15 cm depth. The fabric is chambered (Brewer and Sleeman, 1988) with many connected pores.

Plate 24 shows an iron oxide nodule (30.7% FeO) identified by microprobe analysis and by optical properties at 46 cm depth. This is a feature associated with reddish brown nodules observed in the field soil.

Plate 25 shows a photomicrograph of a thin section of material at 46 cm depth. The fabric is chambered and vughy. Vughy structure is that fabric having large voids, irregular in shape and normally not interconnected. The chambered fabric has interconnected large voids usually irregular in shape with smooth walls (Brewer and Sleeman, 1988).

Plate 26 is a photomicromograph of a thin section of material at 86 cm depth. The features have been proven by both petrographic examination and microprobe analysis to be iron oxide and clay accumulations (6.4% FeO, 45.5% SiO_2 and 25% Al_2O_3).

Plate 27 is a photomicrograph of a thin section of the soil at 86 cm depth. The features marked (A) have been identified as carbonate glaebules (28.5% CaO). This is associated with the presence of free carbonate accumulations in this horizon.

Plate 28 is a photomicrograph of the material at 86 cm depth in thin section. The fabric is fissured and channelled. The fabric is fissured with skew planes and planar voids traversing the soil mass in an irregular manner. Channels are elongated tubular-shaped voids with a circular cross-section (Brewer and Sleeman, 1988).

Plate 29 displays the micromorphological features of the soil at 93 cm depth. The feature marked (A) appears to be albite with twinning seen clearly using doubly polarised light (2.07 % MgO, 26.8% Al_2O_3, 57% SiO_2). The features marked (B) were identified as quartz (91.3% SiO_2), confirmed by electron microprobe analysis.

Plate 30 shows carbonate nodules at 93 cm depth (21.9% CaO by electron microprobe analysis).

Plate 31 shows a photomicrograph of the material at 93 cm depth in thin section. The fabric is channelled with relatively dense packing of fine grained iron oxide in the coarser soil matrix this fabric is termed fragmoidic ferraric porphyric texture by Brewer and Sleeman (1988).

5.3.6. Mineralogy of sand fraction

The heavy mineral fraction contained ilmenite, iron oxide, pyroxene, zircon, rutile, tourmaline and leucoxene (Table 14). There is a tendency for zircon, rutile and leucoxene to increase with depth. This may indicate a facies change in the Tertiary sediments. The occurrence of ilmenite, pyroxene and K-feldspar follow the separation of the sandy surface horizons and the clay subsoil (see Table 15). Tourmaline is present in trace amount throughout the profile.

Table 14. Heavy mineral analysis of sand fraction (177 micron), UF3.

Depth (cm)	(0 - 5)	(10 - 15)	(95 - 100)	(125 - 135)	(> 135)
Minerals					
Ilmenite	moderate	moderate	little	little	little
Leucoxene	trace	trace	little	little	little
Zircon	trace	trace	trace	little	trace
Tourmaline	trace	trace	trace	trace	trace
Rutile	little	little	trace	moderate	moderate
Iron oxides	little	little	moderate	trace	little
Pyroxene	little	little	n.d	n.d	n.d

n.d = not detected

Quartz (Table 15) is relatively high throughout the profile while traces of K-feldspars are present in the topsoil. Calcic plagioclase tends to increase with depth suggesting less weathering of material deeper in the profile.

The presence of calcic plagioclase throughout the profile indicates the possibility of a contribution of doleritic material. Perhaps this is due to the partial doleritic provenance of the Tertiary clay sediments (Leaman, 1971) or due to stratification of sediments forming the lower profile. The presence of pyroxene and ilmenite in higher amounts in the topsoil suggests some stratification of the profile and can be taken to indicate a larger doleritic component in the surface layers.

Table 15. Light mineral analysis of sand fraction (177 micron), UF3.

Depth (cm)	(0 - 5)	(10 - 15)	(95 - 100)	(125 - 135)	(> 135)
Minerals					
K-Feldspar	trace	trace	n.d	n.d	n.d
Plagioclase	little	trace	moderate	little	little
Quartz	much	much	much	much	much

n.d = not detected

5.3.7. Origin of materials and soil formation

The UF3 soil profile is located on a toeslope (slope, 9%) (profiles UF4 and UF5 being directly downslope) beneath a steeper footslope and very steep backslope extending to a ridge of dolerite.

The profile to a depth of 145 cm appears to comprise several distinct layers distinguished by a marked difference in macromorphological (texture, colour, pedality), physical, chemical and mineralogical characteristics. The upper profile is quite sandy but below 15 cm clay content steadily increases and the soil can be considered duplex.

The high percentage of fine sand together with the presence of calcic plagioclase, pyroxene and ilmenite in the topsoil suggests that the material may be partly from doleritic materials, perhaps transported by aeolian processes or as colluvium from upslope exposures. The high percentage of fine sand, presence of well-rounded grains, and

absence of any dolerite clasts indicate aeolian origin is more likely. Also, the presence of both K-feldspar and quartz indicates the topsoil may be partly derived from Triassic sandstone and/or Permian mudstone sources (Leaman, 1971) possibly being transported to the site via aeolian processes from an exposed Pitt Water Bay area during a previous glaciation (Doyle, personal communication).

Relatively high amounts of quartz, zircon and rutile along with the high clay content in the subsoil suggests that the material is probably derived from Tertiary sediments (Beattie, personal communication). The particle size analysis (see Figure 13) indicates the subsoil material is stratified, probably reflecting the nature of the parent sediment since there are no associated stonelines or clasts. This stratification is emphasised by the deposition of secondary iron oxides in coarser (sandier) textured layers. This secondary iron oxide, in the form of iron glaebules and iron pans below 22 cm, could be sourced from the weathering of exposed dolerite above the site (western ridge of the Coal River valley). Dolerite, a rock high in ferromagnesian minerals, could supply much iron, and also calcium and magnesium, on weathering. The iron, once supplied from the weathering of dolerite sources, may then move in suspension or solution along preferred sub-surface drainage lines, in particular in the more sandy layers directly above the clayey subsoil. In summary iron is thought to have moved laterally, downslope across and through the sloping stratified substrate of UF3 (see figure 2), iron oxides being precipitated as pans, laminae and nodules in the sandier layers during drier, aerobic, periods, as observed in the subsoil of this profile.

Relatively high clay content and high percent exchangeable Na^+ and Mg^{2+} in the subsoil are common features of many Australian sodic soils. Australian sodic and magnesic soils commonly have poor physical and chemical characteristics (Rengasamy and Olsson, 1991). They are hard and tough when dry and have coarse prismatic structure in the clayey subsoil. In addition, marked swelling and dispersion of the clayey subsoil occurs on wetting. These properties are amplified by the low levels of exchangeable calcium, apart from a moderate accumulation in the topsoil, and the alkalinity of the subsoil.

5.3.8. Soil classification

According to a new classification system for Australian soils (Isbell, 1996) this profile may be classified as "ferric endocalcareous subnatric brown sodosol". This classification highlights the key feature of the overall profile, such as texture contrast, high sodium percentage, the presence of secondary carbonate, brown colour and the presence of iron oxide rich layers.

The US Soil Taxonomy (Soil Survey Staff, 1975) classification is "Typic Natrustalf". This classification emphasises the sodic nature of soil, the ustic moisture regime and texture contrast but it does not highlight its iron oxide layers or the secondary carbonate.

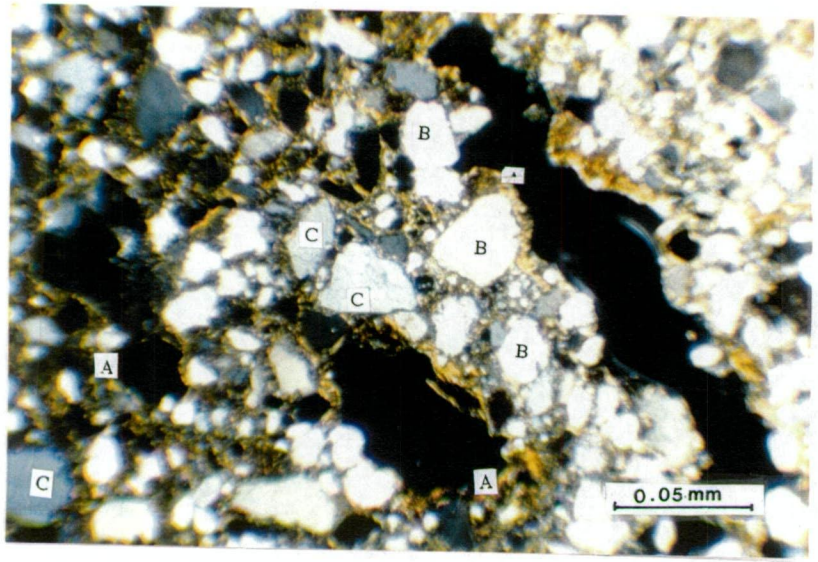

Plate 22.Fabric, UF3, 15 cm depth, (A). Iron oxide (FeO 82%); (B). Quartz (SiO_2 95.9%); (C). Feldspar (K_2O 12.5%, Al_2O_3 30.6%, SiO_2 67.2%). (X 50 crossed polarizers).

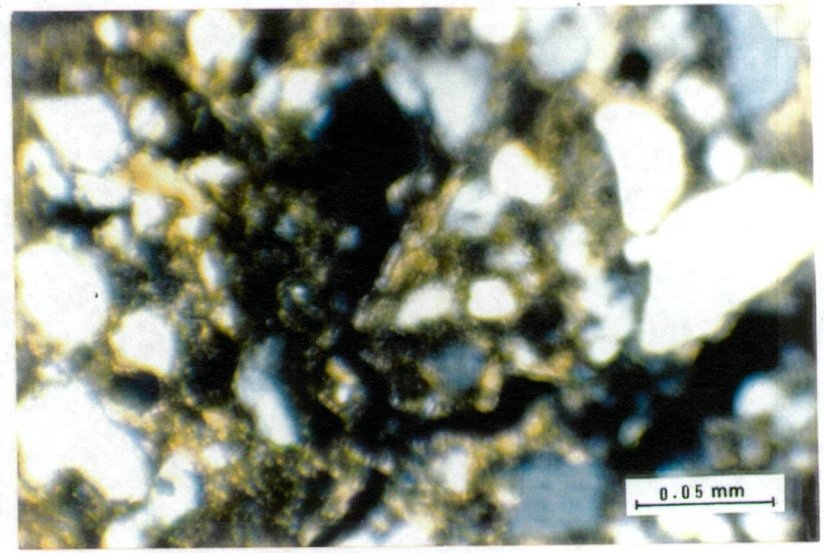

Plate 23.Fabric, UF3, 15 cm depth Chambered structure.(X 50 crossed polarizers).

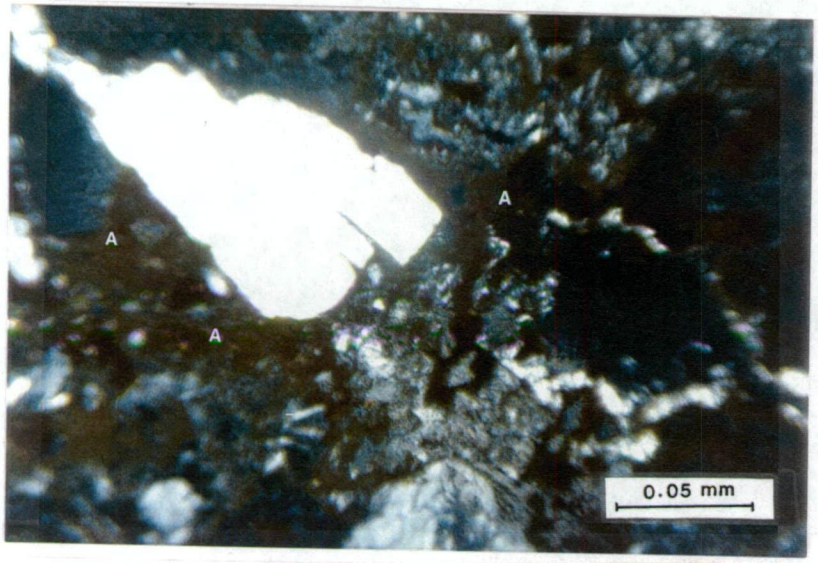

Plate 24.Fabric, UF3, 46 cm depth, (A). Iron oxide (FeO 30.7%). (X 50 crossed polarizers).

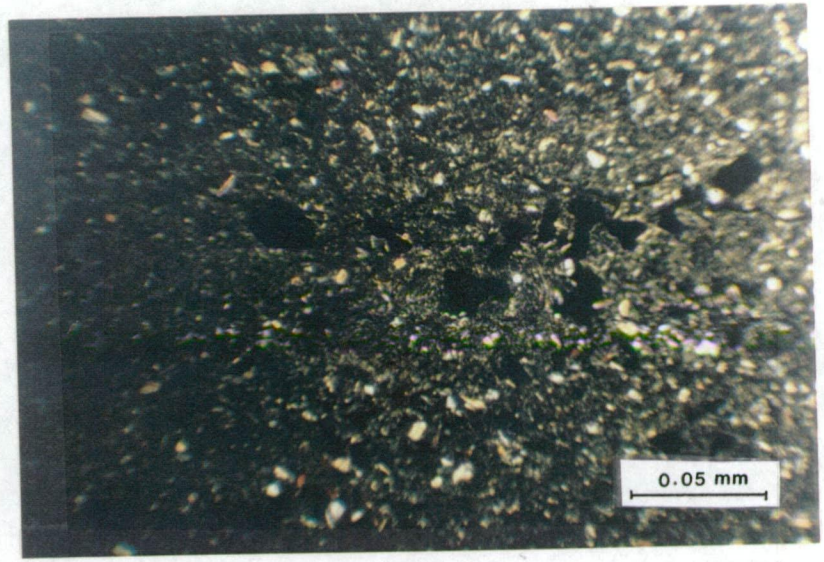

Plate 25.Fabric, UF3, 46 cm depth Chanbered and Vughy structures.(X 50 crossed polarizers).

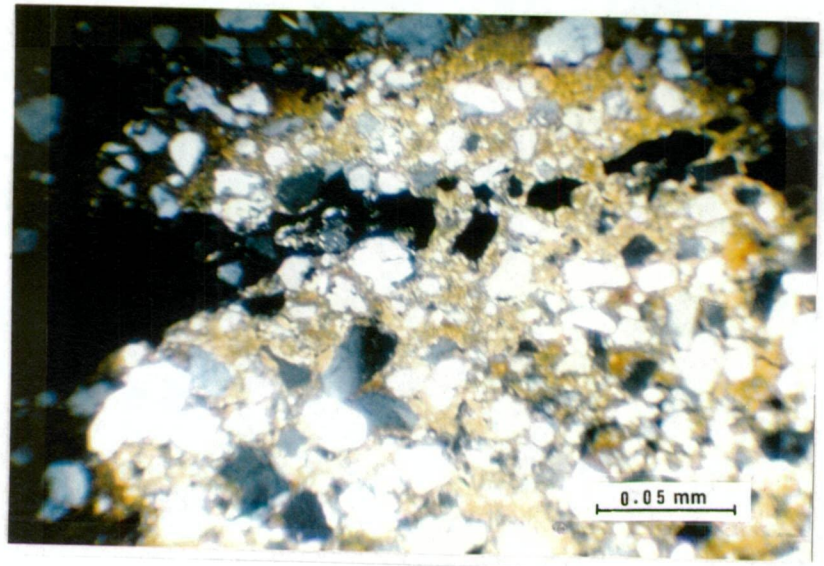

Plate 26 Fabric, UF3, 86 cm depth, Iron Oxide and clay accumulations (FeO 6.4%, 45.5% SiO_2 and 25% Al_2O_3).(X 50 crossed polarizers).

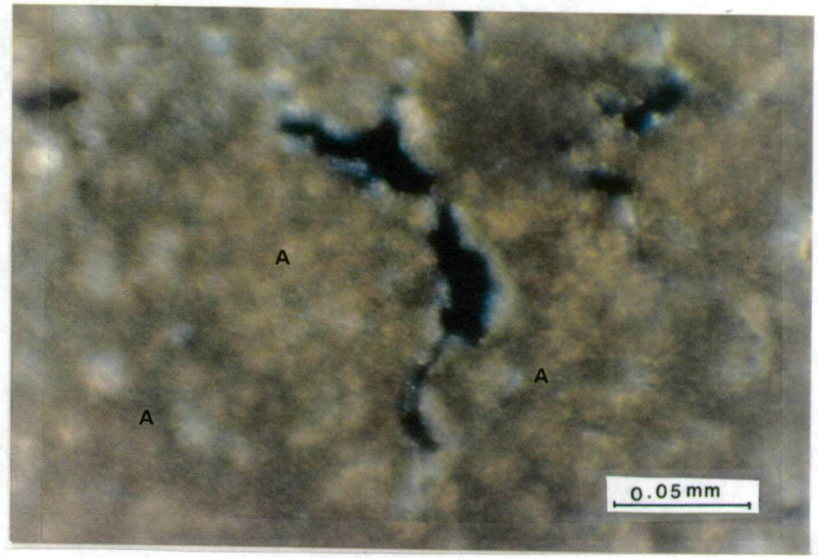

Plate 27.Fabric, UF3, 86 cm depth, (A). Carbonate glaebules (CaO 28.5%) (x 50 crossed polarizers).

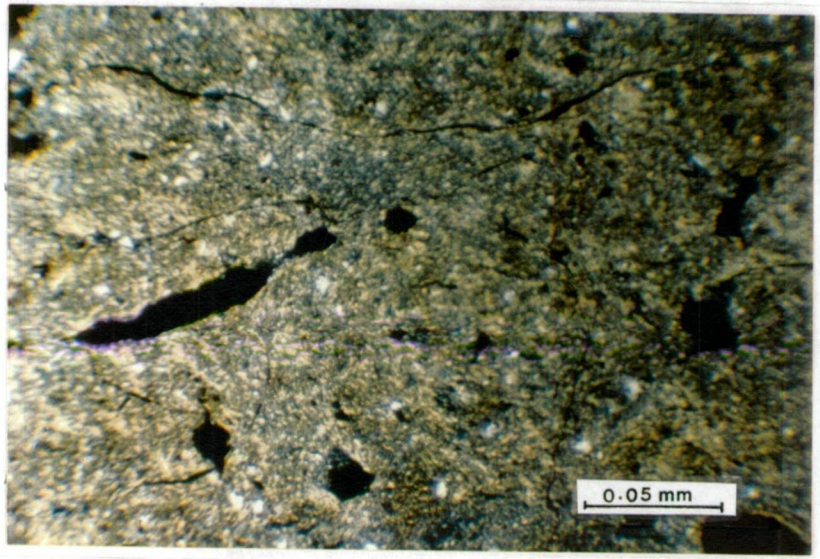

Plate 28.Fabric, UF3, 86 cm depth, Fissured and chanelled structures.(X 50 crossed polarizers).

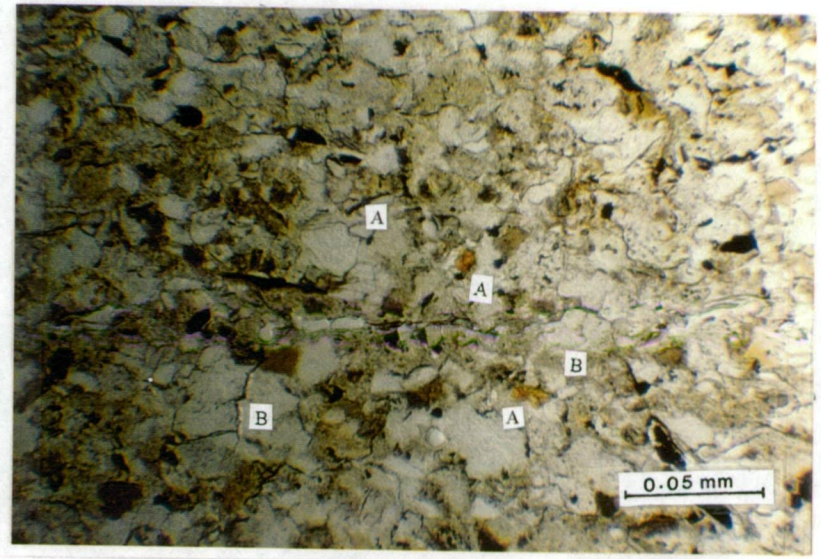

Plate 29.Fabric, UF3, 93 cm depth, (A). Albite (MgO 2.07%, Al_2O_3 26.8%, SiO_2 57%); (B).Quartz. (SiO_2 91.3%). (X 50 plain light).

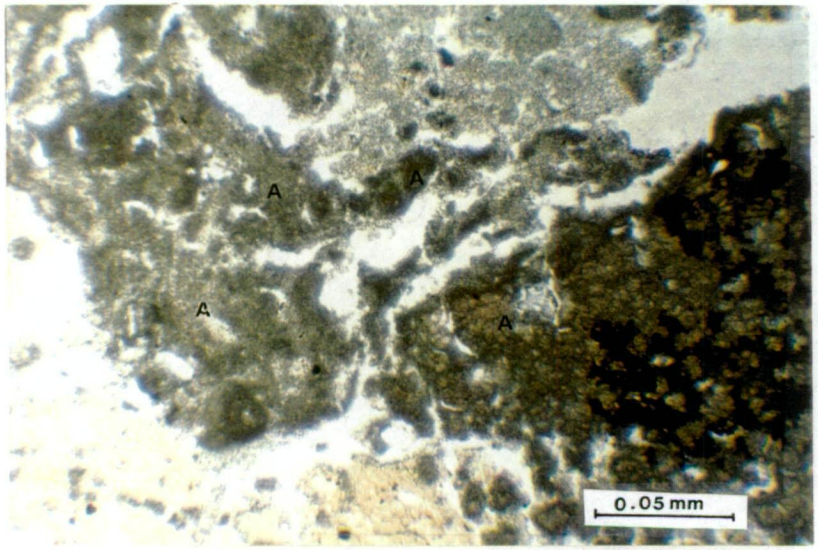

Plate 30.Fabric, UF3, 93 cm depth, (A). Carbonate nodules (CaO 21.9%) (x 50 crossed polarizers).

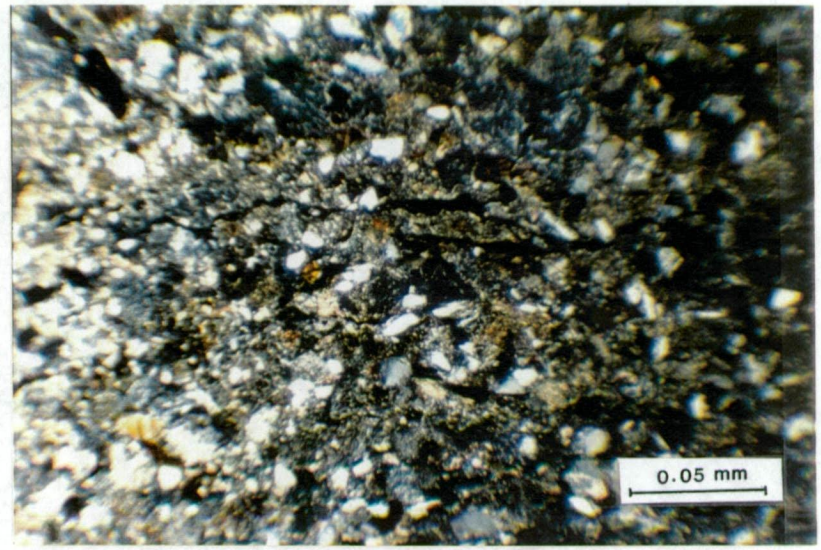

Plate 31.Fabric, UF3, 93 cm depth, Chanelled structure; more specifically fragmoidic ferraric porphyric.(X 50 crossed polarizers).

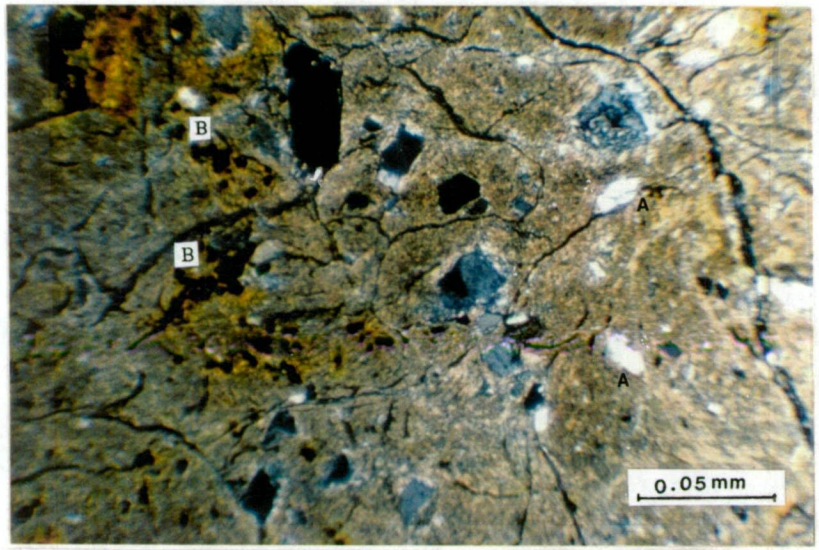

Plate 32.Fabric, UF4, 70 cm depth , (A). Quartz (SiO_2 95.3%) ; (B). iron nodules (FeO 12.7%). (X 50 crossed polarizers).

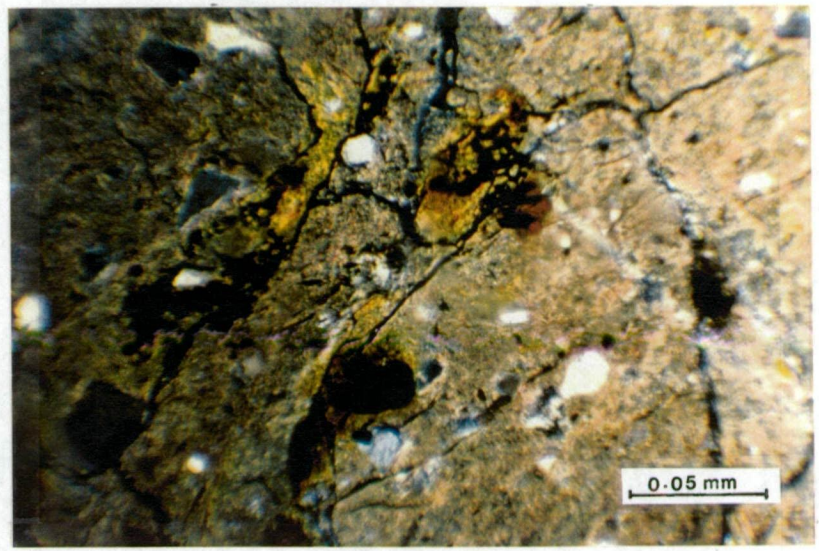

Plate 33.Fabric UF4, 70 cm depth, Ferraric plectic porphyric.(X 50 crossed polarizers).

5.4. UF4 (Duplex soil)

5.4.1. Field-observed soil morphology

A detailed profile description and photograph (plate 4) of the duplex soil UF4 are given on page 109. The surface horizon from 0 to 10 cm depth, is a sandy loam with weak medium angular blocky structure and an abrupt irregular boundary. Below 10 cm depth the profile is dominated by medium heavy clay to heavy clay with a moderate, coarse, prismatic structure. It is also very firm and of low permeability. The heavy clay subsoil shows planar voids and sand infills down cracks which have developed due to shrinking and swelling. This profile shows the characteristics of a mottled, brown, duplex soil (Northcote *et al,* 1975).

Soil colour is brown to greyish brown (10YR 4/2 - 5/2) in the surface changing to dark brown (10YR 3/4) from 10 to 38 cm depth. Below 38 cm depth the colour changes again to dark greyish yellow (2.5Y 5/2). The black mottles in the upper clay subsoil represent mixing by earthworms and movement of dispersed organic matter down cracks, while the brighter yellowish brown mottles and paler matrix colours suggest periodic reducing conditions existed during soil formation. Many soft segregation of iron in voids and coating the outside of some peds are found below 27 cm depth.

5.4.2. Physical characteristics

Figure 18 shows the depth functions for the various particle size fractions; detailed data are given in Appendix 1, Table 25. Clay and fine sand content have an opposite trend with depth.

Clay content increases sharply with depth going from 25 to 58 % from the surface to 27 cm depth before also dropping back sharply to about 35% by 50 cm depth. This is followed by a slower decrease to 28% for the 70 - 86 cm depth interval. Below this there are highs (33.5% and 35%) at 98 - 109 cm and 128 - 142 cm and lows (28% and 23.5%) at 117 - 128 cm and142 - 160 cm depth.

Fine sand decreases rapidly with depth from 51.1% in the surface (0 - 5 cm) to 27-29% at 20 - 40 cm. Below this fine sand increases sharply to about 39% by 46 cm then

Depth (cm)	Description UF4
0 - 5.	Dark greyish brown (10 YR 4/2 moist); sandy loam; weak medium (5-10 mm) subangular blocky structure; weak moist strength; slightly sticky; slightly plastic, normal plastic; many medium roots; diffuse smooth boundary,
5 - 10.	Greyish brown (10 YR 5/2 moist); very few fine distinct black (10 YR 2/1) mottles; sandy loam; weak medium (5-10 mm) subangular blocky structure; weak moist strength; slightly sticky; slightly plastic, normal plastic; many medium roots; abrupt irregular boundary,
10 - 27	Dark yellowish brown (10 YR 3/4 moist); few medium distinct yellowish brown (10 YR 5/4) and few black (10 YR 2/1) mottles; medium heavy clay; moderate coarse (10-20 mm) prismatic structure; very firm moist strength; very sticky; very plastic, normal plastic; many medium roots; common iron rich soft segregations; diffuse smooth boundary,
27 - 38	Dark yellowish brown (10 YR 3/4 moist); common coarse distinct brownish yellow (10 YR 6/8) mottles; medium heavy clay; moderate coarse (10-20 mm) prismatic structure; very firm moist strength; very sticky; very plastic, normal plastic; many medium roots, many iron rich soft segregations; diffuse smooth boundary,
38 - 98	Greyish brown (2.5 Y 5/2 moist); common coarse distinct yellowish brown (10 YR 5/8) and few dark red (2.5 YR 3/6) mottles; medium heavy clay; moderate coarse (10-20 mm) prismatic structure; strong moist strength; very sticky; very plastic, normal plastic; few fine roots; many iron rich soft segregations; diffuse smooth boundary,
98 - 128	Dark greyish yellow (2.5 Y 4/2 moist); few medium distinct yellowish brown (10 YR 5/8) and few dark red (2.5 YR 3/6) mottles; sandy medium heavy clay; moderate medium (5-10 mm) prismatic structure; strong moist strength; moderately sticky; moderately plastic, normal plastic; many iron rich soft segregations; diffuse smooth boundary,
128 - 160	Greyish yellow (2.5 Y 5/2 moist); few medium distinct yellowish brown (10 YR 5/8) mottles; sandy medium heavy clay; moderate medium (5-10 mm) prismatic structure; strong moist strength; moderately sticky; moderately plastic, normal plastic; many iron rich soft segregations.

Plate 4. Profile UF4

increasing gradually to peak at 44% just above 90 cm depth before dropping back to 40% just above 110 cm depth and then rising gradually to 50% in the 142 - 160 cm depth interval. Infills of fine sandy materials were observed in the subsoil and may be due to fine sand entering cracks produced due to shrinking of the clayey subsoil on drying.

The silt fraction is high (17%) in the topsoil to about 20 cm but then drops to lower levels throughout the lower profile ranging from about 8 to 13%.

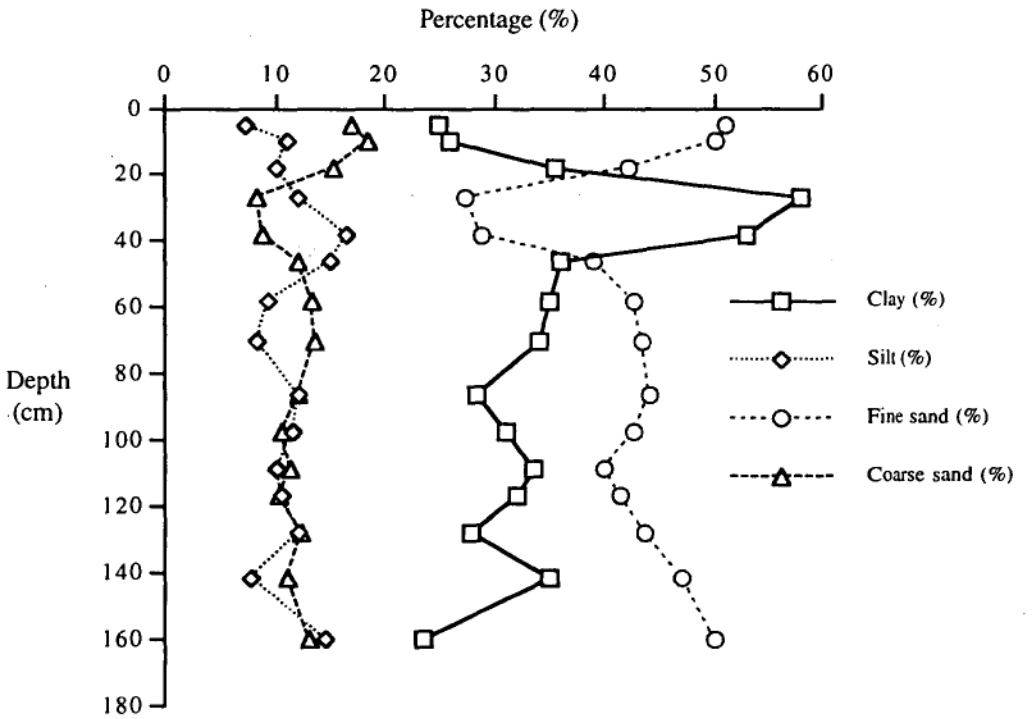

Figure 18. Depth functions of clay, silt, fine sand and coarse sand, UF4

Figure 19 shows depth functions of bulk density and clay content. There is no parallelism between bulk density and clay content with depth apart from the initial increase in both above 20 cm.

Bulk density increases steadily from the surface to 27 cm depth ranging from 1.43 to 1.65 g/cm^3 possibly due to soil compaction associated with soil cultivation when wet or to increased clay content. Bulk density gradually increases to 1.93 g/cm^3 by 98 cm. This may be due to regular shrinking and swelling associated with wetting and drying cycles.

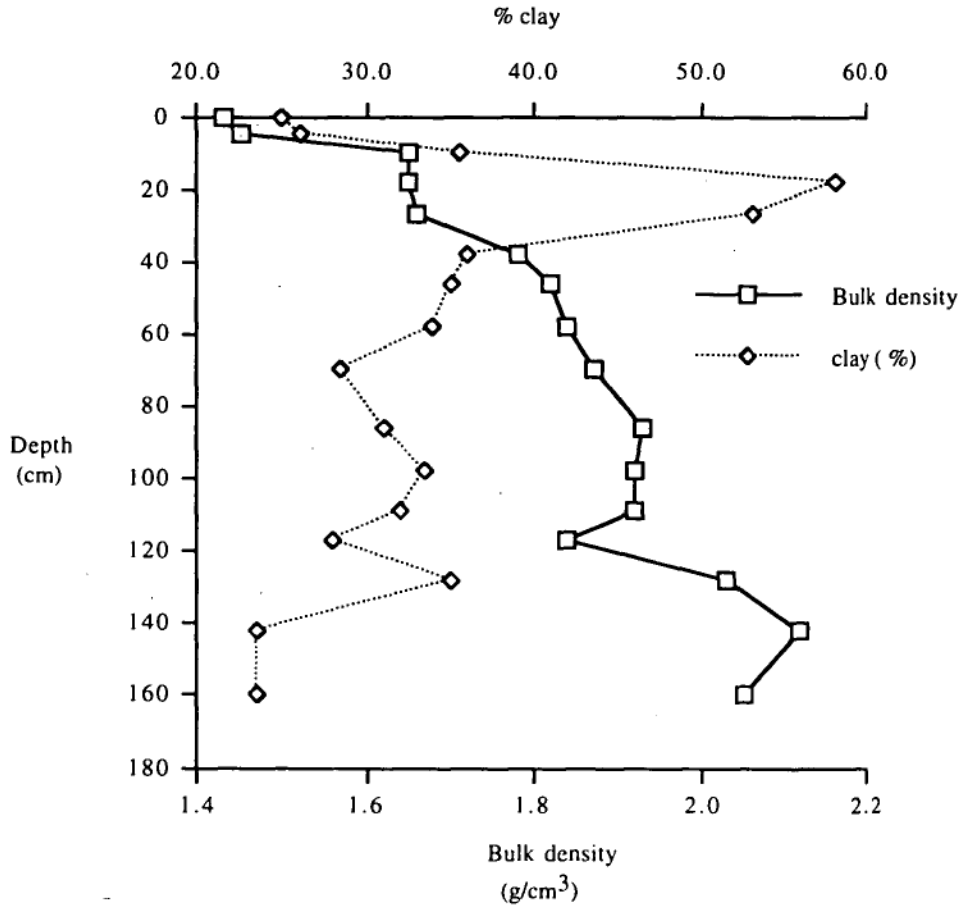

Figure 19. Depth functions of clay content and bulk density, UF4

This vertic behaviour attributable to a mixed smectite and kaolinite mineralogy (refer to Table 16). As previously discussed the shrinking allows sandy surface material to enter the subsoil, via cracks, increasing the volume of material in a confined in the subsoil. The bulk density then slowly decreases to 1.84 at 128 cm. Below 128 cm depth bulk density increases to 2.12 g/cm^3. The relatively high bulk density in the subsoil is also partly due to the presence of many soft segregations of iron (see Plate 4).

As already mentioned the clay content increases rapidly with depth, 25% up to 58%, from the surface to 27 cm depth. This highlights the major textural boundary between the sandy topsoil and a clay rich subsoil. The clay content decreases gradually reaching 28.5% at 86 cm depth. The high clay content in the 20-50 cm "clay bulge" zone is possibly due clay translocation from the topsoil layers. Translocation of clay would be aided by clay dispersion associated with high levels of exchangeable Na^+ (Figure 21).

The clay content increases again between 86 and 109 cm depth, changing from 28.5 to 33.5%. Below 109 cm clay content tends to decrease to 23.5 %. This sharp decrease in clay content in the lower profile may represent a discontinuity in the Tertiary sediment substrate (see section 5.4.7).

5.4.3. Chemical characteristics

Detailed data are given in Appendix 1, Table 25.

Figure 20 shows depth functions for both pH (H_2O) and electrical conductivity. The pH (H_2O) and electrical conductivity to have a somewhat opposite trends with depth.

The profile is moderately to strongly acid to a depth of about 130 cm with pH ranging between 5.7 and 5.3. Below this the soil is slightly acid. The pH (1:5 H_2O) increases from 5.5 at the surface to 5.7 at 18 cm depth. Below 18 cm the subsoil pH is strongly acid (pH 5.3 at 86 cm depth) but rises to just above pH 6 by 142 cm depth.

Electrical conductivity decreases from 0.11 dS/m at the surface to 0.06 dS/m at 18 cm depth. Below 18 cm depth electrical conductivity gradually increases to 0.19 dS/m at 109 cm depth before decreasing below 109 cm to 0.12 dS/m. Thus this soil would be classified as non saline according to Doyle (1993).

Figure 21 shows the depth functions of basic exchangeable cations; Ca^{2+}, Mg^{2+} and Na^{+}. There is a clear dominance of exchangeable Mg^{2+} in the subsoil although levels of magnesium decrease below 117 cm. Exchangeable Ca^{2+} and Mg^{2+} are co-dominant in the upper profile.

Exchangeable Na^{+} decreases slightly from the surface to 10 cm depth dropping from 0.72 to 0.38 cmol(+)/kg. Below 10 cm exchangeable Na^{+} gradually increases from 0.38 reaching 5.8 cmol(+)/kg by 117 cm. Below 117 cm exchangeable Na^{+} slowly decreases to 4.66 cmol(+)/kg at 160 cm depth. The exchangeable sodium percentage (ESP) is about 7 or 8 in the surface layers but increases below 46 cm to values between 10 and 20. This indicates the subsoil would be classed as sodic in the schemes of both Northcote and Skene (1972) and Isbell (1996). The moderate levels of exchangeable sodium explain the clay dispersivity observed in the field profile.

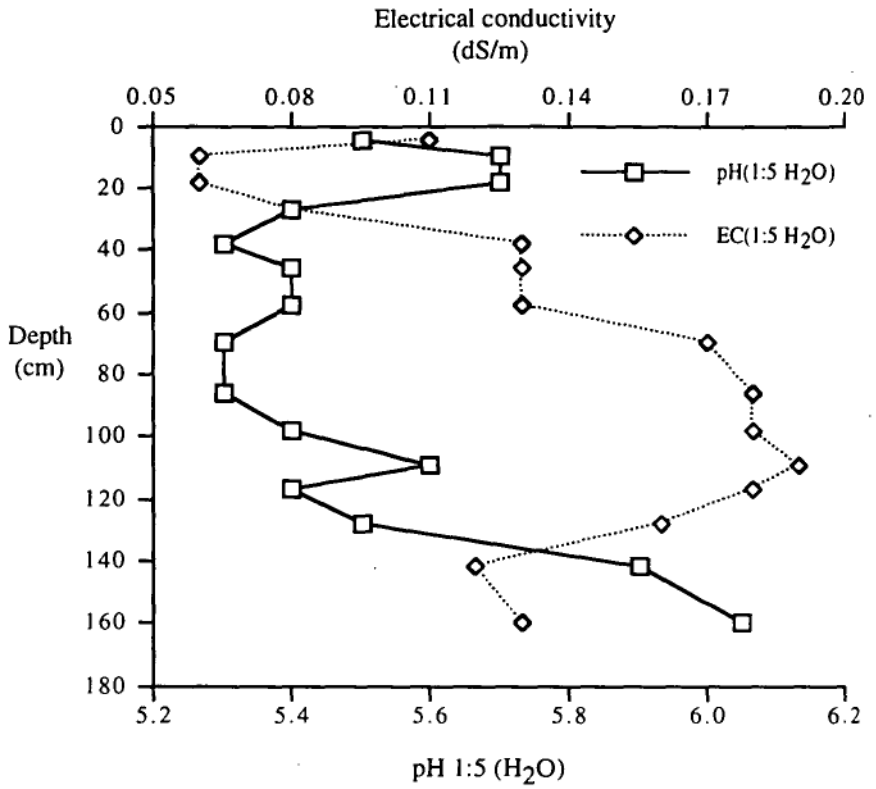

Figure 20. Depth functions of pH (1: 5 H_2O) and electrical conductivity (EC 1: 5 H_2O), UF4

Exchangeable Mg^{2+} is 8.5 cmol(+)/kg in the surface 0 - 5 cm, then decreases to 5.6 cmol(+)/kg at 10 cm depth but increases steadily to 24.8 cmol(+)/kg at 117 cm depth. Below 117 cm depth exchangeable Mg^{2+} decreases abruptly to be only 14.8 cmol(+)/kg by 160 cm.

High exchangeable Na^+ and Mg^{2+} in the subsoil are common to most Australian sodic soils which also exhibit poor physical conditions such as very tough dry soil strength, low permeability, poor aeration and clay dispersivity (Rengasamy and Olsson, 1991).

Although co-dominant with exchangeable Mg^{2+} above 30 cm, exchangeable Ca^{2+} decreases rapidly from the 0 - 5 cm value of 12.6 to about 6 cmol(+)/kg by 40 cm. Below 40 cm calcium continues to decrease to values less than 4.0 cmol(+)/kg.

Exchangeable K^+ (not shown in Figure 21) is relatively low throughout the profile ranging from 0.15 to 0.55 cmol(+)/kg (Table 25).

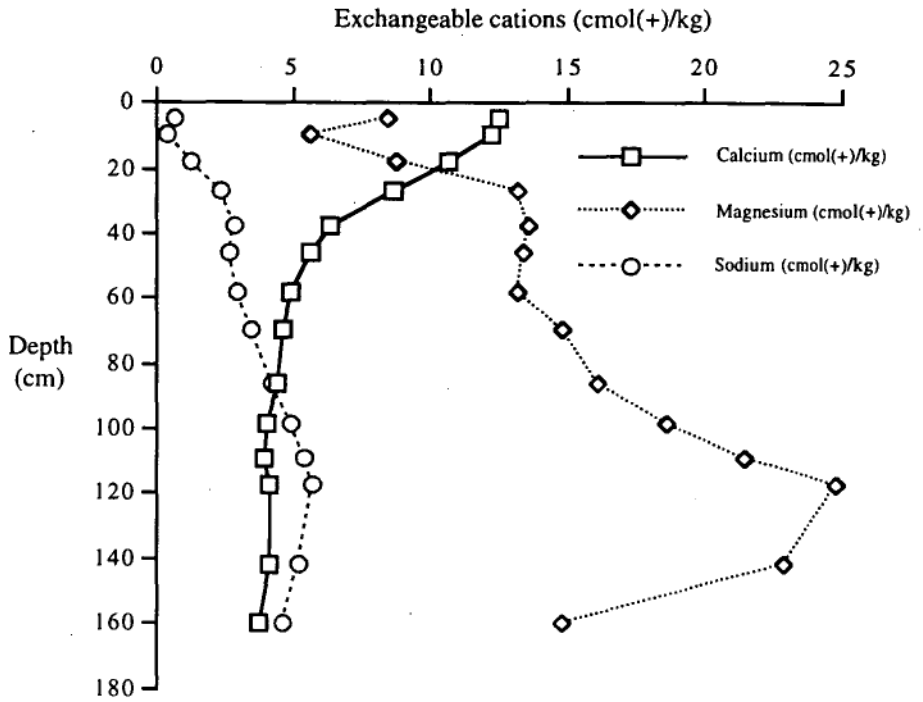

Figure 21. Depth functions of exchangeable Ca^{2+}, Mg^{2+}, and Na^{+}, UF4

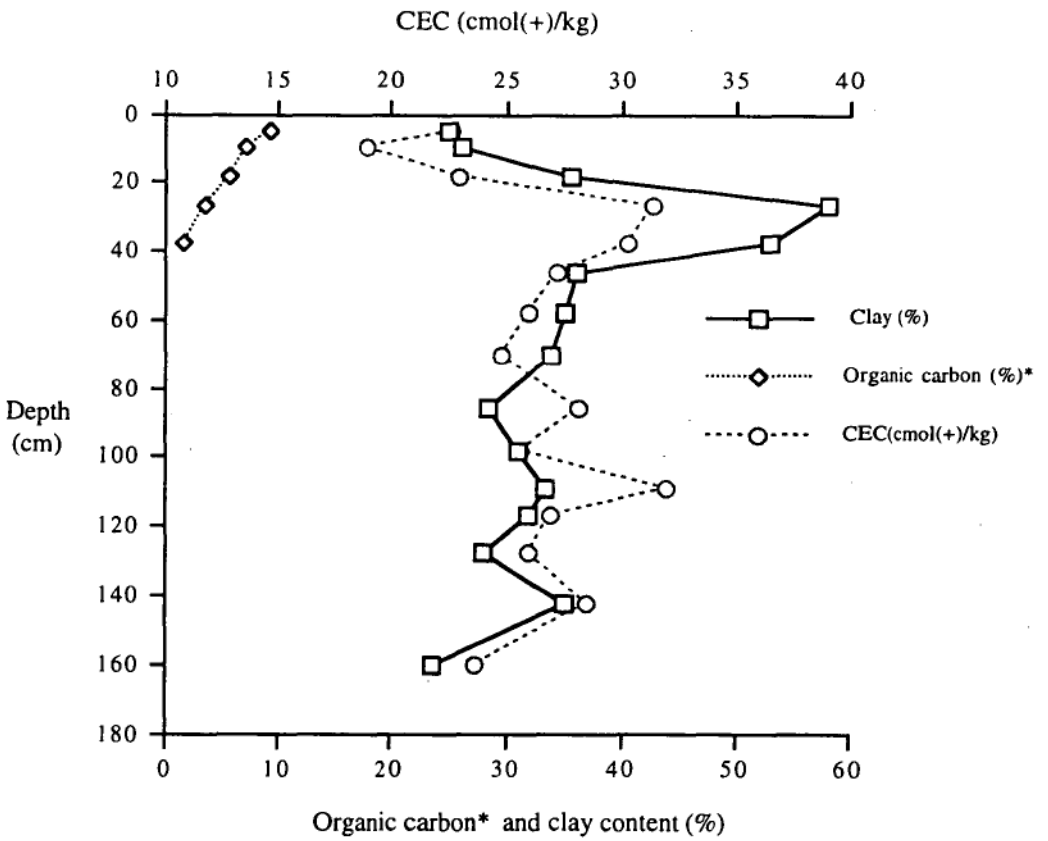

Figure 22. Depth functions of CEC, organic carbon and clay content, UF4.
*Organic carbon data are x 4

Figure 22 shows the depth functions of clay content, organic carbon and cation exchangeable capacity (CEC). There is a close relationship between clay content and CEC with depth. Organic carbon decreases steadily from the surface to 40 cm.

Clay content increases sharply from the surface to 27 cm increasing from 25% to about 58% in the area of the "clay bulge". Higher CEC is also associated with this zone of high clay content.

Cation exchange capacity is 22.6 cmol(+)/kg in the surface 0 - 5 cm then decreases to 18.9 cmol (+)/kg at 10 cm depth in association with decreasing organic carbon levels. The organic carbon gradually decreases from 2.26 % in the surface 0 - 5 cm to 0.39 % at 38 cm depth (Table 18). Cation exchange capacity rapidly increases to 31.4 cmol(+)/kg at 27 cm depth in the region of the "clay bulge". Below 27 cm depth CEC tends to decrease gradually to 23.7 cmol(+)/kg along with the decrease in clay content. Clearly in all but the upper 20 cm the CEC is dictated by the clay content. However, the relatively higher ratio of clay content to CEC in the upper 80 cm of the profile, in comparison with the lower 80 cm of the profile, suggests a change in the clay mineral composition. This is supported by the X-ray diffraction data which show a high amount of kaolinite in the topsoil and greater amounts of smectite in the subsoil (refer to Table 16).

5.4.4. X ray diffraction analysis of clay fractions

Table 16 shows the dominance of kaolinite throughout the profile with smectite in moderate proportion in the subsoil (below 98 cm). The domination of kaolinite in the upper layers is probably due to greater weathering effects near the surface. This feature of higher amounts of kaolinite in the surface was also seen in profiles UF2 and UF3. The domination of smectite in the subsoil causes shrinking when the subsoil dries, and swelling on re-wetting. This swelling causes low permeability, poor aeration and can result in saturation of the upper profile in wet periods.

Table 16. Semi quantitative X ray diffraction analysis, UF4
t - trace (<10%); l - little(11-25%) ; md - moderate(26-50%); m - much(>50%)

profile	depth (cm)	Smectite	Kaolinite	Illite
UF4	27 - 38	l	m	-
	98 - 109	md	m	-
	>160	md	m	-

5.4.5. Micromorphology

Detailed analytical data are given in Table 48 and 49 (see Appendix 2).

Plate 32 shows detailed features of a sample taken at 70 cm depth. Features marked (A) have proven to be quartz (95.3 % SiO_2) by both electron microprobe analysis and petrographic microscopy. Features marked (B) are considered small iron oxide accumulations (12.7 % FeO).

Plate 33 shows the micromorphological structure at 70 cm depth. The plate illustrates iron oxide coating coarse quartz grains with the surrounding matrix of soil identified as ferraric plectic porphyric fabric (Brewer and Sleeman, 1988).

5.4.6. Mineralogy of sand fraction

Table 17 shows that ilmenite and iron oxide are more dominant throughout the profile while leucoxene, zircon, tourmaline, rutile and pyroxene are minor minerals.

Zircon is relatively high in the surface horizons then decreases abruptly in the subsoil. Tourmaline and leucoxene occur in only trace amounts throughout the profile.

The distribution of quartz (Table 18) is high throughout the profile while K-Feldspar is at trace levels throughout the profile. Calcic plagioclase is low in the topsoil and not detected between 38 cm and 86 cm depth but increases again below 128 cm depth. The increase in both pyroxene and plagioclase below 128 cm support the idea of a doleritic provenance for the Tertiary sediments forming the substrate in this soil.

Table 17. Heavy mineral analysis of sand fraction, (177 micron) UF4.

Depth (cm)	(0 - 5)	(5 - 10)	(38 - 46)	(70 - 86)	(128 - 142)	(> 160)
Minerals						
Ilmenite	moderate	moderate	moderate	moderate	moderate	moderate
Leucoxene	trace	trace	trace	trace	trace	trace
Zircon	moderate	little	trace	trace	trace	trace
Tourmaline	trace	trace	trace	trace	trace	trace
Rutile	little	trace	little	little	trace	trace
Iron oxide	little	moderate	moderate	moderate	moderate	moderate
Pyroxene	trace	little	n.d	trace	trace	moderate

n.d = not detected

Table 18. Light mineral analysis of sand fraction, (177 micron) UF4.

Depth (cm)	(0 - 5)	(5 - 10)	(38 - 46)	(70 - 86)	(128 - 142)	(> 160)
Minerals						
K-Feldspar	trace	trace	trace	trace	trace	trace
Plagioclase	trace	trace	n.d	n.d	little	little
Quartz	much	much	much	much	much	much

n.d = not detected

5.4.7. Origin of materials and soil formation

The UF4 profile lies on a gentle footslope position (7% slope) 50 m down slope and 6 m below UF3 and 60 m up slope of UF5.

This duplex profile examined to a depth of 170 cm comprises at least two distinct kinds of material. A clear textural boundary exists between the sandy topsoil and a clay rich subsoil. These two materials are also distinguished by marked changes in macro-morphological (colour, pedality, consistence), physical, chemical and mineralogical characteristics.

The presence of calcic plagioclase and pyroxene in the topsoil suggests that this upper material is partly derived from doleritic materials. However the high percent fine sand, much of which is well rounded, together with the presence of high amounts of quartz and zircon and minor K-feldspar and rutile in the topsoil suggests it is also partly derived from Triassic sandstone and/or Permian mudstone sources. Thus the sandy surface soil may be

reworked more recent sand deposits derived by aeolian transport from an exposed Pitt Water Bay floor as in the case of UF2 and UF3 (Holz, 1994; Leaman, 1971).

The mixed kaolinite and smectite mineralogy of the subsoil results in shrinkage and cracking on drying and the development of planar voids. These planar voids allowed translocation of fine sand from the upper profile down open cracks into the clayey subsoil to a depth of about 80 cm.

The subsoil material below 120 cm has less clay and more pyroxene and plagioclase and thus represents a less weathered layer of Tertiary sediment, possibly of more doleritic provenance.

As seen in UF2 the clay bulge in the upper subsoil (30 cm - 50 cm) may be due to one of three processes or some combination of them. These are: 1) more intense weathering of primary and secondary minerals near the soil surface, 2) clay translocation from the topsoil, or 3) the clay may be an inherited feature of the apparent parent Tertiary sediment. The higher proportion of kaolinite and lower amounts of pyroxene and plagioclase, in the upper profile, support the former view. The absence of depositional argillans suggests that clay translocation cannot have been a significant process and the extremely slow permeability of the clay would also seem to preclude its occurrence. Weathering and inheritance seem to be the best options.

A gradual increase in exchangeable sodium and ESP was evident from 0 to 120 cm with a slight decrease below 120 cm depth. Magnesium was the dominant exchangeable cation, apart from the topsoil where calcium is co-dominant. Magnesium increases with depth to very high levels between 100 cm and 140 cm. These properties and the acidity of the profile are in accord with properties of soloths (Stace *et al*, 1968). The high clay content together with high levels of exchangeable Na^{+} and Mg^{2+} in the subsoil is a common feature of Australian sodic soils (Rengasamy and Olsson, 1991). These soils exhibit poor physical conditions ie. tough and compact pedality, poor aeration and poor plant root environments and both swelling and dispersivity on wetting. Salinity, although increasing to nearly a metre depth, is never more than slight.

5.4.8. Soil classification

According to a new classification system for Australian soil (Isbell, 1996) this profile may be classified as "Brown Mottled Subnatric Sodosol". This classification explains the key features of the overall profile such as texture contrast, high sodium percentage and subsoil colour with significant mottling.

The US Soil Taxonomy classification(Soil Survey Staff, 1975) is "Typic Natrustalf". This emphasises the sodic nature of soil, the ustic moisture regime and texture contrast.

5.5. UF5 (Duplex soil)

5.5.1. Field-observed soil morphology

A detailed profile description and photograph (plate 5) of the duplex soil, UF5, are given on page 121. The surface horizon is sandy loam down to 20 cm depth with very weak medium angular blocky structure and a clear lower boundary. Below 20 cm depth the profile is dominated by medium clay to 85 cm before changing to a light clay below 85 cm. A moderate, coarse prismatic structure is typical of the upper clayey subsoil changing to weak, coarse angular blocky structure in the lower subsoil. Many soft segregations of iron oxide occur below 30 cm depth. Examination of the subsoil showed sand infills down cracks. These cracks have developed due to shrinking on drying. Dolerite clasts were found continuing from 156 cm depth making up about 50% of the material. According to Northcote *et al,* (1975) this profile is a mottled, brown, duplex soil.

The matrix colour is dark greyish brown (10YR 4/2) in the surface horizon changing to greyish brown (10YR 5/2) in the lighter lower topsoil (10-20 cm). In the upper subsoil, below 20 cm, the matrix colour is brown (10YR 4/4) with a few reddish brown (5YR 5/8) and some black (10YR 5/3) mottles. These mottle patterns are an indication of oxidation and reduction processes causing iron and manganese mobilisation and re-precipitation. Below 85 cm depth the matrix colour changes to greyish olive (5Y 5/3) with some yellowish brown (10YR 5/6) mottling. These redoximorphic features (Soil Survey Staff, 1975) suggest poor aeration and restricted drainage in the clay subsoil.

5.5.2. Physical characteristics

Detailed physical data are given ion Appendix 1, Table 26.

Figure 23 shows depth functions for the various particle size fractions. The clay content and coarse sand have an opposite trend with depth. Clay content is 20.5% in the surface 0 - 10 cm but increases abruptly to 37% at 30 cm and reaches 47% by 40 cm depth. Below 40 cm clay content then gradually decreases to reach about 20% at 150 cm. Below 150 cm, clay again increases from 20% to 28.5%. This clay content trend, once again, illustrates a "clay bulge" in the 30-70 cm depth range. This "clay bulge" may have formed due to one or more of three main factors; 1) preferential weathering of primary minerals in the upper subsoil due to its proximity to the soil surface, 2) clay translocation form the topsoil to the subsoil, or 3) the clay may be an inherited feature of the parent Tertiary sediment (Doyle, personal communication). The relative merits of each of these possibilities will be discussed more fully in the soil formation section (5.5.6). The zone of low clay content between 130 cm and 156 cm and may represent stratification of the parent sediment (discussed further in the section on soil formation).

Fine sand is relatively variable throughout the profile ranging from 12.1% to 21.5%. However there is a clear accumulation of fine sand in the surface material (0-20 cm). The variations in the silt content down the profile (ranging from 8.5% to 14.5%) generally follow the clay content changes.

Coarse sand increases slightly from the surface to 20 cm depth going from 53.5 to 57%. Below 20 cm coarse sand decreases sharply reaching 37 % at 40 cm depth. Coarse sand then gradually increases to 58.7 % by 150 cm depth. The increase in coarse sand with depth in the lower subsoil may be due to infilling of sandy materials down cracks, less weathering of primary minerals in the lower subsoil or stratification of the parent sediments. Below 150 cm the coarse sand decreases to between 43% and 50%. This profile has a high coarse sand content in comparision to the UF2, UF3 and UF4 soils. The

Depth (cm)	Description UF5
0 - 10.	Dark greyish brown (10 YR 4/2 moist); sandy loam; very weak medium (5-10 mm) angular blocky structure; weak moist strength; slightly sticky; slightly plastic, normal plastic; many medium roots; clear wavy boundary,
10 - 20	Greyish brown (10 YR 5/2 moist); few medium distinct yellowish red (5 YR 5/8) and black (10 YR 2/1) mottles; sandy loam; weak medium (5-10 mm) angular blocky structure; weak moist strength; slightly sticky; slightly plastic, normal plastic; many medium roots; many planar voids; few iron nodules; with clear smooth boundary,
20 - 30	Brown (10 YR 4/4 moist); few medium distinct dark red (2.5 YR 4/8), yellowish red (5 YR 5/8) and black (10 YR 2/1) mottles; medium clay; moderate coarse (10-20 mm) prismatic structure; very firm moist strength; very sticky; very plastic, normal plastic; many medium roots; many iron soft segregations; many planar voids; diffuse smooth boundary,
30 - 85	dark greyish brown (10 YR 4/2 moist); few medium distinct dark red (2.5 YR 4/8), yellowish red (5 YR 5/8), and black (10 YR 2/1) mottles; medium clay; moderate coarse (10-20 mm) angular blocky structure; very firm moist, strength; very sticky; very plastic, normal plastic; common fine roots; many iron soft segregations; diffuse smooth boundary,
85 - 123	Olive (5 Y 5/3 moist); few medium distinct yellowish brown (10 YR 5/6) mottles; light clay; weak coarse (10-20 mm) angular blocky structure; very firm moist strength; very sticky; very plastic, normal, plastic; many iron soft segregations; gradual wavy boundary,
123 - 145	Olive (5 Y 5/3 moist); few medium distinct olive yellow (2.5 Y 6/6) and yellowish red (5 YR 5/8) mottles; light clay; weak medium (5-10 mm) prismatic and angular blocky structure; firm moist, strength; very sticky; very plastic, normal plastic; many iron soft segregations; gradual wavy boundary,
145 - 156	Olive (5 Y 4/4 moist); few medium distinct light olive brown (2.5 Y 5/6) and black (10 YR 2/1) mottles; light clay; weak medium (5-10 mm) angular blocky structure, firm moist strength; very sticky; very plastic, normal plastic; many iron soft segregations; diffuse smooth boundary,
156 - 190	Olive brown (2.5 Y 4/4 moist); few medium distinct light olive brown (2.5 Y 5/6) and black (10 YR 2/1) mottles; light clay; weak medium (5-10 mm) angular blocky structure; firm moist strength; very sticky; very plastic, normal plastic; about 50% of the material is very coarse cobbles (>60 mm diameter) of weathered dolerite.

Plate 5. Profile UF5

coarse sand may be a reflection of a mixed parent material and this is supported by the presence of dolerite clasts in the lower profile.

Figure 24 shows the relationship between bulk density and clay content of the fine earth with depth. Clay content and bulk density have a weakly similar trend, although the bulk density is relatively considerably higher in the 100 to 140 cm depth range.

Bulk density increases sharply from the surface horizon to 40 cm depth rising from 1.43 to 1.83 g/cm^3. Bulk density then decreases slightly to 1.77 g/cm^3 at 60 cm before increasing to 2.02 g/cm^3 at 115 cm depth. Below 115 cm bulk density decreases gradually reaching 1.63 g/cm^3 by 190 cm depth. The high bulk density and high clay content in the subsoil result in low permeability, poor aeration and the development of redoximorphic features (Soil Survey Staff, 1975).

5.5.3. Chemical characteristics

Detailed chemical data are given in Appendix 1, Table 26.

Figure 25 shows depth functions for pH(H_2O) and electrical conductivity. The surface soil is slightly acid and decreases to moderately acid in the upper clay subsoil (30-70 cm). Below 70 cm the pH increases gradually from neutral to slightly alkaline.
The electrical conductivity decreases slightly from the surface to 20 cm depth from 0.06 to 0.04 dS/m. It then increases to 0.33 dS/m in the upper subsoil. The EC then decreases slowly reaching 0.24 dS/m by 150 cm before slightly increasing to 0.33 dS/m in the very lower subsoil. The topsoil is considered non saline while the subsoil is slightly saline (Doyle, 1993).

Figure 26 shows depth functions of basic exchangeable cations; Ca^{2+}, Mg^{2+} and Na^{+}. As with profiles UF2, UF3 and UF4, exchangeable Mg^{2+} and Ca^{2+} are co-dominant in the top soil, while magnesium is the dominant exchangeable cation in the subsoil. Exchangeable Na^{+} also follows the trends seen in the other three duplex soils, increasing gradually with depth.

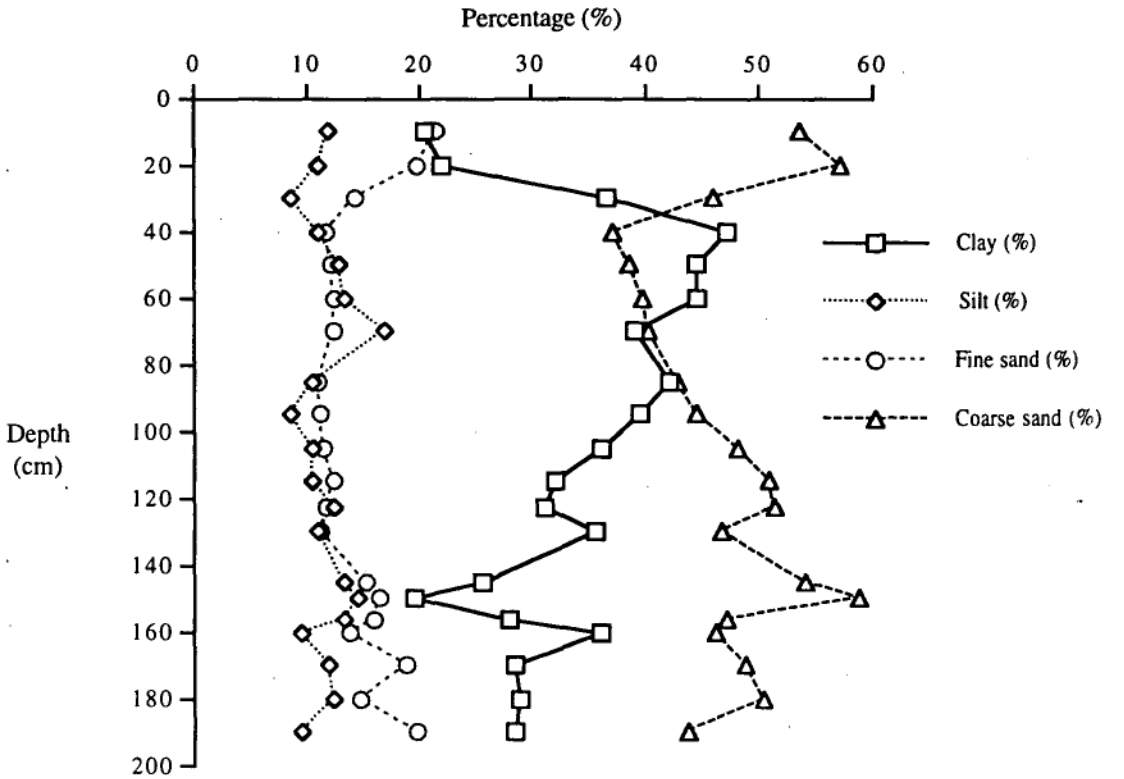

Figure 23. Depth functions of clay, silt, fine sand and coarse sand, UF5

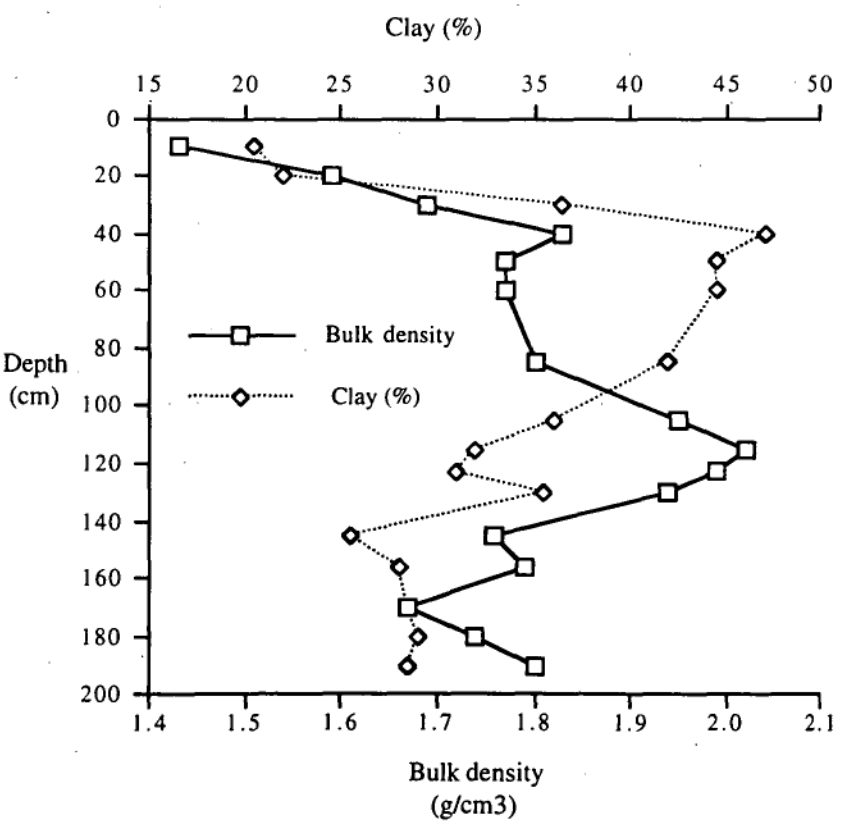

Figure 24. Depth functions of clay content and bulk density, UF5

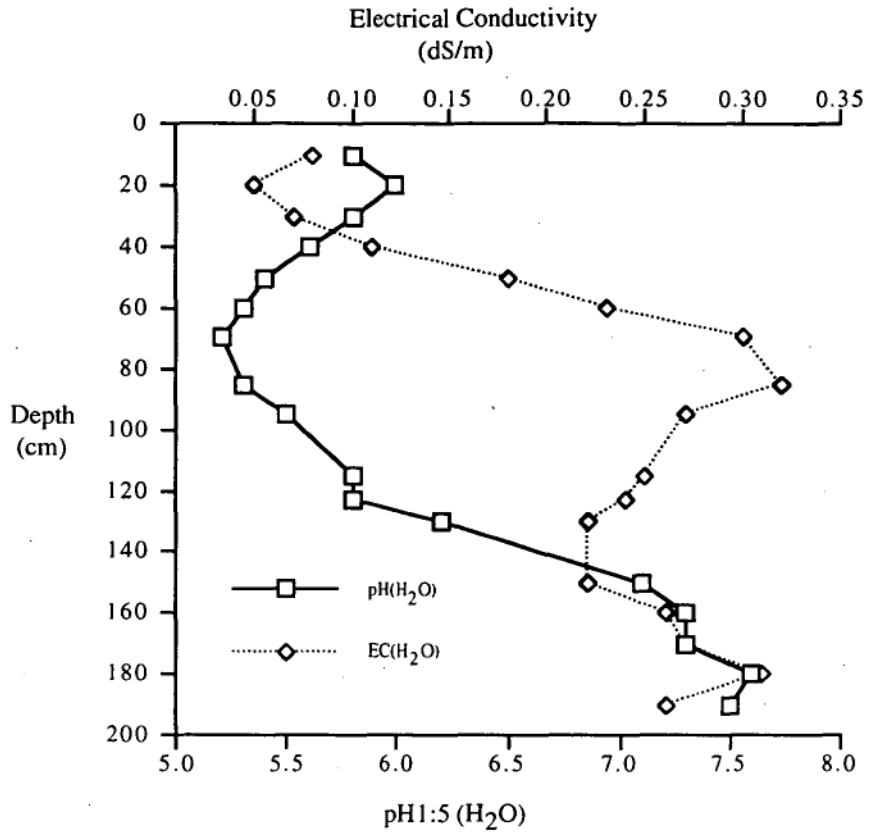

Figure 25. Depth functions of pH(1:5 H_2O) and electrical conductivity (EC 1:5 H_2O), UF5

Exchangeable Mg^{2+} decreases from 13.2 cmol(+)/kg in the surface to 10.4 cmol(+)/kg at 20 cm depth. It then gradually increases reaching 29 cmol(+)/kg at 105 cm. Exchangeable Mg^{2+} decreases sharply to 12.1 cmol(+)/kg between 130 cm and 160 cm, suggesting some kind of discontinuity at this depth. Below 156 cm depth Mg^{2+} increases to 23.4 cmol(+)/kg.

Exchangeable Na^{+} gradually increases from 0.1 cmol(+)/kg at the surface to about 6.0 cmol(+)/kg at 130 cm. From 130 cm to 150 cm exchangeable Na sharply decreases to 3.5 cmol(+)/kg and then sharply increases again to 7.6 cmol(+)/kg at 160 cm, also suggesting some kind of discontinuity. Sodium then gradually decreases below 160 cm to about 6.5 cmol(+)/kg. Exchangeable sodium percentage is below 10% from the surface to 30 cm depth then increases from 10% to 23% below 30 cm. Thus this soil can be considered sodic in both the schemes of Northcote and Skene (1972) and Isbell (1996).

Exchangeable Ca^{2+} which is co-dominant in the surface decreases rapidly, along with organic carbon, from 15.2 cmol(+)/kg to about 7.0 cmol(+)/kg by 50 cm depth.

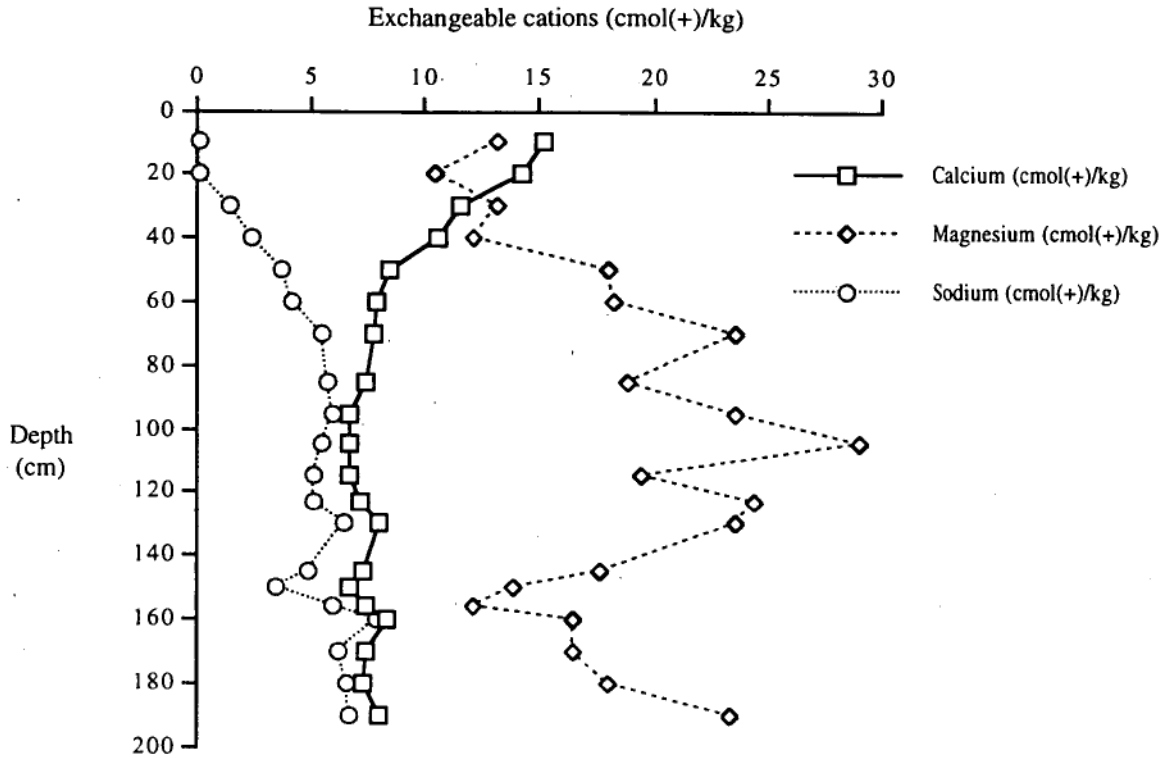

Figure 26. Depth functions of exchangeable Ca^{2+}, Mg^{2+}, and Na^{+}, UF5

The decrease continues more gradually between 50 cm and 115 cm reaching 6.5 cmol(+)/kg. A slight increases to 8.3 cmol(+)/kg occurs below 120 cm.

Exchangeable K^{+} (not shown) is relatively low throughout the profile ranging from 0.1 cmol(+)/kg at the surface to 0.4 cmol (+)/kg in the subsoil (see Table 26).

Figure 27 presents the depth functions of clay content, organic carbon and CEC. There is a tendency for clay content and CEC to have a similar trend with depth. Organic carbon decreases rapidly below the surface. The clay content increases from about 20 % in the surface layers to 47% in the upper subsoil. Below 40 cm clay content of the fine earth gradually decreases to a depth of 190 cm.

The cation exchange capacity decreases from 29 cmol(+)/kg in the surface to 24.8 cmol(+)/kg at 20 cm. This is probably related to the drop in organic carbon which decreases fro 2.0 in the surface to 1.28 % at 30 cm depth. Below 20 cm the CEC increases gradually reaching 41.8 cmol(+)/kg at 105 cm. CEC then slowly decreases to reach 24.2 cmol(+)/kg at 156 cm. Below 156 cm CEC increases to 38.4 cmol(+)/kg.

The rapid increase in CEC below 20 cm is clearly related to the sharp increase in clay content. However, the clay in the upper subsoil is higher in kaolinite while in the subsoil smectite is dominant (Table 19). This factor results in higher CEC values in the lower subsoil, below about 70 cm, despite lower clay contents when compared with the upper subsoil.

The sharp decrease in both CEC and clay content between 130 cm and 160 cm may indicate a discontinuity in the profile (Figure 27). Both CEC and clay content increase again in the lower subsoil. The increase in CEC is due to clay content increase and the dominance of smectite (Table 19).

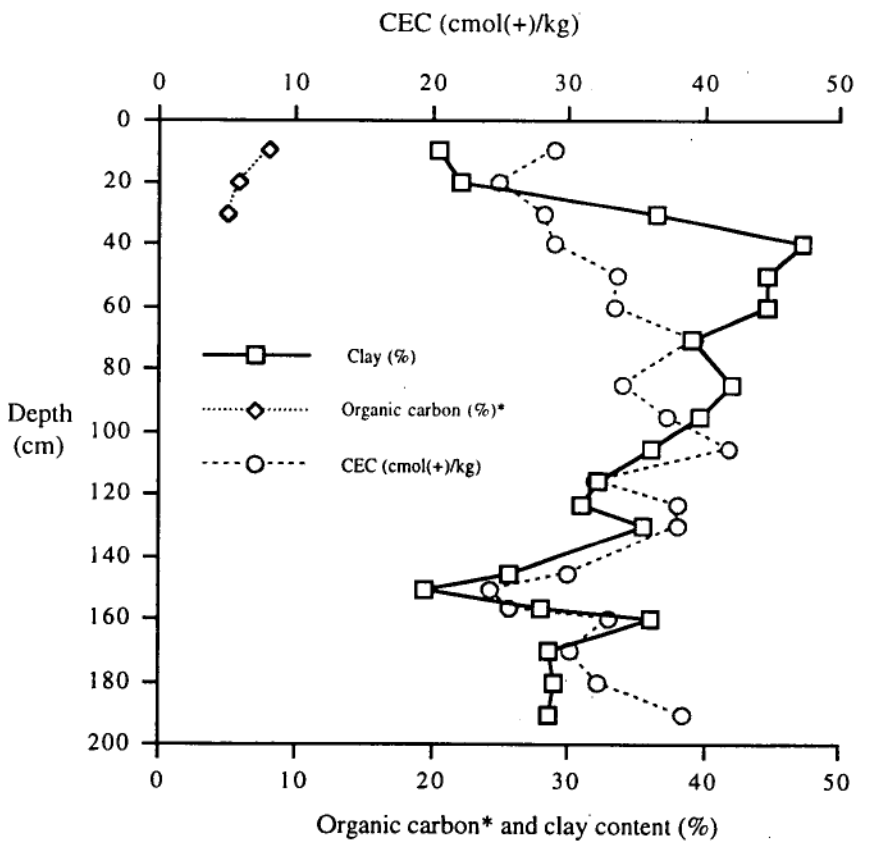

Figure 27. Depth functions of CEC, organic carbon and clay content, UF5
* Organic carbon data are x 4

5.5.4 X ray diffraction analysis of clay fractions

Table 19. Semi quantitative X ray diffraction analysis, (UF5)
t - trace (<10%); l - little(11-25%) ; md - moderate(26-50%); m - much(>50%)

profile	depth (cm)	Smectite	Kaolinite	Illite
UF5	10 - 20	md	m	-
	85 - 95	md	m	-
	180 - 190	m	md	-

Data in Table 19 show kaolinite is dominant over smectite in the upper profile while smectite is dominant over kaolinite in the deep subsoil. The domination of kaolinite in the upper profile indicates that more intense weathering has occurred in the surface materials. The "clay bulge" may be due to greater *in situ* weathering of primary minerals to form secondary minerals and/or to inheritance of the clay of the parent sediment.

The presence of moderate amounts of smectite may be implicated in the shrinkage and swelling behaviour of the upper subsoil with changing moisture content. in the lower profile the domination of smectite indicates a lower intensity of clay mineral weathering. As discussed earlier the high CEC of smectite and lower CEC of kaolinite clay minerals results in relatively higher CEC in the lower subsoil in contrast to the upper subsoil.

5.5.5. Mineralogy of sand fraction

Table 20 shows ilmenite, pyroxene and plagioclase occur throughout the profile and indicate dolerite as one of the source materials. The increase in pyroxene with depth probably relates to greater weathering in the surface layers. Zircon and rutile are higher in the fine sandy surface layers and then gradually decrease with depth. Leucoxene and tourmaline are relatively minor minerals throughout the profile. Iron oxide nodules have clearly accumulated in the middle profile (70-85 cm).

Quartz (Table 21) is in relatively high amounts throughout the profile, as in all soils in this study and supports the idea of Triassic sandstone and/or Permian mudstones as source rocks. Calcic plagioclase is relatively low in the surface but higher in the deep subsoil probably relating to a more dominantly dolerite source as indicated by rounded dolerite

stones found at the base of the profile. K-Feldspar is minor in the upper layers and was not detected in the lower profile.

Table 20. Heavy mineral analysis of sand fraction (177 micron), UF5.

Depth (cm)	(0 - 5)	(20 - 30)	(70 - 85)	(115 - 123)	(145 - 150)	(180 - 190)
Minerals						
Ilmenite	moderate	moderate	moderate	moderate	much	moderate
Leucoxene	trace	trace	trace	trace	trace	trace
Zircon	little	trace	trace	trace	trace	trace
Tourmaline	trace	trace	trace	n.d	trace	n.d
Rutile	little	little	trace	trace	trace	trace
Iron oxides	trace	little	moderate	trace	trace	trace
Pyroxene	little	trace	trace	much	moderate	much

n.d = not detected

Table 21. Light mineral analysis of sand fraction (177 micron), UF5

Depth (cm)	(0 - 5)	(20 - 30)	(70 - 85)	(115 - 123)	(145 - 150)	(180 - 190)
Minerals						
K-Feldspar	trace	trace	n.d	n.d	n.d	n.d
Plagioclase	little	trace	trace	trace	little	moderate
Quartz	much	much	much	much	much	much

n.d = not detected

The mineralogical data support the idea that the profile comprises three somewhat different kinds of material. The presence of K-feldspar, zircon and rutile and the high amount of fine sand in the upper profile suggests that this material was probably derived originally from Triassic sandstone and/or Permian mudstones, possibly being transported by aeolian processes from more recent sandy deposits of Pitt Water Bay (Leaman, 1971; Holz, 1994).

The high amounts of pyroxene, ilmenite and calcic plagioclase in the lower subsoil along with quartz, rutile and some zircon suggest this material is colluvium/alluvium originally derived from both Tertiary sediment and dolerite sources. The presence of rounded dolerite clasts below 156 cm would suggest a dolerite channel deposit, above which lies a mixed colluvium/alluvium. *In situ* Tertiary sediment must lie below (contact not observed).

5.5.6. Origin of materials and soil formation

The UF5 soil is located on a gentle (6% slope) lower toeslope 60 m down slope from UF4. The site is 40 m upslope from a linear, in-filled, drainage depression and is not more than 2 m above the channel floor (Figure 2a).

The profile to a depth of 190 cm comprises three distinct kinds of material distinguished by marked differences in macromorphological (colour, pedality, consistence), physical, chemical and mineralogical characteristics. The boundaries are clear between a sandy topsoil and clay-rich subsoil with the lower profile resting on well-rounded, water-worn dolerite clasts at 156 cm depth.

The presence of planar voids in the subsoil is due to shrinkage and expansion associated with a mixed kaolinite and smectite clay mineralogy. This has allowed the translocation of sandy materials down cracks into the upper subsoil.

High fine sand percentage and the presence of K-feldspar along with relatively small amounts of calcic plagioclase in the sandy topsoil suggests that the material was probably derived from Triassic sandstone and/or Permian mudstone perhaps reworked from recent sandy beach deposits close to Pitt Water (Leaman, 1971). The sandy topsoil may be largely windblown sand. The numerous occurrences of low dunes, sheets and pillows of windblown sand within the boundaries of the University Farm (Beattie, pers. comm.) provide evidence of previously active aeolian processes while modern agricultural activities often result in wind erosion and sand blasting of young crops.

The high clay content in the upper subsoil, from 30 cm to 70 cm, forms a clear "clay bulge". At least three possibilities can be proposed for the formation of this clay-rich zone. The first is that the clay bulge is due to more intense weathering of clay-forming minerals (pyroxene and feldspar) in this subsoil zone relative to that below. This is supported by the fact that kaolinite is in greater abundance while pyroxene and plagioclase are in lower amounts in the "clay bulge". Also both exchangeable calcium and magnesium have been relatively depleted in this part of the profile. The second is that the clay-rich zone represents material translocated from the topsoil by percolating soil water. This mechanism would have been supported by the presence of many clay coatings on soil peds, but these

were not evident in the field profile. In addition the high clay content and dispersive nature of the soil on wetting result in very low permeability, thus greatly reducing the possibility of vertical clay movement. The third possibility is that the clay layer represents sedimentary layering resulting from a variation in flow regime or sedimentary process during deposition. This is supported by the known stratified character of the Tertiary sediments discussed by other workers (Leaman, 1971; Holz, 1994) and cannot be discounted. Thus increased weathering and clay formation in the "clay bulge" zone and inheritance from the parent sediments are favoured.

However, the presence from 156 cm depth of basal, densely packed, well-rounded dolerite clasts of moderate size (5 - 10 cm) introduces a new factor not noted in the case of UF2, UF3, or UF4. The UF5 site was excavated with difficulty below 156 cm to 190 cm depth, with no reduction in the amount of dolerite clasts. This suggests that the clasts are not part of a stoneline marking a subaerial erosion surface but that they represent bed-load material (more than 34 cm thick) of a former stream now seen as the minor, infilled drainage line centred 40 metres downslope from the UF5 soil site. Thus the parent sediments of the UF5 soil may be part alluvial or colluvial and more recent in origin than the Tertiary sediments in which the presence of dolerite clasts appears not to have been recorded (Leaman, 1971). The high level of coarse sand in the subsoil of the UF5 profile in comparison with the UF3 and UF4 profiles may also reflect an alluvial origin and/or colluvial activity during formation of the lower footslope.

High clay content in the lower profile and high amounts of pyroxene, ilmenite and calcic plagioclase are indicative of a dolerite source while zircon, tourmaline and rutile indicate a more ancient Triassic sandstone and/or Permian mudstone source. All these sources are known to have contributed to the Tertiary sediments formation (Holz, 1994). The irregular depth function of particle size, exchangeable magnesium and CEC, below 20 cm and the mixed mineralogy support the idea that colluvium from upslopes sources forms the materials down to about 156 cm. Below this depth dolerite clast-supported channel deposits occur as discussed above.

Exchangeable sodium and ESP gradually increase with depth while magnesium, although co-dominant with calcium in the upper 40 cm, is the dominant cation in much of the profile. These properties and the acidity to 130 cm depth indicate the soil is a soloth (Stace *et al*, 1968), although the profile is neutral to slightly alkaline between 140 and 190 cm. The relatively high clay content and high percent exchangeable Na^{+} and Mg^{2+} in the subsoil are common features of many Australian sodic soils. These soils are associated with poor physical and chemical characteristics including: a hard tough soil strength when dry and coarse prismatic structure in the subsoil, swelling and dispersion of the clayey subsoil on wetting and commonly a distinct texture contrast profile (Rengasamy and Olsson, 1991).

The soil is never more than slightly saline with electrical conductivity increasing to 80 cm depth before decreasing to 140 cm depth below which it increases again.

5.5.7. Soil classification

According to the Isbell classification (1996) this soil is classified as "Brown Subnatric Sodosol". This explains the key feature of the profile such as texture contrast, high ESP and colour.

Soil Taxonomy (Soil Survey Staff, 1975) classification is "Typic Natrustalf". This classification focuses on the sodic nature of soil, the ustic moisture regime and texture contrasts.

V1. GENERAL DISCUSSION AND CONCLUSION

The study of the five soils above Tertiary clay sediments in the lower Coal River Valley reported in this thesis has provided data on soil morphology, physical and chemical characteristics, clay mineralogy, micromorphology and the mineralogy of sand fraction. The relationship between depth functions of these properties along with an understanding of the site geomorphology and surrounding geology has provided information about soil formation and an understanding of soil properties. Classification of the profiles in the new scheme of Isbell (1996) expresses the key attributes of each of the profiles.

Two very different primary profile forms have been studied, namely a uniform black cracking clay soil and four duplex profiles where fine sandy topsoils abruptly overlie clay-rich subsoils.

6.1. Uniform black cracking clay soil

The key morphological characteristics of UF1, a black cracking clay soil, include three different kinds of material: 1) a black, grading with depth to brown, cracking clay layer from 0 to 74 cm, 2) a pale yellow, low bulk density, crumbly material from 74 cm to 150 cm and 3) a greyish olive heavy clay below 150 cm depth. The bulk density and clay content are relatively high from the surface to 74 cm depth and below 150 cm.

The apparent parent material of this uniform black, cracking clay is a granular basalt glass deposit, little altered from 74 cm to 150 cm depth (on the basis of persistence of fragile amygdule structures of which there are only few above 74 cm). These structures in the light crumbly layer (74 cm - 150 cm) and its identification as basalt glass (Dr. J. McPhie, pers. comm.) indicate a volcanic (phreatomagmatic) event. Baillie and Leaman (1989) found that volcanic activity during Late Eocene to Early Miocene time was represented in the Coal River Valley by basaltic volcanics which overlie and interfinger with the Tertiary sediments. However, the soil is unlikely to date from this time and the fragility of the basalt glass deposit features may suggest a more recent volcanic event.

The olive heavy clay horizon below 150 cm with a sand mineralogy containing high amounts of iron oxide, pyroxene and quartz is in accordance with the provenance of materials forming the Tertiary sediments, i.e., Triassic sandstone, Permian mudstone and Jurassic dolerite (Nye, 1924).

6.2. Salinity, sodicity and magnesic characteristics

One feature common to all the soils studied is the increase in salinity, sodicity and magnesic characteristics of subsoils although sodicity tended to decrease towards the base of most profiles.

The basalt glass parent material of the black cracking clay soil would not be a likely source of salt; rather there is a dominance of ferromagnesian minerals and smectite clays derived from them. The immediate source of salt for this soil is therefore thought to be atmospheric cyclic salt of marine origin (Hutton and Leslie, 1958; Hutton, 1962; Jackson, 1977; Bowman *et al*, 1981) which is a major means of salt accession to soils in southern Australia (Teakle, 1937; Downes, 1954; Gunn, 1967; Chartres, 1993). The west to east air stream and the proximity of the Southern Ocean make the soils of the drier areas of Tasmania especially prone to retention of salt from this source. Also South-East Tasmania and The Coal River Valley in particular are now notably dry (Beattie, pers. comm.) with low levels of leaching intensity.

As the salinity profiles are similar in both magnitude and trend in the four duplex soils to that of UF1 the source of salt is thought to have been the same and to be continuing.

6.3. Genesis of the duplex soils

Generally these profiles are comprised of two major horizons constituting strongly duplex soils. However, UF3 is not as strongly duplex as UF2, UF4 and UF5 and shows much greater accumulation of glaebular iron oxide deposits. These iron oxides have evidently precipitated from iron-rich groundwaters moving downsolpe from the steep Jurassic dolerite ridge west of the Cambridge - Richmond road (Beattie, pers. comm.).

Profiles UF2, UF4 and UF5 were recorded as very similar in their main morphological features, ie, a very sandy topsoil with weak pedality in which the sand fraction in dominantly fine sand, resting abruptly on a dispersed clay subsoil of very to extremely slow internal drainage. This subsoil is dense and extremely hard when dry and very firm and sticky when moist or wet. Clay coatings, indicative of clay illuviation were not recorded. On the other hand all profiles showed a pronounced clay maximum in the upper B2 horizon, probably due to *in situ* clay formation and/or inheritance from the parent Tertiary sediment.

There is much evidence of wind action in prior transport of medium to fine sand all over the University Farm (Holz, 1994; Beattie, pers. comm). Holz (1994) suggested that sandy beach deposits of Pitt Water were the source of sand blown over a substrate of Tertiary sediments and debris flow deposits in which Tertiary sediment was a major constituent together with material of Jurassic dolerite, Triassic sandstone and Permian mudstone origin.

Thus it seems probable that the clay bulge in the duplex soils is the result of inheritance from the parent sediment or weathering rather than illuviation, certainly an improbable process now in these sodic, dispersed, impermeable materials.

It follows that dominantly fine sandy topsoils may have formed from wind-blown sand deposited above Tertiary sediments, whether or not the Tertiary sediments have been re-worked as colluvium. The dilemma of relatively thin sandy topsoils above a much thicker, high clay, subsoil has never been resolved satisfactorily in terms of classical ideas of soil horizon differentiation and of the formation of natural soils in a state of dynamic equilibrium with their environment (Nikiforoff, 1959; Butler, 1959).

The mineralogical data support the concept that the parent sediments of these soils are stratified. The presence of calcic plagioclase, K-feldspar, zircon, tourmaline and rutile in the sandy topsoils suggests that the surface materials are a mixture derived from Triassic sandstones and/or Permian mudstone and Jurassic dolerite, perhaps with a more recent contribution due to aeolian transport from sandy beach deposits fringing the western side of Pitt Water (Leaman, 1971; Holz, 1994).

Obvious differences between the duplex soils are those arising from differential occurrences of secondary pedological features (Brewer, 1964) in the form of glaebules of iron oxides, manganese oxides, and alkaline earth carbonates. These features separate UF2 (with a distinct manganese layer) and UF3 (with much iron oxide precipitation) from UF4 and UF5. An obvious source of iron, manganese, magnesium and calcium is the ridge of weathering dolerite into which a steep backslope has been cut above a footslope on which the UF3, 4 and 5 soils occur. Movement of iron, manganese and calcium in groundwaters and subsequent precipitation as the solutes were concentrated by drying is considered to be the mechanism involved. There is no reason to suppose that these processes are not on-going. Drainage of these soils occurs preferentially by down slope flow through the sandy topsoil above the clay subsoil which is very impermeable. Very large concretionary glaebules of iron oxides have been found straddling the boundary separating the topsoil and subsoil. In the case of the UF3 soil another form of iron oxide precipitation was recorded, ie, repeated thin laminae co-incident with the more sandy and more permeable layers of stratified Tertiary sediments. However the down slope limit of the very large concretionary glaebules of iron oxide in the presently studied sloping site is between profiles UF3 and UF4. This is in accord with local knowledge concerning the location of near-surface masses of "ironstone" in a band just below the Cambridge - Richmond road that have interfered with ploughing.

The cation exchange capacity (CEC) is relatively low in the topsoil of all the duplex soils due to the low levels of organic matter and clay (dominantly kaolinite). The CEC then increases in the subsoil due to initially high clay contents and continues to rise with increased smectite in the lower profile.

6.4. Soil management considerations

Physical and chemical characteristics and the clay mineralogy of all the soils studied confirm and explain management problems which reduce their suitability for agricultural uses. The sodic, smectite-rich clay of the UF1 soil cracks widely and deeply on drying. Sodicity and dispersivity are associated with very high bulk density and

unfavourable pore size distribution (Rengasamy and Olsson, 1991). Such soils have a very narrow range of moisture content for satisfactory cultivation and trafficking. On the other hand the sodic and magnesic clay subsoils of the duplex soils are protected from rapid drying by fine sandy topsoils, with greatly reduced shrinkage and cracking. It seems that these subsoils rarely if ever dry beyond the moist state below a depth of about 50 cm from the soil surface (Beattie, pers. comm) nor indeed do they appear to become much wetter than this. The high bulk densities and predominance of very fine voids means that water is held very strongly as well as access by roots being physically restricted. The observed extremely slow internal drainage, poor aeration, poor root development and overall shallow effective depth of these soils may thus be explained.

The timely publication of a new Australian Soil Classification (Isbell, 1996) has provided a much more precise system for classification of each of the soils studied. The nomenclature has also provided an accurate summary of their important properties.

REFERENCES

Abedine, A.Z., and Robinson, G.H. (1971). A study on cracking in some vertisols of the Sudan. Geoderma. 5, 229 - 41.

Adams, S.N., Honeysett, J.L., Tiller, K.G., and Norrish, K. (1969). Factors controlling the increase in cobalt in plants following the addition of cobalt fertilizers. Aust. J. Soil. Res. 7, 29-42.

Ahmad, N .,and Jones, R.L. (1969). Genesis, chemical properties and mineralogy of Caribbean grumusols. Soil Sci. 107, 166 - 74.

Akram, M., Hassan, G., Ashraf, M., and Chaudhary, E.H. (1989). Effect of gypsum and sulphuric acid on soil properties and dry matter yield of wheat grown in a highly saline-sodic soil. J. Agric Res Lahore. 27, 113 - 19.

Alprovitch, N., Shainberg, I., and Keren, R. (1981). Specific effect of magnesium on the hydraulic conductivity of sodic soils. J. Soil Sci. 32: 543 - 54.

Anderson, J.U., Fadul, K.E .,and O'Connor, G.A. (1973). Factors affecting the COLE in vertisols. Soil Sci. Soc. Am. Proc. 37, 296 - 99.

Aragues, R., and Amezketa, E. (1991). Clay dispersion and hydraulic conductivity of five horizons of a saline-sodic soil. investigation-Agraria, production-y-proteccion-vegetales. 6, 161 - 69.

Australian Bureau of Meteorology (1992). Hobart Region.

Australian Water Resources Council (1975). Review of Australia's Water Resources. Dept. of National Resources, Canberra.

Bailey, E.H., and Stevens, R.E .(1960). Selective staining of K felspar and plagioclase on rock slabs and thin sections. American Mineralogist. 45,1020 - 25.

Baillie, P.W., and Leaman, D.E (1989). South-eastern Tasmania. IN: Burrett.C.F., and Martin.E.L (Eds) Geology and mineral resources of Tasmania. Geological society of Australia Inc. Special Publication No.15, 365 - 67.

Bakker, A.C., Emerson, W.W., and Oades, J.M .(1973). The comparative effects of exchangeable calcium, magnesium and sodium on some physical properties of red-brown earth subsoils. III. The permeability of Shepparton soil and comparison of methods. Aust. J. Soil. Res. 11, 159 - 65.

Bakker, A.C., Emerson, W.W., and Oades, J.M. (1973). The comparative effects of exchangeable calcium , magnesium and sodium on some physical properties of red-brown earth subsoils. I. Exchange reactions and water contents for dispersion of Shepparton soil. Aust. J. Soil. Res. 11, 143 - 50.

Banks, M.R. (1962). The geology of Tasmania. J. Geol.Soc. Aust. 9: 189 -215.

Baver, L.D., Gardner, W.H., and Gardner, W. R. (1972). Soil Physics. John Wiley & Sons. Inc. New York. 130 - 31.

Beattie, J.A. (1970). Peculiar features of soil development in parna deposits in the Eastern Riverina, NSW. Aust. J. Soil. Res. 8, 145 - 56.

Beattie, J.A. (1972) Groundsurfaces of the Wagga Wagga Region NSW. CSIRO (Aust.) Soil Publ. No.28.

Beattie, J.A. (1995). Anomalous soloths, Lower Coal River Valley, South-East Tasmania. IN: Australian Sodic Soils: distribution, properties and management. Eds. R. Naidu, P. Rengasamy and M.E. Sumner (Eds). CSIRO (Aust.) Melbourne.

Berndt, R.D,. and Coughlan, K.J. (1976). The nature of change in bulk density with water content in a cracking clay. Aust. J. Soil. Res. 15, 27 - 37.

Black, C.A. (1965). Methods of soil analysis. Parts I and II. Agronomy No.9. American Society of Agronomy. Inc. Madison, Wisconsin.USA.

Blake, G., Schlichting, E., and Zimmermann, U. (1973). Water recharge in a soil with shrinkage cracks. Soil Sci. Soc. Am. Proc. 37, 669 - 72.

Bowman, D.M.J.S., and Jackson, W.D. (1981). Vegetation succession in Southwest Tasmania. Search. 12: 358 - 62.

Bowler, J.M., (1976). Aridity in Australia: age, origins and expression in aeolian landforms and sediments. Earth Sci. Rev. 12, 176 - 310.

Brewer, R. (1964). Fabric and Mineral Analysis of soils. John Wiley & Sons. Inc. Sydney.

Brewer, R., Protz, R., and McKeague, J.A. (1973). Microscopy and electron microporobe analysis of some iron-manganese pans from Newfoundland. Canadian J. Soil Sci. 53, 349 - 61.

Brewer, R and Sleeman, J.R. (1988). Soil structure and Fabric. CSIRO Publishing Melbourne.

Bronswijk, J.J.B. (1989). Prediction of actual cracking and subsidence in clay soils. Soil Science. 148, 87 - 93.

Bronswijk, J.J.B., and Evers-vermeer, J.J. (1990). Shrinkage of Dutch clay soil aggregates. Netherlands Journal of Agricultural Science. 38, 175 - 94.

Buol, S.W., Hole, F.D., and McCracken, R.J. (1980). Soil Genesis and Classification. Iowa state University Press. Ames. 2nd Edn.

Burns, R.G., and Burns, V.M., (1975). Mechanism for nucleation and growth of manganese nodules. Nature (London) 255, 130-131.

Butler, B.E. (1950). A theory of prior streams as a casual factor of soil occurrence in the Riverine Plain of South-Eastern Australia. Aust. J. Agric. Res. 1, 231 - 52.

Butler, B.E. (1955). A system for the description of soil structure and consistence in the field. J. Aust. Inst. Agric. Sci. 21, 239 - 49.

Butler, B.E. (1956). Parna - an aeolian clay. Aust. J. Sci. 18, 145 - 51.

Butler, B.E. (1958a). Depositional systems of the Riverine Plain of South-Eastern Australia in relation to soils. CSIRO (Aust). Soil Publ. No. 10.

Butler, B.E (1958b). The diversity of concepts about soil. J. Aust. Inst. Agric. Sci. p. 14 - 20.

Butler, B.E. (1959). Periodic phenomena in landscapes as a basis for soil studies. CSIRO (Aust). Soil Pub. No 14.

Butler, B.E. (1982). A new system for soil studies. J. Soil Sci. 33: 581 - 595.

Butler, B.E., and Churchward, H.M (1983). Aeolian processes. IN: Soils an Australian viewpoint. CSIRO. Australia, Melbourne / Academic Press, London.

Butler, B.E., and Hubble, G.D (1977). Morphologic properties. IN: Soil Factors in Crop Production in a Semi-Arid Environment. Russell, J.S., and Greacen, E.L. (Eds). Queensland University press. Brisbane.

Butler, B.E., and Hutton, J.T. (1956). Parna in the Riverine Plain of South-Eastern Australia and the soils thereon. Aust. J. Agric. Res. 7, 536 - 53.

Campbell, A.S., and Schwertmann, U. (1984). Iron oxide mineralogy of placic horizons. J. Soil Sci 35: 154 - 62.

Chan, K.Y. (1981). Representative sampling for bulk density in a vertisol. Soil Sci. Soc. Am. J 45, 668 - 69.

Charles, S.H., Chesters, G., and Corey, R.B. (1964). Contribution of organic matter and clay to soil cation exchange capacity as affected by pH of the saturating solution. Soil Sci. Soc. Am. Proc. 28, 517 - 20.

Chartres, C.J. (1993). Sodic soils: an introduction to their formation and distribution in Australia. Aust. J. Soil. Res. 31, 751 - 60.

Chartres, C.J., Greene. R.S., Ford, G.W., and Rengasamy,P. (1985). The effects of gypsum on macroporosity and crusting of two red duplex soils. Aust. J. Soil. Res. 23, 467 - 79.

Churchman, G.J., Skjemstad, J.O., and Oades, J.M. (1993). Influence of clay minerals and organic matter on effects of sodicity on soils. Aust. J. Soil. Res. 31, 779 - 800.

Churchward, H.M. (1961). Soil studies at Swan Hill, Victoria, Australia. I. Soil layering. J. Soil Sci. 12, 73 - 86.

Coventry, R.J., Taylor, R.M., and Fitzpatrick, R.W. (1983). Pedological significance of the gravels in some red and grey earths of Central North Queensland. Aust. J. Soil. Res. 21, 219-40.

Davidson, S. E., and Page, J.B. (1956). Factors influencing swelling and shrinking in soils. Soil Sci. Soc. Am. Proc. 20: 320 - 24.

Davies, J. (1988). Land systems of Tasmania. Region 6: South, East and Midlands.-A Resource Classification Survey. Department of Agriculture, Tasmania.

De Sigmond, A.A.J (1926). The classificastion of alkali and salty soils. First International Congress Soil Science Proceedings I , 330 - 44.

De vos, J.H., and Virgo, K.J. (1969). Soil structure in vertisols of the Blue Nile clay plains, Sudan. J. Soil Sci. 21, 189 - 205.

Downes, R.G. (1954). Cyclic salt as a dominant factor in the genesis of soils in South-Eastern Australia. Aust. J. Soil Res. 5: 448 - 64.

Doyle, R.B.(1993). Soils of the South Esk sheet Tasmania (southern half). Department of Primary Industry and Fisheries, Tasmania.

Dudal, R. (1963). Dark clay soils of tropical and subtropical regions. Soil Sci. 95: 264 - 70.

Emerson, W.W. (1967). A classification of soil aggregates based on their coherence in water. Aust. J. Soil. Res. 5: 47 - 57.

Emerson, W.W (1977). Physical properties and structure. IN: Russell J.S,. and Greacen, E.L (Eds) : Soil Factors in Crop Production in a Semi-Arid Environment. Queensland University press, Brisbane.

Emerson, W.W. (1983). Interparticle bonding. IN: Division of Soils (1983). Soils, an Australian Viewpoint. CSIRO (Aust.) Melbourne / Academic Press.

Emerson, W.W., and Bakker, A.C. (1973). Comparative effects of exchangeable calcium, magnesium and sodium on some physical properties of red-brown earth subsoils II. The spontaneous dispersion of aggregates in water. Aust. J.Soil. Res. 11, 151 - 7.

Eswaran, H. and Raghu Mohan, N.G. (1973). The microfabric of petroplinthite. Soil Sci. Soc. Am. J. 37, 79-82.

Evans, K.J, Mitchel, I.G, and Salan, B., (1978). Heavy metal accumulation in soils irrigated by sewage and effect in plant-animal system. IN: International conference on developments in land methods of waste water treatment and utilization. 24: 1 - 14.

Fox, W.E. (1964a). A study of bulk density and water in a swelling soil. Soil Sci. 98, 307 - 16.

Fox, W.E. (1964b). Cracking characteristics and field capacity in a swelling soil. Soil Sci. 98, 413.

Franzmeier, D.P., and Ross, S.J.Jr. (1968). Soil swelling: laboratory measurement and relation to other soil properties. Soil Sci. Soc. Am. Proc. 32, 573 - 77.

Gatehouse, C.G (1967) The geology of the Richmond-Sorell area. Papers and Proceedings of the Royal Society of Tasmania. 6, 101 - 07.

George, N.C., and Bridge, B.J. (1973). The effect of height of sample and confinement on the moisture characteristic of an aggregated swelling clay soil. Aust. J. Soil. Res. 11, 107 - 20.

Gillman, G.P., and Bell, L.C. (1976). Surface charge characteristics of six weathered soils from tropical north Queensland. Aust. J. Soil. Res. 16, 67-77.

Goldberg, S., and Forster, S. (1990). Flocculation of reference clays and arid-zone soil clays. Soil Sci. Soc. Am. J. 54, 714 - 18.

Graham, E.R. (1955). Rapid determination of quartz, potash minerals and plagioclase felspar in soils. Chem. Anal. 44 , 37 - 38.

Greene, R.S.B., and Ford, G.W. (1985). The effect of gypsum on cation exchange in two red duplex soils. Aust J Soil Res. 23, 61 - 74.

Gumbs, F.A and Warkentin, B.P. (1972). The effect of bulk density and initial water content on infiltration in clay soil samples. Soil Sci. Soc. Am. Proc. 36, 720 - 24.

Gunn, R.H. (1967). A soil catena on a denuded laterite profile in Queensland. Aust. J. Soil Res. 5, 117 - 32.

Gunn, R.H (1985) Shallow groundwaters in weathered volcanic, granitic and sedimentary rocks in relation to dryland salinity in Southern New South Wales. Aust. J. Soil Res. 23, 355 - 71.

Gunn, R.H., and Richardson, D.P., (1979). The nature and possible origins of soluble salts in deeply weathered landscapes of Eastern Australia. Aus. J. Soil Res. 17, 179 - 215.

Harte, A.J. (1988). The effect of management on the physical properties of soils of the northern NSW Wheat bealt. IN: Coughlan. K.J and Troung. P.N.(Eds) Effects of management practices on soil physical properties. DPI. Brisbane.

Hewett, D.F and Fleischer, M. (1960). Deposits of the manganese oxides. Econ. Geol. 55, 1 - 53.

Holmes, J.W. (1955). Water sorption and swelling of clay blacks. J. Soil Sci. 6, 200 - 08.

Holz, G.K. (1994). Principles of soil occurrence in the lower Coal River Valley, South-East Tasmania. Unpublished PhD Thesis. Department of Agricultural Science, University of Tasmania -Hobart.

Hoogmoed, W.B and Bouma, J (1980). A simulation model for predicting infiltration into cracked clay soil. Soil Sci. Soc. Am. J. (44): 458 - 61.

Hubble, G.D., Isbell, R.F., and Northcote, K.H. (1983). Features of Australian soils. IN: Soils, an Australian viewpoint. CSIRO, Melbourne/Academic Press: London.

Hutton, J.T (1962). Rain water analysis July 1957 to March 1961. CSIRO (Aust). Div. Soils. Div. Rpt. No.7.

Hutton, J.T., and Leslie, T.I. (1958). Accession of non-nitrogenous ions dissolved in rainwater to soils in Victoria. Aust. J. Agric. Res. 9, 492 - 507.

Isbell, R.F. (1996). The Australian soil classification. CSIRO Publishing. Collingwood. Victoria. Australia.

Isbell, R.F, Reeve, R and Hutton, J.T. (1983). Salt and sodicity. IN: Soils, an Australian viewpoint . CSIRO:Melbourne/Academic Press: London.

Jackson, M.L. (1968). Weathering of primary and secondary minerals in soils. 9th Int. Congr. Soil. Sci. Trans. Adelaide, Australia. 4, 281 - 92.

Jackson, M.L., and Sherman, G.D (1953). Chemical weathering of minerals in soils. Adv.Agron. 5: 219 - 318.

Jackson, W.D. (1965) Vegetation. IN: Davies, J.L (Ed.) Atlas of Tasmania, Department of Lands and Surveys, Hobart.

Jackson, W.D. (1977). Nutrient cycling in Tasmanian oligotrophic environments. IN: Proc. Symp. Nutrient Cycling and Indigenous Forest Ecosystems. CSIRO Aust. Div. Land Mgt. Perth.

Jayawardane, N.S. (1984). Determination of the swelling characteristics of a soil using a neutron and gamma density meter. Aust. J. Soil. Res. 22, 389 - 99.

Jayawardane, N.S and Greacen. E.L (1987). The nature of swelling in soils. Aust. J. Soil. Res. 25, 107 - 13.

Jenny, H. (1941). Factors of Soil Formation. McGraw-Hill. New York.

Joffe, J.S., (1949). Pedology. Pedology Publications. New Brunswick, New Jersey. 2nd. Ed'n.

Johns, W.D., and Huang, W.H. (1966). Distribution of chlorine in terrestrial rocks. Geochim. Cosmoschim. Acta. 31, 35 - 49.

Johnson, W.M, Cady, J.D, and James, M.S. (1962). Characteristics of some brown grumusols of Arizona. Soil Sci. Soc. Am. Proc. 26, 389 - 93.

Kodama, H., McKeague, J.A., Tremblay, R.J.,Gosselin, J.R., and Townsend, M.G. (1977). Characterisation of iron oxide compounds by Mossbower and other methods. Canadian J. Earth Sci. 14, 1-15.

Lal, R, Bridge, B.J. and George, N.C. (1970). The effect of column diameter on the infiltration behaviour of a swelling soil. Aust. J. Soil. Res. 8, 185 - 93.

Leaman, D.E. (1971). The geology and ground water resources of the Coal River Basin. Underground Water Supply Paper. No.7. Dept. of Mines.Tasmania.

Leaman, D.E. (1972). Gravity survey of the Hobart District. Geological Survey Bulletin. No.52. Dept. of Mines. Tasmania.

Leeper, G.W. (1970). The Australian Environment. CSIRO and Melbourne Univ. Press.

Letey, J. (1991). The study of soil structure: science or art. Aust. J. soil Res. (29): 699 - 7087.

Little, I.P. (1992). The relationship between soil pH measurements in calcium chloride and water suspensions. Aust. J. Soil. Res. 30, 587 - 92.

Loveday, J. (1955). Reconnaissance soil map of Tasmania. Sheet 82 - Hobart. CSIRO Aust. Div. of Soils, Divisional Report 13/55.

Loveday, J. (1974a). Methods for Analysis of Irrigated soils. Cwth. Bur. Soils. Tech. Pub. No.54.

Loveday, J. (1974b). Recognition of gypsum responsive soils. Aust. J. Soil Res. 12, 87 - 96.

Marshall, C.E. (1977). The physical chemistry and mineralogy of soils. Wiley-Interscience Publications. John Wiley & sons.Inc. New York.2nd. Edn.

McCown, R.L.,Murtha, G.G., and Smith, G.D. (1976). Assessment of available water storage capacity of soils with restricted subsoil permeability. Water Resources Research. 12, 1255-9.

McDaniel, P.A, Bathke, G.R, Buol, S.W, Cassel, D.K and Falen, A.L. (1992). Secondary manganese/iron ratios as pedochemical indicators of field-scale through flow water movement. Soil Sci. Soc. Am. J. 56, 1211 - 17.

McDonald, R.C, Isbell. R.F, Speight, Walker, J, and Hopkins, M.S. (1984). Australian Soil and Land Survey, Field Handbook. Inkata press. Melbourne.

McIntyre, D.S (1956). The effect of free ferric oxide on the structure of some terra rossa and rendzina soils. J. Soil Sci. 7, 302-06.

McIntyre, D.S, Loveday, J, and Watson, C.L.(1982). Field studies of water and salt movement in an irrigated swelling clay soil: I. Infiltration during ponding. Aust. J. Soil. Res. 20, 81 - 90.

McKeague, J.A., Brydon, J.E., and Miles, N.M. (1971). Differentiation of forms of extractable iron and aluminium in soils. Soil Sci. Soc. Am. Proc. 35, 33-8.

McKenzie, D.C, Humble. P.J, Abbott. T.S, Macleod. D.A, and Cass.A. (1988). Vertisol structure dynamics following irrigation of cotton, as influenced by prior rotation crops. IN: Coughlan. K.J and Troung. P.N (Eds). Effects of Management Practices on Soil Physical Properties. DPI. Queensland.

McKenzie, R.M. (1971).The synthesis of cryptomelane and some other oxides and hydroxides of manganese. Miner Mag. 38, 493-502.

McKenzie, R.M. (1975). An electron microprobe study of the relationships between heavy metals and manganese and iron in soils and ocean floor nodules. Aust. J. Soil. Res. 13, 177-88.

McKenzie, R.M. (1978). The effect of two manganese oxides on the uptake of lead, cobalt, nickel, copper and zinc by subterranean clover. Aust. J. Soil. Res. 16, 209-14.

McLean, E.O. (1965) Exchangeable Aluminium. IN: C.A. Black (ed). Methods of Soil Analysis. Part 2. Agronomy 9. Amer. Soc. of Agron. Madison. Wis.

McNeal, B.L,. Layfield, D.A,. Norvell, W.A., and Rhoades, J.D. (1968). Factors influencing hydraulic conductivity of soils in the presence of salt solutions . Soil. Sci. Soc. Am. J. 32, 187 - 9.

Mehra, O.P., and Jackson, M.L. (1958). Iron oxide removal from soils and clays by dithionite-citrate system buffered with sodium bicarbonate. Clays Clay Miner. 7, 317-27.

Milner, H.B. (1962). Sedimentary Petrography. Allen & Unwin. London.

Munsell color (1994). Munsell soil color charts. Macbeth Division of Kollmorgan Instruments Corporation. New York. Revised Edn.

Murphy, C.P. (1986). Thin section preparation of soils and sediments. A.B. Academic Publishers. U.K.

Nikiforoff (1959). Reappraisal of the soil. Science. 129, 186 - 96.

Norrish, K. (1975). Geochemistry and Mineralogy of trace elements. IN: Trace elements in the Soil-Plant-Animal System. D.J. Nicholas and A.R. Egan (Eds). Academic Press, New York.

Norrish, K., and Rosser, H. (1983). Mineral phosphate. IN: Soils, an Australian viewpoint. CSIRO, Melbourne. Academic Press: London.

Northcote, K.H. (1979). A Factual Key for the Recognition of Australian Soils. Rellim Technical Publication: Glenside, S.A.4th.edition.

Northcote, K.H and Skene, J.K.M. (1972). Australian Soils with Saline and Sodic Properties. CSIRO (Aust.) Soil Publication No.27.

Northcote, K.H,.Hubble, G.D.,Isbell,R.F., Thompson,C.H., and Bettenay,E. (1975). A description of Australian Soils. CSIRO (Aust.). Melbourne.

Nye, P.B. 1924). Underground water resources of the Richmond- Bridgewater- Sandford Districts. Dept. of Mines. Tasmania. Bull. No.3. 1 - 67.

Oakes, H., and Thorp, J. (1950). Dark clay soils of warm regions variously called rendzina, black cotton soils, regurs and tirs. Soil Sci. Soc. Am. Proc. 15, 347 - 54.

Omar, M.S, Hammad, S.A and Gouda, M (1990). Infiltration characteristics of sodium affected soil as related to soil management. Egyptian J. Soil Sci. 30, 579 - 86.

Oster, J.D., Shainberg, I., and Wood, J.D. (1980). Flocculation value and gel structure of sodium/calcium montmorillonite and illite suspensions. Soil Sci. Soc. Am. J.. 44, 955 - 59.

Peck, A.J. (1977). Development and reclamation of secondary salinity. IN: Soil Factors in Crop Production in a Semi-Arid Environment. Russell,J.S,. and Greacen, E.L.(Eds.) University of Queensland Press, Brisbane.

Perfect, E, Van Loon, W.K.P, Kay, B.D and Groenevelt, P.H (1990). Influence of ice segregation and solutes on soil structural stability. Canadian J. Soil Sci. 70, 571 - 81.

Pojasok, T and Kay, B.D (1990). Effect of root exudates from corn and brome grass on soil structural stability. Canadian J. Soil Sci. 70, 351 - 62.

Prathapar, S.A, Meyer, W.S and Cook, F.J (1989). Effect of cultivation on the relationship between root length density and unsaturated hydraulic conductivity in a moderately swelling clay soil. Aust. J. Soil. Res. 27, 645 - 50.

Prebble, R.E (1987). Effect of cultivation on aggregate stability, micro-aggregation and organic carbon of vertisols. CSIRO(Aust.) Soil Publ. No.91.

Rayment, G.E and Higginson, F.R (1992). Australian Laboratory Handbook of Soil and Water Chemical Methods. Inkata press, Melbourne, Sydney.

Rengasamy, P. (1990). Water quality and soil structure. IN: Management of Soil Salinity in South-East Australia. Humphreys, E., Muirhead.W.A., Van der Leiij, A. (Eds.) Aust. Soc.Soil. Sci. Inc. Riverina Branch.

Rengasamy, P and Olsson, K.A (1991). Sodicity and Soil Structure. Aust. J. Soil. Res. 29,. 935 - 52.

Rengasamy, P., Ford, G.W and Greene, R.S.B (1988). Classification of aggregate stability. IN: Coughlan. K.J and Troung. P.N.(Eds). Effects of Management Practices on Soil Physical Properties. DPI. Queensland. Brisbane.

Rengasamy, P., Greene, R.S.B., Ford, G.W., and Mehanni, A.H (1984). Identification of dispersive behaviour and the management of red-brown earths. Aust. J. Soil. Res. 22, 413 - 31.

Ritchie, J.T, Kissel, D.E and Burnett, E (1972). Water movement in undisturbed swelling clay soil. Soil Sci. Soc. Am. Proc.. 36, 874 - 79.

Schwertmann, U. (1985). The effect of pedogenic environments on iron oxide minerals. Adv. Soil Science 1, 171-200.

Schwertmann, U., and Taylor,R.M. (1977). Iron oxides. IN: Minerals in Soil Environments.Special Publication No.15. Soil Sci. Am. Madison.Wis.

Scotter, D.R (1985). The effect of electrolyte solutions on the unsaturated hydraulic conductivity of a sodic clay soil. Aust. J. Soil. Res. 23, 301 - 07.

Shainberg, I., and Letey, J. (1984). Response of soils to sodic and saline conditions. Hilgardia. 52 (2), 1 - 57.

Shaw, R., Brebber, L., Ahem, C., and Weinand,M. (1994). A review of sodicity and sodic soil behaviour in Queensland Aust. J.Soil. Res. 32, 143 - 72.

Simonson, R.W (1954). Morphology and classification of the regur soils of India. J. Soil Sci. 5, 275 - 88.

Simonson, R.W (1959). Outline of a generalized theory of soil genesis.Soil Sci. Soc. Am. Proc. 23, 152 - 56.

Smith, A.N. (1965). Aluminium and iron phosphates in soils. J. Aust. Inst. Agric. Sci. 31, 110-26.

So, H.B., and Aylmore, L.A.G (1993). How do sodic soils behave? The effects of sodicity in soil physical behaviour. Aust. J.Soil. Res. 31, 761 - 77.

So, H.B and Cook, G.D (1993). The effect of slaking and dispersion on the hydraulic conductivity of clay soils. Catena Supplement. 24, 55 - 64.

Soil Survey Staff (1975). Soil Taxonomy : A Basic System of Soil Classification for Making and Interpreting Soil Surveys.

SSSA (1987). Glossary of Soil Science Terms. Soil Scie. Soc. Am. Madison. Wisc.

Stace, H.C.T., Hubble,G.D., Brewer, R., Northcote,K.H., Sleeman,J.R.,Mulcahy, M.J., and Hallsworth, E.G. (1968). A Handbook of Australian Soils. Rellim. Glenside. S. Aust. (CSIRO and ISSS).

Stephens,.C.G (1962). A Manual of Australian Soils. Third edition. CSIRO.(Aust), Melbourne.

Sullivan, L.A., and Koppi,A.J. (1992). Manganese oxide accumulations associated with some soil structural pores I. Morphology, composition and genesis. Aust. J. Soil. Res. 30, 409-27.

Sumner, M.E (1993). Sodic soils: new perspectives. Aust. J. Soil. Res.31, 683 - 750.

Symons, B.E. (1975). Geological map of Hobart. Tasmania Department of Mines.

Taslma, T, (1967). Leaching of tile-drained saline soils. Aust. J. Soil. Res. 5, 37 - 46.

Taylor, R.M. (1968). The association of manganese and cobalt in soils- further observations. J. Soil Sci. 19,77-80.

Taylor, R.M., and McKenzie,R.M (1966). The association of trace elements with manganese minerals in some Australian soils. Aust. J. Soil. Res 4, 29-39.

Taylor, R.M., and Schwertmann,U. (1974). Maghemite in soils and its origin I. Properties and observations of soil maghemites. Clay Miner. 10, 299-310.

Taylor, R.M., McKenzie,R.M., Fordham, A.W., and Gillman, G.P. (1983). Oxide minerals. IN: Soils, an Australian viewpoint. CSIRO: Melbourne/Academic Press London.

Taylor, R.M., McKenzie. R.M., and Norrish, K (1964). The mineralogy and chemistry of manganese in Australia. Aust. J. Soil. Res. 2, 235 - 48.

Taylor, S.A and Ashcroft, G.L (1972). Physical Edaphology. W.H Freeman & Company.San Francisco.

Teakle, L.J.H (1937). Salt (sodium chloride) content of rain water. J.Dept. Agric. West Aust. 14, 115 - 23.

Templin, E.H, Mowery, I.C and Kunze, G.W (1956). Houston black clay, the type grumusol:I. Field morphology and geography. Soil Sci. Soc. Am. Proc. 20, 88 -90.

Tiwary, K.N, Kumar, A, Carter, M.R, Gupta. U.C (1989). Evaluation of sedimentary iron pyrites as an ameliorant for a saline-sodic soil in Uttar Pradesh, India. Arid-Soil-Research and Rehabilitation 3, 361 - 68.

United States Salinity Laboratory Staff (1954). Diagnosis and Improvement of Saline and Alkaline Soils. USDA, Agric. Handbook No. 60, U.S. Salinity. Lab., Riverside, CA.

United States Salinity Laboratory Staff (1964). Elimination of boundary-flow errors in laboratory hydraulic conductivity measurement. Soil Sci. Soc. Am. Proc 28, 713 - 14.

Van Dijk, D.C. (1958). Soil distribution in the Griffith - Yenda district, NSW. CSIRO (Aust). Soil Publ. No.11.

Virgo, K.J (1981). Observations of cracking in Somali vertisols. Soil Science 131, 60 -61.

Walker, P.H., and Costin, A.B. (1971). Atmospheric dust accession in South-Eastern Australia. Aust. J. Soil Res. 9, 1 - 6.

Walker, J., and Hopkins, M.S. (1990). Vegetation. IN: McDonald, R.C., Isbell, R.F., Speight, J. G., Walker, J., and Hopkins, M.S.(Eds). Australian Soil and Land Survey Field Handbook. Inkata Press. Melbourne.

Weber, M.D., McKeague, J.A., Road, A.T., De Kimpe,C.P., Chang wang., Haluschak, P.,Stonehouse, H.B., Pettapiece,W.W., Osborne,V.E and Green, A.J. (1974). A comparison among nine Canadian laboratories of dithionite-oxalate-, and pyrophosphate-extractable Fe and Al in soils. Canadian J. Soil Sci. 54, 293-98.

Wild, A., (1958). The phosphate content of Australian soils. Aust. J. Soil Res. 9, 193 - 204.

Wilding, L.P and Hallmark, C.T (1984). Development of structural and microfabric properties in shrinking and swelling clays. IN: Proceedings of the ISSS Symposium on Water and Solute Movement in Heavy Clay Soils.

Wilding, L.P., Smeck, N.E., and Hall, G.F. (1983). Pedogenesis and Soil Taxonomy. I. Concepts and Interactions. Elsevier. Amsterdam - Oxford - New York.

Williams, J. (1983). Physical properties and water relations: soil hydrology. IN: Soils, an Australian viewpoint. CSIRO:Melbourne/Academic Press: London.

Yaalon, D.H and Kalmar, D (1972). Vertical movement in an undisturbed soil : continuous measurement of swelling and shrinkage with a sensitive apparatus. Geoderma 8,231 - 40.

Young, A. (1976). Tropical Soils and Soil Surveys. Cambridge University press. 180 - 191.

Yule, D.F and Ritchie, J.T (1980). Soil shrinkage relationships of Texas vertisols : I. Small cores. Soil Sci. Soc. Am. J. 44, 1285 - 91.

Appendix 1. Physical and chemical analysis data

Table 22. Chemical and physical data analysis UF1

Depth (cm)	Bulk Density (gr/cm3)	% clay <0.002 mm	% silt 0.002-0.02 mm	% fine sand 0.02 - 0.2 mm	% coarse sand 0.2 - 2.0 mm	pH (H2O)	pH (CaCl2)	EC (dS/m)	% C-organic	Na+	K+	Ca++	Mg++	CEC	ESP
										cmol(+)/kg					
0 - 2	1.41	65	17.5	5.14	3.9	6.7	5.8	0.14	3.22	2.7	1.81	9.55	12.46	26.52	10.2
2. - 5	1.55	64.5	21	5.26	3.48	6.8	5.8	0.12	2.78	2.7	0.63	9.73	12.66	25.72	10.5
5. - 10	1.55	66	19.5	5.46	3.64	7.0	5.9	0.17	2.56	2.99	0.48	9.73	13.01	26.21	11.4
10. - 15	1.54	71.5	18	4.86	3.12	6.9	5.7	0.2	2.48	3.73	0.33	8.81	13.79	26.66	14.0
15 -18.	1.53	72	16.5	5.9	3.34	6.8	5.7	0.19	2.15	4.03	0.19	8.39	13.71	26.32	15.3
18 - 23.	1.54	67.5	14.5	9.2	4.48	6.5	5.4	0.21	2.09	4.17	0.19	8.02	13.83	26.21	15.9
23 - 30.	1.44	70.5	13.5	9.02	4.24	6.5	5.3	0.23	2.06	4.76	0.19	7.88	15.2	28.03	17.0
30 - 40.	1.49	79	11.5	8.02	3.62	7.0	6.3	0.25	1.65	5.65	0.04	7.42	16.02	29.13	19.4
40 - 50.	1.22	79	13	8.14	5.38	7.8	7	0.35	1.44	6.82	0.04	8.2	17.78	32.84	20.8
50 - 55.	1.54	80	9.5	8.6	5.64	7.9	7.2	0.46	1.28	7.12	0.04	6.77	15.28	29.21	24.4
55 - 60.	1.42	80	13.5	8.78	6.72	8.1	7.3	0.46	1.07	7.41	0.04	6.88	15.94	30.27	24.5
60 - 70.	1.55	81	12.5	7.22	7.62	8.3	7.6	0.5		7.56	0.04	6.98	15.43	30.01	25.2
70 - 74.	1.52	79.5	8	7.56	8.22	8.7	7.8	0.54		8.3	0.04	6.72	14.73	29.79	27.9
74 - 80.	1.25	32.5	19	38.02	8.92	8.8	7.8	0.49		11.83	0.04	10.19	23.52	45.58	26.0
80 - 100.	1.11	26.5	17	41.02	16.54	8.9	7.7	0.56		12.13	0.04	11.94	23.17	47.28	25.7
100 - 120.	1.06	25.5	12.5	45.16	13.5	8.7	7.7	0.4		13.6	0.04	9.06	25.35	48.05	28.3
120 - 140.	1.58	27	14.5	42.52	13.92	8.9	7.7	0.5		13.6	0.04	10.46	25.74	49.84	27.3
140 - 150.	0.93	37	20	29.08	11.14	9.0	7.8	0.59		12.72	0.04	12.28	26.6	51.64	24.6
150 - 160.	1.31	76	17	8.28	364	9.0	7.8	0.53		10.95	0.04	8.98	20.04	40.01	27.4
> 160	1.49	83.5	11	7.66	3.46	8.8	7.8	0.53		9.77	0.04	8.93	21.49	40.23	24.3

Table 23. Chemical and physical data analysis UF2

Depth (cm)	Bulk density gr/cm3	% clay < 0.002 mm	% silt 0.002-0.02 mm	% fine sand 0.02-0.2 mm	% Coarse sand 0.2-2.0 mm	pH(H2O)	pH (CaCl2)	EC (dS/m)	% C-organic	Na+	K+	Ca++	Mg++	CEC	ESP
										cmol(+)/kg					
0 - 5	1.36	16.5	10	56.9	20.4	5.8	4.6	0.075	2.22	0.06	0.11	6.41	5.36	11.94	0.5
5 - 10.	1.36	17.5	8.5	57.9	19.6	5.7	4.3	0.064	1.96	0.06	0.01	5.33	5.01	10.41	0.6
10 - 19.	1.41	14	11	58.5	20.6	5.7	4.2	0.053	1.53	0.06	0.01	4.37	4.49	8.93	0.7
19 -28.	1.66	46.5	11.5	32.6	10.4	5.8	4.1	0.11	1.12	2.78	0.01	8.83	25.02	36.64	7.6
28 -37.	1.64	46.5	10.5	33.6	10.7	5.7	4.2	0.15	0.59	3.99	0.01	7.36	25.12	36.48	10.9
37 -46.	1.65	47	10.5	31.5	9.7	5.5	4.2	0.208		5.19	0.01	7.58	27.92	40.7	12.8
46 - 62.	1.68	41	11.5	35.9	10.7	5.6	4.3	0.27		5.8	0.01	6.63	27.04	39.48	14.7
62 - 75.	1.79	40.5	12.5	37.2	10.2	5.6	4.5	0.284		6.4	0.01	6.03	26.83	39.27	16.3
75 - 89.	1.62	34	10	42.6	12.1	6	5.1	0.327		7.01	0.06	5.99	26.21	39.27	17.9
89 - 95.	1.68	33	10	39.4	12.7	6.6	6	0.335		8.21	0.11	6.99	32.89	48.2	17.0
95 - 100.	1.71	33	11.5	37	14	6.9	6.2	0.33		8.21	0.21	7.18	34.7	50.3	16.3
100 - 110.	1.79	34	11	35.3	16.2	7.2	6.4	0.309		8.06	0.21	7.03	29.32	44.62	18.1
110 - 112.	1.77	32	11	38.2	15.9	7.4	6.4	0.28		7.91	0.21	6.85	26.62	41.59	19.0
112 - 120.	1.79	30.5	11.5	43.9	12.2	7.6	6.5	0.279		7.76	0.26	6.68	28.49	43.19	18.0
120 - 138.	1.71	26	11	46.5	14.5	9.1	7	0.38		7.01	0.26	9.22	24.55	41.04	17.1
138 - 156.	1.6	23	13	49.8	14.6	8.5	6.8	0.26		6.4	0.31	5.41	19.73	31.85	20.1
> 156	1.64	24	11	37.1	25	9.2	7.2	0.38		7.61	0.51	12.26	23.05	43.43	17.5

Table 24. Chemical and physical data analysis UF3.

Depth (cm)	Bulk Density (gr/cm3)	% clay <0.002 mm	% silt 0.002-0.02 mm	% fine sand 0.02-0.2 mm	% coarse sand 0.2-2.0 mm	pH(H2O)	pH(CaCl2)	EC (dS/m)	% C-organic	Na+	K+	Ca++	Mg++	CEC	ESP
										(cmol(+)/kg)					
0 - 6	1.78	16.5	15	57.3	13.4	6.6	6.2	0.11	2.34	0.38	0.29	6.69	13.72	21.08	1.8
6 - 12 .	1.5	11.5	18.5	55.3	14.7	6.1	5.5	0.06	2.06	0.38	0.04	9.3	6.86	16.58	2.3
12 - 20.	1.4	12	17.5	58.5	14.3	5.8	5.2	0.06	2.1	0.38	0.04	11.56	7.93	19.91	1.9
20 - 32 .	1.99	11.5	20	52.1	17.9	6	5.3	0.05	0.98	0.38	0.04	9.09	6.71	16.22	2.3
32 - 42 .	1.91	23.5	12	47.9	15.6	6.3	5.5	0.06	0.51	0.93	0.04	7.24	12.2	20.41	4.6
42 - 59.	1.86	27	9	50.9	12.3	6.7	6	0.12		1.48	0.04	4.98	17.38	23.88	6.2
59 - 75.	1.85	38	10	38.5	11.3	7.7	6.7	0.31		4.52	0.29	3.74	35.21	43.76	10.3
75 - 80.	1.72	43.5	29	29.3	1.8	8.1	7.3	0.42		6.17	0.37	3.88	38.11	48.53	12.7
80 - 95	1.77	49	36.5	10.9	0.7	8.3	7.7	0.43		6.72	0.49	5.05	39.33	51.59	13.0
95 - 100	1.96	44	34	21.5	1.4	8.3	7.7	0.37		5.89	0.37	4.16	36.28	46.70	12.6
00 - 108	2.16	35	18.5	34.5	7.5	8.2	7.6	0.31		4.52	0.2	3.61	25.61	33.94	13.3
08 - 114	1.98	42	33.5	24.2	0.3	8.2	7.5	0.34		5.62	0.37	4.16	36.28	46.43	12.1
14 - 126	2.07	24	15	53.5	7.9	8.2	7.3	0.23		2.59	0.12	2.3	17.23	22.24	11.6
26 - 135	1.99	22	17	49	10.6	8	7.2	0.25		2.31	0.12	2.37	17.23	22.03	10.5
> 135	1.93	25	19.5	47.1	10.5	8.2	7.4	0.26		2.86	0.2	2.72	17.84	23.62	12.1

Table 25. Chemical and physical data analysis UF4.

Depth (cm)	BD gr/cm3	% clay < 0.002 mm	% silt 0.002-0.02 mm	% fine sand 0.02-0.2 mm	% Coarse sand 0.2-2.0 mm	pH(H2O)	pH (CaCl2)	EC (dS/m)	% C-organic	Na+	K+	Ca++	Mg++	Al3+	H+	CEC	ESP (cm)
										(cmol/kg)							
0 - 5	1.43	25	7.5	51.1	17.1	5.5	5.4	0.11	2.26	0.72	0.55	12.58	8.54	0.15	0.05	22.59	3.2
5 - 10.	1.45	26	11	50.2	18.5	5.7	5.6	0.06	1.77	0.38	0.25	12.3	5.64	0.25	0.05	18.87	2.0
10. - 18	1.65	35.5	10	42.2	15.4	5.7	5.6	0.06	1.45	1.26	0.25	10.7	8.76	1.65	0.25	22.87	5.5
18 - 27	1.65	58	12	27.3	8.4	5.4	5.3	0.08	0.94	2.35	0.35	8.67	13.23	6.3	0.5	31.4	7.5
27 - 38	1.66	53	16.5	28.9	8.9	5.3	5.2	0.13	0.39	2.82	0.25	6.37	13.67	6.25	0.95	30.31	9.3
38 - 46	1.78	36	15	38.9	12	5.4	5.3	0.13		2.62	0.15	5.67	13.45	4.9	0.4	27.19	9.6
46 - 58	1.82	35	9.5	42.6	13.4	5.4	5.3	0.13		2.96	0.15	4.97	13.23	4.25	0.4	25.96	11.4
58 - 70	1.84	34	8.5	43.5	13.6	5.3	5.2	0.17		3.44	0.15	4.69	14.79	2.75	0.6	24.86	13.8
70 - 86	1.87	28.5	12	44.1	12.2	5.3	5.2	0.18		4.25	0.15	4.48	16.13	2.25	0.9	28.16	15.1
86 - 98	1.93	31	11.5	42.6	10.6	5.4	5.2	0.18		4.93	0.15	4.06	18.58	1.3	0.45	25.68	19.2
98 - 109	1.92	33.5	10	39.9	11.4	5.6	5.4	0.19		5.41	0.15	3.92	21.49	0.65	0.3	31.92	16.9
109 - 117	1.92	32	10.5	41.4	10.4	5.4	5.4	0.18		5.75	0.15	4.13	24.83	0.6	0.25	27.01	21.3
117 - 128	1.84	28	12	43.8	12.3	5.5	5.5	0.16		5.20	0.15	4.06	15.91	0.55	0.1	25.97	20.0
128 - 142	2.03	35	8	47.1	11	5.9	5.7	0.12		5.20	0.15	4.13	22.83	0.3	0.15	28.51	18.2
142 - 160	2.12	23.5	145	50.2	13.1	6.05	5.8	0.13		4.66	0.15	3.78	14.79	0.2	0.1	23.68	142 - 19760
> 160	2.05	23.5	16.5	48.4	13.1	6.05	5.9	0.12		4.79	0.15	3.78	18.58	0.2	0	30.41	> 165.8

Table 26. Chemical and physical data analysis UF5

Depth (cm)	BD gr/cm3	% clay < 0.002 mm	% silt 0.002-0.02 mm	% fine sand 0.02-0.2 mm	% Coarse sand 0.2-2.0 mm	pH(H2O)	pH (CaCl2)	EC (dS/m)	% C-organic	Na+	K+	Ca++	Mg++	Al3+	H+	CEC	ESP
										(cmol(+)/kg							
0 - 10	1.43	20.5	12	21.5	53.5	5.8	5.6	0.08	2.02	0.1	0.4	15.2	13.2	0.0	0.1	29.0	0.4
10 - 20.	1.59	22	11	19.9	57.1	6	5.9	0.05	1.53	0.1	0.1	14.2	10.4	0.1	0.1	24.8	0.2
20 - 30	1.69	36.5	8.5	14.3	45.8	5.8	5.7	0.07	1.28	1.4	0.2	11.5	13.2	1.7	0.2	28.1	4.9
30 - 40	1.83	47	11	11.8	37	5.6	5.4	0.11		2.4	0.2	10.6	12.1	3.3	0.4	28.9	8.2
40 - 50	1.77	44.5	13	12.1	38.6	5.4	5.3	0.18		3.6	0.2	8.4	18.0	2.9	0.4	33.4	10.9
50 - 60	1.77	44.5	13.5	12.4	39.8	5.3	5.2	0.23		4.1	0.2	7.8	18.3	2.5	0.4	33.2	12.4
60 - 70	1.82	39	17	12.4	40.2	5.2	5.1	0.3		5.5	0.2	7.7	23.6	1.9	0.3	39.1	13.9
70 - 85	1.8	42	10.5	10.9	42.7	5.3	5.2	0.32		5.8	0.2	7.4	18.8	1.6	0.2	33.8	17.0
85 - 95	1.73	39.5	8.5	11.3	44.5	5.5	5.3	0.27		6.0	0.2	6.6	23.6	0.6	0.3	37.2	16.1
95 - 105	1.95	36	10.5	11.5	48	5.8	5.5	0.2		5.5	0.2	6.6	29.0	0.3	0.3	41.8	13.0
105 - 115	2.02	32	10.5	12.5	50.9	5.8	5.7	0.25		5.1	0.2	6.6	19.5	0.3	0.2	31.8	15.9
115 - 123	1.99	31	12.5	11.7	51.3	5.8	5.7	0.24		5.1	0.2	7.1	24.4	0.7	0.5	37.9	13.4
123 - 130	1.94	35.5	11	11.3	46.6	6.2	6	0.22		6.4	0.2	7.9	23.6	0.0	0.0	38.0	16.7
130 - 145	1.76	25.5	13.5	15.4	54	6.5	6.4	0.27		4.9	0.2	7.2	17.7	0.0	0.0	29.9	16.2
145 - 150	1.79	19.5	14.5	16.5	58.7	7.1	6.6	0.22		3.5	0.2	6.6	13.9	0.0	0.0	24.2	14.4
150 - 156	1.79	28	13.5	16	47.2	7.4	6.7	0.29		5.9	0.3	7.3	12.1	0.0	0.0	25.6	23.0
156 - 160	1.63	36	9.5	13.8	46.2	7.3	6.8	0.26		7.8	0.4	8.3	16.5	0.0	0.0	32.9	23.6
160 - 170	1.67	28.5	12	19	48.8	7.3	7.1	0.27		6.1	0.3	7.3	16.5	0.0	0.0	30.2	20.3
170 - 180	1.74	29	12.5	14.8	50.5	7.6	7.2	0.31		6.5	0.4	7.2	18.0	0.0	0.0	32.0	20.3
180 - 190	1.8	28.5	9.5	19.8	43.8	7.5	7.4	0.26		6.7	0.4	8.0	23.4	0.0	0.0	38.4	17.3

Appendix 2. Microprobe analysis data.

Table 27. Microprobe data analysis UF1 at 20 cm depth (quartz grain, marked "A" in plate 6).

Elements	I*	II	III	IV	V	VI	VII	VIII	IX	X
Al2O3	0.592	2.1	0.806	0.795	0.775	0.945	0.833	0.866	1.115	1.588
SiO2	89.748	78.563	77.535	83.125	96.512	89.952	93.855	87.792	85.783	90.163
P2O5	0	0	0	0.053	0.053	0	0	0	0	0.025
MgO	0.061	0.141	0.07	0.069	0.083	0.07	0.076	0.098	0.213	0.115
CaO	0.039	0.19	0.083	0.096	0.066	0.061	0.025	0.055	0.228	0.121
K2O	0	0.018	0.009	0.005	0	0	0	0.008	0.042	0.038
MnO	0.036	0.025	0.023	0	0	0	0.042	0.025	0	0
FeO	0.242	1.167	0.701	0.584	0.568	0.482	0.436	0.542	0.652	0.649
TiO2	0.109	0.164	0.113	0.066	0.031	0.069	0.092	0.03	0.064	0.067
Total	**90.827**	**82.368**	**79.34**	**84.793**	**98.088**	**91.579**	**95.359**	**89.416**	**88.097**	**92.766**

Table 28. Microprobe data analysis UF1 at 20 cm depth (clay microped with iron oxide coating, marked "B" in plate 6).

Elements	I	II	III	IV	V	VI	VII	VIII	IX	X
Al2O3	19.342	18.745	23.92	23.451	20.16	17.64	17.999	18.024	19.269	18.511
SiO2	49.478	52.946	47.286	49.653	44.474	56.596	58.001	48.906	49.737	45.03
P2O5	0.113	0.179	0.109	0.068	0.127	0.12	0.183	0.179	0.196	0.245
MgO	2.21	2.137	1.804	1.922	1.637	1.616	2.194	2.326	1.975	2.02
CaO	1.153	1.18	1.038	1.062	1.196	1.019	0.976	1.131	1.398	1.684
K2O	0.233	0.215	0.179	0.121	0.324	0.179	0.378	0.239	0.249	0.274
MnO	0.072	0	0.031	0.075	0.059	0	0	0	0	0.095
FeO	13.607	11.627	10.537	10.848	9.922	9.774	11.394	13.161	10.128	11.267
TiO2	1.247	1.212	1.139	1.184	4.101	1.273	1.592	1.678	1.31	1.332
Total	**87.455**	**88.241**	**86.043**	**88.384**	**82**	**88.217**	**92.717**	**85.644**	**84.262**	**80.458**

Table 29. Microprobe data analysis UF1 at 20 cm depth (iron nodules, marked "C" in plate 6).

Elements	I	II	III	IV	V
Al2O3	5.13	5.86	9.276	6.237	9.317
SiO2	7.414	7.235	14.277	8.741	14.075
P2O5	0.505	0.432	0.37	0.437	0.347
MgO	0.334	0.472	0.569	0.388	0.676
CaO	0.448	0.241	0.395	0.243	0.482
K2O	0.023	0.014	0.024	0.061	0.076
MnO	0.22	0.287	0.279	0.336	0.028
FeO	48.747	58.298	52.848	57.696	50.72
TiO2	0.336	0.395	0.722	0.556	0.779
Total	**63.157**	**73.234**	**78.76**	**74.695**	**76.5**

Table 30. Microprobe data analysis UF1 at 90 cm depth (coating of oriented clays, marked "A" in plate 15).

Elements	I	II	III	IV	V	VI	VII	VIII
Al2O3	15.166	15.691	13.142	13.752	13.258	10.585	15.611	18.164
SiO2	49.758	51.199	54.383	52.850	52.633	53.860	52.661	53.661
P2O5	0.154	0.004	0.041	0.055	0.102	0.022	0.067	0.024
MgO	3.365	3.307	3.825	3.046	3.128	3.534	2.715	2.735
CaO	0.881	0.785	0.733	0.859	0.881	0.887	0.737	0.779
K2O	0.039	0.037	0.012	0	0.018	0.008	0	0.012
MnO	0.091	0.103	0.163	0.064	0.158	0	0.055	0.079
FeO	9.056	9.611	12.682	17.195	17.764	19.876	16.195	14.468
TiO2	1.81	1.903	0.716	1.057	0.846	0.689	1.108	1.17
Total	**80.32**	**82.64**	**85.697**	**88.878**	**88.788**	**89.461**	**89.149**	**91.092**

Table 31. Microprobe data analysis UF1 at 90 cm depth (chalcedony, marked "A" in plate 14).

Elements	I	II	III
Al2O3	0.016	0.078	0.011
SiO2	95.166	93.782	94.398
P2O5	0.008	0.036	0.013
MgO	0	0.002	0.017
CaO	0	0.005	0.018
K2O	0	0	0.002
MnO	0.011	0	0.000
FeO	0.034	0.013	0.036
TiO2	0	0	0.020
Total	**95.235**	**93.916**	**94.515**

* Roman numerals indicate replicate analysis within one thin section.

Table 32. Microprobe data analysis UF1 at 90 cm depth (feldspar, marked "B" in plate 15).

Elements	I
Al2O3	13.33
SiO2	52.46
P2O5	0.057
MgO	2.409
CaO	0.279
K2O	1.105
MnO	0.079
FeO	15.011
TiO2	0.999
Total	**85.729**

Table 33. Microprobe data analysis UF1 at 90 cm depth (iron oxide glaebules, marked "B" in plate 14).

Elements	I	II
Al2O3	7.512	4.735
SiO2	27.44	9.994
P2O5	0.616	1.751
MgO	1.873	0.718
CaO	0.71	0.242
K2O	0.022	0.219
MnO	0.118	0.588
FeO	29.14	52.72
TiO2	1.056	1.054
Total	**68.487**	**72.021**

Table 34. Microprobe data analysis UF1 at 150 cm depth (iron oxide glaebules, marked "A" in plate 16).

Elements	I	II	III	IV	V	VI	VII	VIII
Al2O3	22.086	20.408	10.616	18.141	22.127	21.473	21.742	22.202
SiO2	54.842	52.113	64.13	50.867	51.398	50.903	50.039	50.432
P2O5	0.173	0.025	0.053	0.068	0.061	0.033	0.038	0.048
MgO	2.511	1.972	0.907	1.926	2.136	2.021	2.155	2.066
CaO	0.638	0.839	0.362	0.665	0.719	1.485	0.743	0.523
K2O	0.08	0.069	0.019	0.1	0.035	0.044	0.048	0.057
MnO	0.035	0.096	0	0.022	0.006	0.042	0.009	0.024
FeO	13.39	11.167	6.237	8.526	10.56	10.266	11.154	11.227
TiO2	0.689	0.594	0.25	0.428	1.2	0.727	0.582	0.541
Total	**94.444**	**87.283**	**82.574**	**80.743**	**88.242**	**86.994**	**86.51**	**87.12**

Table 35. Microprobe data analysis UF1 at 150 cm depth (Feldspar, marked "B" in plate 16).

Elements	I	II	III	IV	V	VI	VII	VIII
Al2O3	11.816	41.368	18.196	7.502	12.865	10.428	6.967	8.032
SiO2	61.898	38.726	56.035	70.821	40.887	53.161	67.014	76.006
P2O5	0.032	0.035	0.031	0	0.077	0.018	0.008	0.015
MgO	0.145	1.823	0.182	0.425	0.135	0.129	0.251	0.847
CaO	0.232	0.944	0.086	0.238	0.174	0.184	0.167	0.208
K2O	6.177	0.056	12.976	1.783	12.606	8.25	3.455	0.026
MnO	0.069	0	0	0	0	0	0.07	0
FeO	1.429	8.652	1.026	2.554	1.226	1.229	1.483	4.693
TiO2	0.146	0.427	0.038	0.127	0.098	0.057	0.052	0.243
Total	**81.944**	**92.031**	**88.57**	**83.45**	**68.068**	**73.456**	**79.467**	**90.07**

Table 36. Microprobe data analysis UF2 at 12 cm depth (quartz, marked "A" in plate 18).

Elements	I	II	III	IV	V	VI	VII	VIII
Al2O3	0.997	0.899	0.723	2.712	0.951	1.45	1.705	4.682
SiO2	94.062	95.971	95.547	93.013	95.448	94.185	89.378	86.751
P2O5	0	0.025	0	0	0	0	0	0
MgO	0.007	0.032	0.041	0.044	0.012	0.06	0.01	0.029
CaO	0.057	0.109	0.06	0.127	0.037	0.088	0.093	0.065
K2O	0.026	0.005	0.012	0.009	0.021	0.056	0.028	0.012
MnO	0.147	0.056	0	0	0	0.002	0.013	0
FeO	0.158	0.154	0.168	0.443	0.095	0.151	0.181	0.016
TiO2	0.039	0.01	0	0.064	0	0.028	0.038	0.025
Total	**95.493**	**97.261**	**96.551**	**96.412**	**96.564**	**96.020**	**91.446**	**91.580**

Table 37. Microprobe data analysis UF2 at 12 cm depth (iron oxide, marked "B" in plate 18).

Elements	I	II	III	IV	V	VI	VII
Al2O3	23.027	20.204	9.95	25.588	21.436	16.313	11.087
SiO2	45.531	34.803	9.349	40.707	46.06	64.117	1.827
P2O5	0.043	0.072	0.053	0.011	0.047	0.02	0.017
MgO	0.841	0.744	0.41	0.856	0.938	0.633	0.409
CaO	0.553	0.423	0.224	0.467	0.503	0.345	2.273
K2O	0.221	0.2	0.013	0.625	0.315	0.148	0.013
MnO	0.024	0.007	0.048	0.086	0	0.041	0.028
FeO	7.386	10.756	37.062	8.905	7.341	4.059	2.548
TiO2	0.313	0.342	0.049	0.686	0.527	0.506	0.016
Total	**77.939**	**67.551**	**57.158**	**77.931**	**77.167**	**86.182**	**18.218**

Table 38. Microprobe data analysis UF2 at 89 cm depth (quartz, marked "A" in plate 20).

Elements	I	II	III	IV	V	VI	VII	VIII	IX
Al2O3	1.178	0.367	1.12	0.483	0.955	1.255	0.993	3.286	1.275
SiO2	96.076	100.524	91.616	91.273	90.046	90.924	91.756	90.985	96.393
P2O5	0.03	0.045	0	0	0.003	0.026	0	0	0
MgO	0.117	0.036	0.112	0.041	0.155	0.116	0.092	0.06	0.108
CaO	0.087	0.049	0.182	0.056	0.148	0.129	0.09	0.023	0.063
K2O	0.193	0.056	0.154	0.069	0.271	0.274	0.254	0.057	0.116
MnO	0.027	0	0.064	0	0.016	0	0.03	0	1.088
FeO	0.531	0.299	0.57	0.209	0.454	0.358	0.411	0.113	0.381
TiO2	0.048	0.008	0	0	0.058	0.042	0.023	0.057	0.017
Total	**98.287**	**101.384**	**93.818**	**92.131**	**92.106**	**93.124**	**93.649**	**94.581**	**99.441**

Table 39. Microprobe data analysis UF2 at 89 cm depth (iron oxide accumulation, marked "B" in plate 20).

Elements	I	II	III
Al2O3	11.911	0.908	1.661
SiO2	27.782	8.067	2.665
P2O5	0.013	0	0.023
MgO	1.638	0.257	0.279
CaO	0.784	0.114	0.173
K2O	0.477	0.034	0.469
MnO	2.57	0.742	0.79
FeO	13.937	39.237	38.455
TiO2	14.509	33.783	28.812
Total	**73.621**	**83.142**	**73.327**

Table 40. Microprobe data analysis UF2 at 89 cm depth(manganese nodules, marked "C" in plate 20).

Elements	I	II	III	IV	V	VI
Al2O3	12.775	10.152	11.966	9.762	10.817	9.407
SiO2	31.396	31.935	33.793	19.197	25.771	22.047
P2O5	0	0	0	0	0	0
MgO	1.368	1.578	1.602	0.993	1.367	1.003
CaO	0.422	0.403	0.422	0.436	0.488	0.361
K2O	0.314	0.373	0.43	0.268	0.251	0.305
MnO	5.111	3.807	4.605	4.96	4.615	3.567
FeO	6.949	6.23	7.048	3.672	4.284	4.503
TiO2	0.259	0.185	0.208	0.133	0.192	0.171
Total	**58.594**	**54.663**	**60.074**	**39.421**	**47.785**	**41.364**

Table 41. Microprobe data analysis UF3 at 15 cm depth (iron oxide, marked "A" in plate 22).

Elements	I	II	III	IV	V	VI	VII
Al2O3	5.405	1.112	9.865	7.579	3.556	7.925	6.14
SiO2	47.403	46.471	4.568	18.047	2.252	14.164	9.793
P2O5	0.055	0.039	0.054	0.044	0	0.177	0.139
MgO	0.318	0.03	0.184	0.38	0.111	0.81	0.388
CaO	0.558	0.033	0.103	0.3	0.053	0.169	0.189
K2O	0.025	0.006	0.026	0.147	0	0.506	0.246
MnO	0.103	0.141	0	0	0.123	0.075	0
FeO	37.624	47.423	72.256	53.88	82.029	63.338	67.812
TiO2	0.318	1.077	0.648	1.285	0.106	0.351	0.488
Total	**91.809**	**96.332**	**87.704**	**81.662**	**88.23**	**87.515**	**85.195**

Table 42. Microprobe data analysis UF3 at 15 cm depth (quartz, marked "B" in plate 22).

Elements	I	II	III	IV	V	VI
Al2O3	1.708	0.406	0.718	0.464	1.911	0.449
SiO2	89.967	93.827	95.97	94.369	87.434	94.944
P2O5	0	0.017	0.008	0	0.012	0
MgO	0.024	0.015	0.013	0.005	0.046	0.012
CaO	0.051	0.063	0.036	0.063	0.05	0.022
K2O	0.01	0.002	0	0.033	0.121	0.01
MnO	0	0.023	0	0.081	0.082	0.004
FeO	0.248	0.106	0.354	0.215	0.763	0.644
TiO2	0	0.017	0.037	0	0.011	0.025
Total	**92.008**	**94.476**	**97.136**	**95.23**	**90.43**	**96.11**

Table 43. Microprobe data analysis UF3 at 15 cm depth (feldspar, marked "C" in plate 22).

Elements	I	II	III	IV	V	VI	VII
Al2O3	18.551	22.244	20.669	18.507	16.632	12.157	30.623
SiO2	67.245	57.532	61.349	63.969	59.375	58.255	29.081
P2O5	0.027	0.079	0.046	0	0.015	0.02	0.063
MgO	0.021	0.018	0.036	0.004	0.005	0	0.327
CaO	0.201	4.97	3.621	0.588	0.153	0.419	1.582
K2O	10.768	0.292	0.261	10.18	12.473	0.026	0.44
MnO	0	0	0	0	0.045	0.079	0.002
FeO	1.153	5.35	7.544	0.657	0.532	15.816	16.769
TiO2	0.086	0.023	0	0.024	0.047	0.126	0.179
Total	**98.052**	**90.508**	**93.526**	**93.929**	**89.277**	**86.898**	**79.066**

Table 44. Microprobe data analysis UF3 at 46 cm depth (iron oxide, marked "A" in plate 24).

Elements	I	II	III	IV
Al2O3	6.316	6.445	8.779	16.234
SiO2	56.127	40.689	13.695	28.002
P2O5	0.129	0.076	0.296	0.217
MgO	0.188	0.274	0.317	0.551
CaO	0.099	0.267	0.139	0.128
K2O	0.086	0.206	0.323	2.526
MnO	0.266	0.189	0.588	0.2
FeO	26.142	11.152	30.689	29.697
TiO2	0.021	0.074	0.133	0.23
Total	**89.374**	**59.372**	**54.959**	**77.785**

Table 45. Microprobe data analysis UF3 at 86 cm depth (iron oxide and clay accumulation, plate 26).

Elements	I	II	III	IV	V	VI	VII	VIII	IX
Al2O3	20.054	23.056	29.745	22.096	9.273	15.036	19.246	24.294	23.24
SiO2	42.69	36.917	38.214	51.556	77.725	66.052	36.9	45.507	42.815
P2O5	0.184	0.041	0.002	0	0	0	0	0.059	0
MgO	2.492	0.861	0.355	1.124	0.708	0.916	1.246	1.674	0.964
CaO	0.151	0.288	0.148	0.167	0.078	0.137	0.135	0.268	0.136
K2O	1.549	0.11	0.153	1.607	2.165	0.94	1.123	1.999	0.939
MnO	0.168	0.049	0	1.411	0.079	0.86	2.213	0	0.013
FeO	5.92	3.227	2.033	1.882	1.83	3.057	4.729	6.359	4.55
TiO2	0.877	3.168	0.042	0.444	1.849	0.213	0.238	0.836	0.321
Total	**74.085**	**67.717**	**70.692**	**80.287**	**93.707**	**87.211**	**65.83**	**80.996**	**72.978**

Table 46. Microprobe data analysis UF3 at 86 cm depth (carbonate glaebules, marked "A" in plate 27).

Elements	I	II	III	IV	V	VI	VII	VIII
Al2O3	3.093	2.411	1.308	1.901	3.057	2.021	1.454	2.495
SiO2	2.969	2.301	1.662	2.216	5.705	3.833	1.704	4.525
P2O5	0.452	0.448	0.512	0.464	0.512	0.455	0.43	0.47
MgO	14.623	17.025	17.244	15.619	15.68	14.62	18.303	14.369
CaO	25.787	27.015	28.528	27.04	25.464	26.75	27.66	25.801
K2O	0.073	0.047	0.084	0.082	0.115	0.151	0.087	0.145
MnO	0.062	0.037	0	0.047	0.096	0.051	0.729	0.159
FeO	0.762	0.274	0.16	0.299	0.346	0.358	0.192	0.248
TiO2	0.032	0	0.036	0.007	0.219	0.056	0.003	0.251
Total	**47.853**	**49.558**	**49.534**	**47.675**	**51.194**	**48.295**	**50.562**	**48.463**

Table 47. Microprobe data analysis UF3 at 93 cm depth (Albite, marked "A" in plate 29).

Elements	I	II	III	IV	V	VI	VII	VIII	IX
Al2O3	13.020	20.193	26.828	7.683	13.963	26.478	22.906	16.874	16.586
SiO2	55.860	51.297	36.094	54.473	57.001	38.671	39.770	32.466	29.606
P2O5	0.010	0.029	0.056	0.036	0.054	0.022	0.049	0.042	0.063
MgO	1.626	1.037	1.793	0.942	1.324	1.929	2.074	1.900	1.192
CaO	0.602	0.711	1.509	0.806	1.682	1.849	2.027	2.177	1.318
K2O	2.205	0.583	1.262	0.340	1.043	1.562	1.247	1.104	0.994
Na2O	0.321	0.235	0.359	0.250	0.202	0.297	0.345	0.270	0.244
MnO	0.000	0.000	0.000	0.019	0.011	0.000	0.051	0.049	0.170
FeO	1.802	1.302	3.096	0.940	1.345	2.036	2.426	4.195	9.425
TiO2	3.885	0.148	0.538	0.260	0.267	0.355	0.460	0.432	0.362
Total	**79.331**	**75.533**	**71.536**	**65.747**	**76.893**	**73.199**	**71.354**	**59.508**	**59.960**

Table 48. Microprobe data analysis UF3 at 93 cm depth (quartz, marked "B" in plate 29).

Elements	I	II	III	IV	V	VI	VII	VIII
Al2O3	1.126	1.383	4.788	2.412	1.063	6.938	1.712	5.677
SiO2	91.314	85.564	80.858	93.498	88.604	65.049	89.218	79.808
P2O5	0.000	0.003	0.021	0.006	0.022	0.011	0.035	0.019
MgO	0.213	0.273	0.494	0.346	0.282	0.294	0.369	0.470
CaO	0.344	0.615	0.637	0.361	0.526	0.642	0.551	0.873
K2O	0.022	0.030	0.064	0.135	0.040	0.024	0.091	0.152
Na2O	0.032	0.070	0.085	0.092	0.097	0.070	0.081	0.079
MnO	0.136	0.000	0.078	0.000	0.064	0.022	0.007	0.000
FeO	0.133	0.124	0.256	0.543	0.115	0.163	0.278	0.271
TiO2	0.000	0.049	0.048	0.037	0.000	0.013	0.060	0.056
Total	**93.320**	**88.110**	**87.328**	**97.430**	**90.812**	**73.225**	**92.400**	**87.405**

Table 49. Microprobe data analysis UF3 at 93 cm depth (carbonate nodules, marked "A" in plate 30).

Elements	I	II	III	IV
Al2O3	2.494	3.120	9.714	4.130
SiO2	3.750	4.483	3.441	6.437
P2O5	0.329	0.384	0.000	0.240
MgO	12.779	12.238	0.377	7.393
CaO	21.913	21.136	0.744	14.178
K2O	0.121	0.125	0.052	0.118
Na2O	0.117	0.129	0.082	0.129
MnO	0.000	0.030	0.038	0.024
FeO	0.351	0.406	0.505	1.445
TiO2	0.017	0.062	0.036	0.064
Total	**41.871**	**42.112**	**14.987**	**34.158**

Table 50. Microprobe data analysis UF4 at 70 cm depth (quartz, marked "A" in plate 32).

Elements	I	II	III	IV	V	VI	VII	VIII
Al2O3	0.918	1.549	1.719	7.084	1.815	5.054	1.815	5.054
SiO2	91.944	94.267	95.26	71.422	91.293	78.598	91.293	78.598
P2O5	0	0.004	0	0.001	0	0	0	0
MgO	0.012	0.02	0.03	0.044	0.081	0.065	0.081	0.065
CaO	0.053	0.054	0.052	0.171	0.047	0.16	0.047	0.16
K2O	0.013	0.023	0.019	0.189	0.034	0.007	0.034	0.007
MnO	0.025	0.006	0.092	0	0.008	0	0.008	0
FeO	0.367	0.279	0.466	0.593	0.351	0.633	0.351	0.633
TiO2	0	0.02	0.094	0.582	0	0	0	0
Total	**93.332**	**96.222**	**97.732**	**80.086**	**93.629**	**84.517**	**93.629**	**84.517**

Table 51. Microprobe data analysis UF4 at 70 cm depth (iron nodules, marked "B" in plate 32).

Elements	I	II	III	IV	V	VI	VII	VIII
Al2O3	11.113	15.704	16.425	22.396	24.858	22.665	15.94	17.118
SiO2	70.227	57.633	37.23	57.687	40.601	45.006	37.157	31.098
P2O5	0.008	0.026	0.014	0	0	0	0	0.012
MgO	0.301	0.484	0.587	0.913	0.712	0.823	0.473	0.595
CaO	0.086	0.043	0.131	0.065	0.366	0.077	0.108	0.095
K2O	1.072	0.509	0.363	0.41	0.301	0.39	0.436	0.319
MnO	0.001	0	0.004	0	0	0.058	0.041	0
FeO	2.516	5.754	9.099	7.121	7.385	9.465	9.336	12.762
TiO2	0.41	0.475	0.704	2.545	0.422	0.883	0.628	0.386
Total	**85.734**	**80.628**	**64.557**	**91.137**	**74.645**	**79.367**	**64.119**	**62.385**

Appendix 3. Mineralogy of sand fraction.

Table 52. Counting heavy mineral grains UF1

Depth (cm)	(0 - 5)	(10 - 15)	(23 - 30)	(60 - 70)	(80 - 100)	(150 - 160)
Minerals						
Ilmenite	216	159	230	242	44	40
Leucoxene	26	6	5	10		9
Zircon	46	16		30	1	3
Tourmaline						
Rutile	38	15	28		11	
Barite					63	5
Iron oxides	286	319	285	256	212	276
Pyroxene	206	139	180	116	241	70
Total	818	656	728	654	572	403

Table 53. Counting heavy mineral grains UF2.

Depth (cm)	(0 - 5)	(10 - 16)	(46 - 62)	(112 - 120)	(138 - 156)	(> 156)
Minerals						
Ilmenite	185	576	58	159	180	178
Leucoxene	44	97	7	74	59	59
Zircon	5	26	12	6	17	28
Tourmaline	1	13	2			1
Rutile	76	35	18	13	39	36
Barite						
Iron oxides	64	20	13	74	208	371
Pyroxene	248	72	16	54	141	312
Total	623	839	126	380	644	985

Table 54. Counting heavy mineral grains UF3.

Depth (cm)	(0 - 5)	(10 - 15)	(95 - 100)	(125 - 135)	(> 135)
Minerals					
Ilmenite	350	361	81	100	90
Leucoxene	75	67	61	109	45
Zircon	61	68	1	108	38
Tourmaline	16	23	22	22	13
Rutile	125	127	16	166	133
Barite					
Iron oxides	193	290	151	46	64
Pyroxene	176	246			
Total	996	1182	332	551	383

Table 55. Counting heavy mineral grains UF4.

Depth (cm)	(0 - 5)	(5 - 10)	(38 - 46)	(70 - 86)	(128 - 142)	(> 160)
Minerals						
Ilmenite	180	42	246	238	294	345
Leucoxene	35	12	46	71	33	50
Zircon	165	41	29	57	14	17
Tourmaline	26	2	12	35	9	7
Rutile	132	17	55	116	22	43
Barite						
Iron oxides	97	114	147	209	380	365
Pyroxene	24	28		1	4	304
Total	659	256	535	727	756	1131

Table 56. Counting heavy mineral grains UF5

Depth (cm)	(0 - 5)	(20 - 30)	(70 - 85)	(115 - 123)	(145 - 150)	(180 - 190)
Minerals						
Ilmenite	325	339	367	189	268	254
Leucoxene	64	25	21	11	25	5
Zircon	152	48	15	1	7	4
Tourmaline	28	3	2		2	
Rutile	103	100	42	11	22	20
Barite						
Iron oxides	60	102	526		30	36
Pyroxene	216	22	60	231	75	533
Total	948	639	1033	443	429	852

Table 57. The percentage of heavy mineral grains UF1.

Depth (cm)	(0-5)	(10 -15)	(23-30)	(60-70)	(80 -100)	(150-160)	(> 160)
Minerals							
Ilmenite	26.4	24.2	31.6	37.0	7.7	9.9	28.9
Leucoxene	3.2	0.9	0.7	1.5		2.2	0.4
Zircon	5.6	2.4		4.6	0.2	0.7	
Tourmaline		0.3					
Rutile	4.6	2.3	3.8		1.9		
Barite					11.0	1.2	
Iron oxides	35.0	48.6	39.1	39.1	37.1	68.5	13.7
Pyroxene	25.2	21.2	24.7	17.7	42.1	17.4	57.0
Total	100	100	100	100	100	100	100

Table 58. The percentage of heavy mineral grains UF2.

Depth (cm)	(0 - 5)	(10 - 16)	(46 - 62)	(112 - 120)	(138 - 156)	(> 156)
Minerals						
Ilmenite	29.7	68.7	46.0	41.8	28.0	18.1
Leucoxene	7.1	11.6	5.6	19.5	9.2	6.0
Zircon	0.8	3.1	9.5	1.6	2.6	2.8
Tourmaline	0.2	1.5	1.6			0.1
Rutile	12.2	4.2	14.3	3.4	6.1	3.7
Barite						
Iron oxides	10.3	2.4	10.3	19.5	32.3	37.7
Pyroxene	39.8	8.6	12.7	14.2	21.9	31.7
Total	100	100	100	100	100	100

Nil = 0%; Trace = 0 - 10%; Little = 10 - 25%; Moderate = 25 - 50 %; Much = > 50%

Table 59. The percentage of heavy mineral grains UF3.

Depth (cm)	(0 - 5)	(10 - 15)	(95 - 100)	(125 - 135)	(> 135)
Minerals					
Ilmenite	35.1	30.5	24.4	18.1	23.5
Leucoxene	7.5	5.7	18.4	19.8	11.7
Zircon	6.1	5.8	0.3	19.6	9.9
Tourmaline	1.6	1.9	6.6	4.0	3.4
Rutile	12.6	10.7	4.8	30.1	34.7
Barite					
Iron oxides	19.4	24.5	45.5	8.3	16.7
Pyroxene	17.7	20.8			
Total	100	100	100	100	100

Nil = 0%; Trace = 0 - 10%; Little = 10 - 25%; Moderate = 25 - 50 %; Much = > 50%

Table 60. The percentage of heavy mineral grains UF4.

Depth (cm)	(0 - 5)	(5 - 10)	(38 - 46)	(70 - 86)	(128 - 142)	(> 160)
Minerals						
Ilmenite	27.3	16.4	46.0	32.7	38.9	30.5
Leucoxene	5.3	4.7	8.6	9.8	4.4	4.4
Zircon	25.0	16.0	5.4	7.8	1.9	1.5
Tourmaline	3.9	0.8	2.2	4.8	1.2	0.6
Rutile	20.0	6.6	10.3	16.0	2.9	3.8
Barite						
Iron oxides	14.7	44.5	27.5	28.7	50.3	32.3
Pyroxene	3.6	10.9		0.1	0.5	26.9
Total	100	100	100	100	100	100

Nil = 0%; Trace = 0 - 10%; Little = 10 - 25%; Moderate = 25 - 50 %; Much = > 50%

Table 61. The percentage of heavy mineral grains UF5.

Depth (cm)	(0 - 5)	(20 - 30)	(70 - 85)	(115 - 123)	(145 - 150)	(180 - 190)
Minerals						
Ilmenite	34.3	53.1	35.5	42.7	62.5	29.8
Leucoxene	6.8	3.9	2.0	2.5	5.8	0.6
Zircon	16.0	7.5	1.5	0.2	1.6	0.5
Tourmaline	3.0	0.5	0.2		0.5	
Rutile	10.9	15.6	4.1	2.5	5.1	2.3
Barite						
Iron oxides	6.3	16.0	50.9		7.0	4.2
Pyroxene	22.8	3.4	5.8	52.1	17.5	62.6
Total	100	100	100	100	100	100

Nil = 0%; Trace = 0 - 10%; Little = 10 - 25%; Moderate = 25 - 50 %; Much = > 50%

Table 62. Counting light mineral grains UF1. Depth (cm) Minerals K-Feldspar Plagioclase Quartz

Depth (cm)	(0 - 5)	(10 - 15)	(23 - 30)	(60 - 70)	(80 - 100)	(150 - 160)	(> 160)
Minerals							
K-Feldspar	231	74	32	90	-	-	16
Plagioclase	185	152	210	63	-	35	42
Quartz	471	376	426	350	42	265	364
Siderómelane					315		
Tachylite					322		
Total	887	602	668	503	679	300	422

Table 63. Counting light mineral grains UF2.

Depth (cm)	(0 - 5)	(10 - 16)	(46 - 62)	(112 - 120)	(138 - 156)	(> 156)
Minerals						
K-Feldspar	-	53	10	-	-	-
Plagioclase	-	-	-	136	288	247
Quartz	350	386	378	367	375	388
total	350	439	388	503	663	635

Table 64. Counting light mineral grains UF3.

Depth (cm)	(0 - 5)	(10 - 15)	(95 - 100)	(125 - 135)	(> 135)
Minerals					
K-Feldspar	22	16	-	-	-
Plagioclase	50	31	95	48	63
Quartz	364	356	326	356	348
Total	436	403	421	404	411

Table 65. Counting light mineral grains UF4.

Depth (cm)	(0 - 5)	(5 - 10)	(38 - 46)	(70 - 86)	(128 - 142)	(> 160)
Minerals						
K-Feldspar	11	5	15	7	3	10
Plagioclase	16	4	-	-	56	53
Quartz	425	415	420	396	382	389
Total	452	424	435	403	441	452

Table 66. Counting light mineral grains UF5.

Depth (cm)	(0 - 5)	(20 - 30)	(70 - 85)	(115 - 123)	(145 - 150)	(180 - 190)
Minerals						
K-Feldspar	12	13	-	-	-	-
Plagioclase	41	15	23	37	49	108
Quartz	294	315	352	346	326	286
Total	347	343	375	383	375	394

Table 67. Microprobe data analysis UF1 at 80 - 100 cm depth (quartz).

Elements	I	II
Al2O3	0.116	0.028
SiO2	97.776	98.368
P2O5	0.001	0
MgO	0.009	0.009
CaO	0	0.016
K2O	0.001	0.027
MnO	0	0.043
FeO	0.174	0
TiO2	0.152	0.006
Total	**98.229**	**98.497**

Table 68. Microprobe data analysis UF1 at 80 - 100 cm depth (Sideromelane).

Elements	I	II	III	IV	V
Al2O3	13.747	13.124	14.625	8.604	9.888
SiO2	53.98	55.372	56.04	57.17	58.671
P2O5	0.158	0.11	0.045	0.241	0.102
MgO	1.175	1.177	1.273	1.818	2.283
CaO	0.219	0.086	0.096	0.617	0.181
K2O	0.22	0.036	0.058	0.706	0.685
MnO	0	0	0	0	0.104
FeO	17.712	18.641	17.397	20.869	19.96
TiO2	1.409	1.269	1.874	1.192	0.94
Total	**88.62**	**89.815**	**91.408**	**91.217**	**92.814**

Table 69. Microprobe data analysis UF1 at 80 - 100 cm depth (Tachylite).

Elements	I	II	III
Al2O3	17.02	17.31	17.549
SiO2	51.918	51.579	47.864
P2O5	0.12	0.256	0.26
MgO	1.545	1.767	1.303
CaO	0.149	0.162	0.095
K2O	1.104	1.128	0.667
MnO	0.047	0.056	0.049
FeO	12.968	12.38	12.102
TiO2	6.282	9.759	12.04
Total	**91.153**	**94.397**	**91.929**

Table 70. The percentage of light mineral grains UF1.

Depth (cm)	(0 - 5)	(10 - 15)	(23 - 30)	(60 - 70)	(80 - 100)	(150 - 160)	(> 160)
Minerals							
K-Feldspar	26	12	5	18		-	4
Plagioclase	21	25	31	13		12	10
Quartz	53	62	64	70	6	88	86
Sideromelane					46		
Tachylite					47		
Total	100	100	100	100	100	100	100

Nil = 0%; Trace = 0 - 10%; Little = 10 - 25%; Moderate = 25 - 50 %; Much = > 50%

Table 71. The percentage of light mineral grains UF2.

Depth (cm)	(0 - 5)	(10 - 16)	(46 - 62)	(112 - 120)	(138 - 156)	(> 156)
Minerals						
K-Feldspar	8	12	9	-	-	-
Plagioclase	-	-	-	27	43	39
Quartz	92	88	81	73	57	61
total	92	100	100	100	100	100

Table 72. The percentage of light mineral grains UF3.

Depth (cm)	(0 - 5)	(10 - 15)	(95 - 100)	(125 - 135)	(> 135)
Minerals					
K-Feldspar	5	4	-	-	-
Plagioclase	11	8	23	12	15
Quartz	83	88	77	88	85
Total	100	100	100	100	100

Table 73. The percentage of light mineral grains UF4.

Depth (cm)	(0 - 5)	(5 - 10)	(38 - 46)	(70 - 86)	(128 - 142)	(> 160)
Minerals						
K-Feldspar	2	1	3	2	1	2
Plagioclase	4	1	-	-	13	12
Quartz	94	98	97	98	87	86
Total	100	100	100	100	100	100

Table 74. Counting light mineral grains UF5.

Depth (cm)	(0 - 5)	(20 - 30)	(70 - 85)	(115 - 123)	(145 - 150)	(180 - 190)
Minerals						
K-Feldspar	3	4	-	-	-	-
Plagioclase	12	4	6	10	13	27
Quartz	85	92	94	90	87	73
Total	100	100	100	100	100	100

Appendix 4. X-ray diffraction analysis.

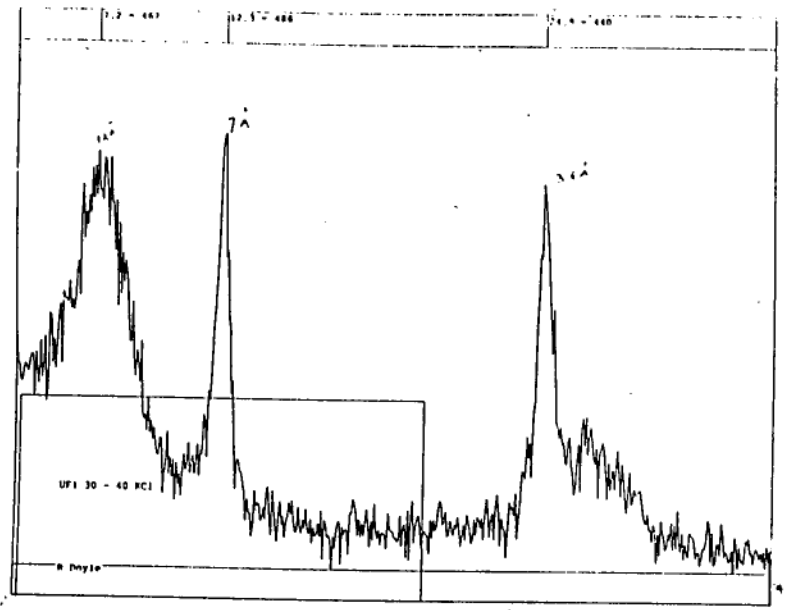
UF1 30 - 40 KCl
R Doyle

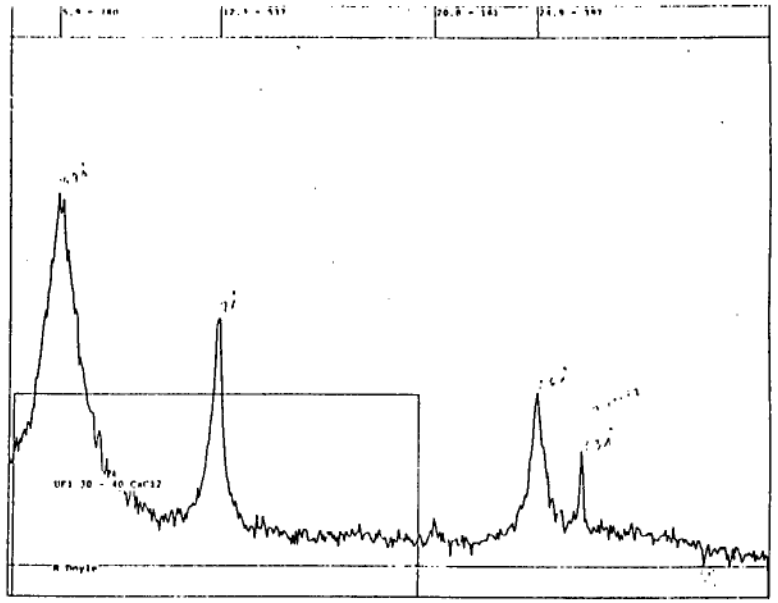
UF1 30 - 40 CaCl2
R Doyle

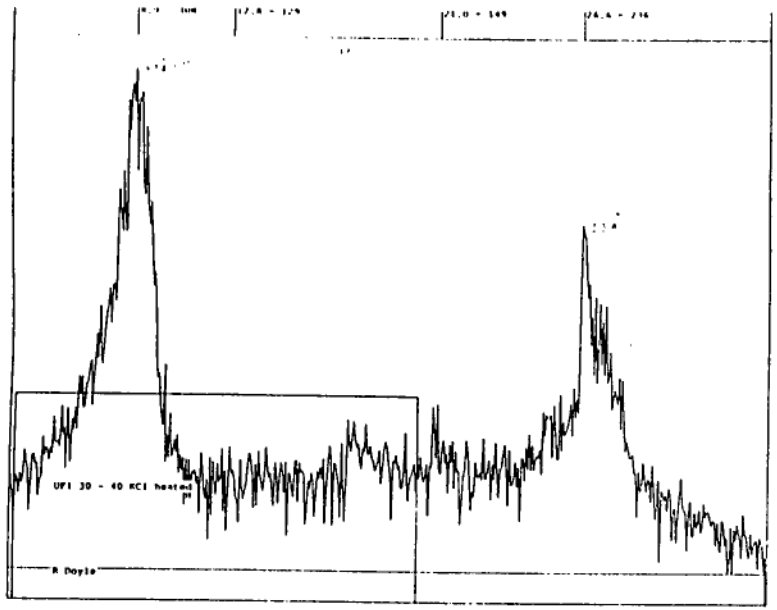
UF1 30 - 40 KCl heated
R Doyle

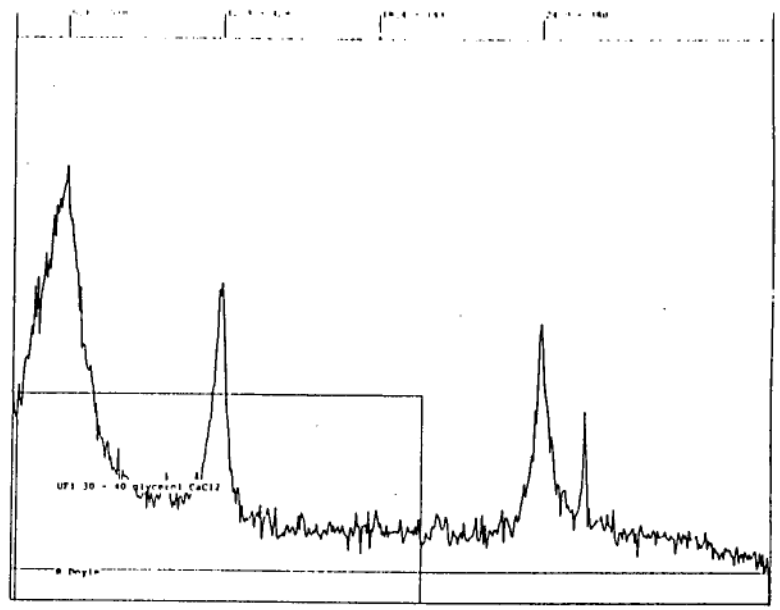
UF1 30 - 40 glycerol CaCl2
R Doyle

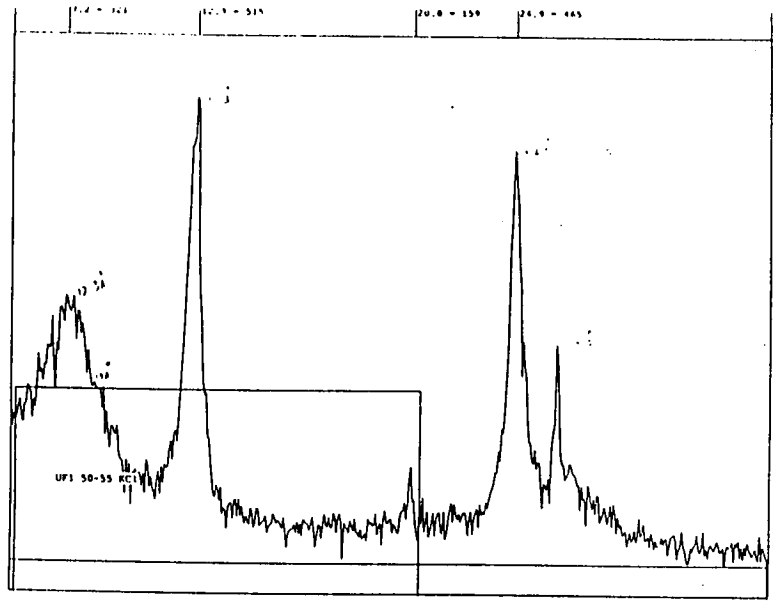
UF1 50-55 KCl

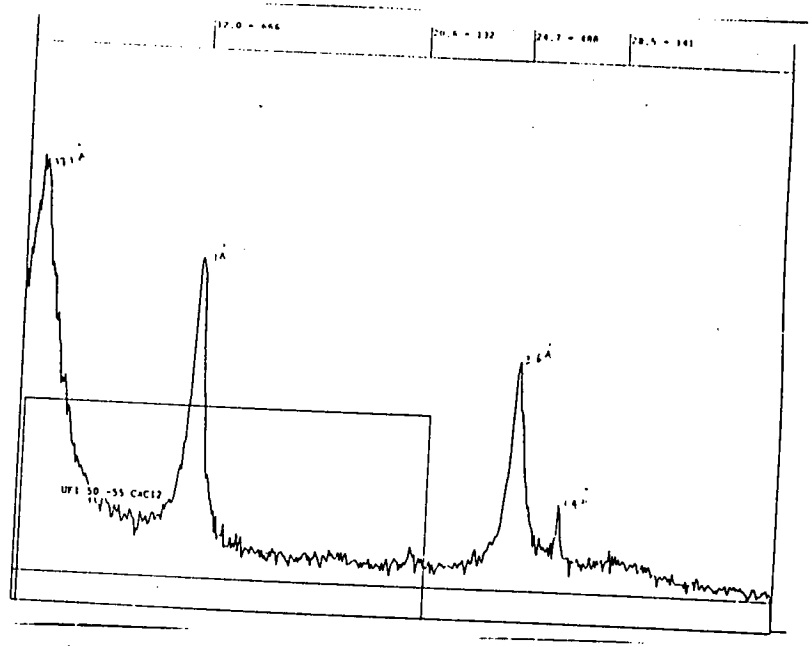
UF1 50 -55 CaCl2

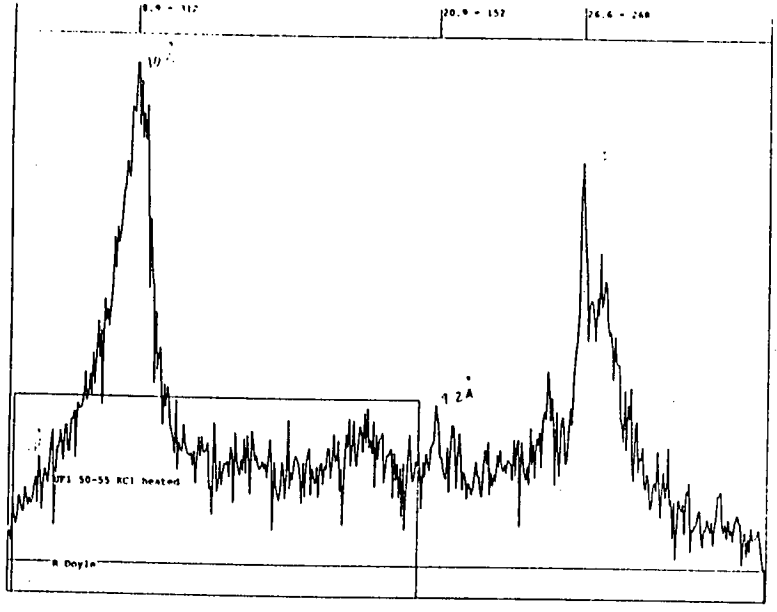
UF1 50-55 KCl heated
R Doyle

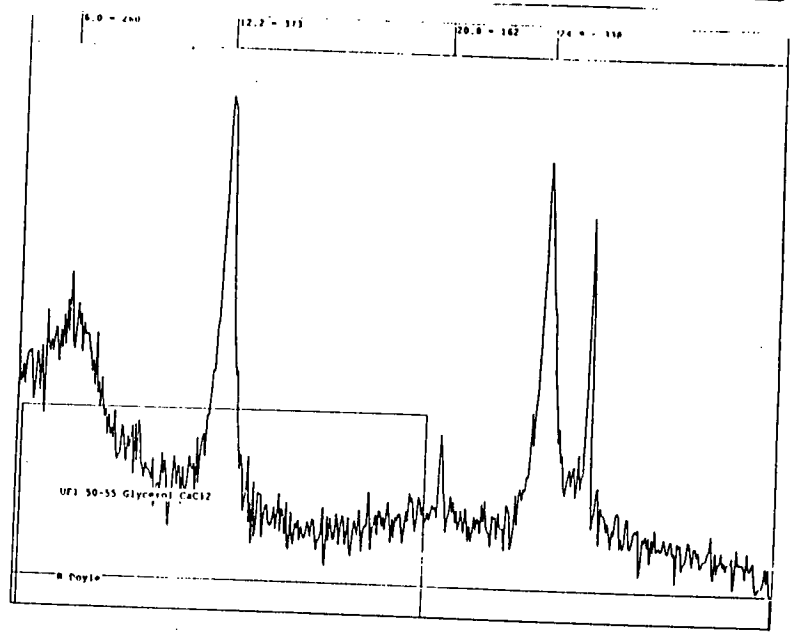
UF1 50-55 Glycerol CaCl2
R Doyle

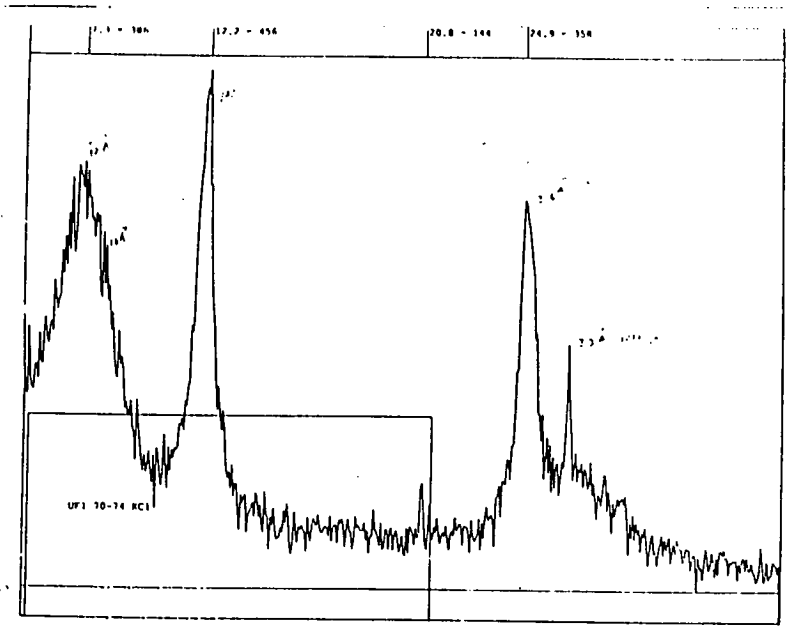
UF1 70-74 RCl

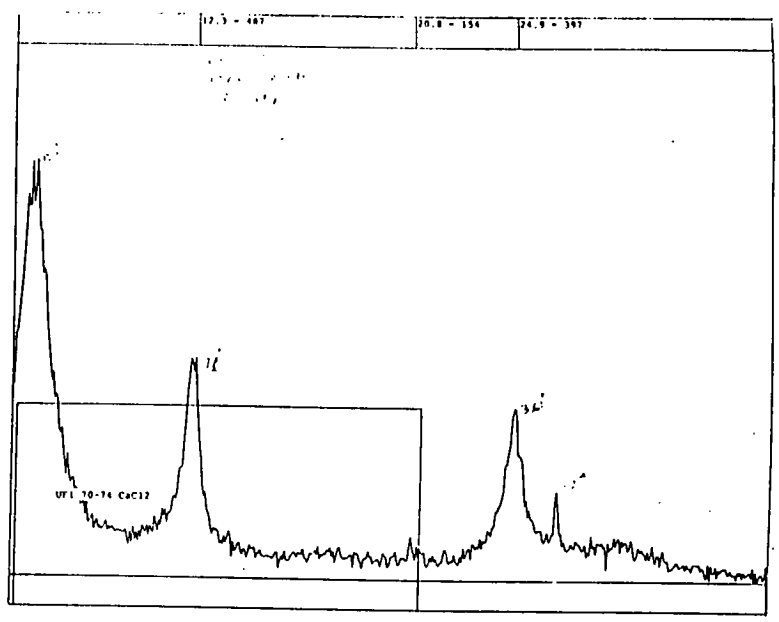
UF1 70-74 CaCl2

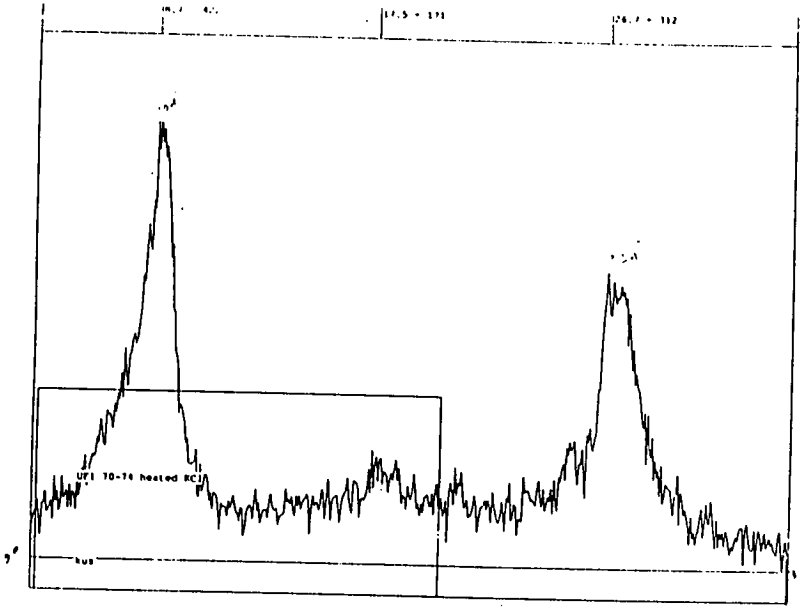
UF1 70-74 heated RCl

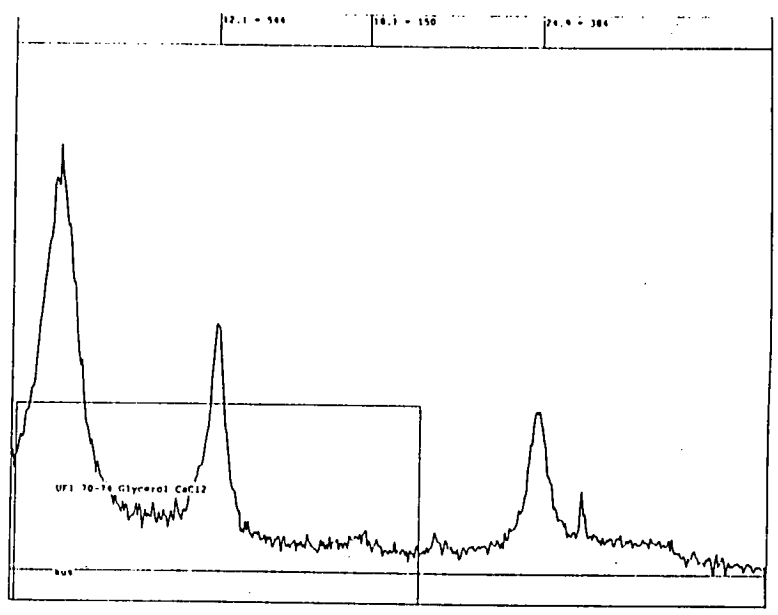
UF1 70-74 Glycerol CaCl2

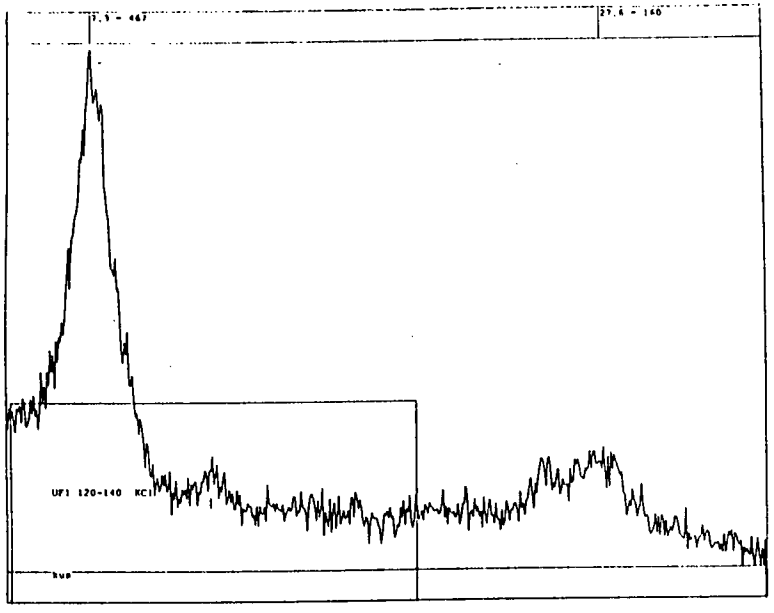
UF1 120-140 KCl
Run

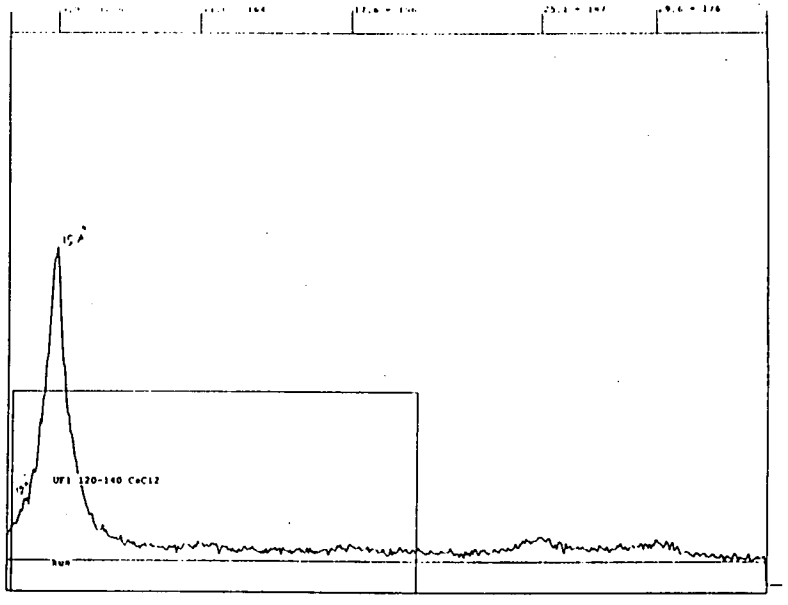
15 Å
UF1 120-140 CaCl2
Run

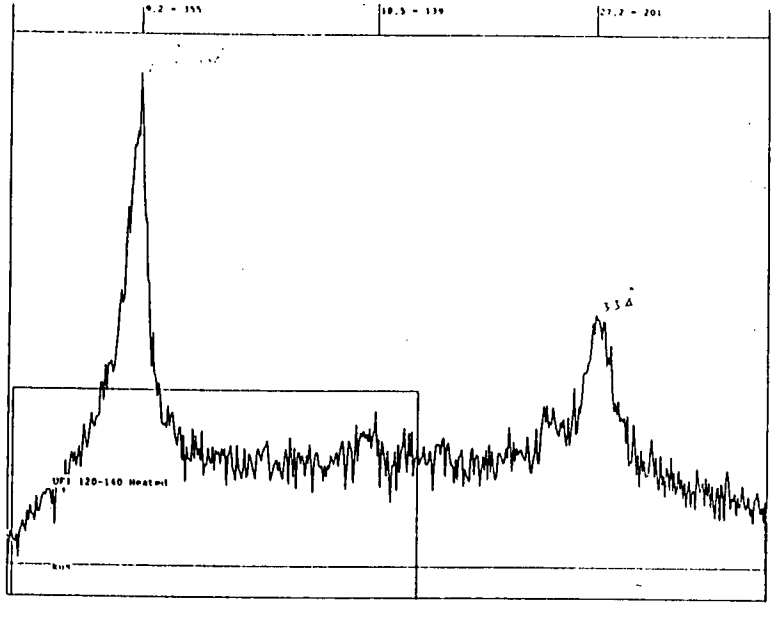
9.2 = 355
10.5 = 139
27.2 = 201
33 Å
UF1 120-140 Heated
Run

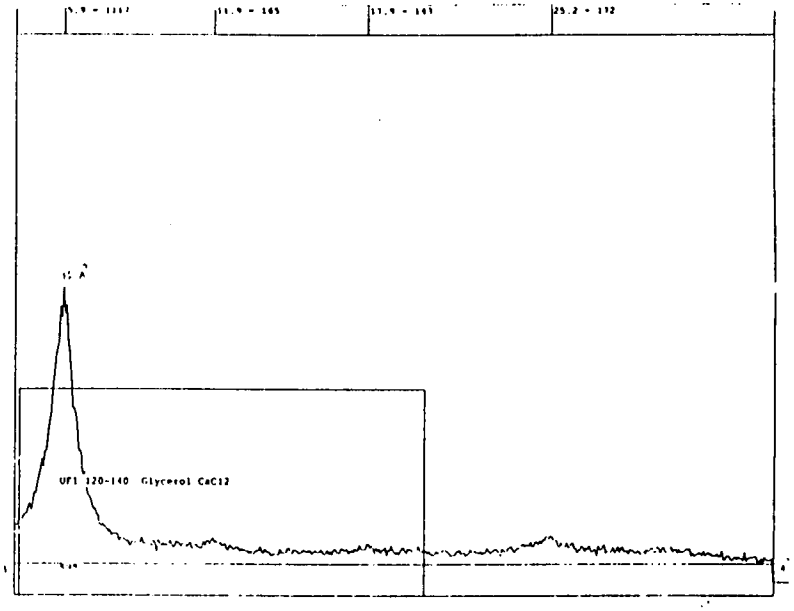
11.9 = 165
25.2 = 172
15 Å
UF1 120-140 Glycerol CaCl2

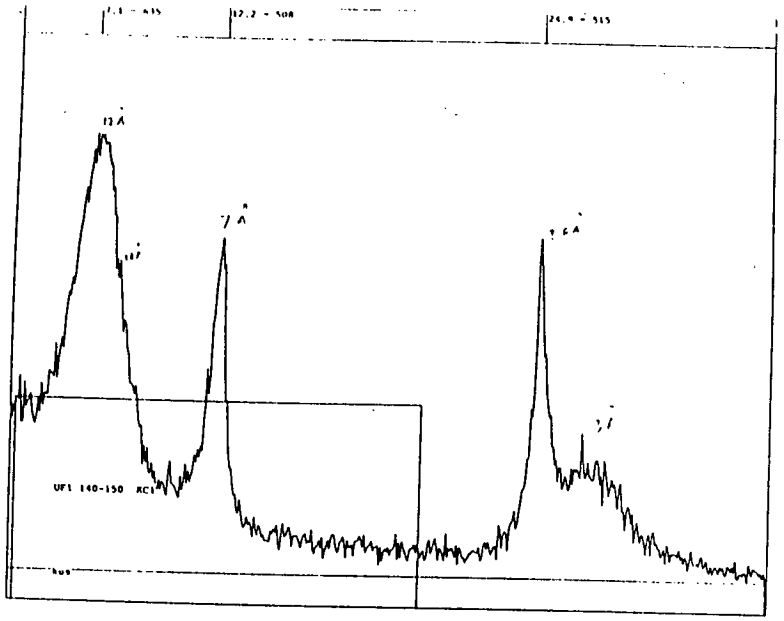
12 Å
7 Å
9.6 Å
UF1 140-150 KCl

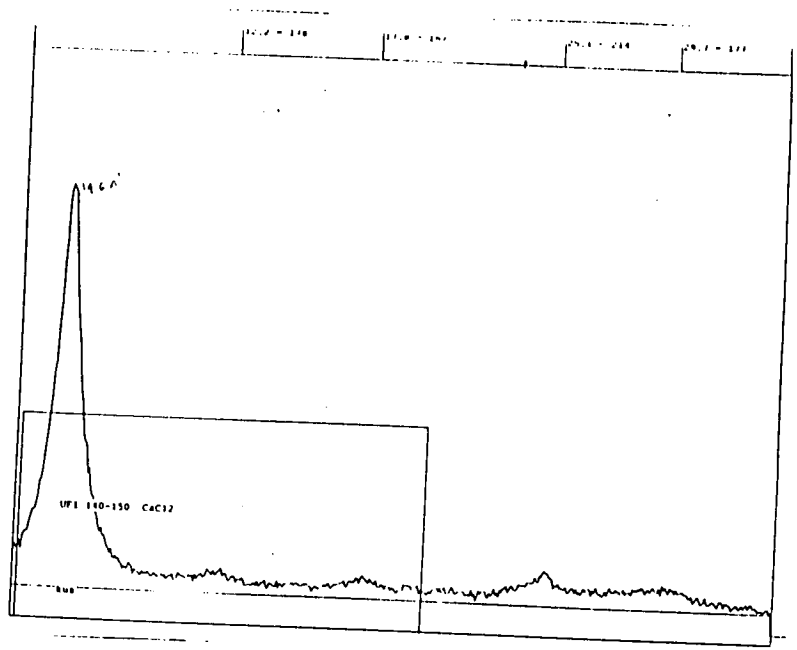
14.6 Å
UF1 140-150 CaCl2

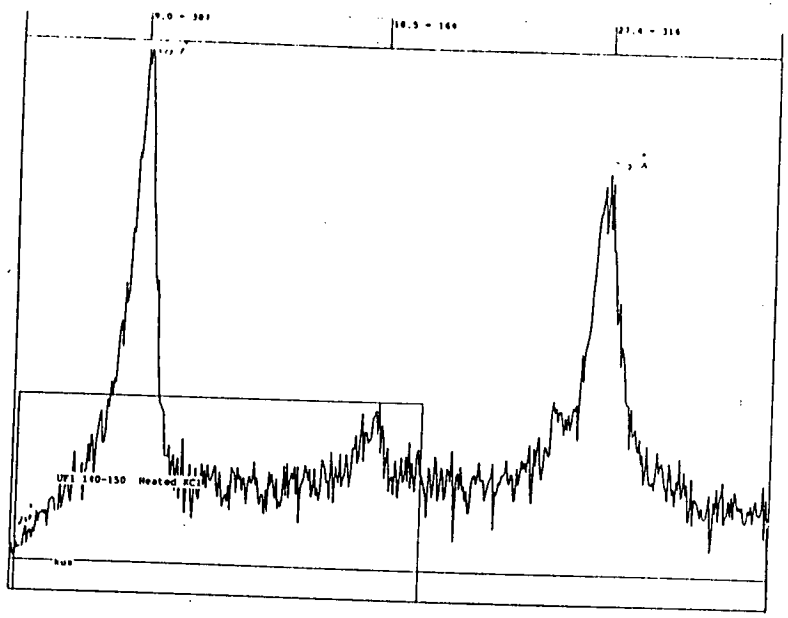
UF1 140-150 Heated KCl

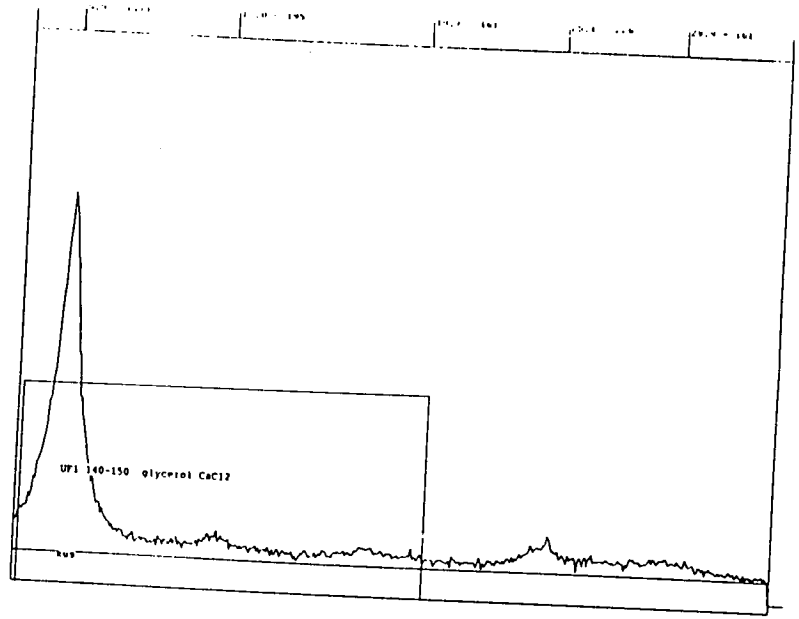
UF1 140-150 Glycerol CaCl2

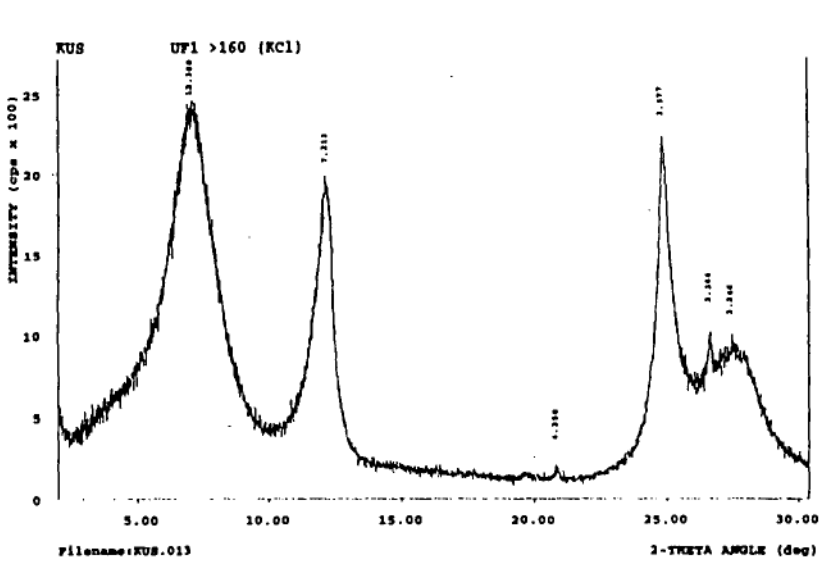
KUS
UF1 >160 (KC1)
INTENSITY (cps x 100)
2-THETA ANGLE (deg)
Filename:KUS.013

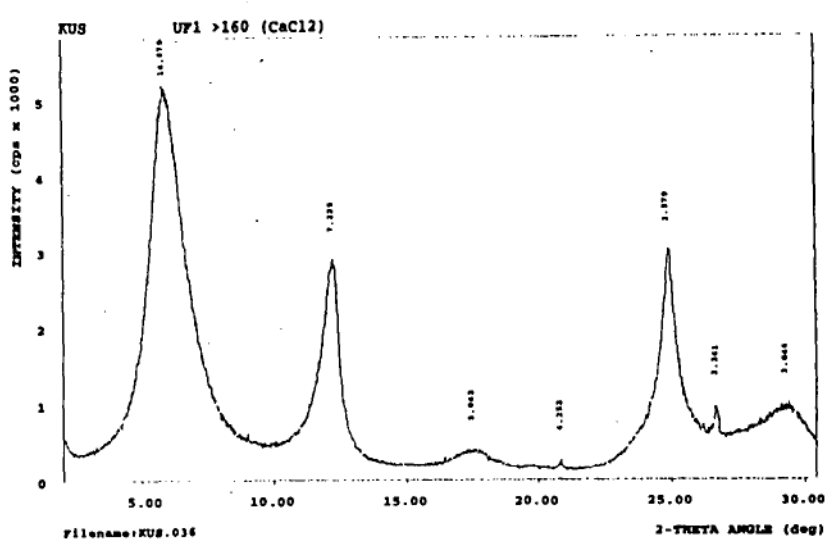
KUS
UF1 >160 (CaCl2)
INTENSITY (cps x 1000)
2-THETA ANGLE (deg)
Filename:KUS.036

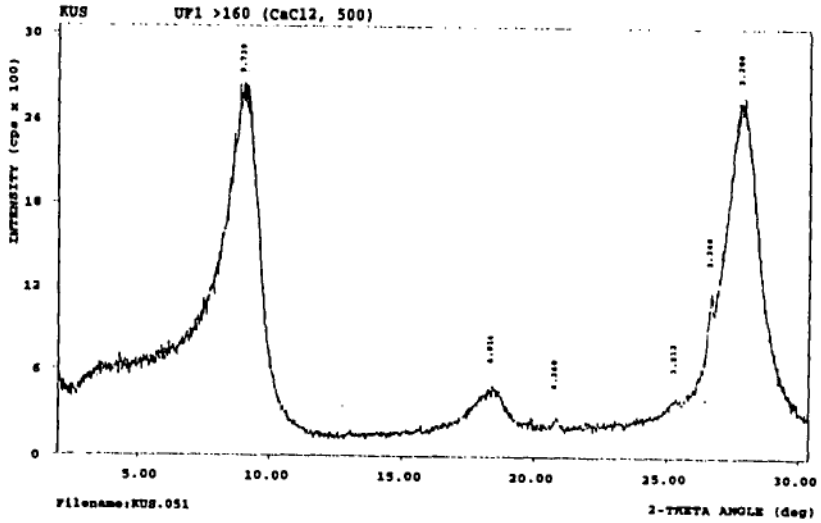
KUS
UF1 >160 (CaCl2, 500)
INTENSITY (cps x 100)
2-THETA ANGLE (deg)
Filename:KUS.051

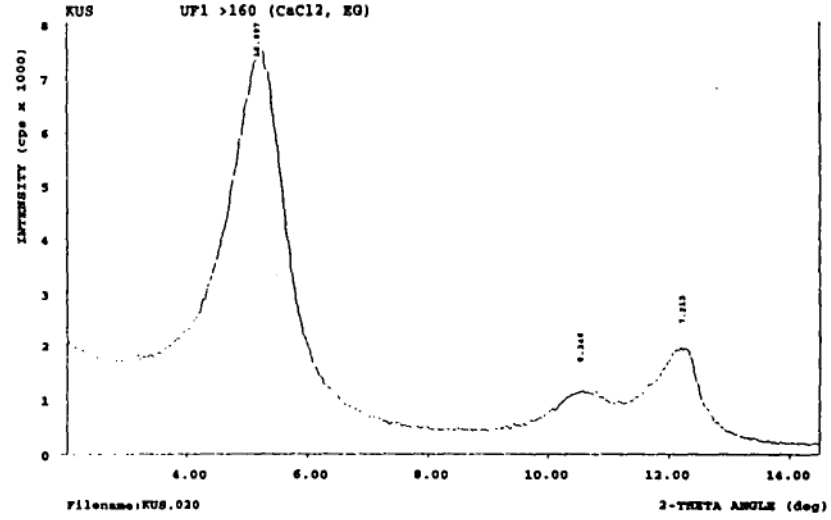
KUS
UF1 >160 (CaCl2, EG)
INTENSITY (cps x 1000)
2-THETA ANGLE (deg)
Filename:KUS.020

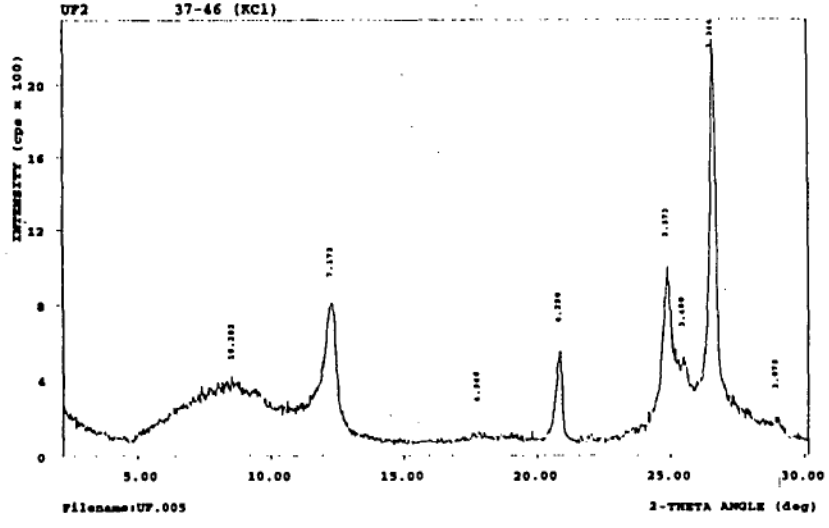
UF2 37-46 (KC1)
INTENSITY (cps x 100)
2-THETA ANGLE (deg)
Filename:UF.005

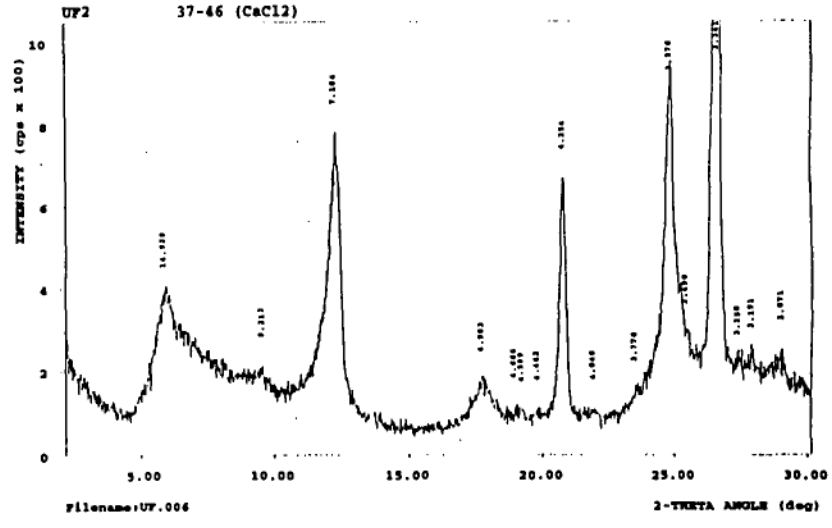
UF2 37-46 (CaC12)
INTENSITY (cps x 100)
2-THETA ANGLE (deg)
Filename:UF.006

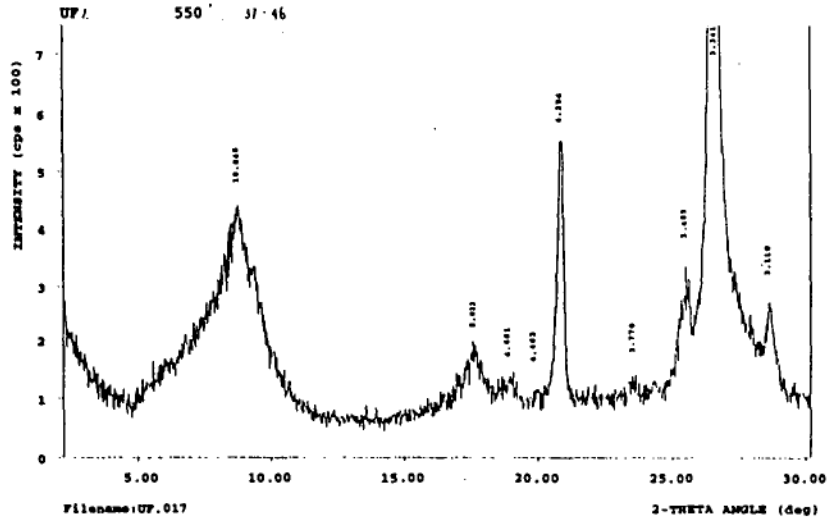
UF
550
37-46
INTENSITY (cps x 100)
2-THETA ANGLE (deg)
Filename:UF.017

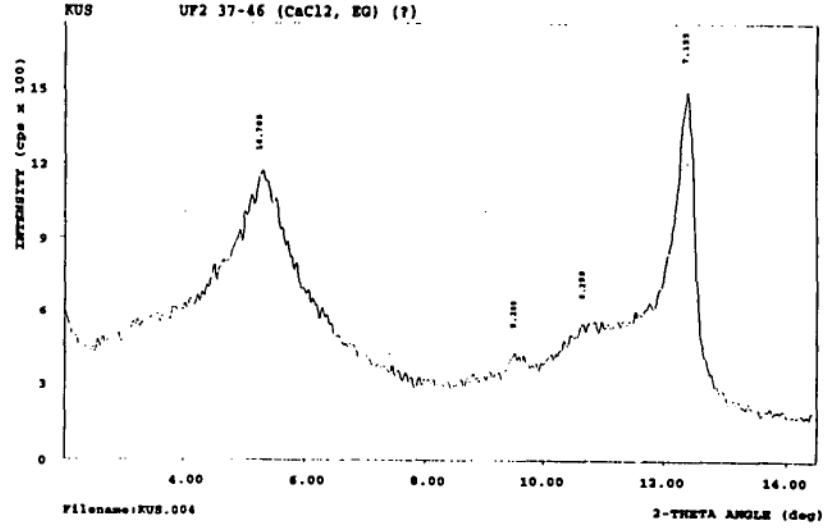
KUS
UF2 37-46 (CaC12, EG) (?)
INTENSITY (cps x 100)
2-THETA ANGLE (deg)
Filename:KUS.004

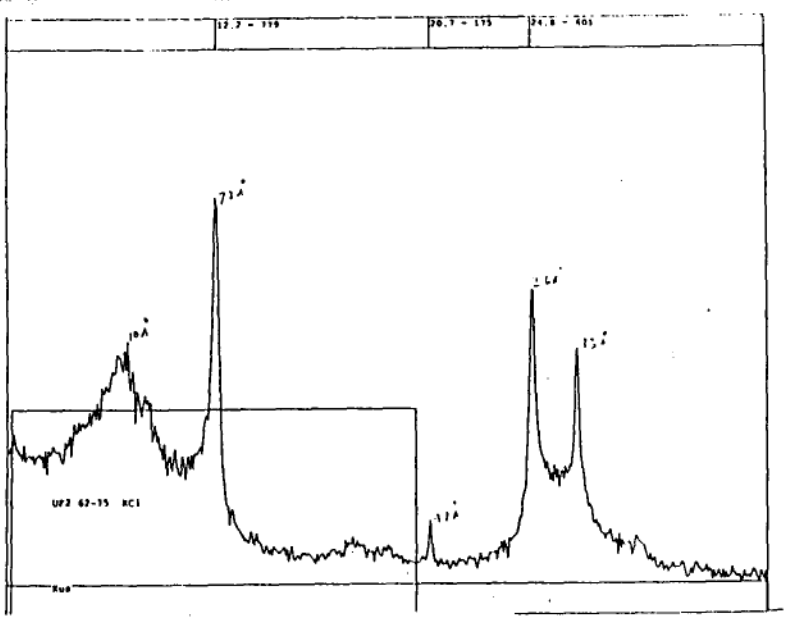
12.7 = 999
20.7 = 175
24.8 = 405
10Å
7.3Å
3.7Å
2.6Å
2.5Å
UF2 62-75 RC1
Run

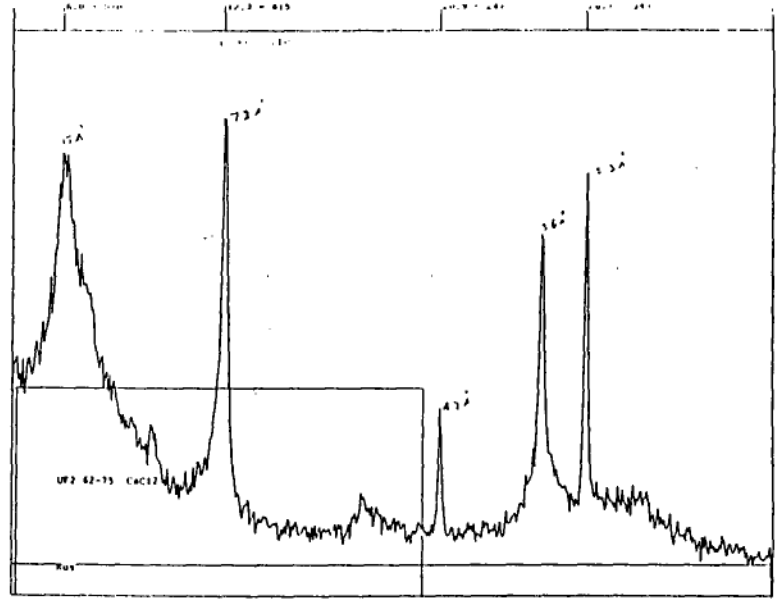
15Å
7.3Å
4.3Å
3.6Å
3.3Å
UF2 62-75 CaCl2
Run

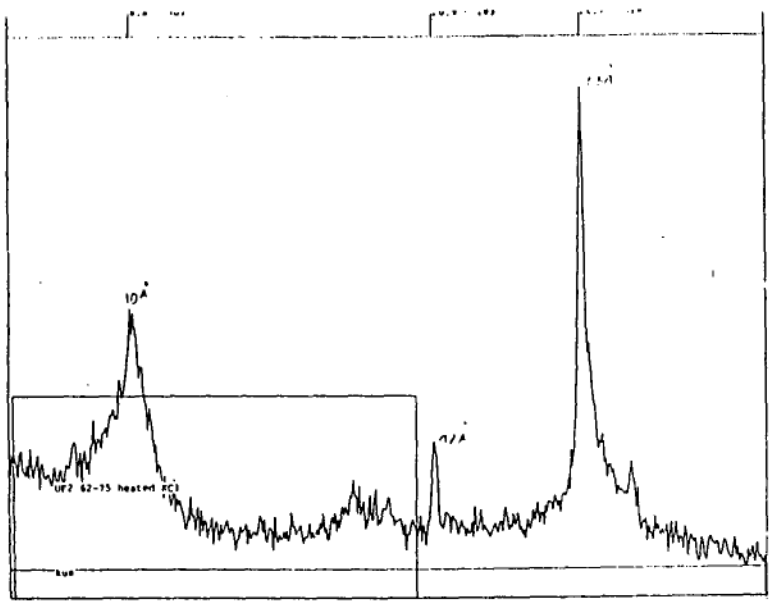
10Å
7.1Å
2.5Å
UF2 62-75 heated RC1
Run

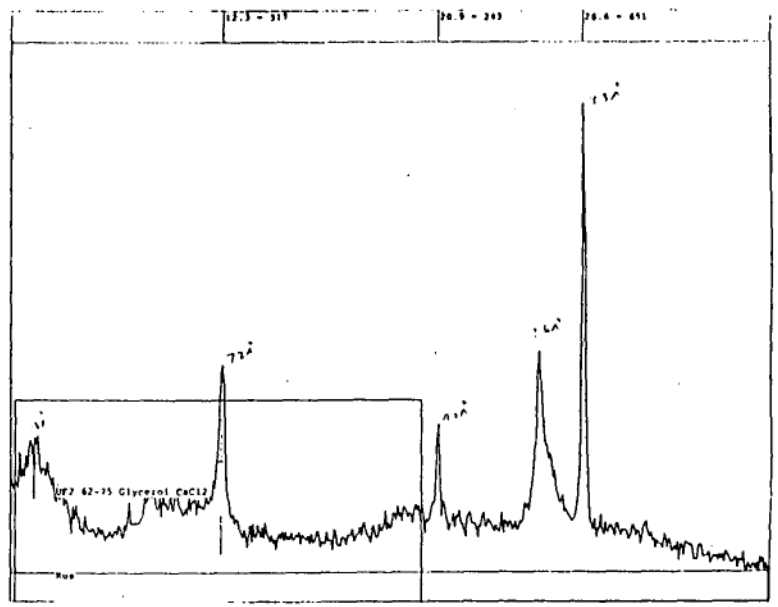
12.3 = 519
20.9 = 203
26.6 = 491
7.3Å
4.3Å
3.6Å
2.5Å
UF2 62-75 Glycerol CaCl2
Run

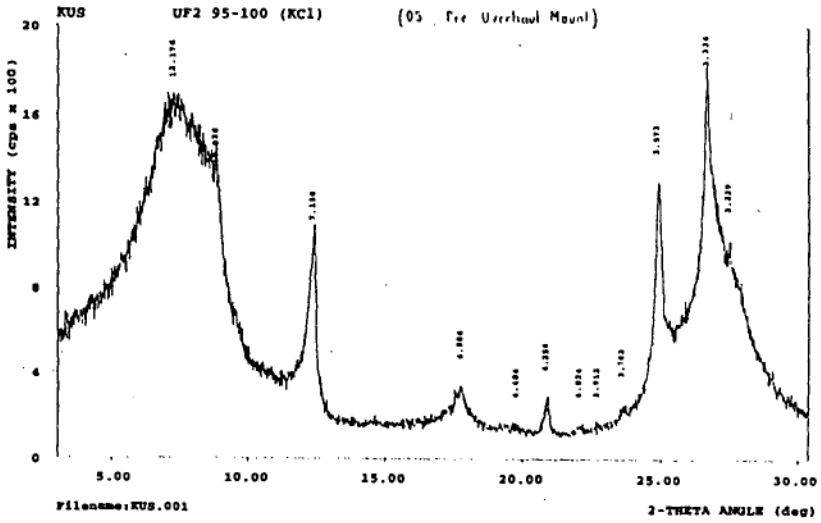
KUS
UF2 95-100 (KC1)
(05 Pre Ovrnlnol Mount)
INTENSITY (cps x 100)
2-THETA ANGLE (deg)
Filename:KUS.001

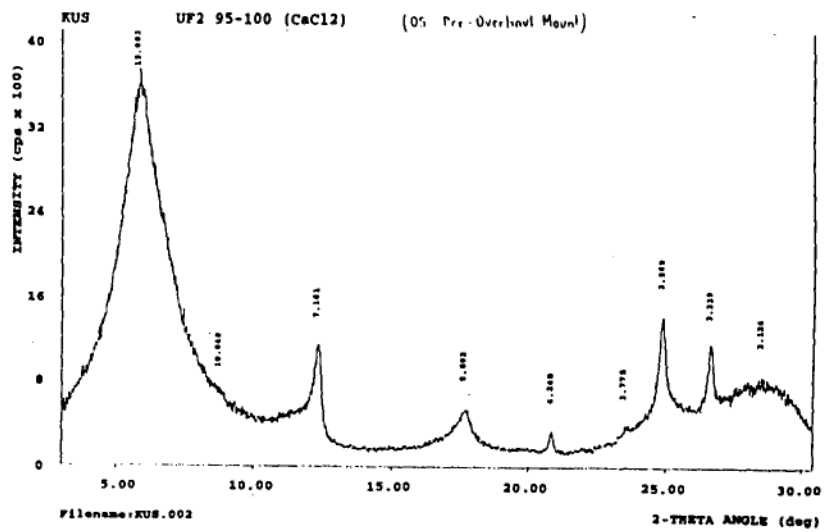
KUS
UF2 95-100 (CaC12)
(05 Pre-Ovrnlnol Mount)
INTENSITY (cps x 100)
2-THETA ANGLE (deg)
Filename:KUS.002

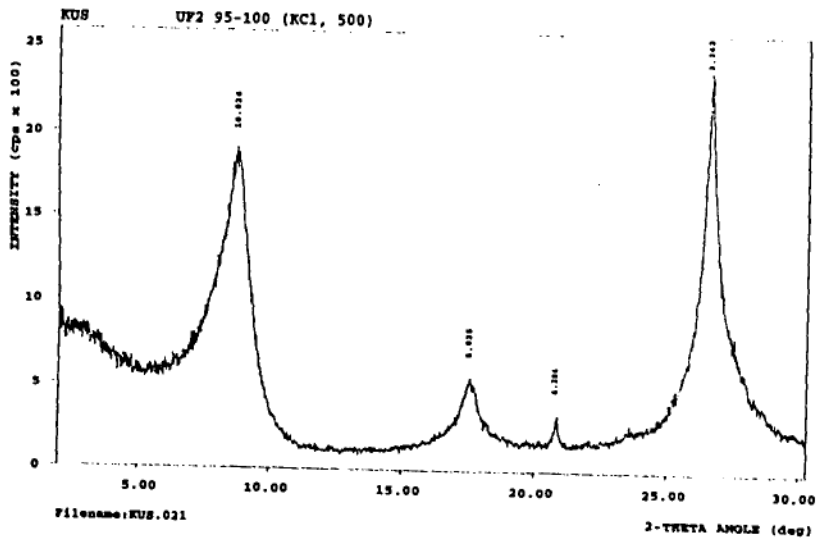
KUS
UF2 95-100 (KC1, 500)
INTENSITY (cps x 100)
2-THETA ANGLE (deg)
Filename:KUS.021

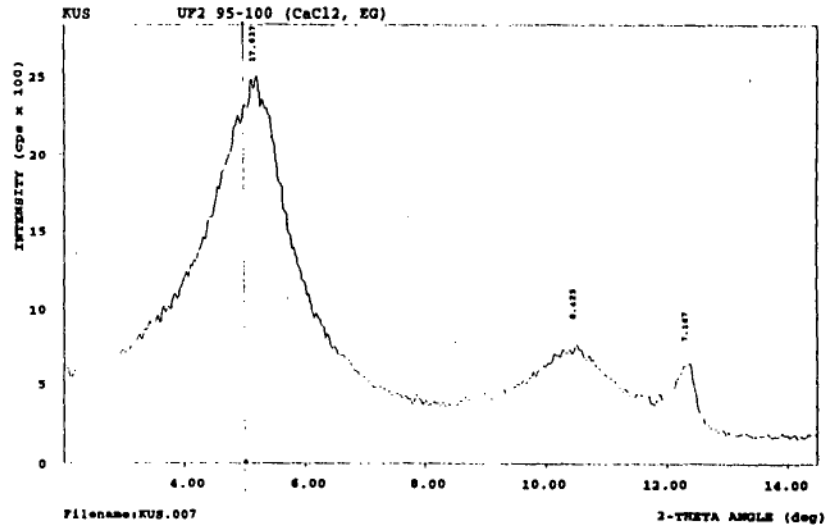
KUS
UF2 95-100 (CaC12, EG)
INTENSITY (cps x 100)
2-THETA ANGLE (deg)
Filename:KUS.007

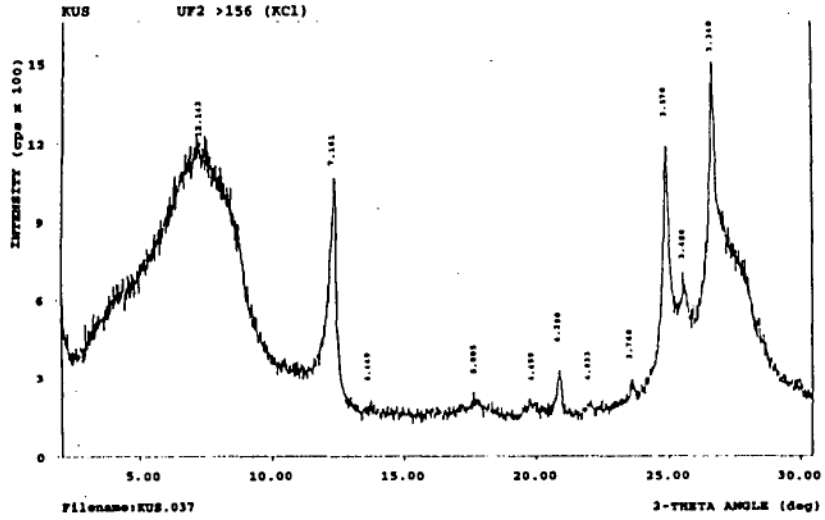
KUS
UF2 >156 (KCl)
INTENSITY (cps x 100)
2-THETA ANGLE (deg)
Filename:KUS.037

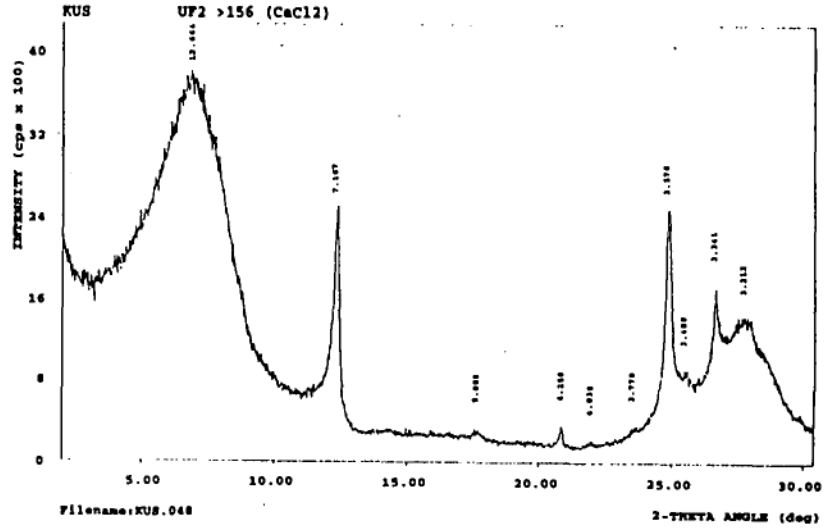
KUS
UF2 >156 (CaCl2)
INTENSITY (cps x 100)
2-THETA ANGLE (deg)
Filename:KUS.048

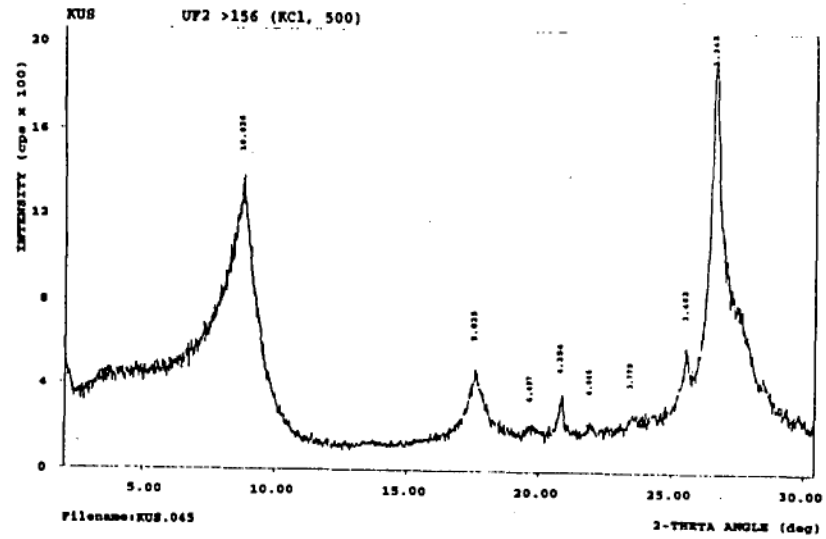
KUS
UF2 >156 (KCl, 500)
INTENSITY (cps x 100)
2-THETA ANGLE (deg)
Filename:KUS.045

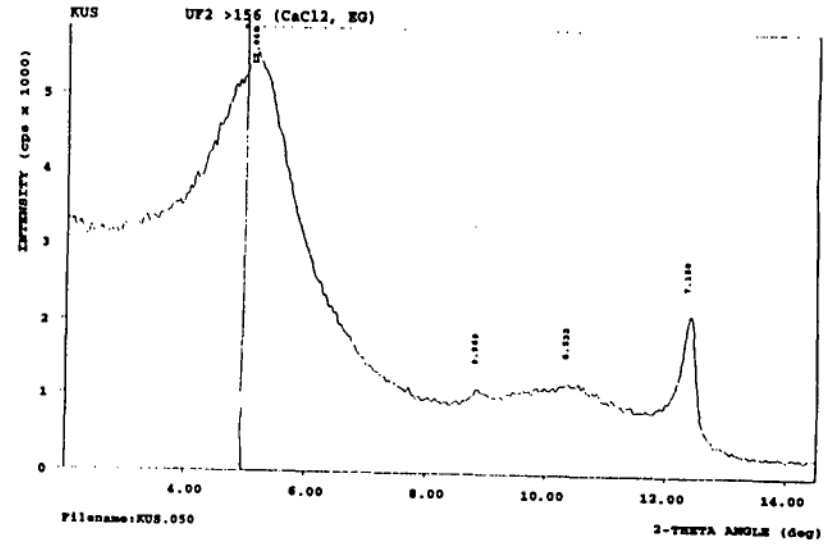
KUS
UF2 >156 (CaCl2, EG)
INTENSITY (cps x 1000)
2-THETA ANGLE (deg)
Filename:KUS.050

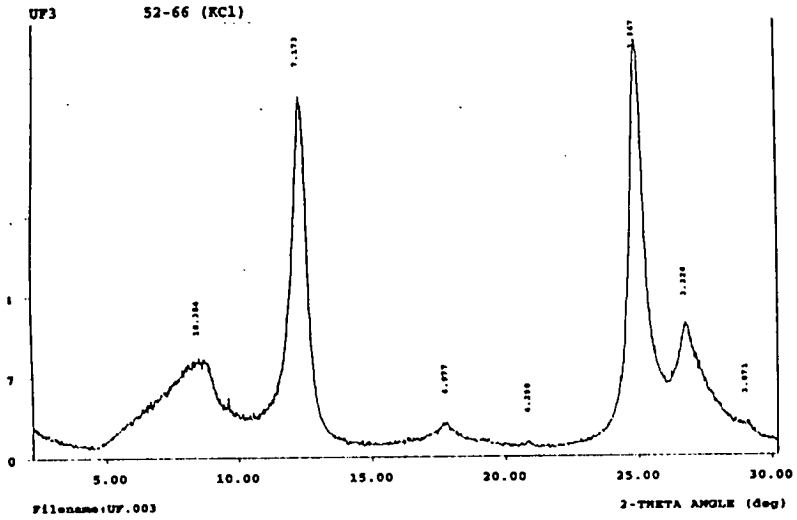
UF3 52-66 (KCl)
5.00
10.00
15.00
20.00
25.00
30.00
2-THETA ANGLE (deg)
Filename:UF.003

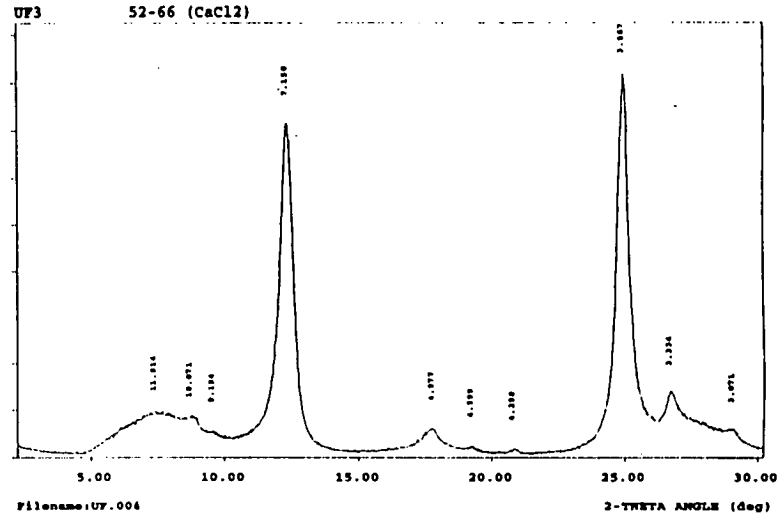
UF3 52-66 (CaCl2)
5.00
10.00
15.00
20.00
25.00
30.00
2-THETA ANGLE (deg)
Filename:UF.004

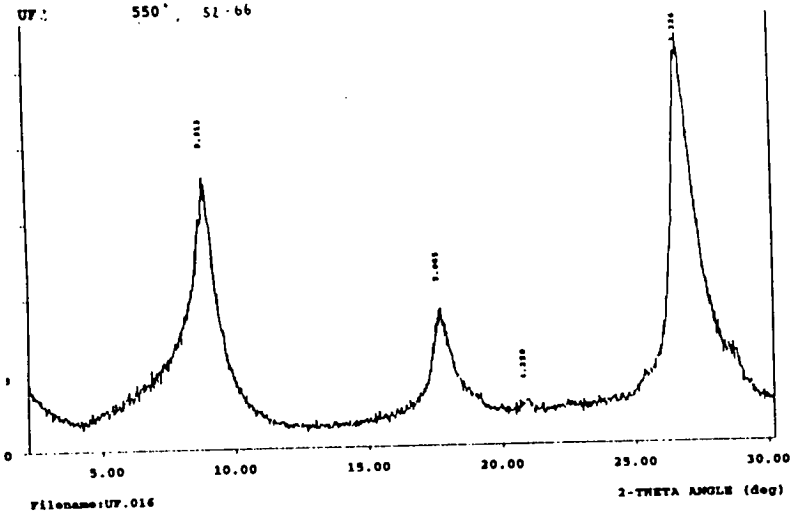
550° 52-66
5.00
10.00
15.00
20.00
25.00
30.00
2-THETA ANGLE (deg)
Filename:UF.016

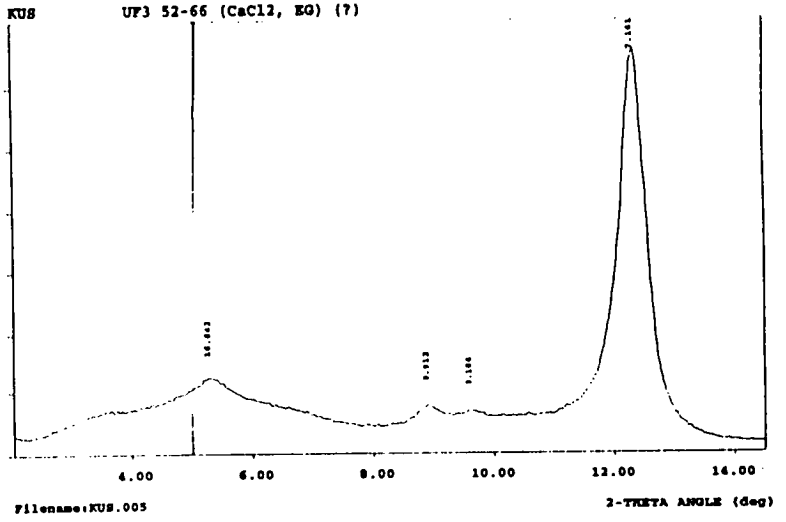
KUS UF3 52-66 (CaCl2, EG) (7)
4.00
6.00
8.00
10.00
12.00
14.00
2-THETA ANGLE (deg)
Filename:KUS.005

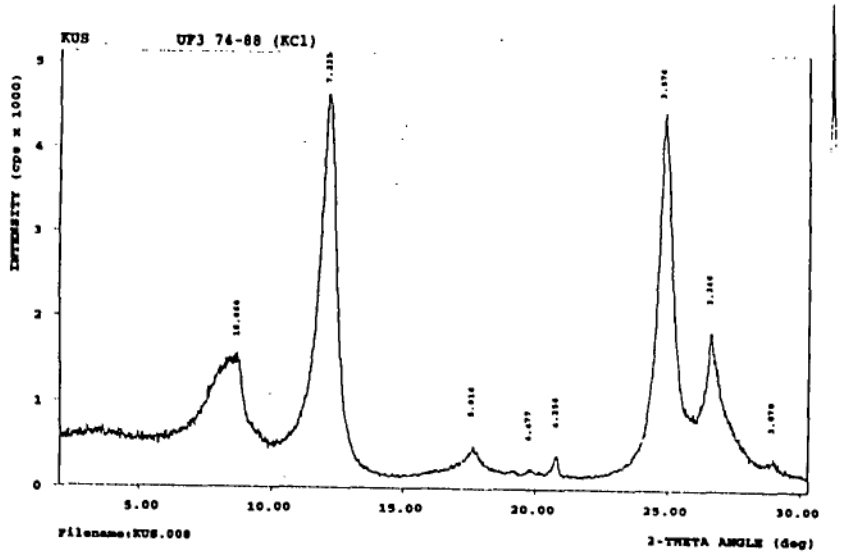
KUS
UF3 74-88 (KCl)
INTENSITY (cps x 1000)
5.00
10.00
15.00
20.00
25.00
30.00
Filename:KUS.008
2-THETA ANGLE (deg)

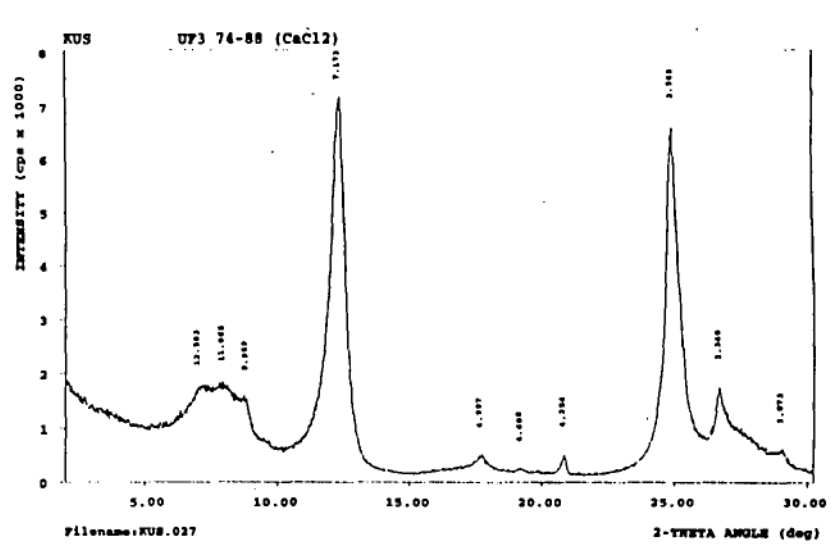
KUS
UF3 74-88 (CaCl2)
INTENSITY (cps x 1000)
5.00
10.00
15.00
20.00
25.00
30.00
Filename:KUS.027
2-THETA ANGLE (deg)

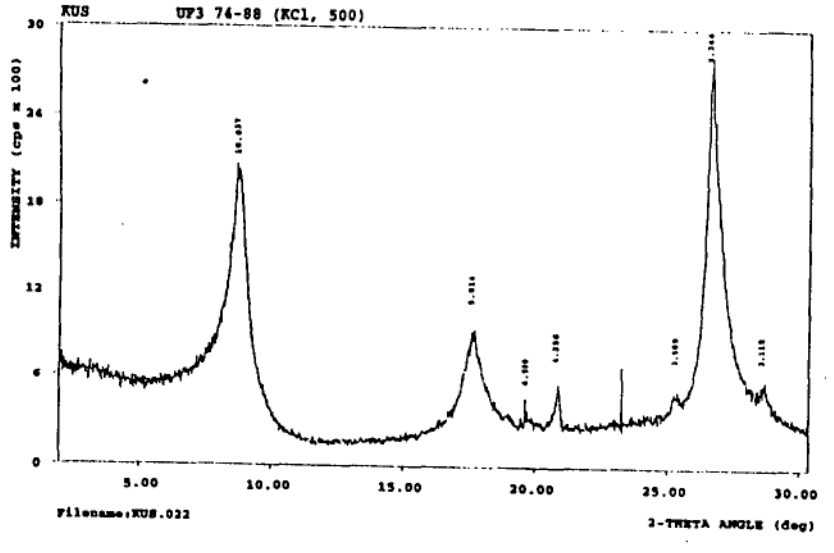
KUS
UF3 74-88 (KCl, 500)
INTENSITY (cps x 100)
5.00
10.00
15.00
20.00
25.00
30.00
Filename:KUS.022
2-THETA ANGLE (deg)

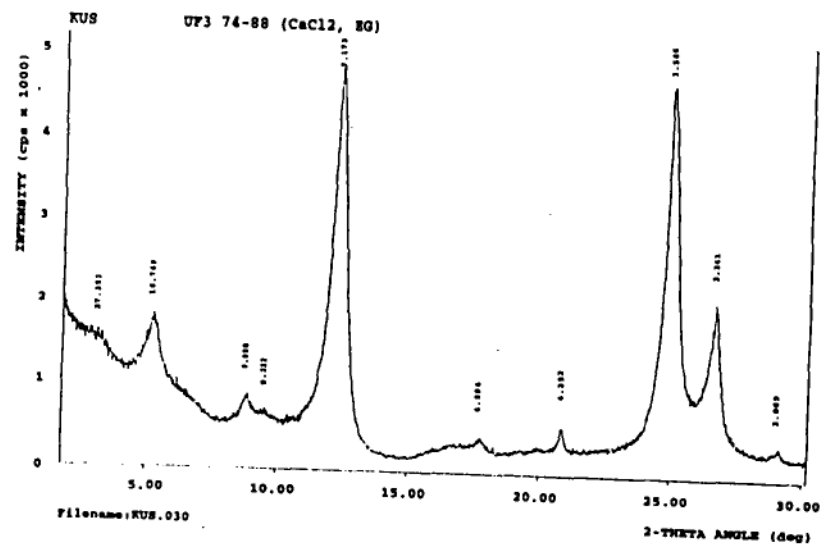
KUS
UF3 74-88 (CaCl2, EG)
INTENSITY (cps x 1000)
5.00
10.00
15.00
20.00
25.00
30.00
Filename:KUS.030
2-THETA ANGLE (deg)

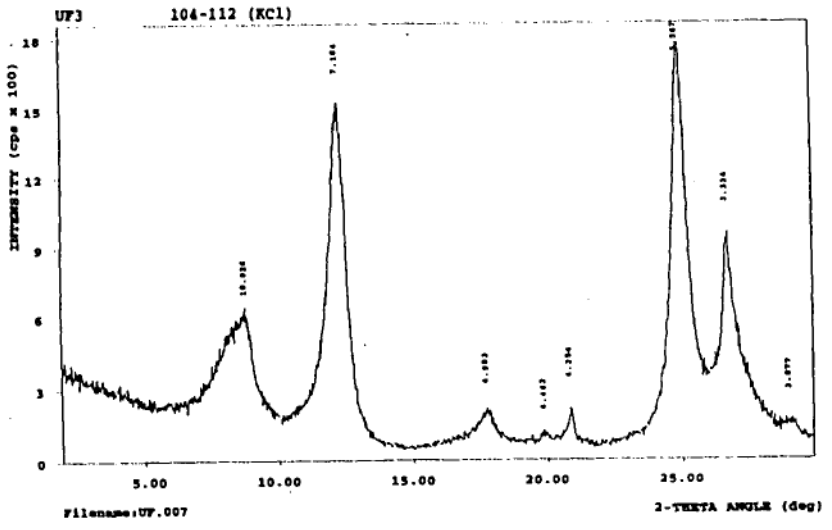
UF3
104-112 (KCl)
INTENSITY (cps x 100)
2-THETA ANGLE (deg)
Filename:UF.007

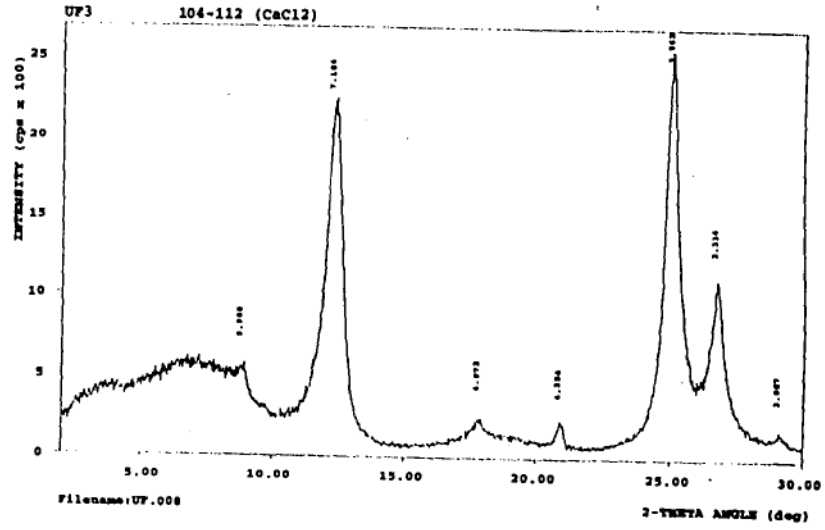
UF3
104-112 (CaCl2)
INTENSITY (cps x 100)
2-THETA ANGLE (deg)
Filename:UF.008

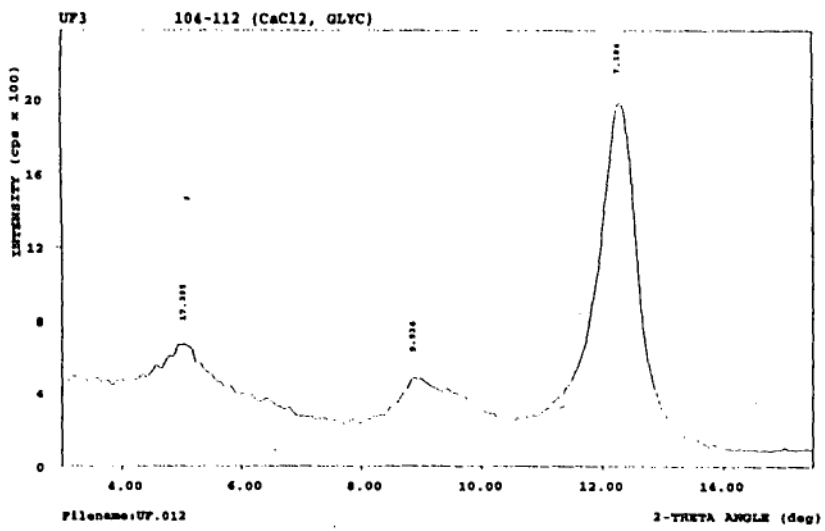
UF3
104-112 (CaCl2, GLYC)
INTENSITY (cps x 100)
2-THETA ANGLE (deg)
Filename:UF.012

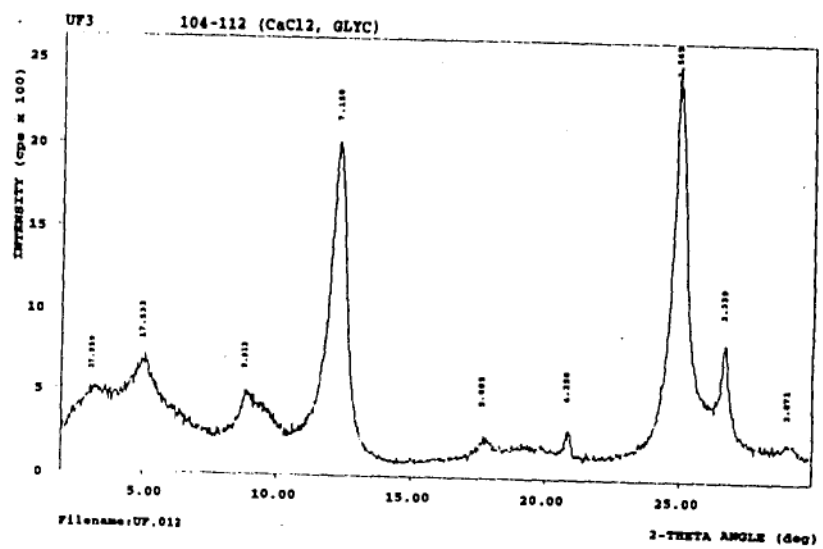
UF3
104-112 (CaCl2, GLYC)
INTENSITY (cps x 100)
2-THETA ANGLE (deg)
Filename:UF.012

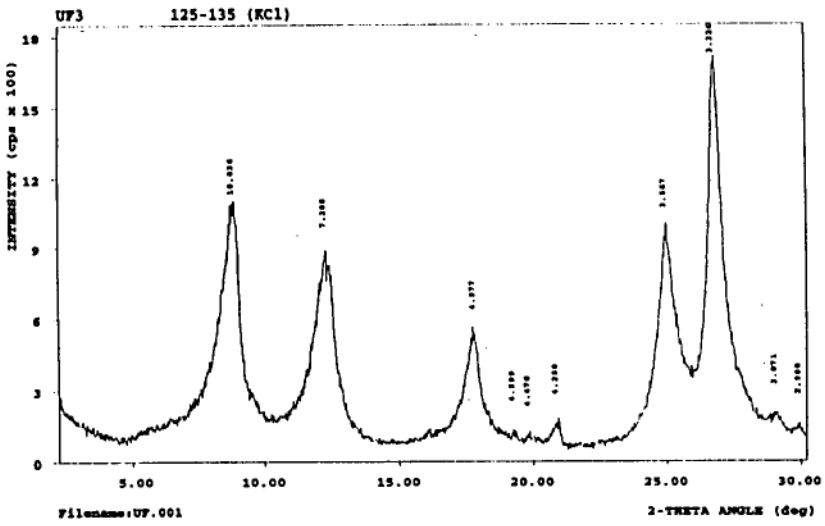
UF3 125-135 (KCl)
INTENSITY (cps x 100)
2-THETA ANGLE (deg)
Filename:UF.001

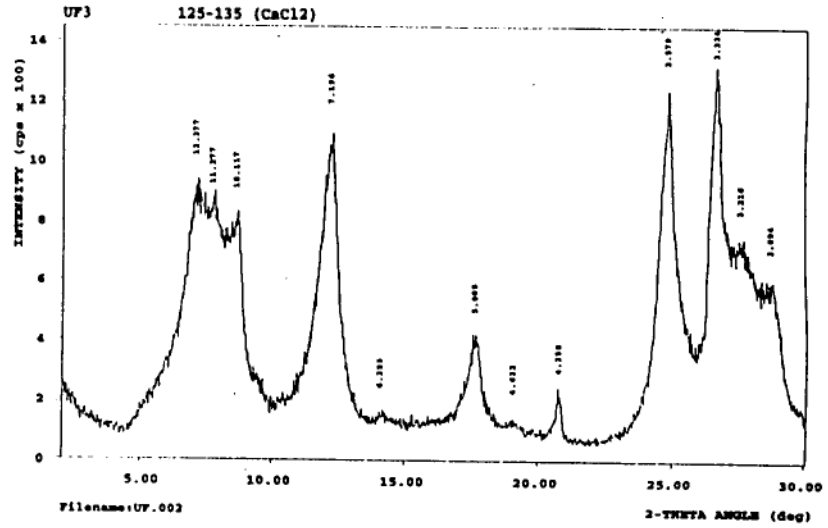
UF3 125-135 (CaCl2)
INTENSITY (cps x 100)
2-THETA ANGLE (deg)
Filename:UF.002

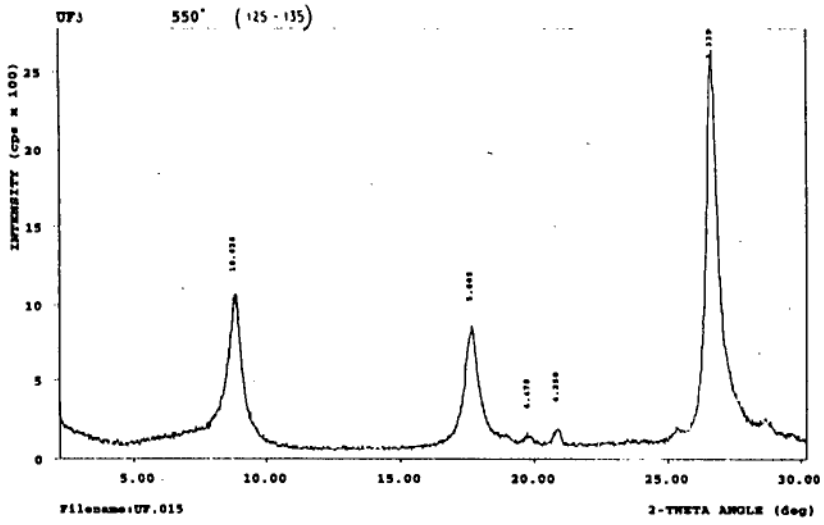
UF3 550° (125-135)
INTENSITY (cps x 100)
2-THETA ANGLE (deg)
Filename:UF.015

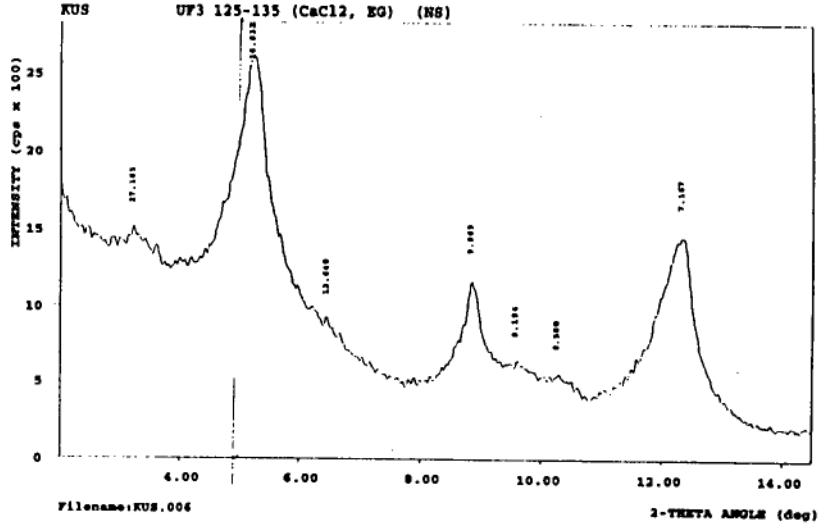
KUS UF3 125-135 (CaCl2, EG) (NS)
INTENSITY (cps x 100)
2-THETA ANGLE (deg)
Filename:KUS.006

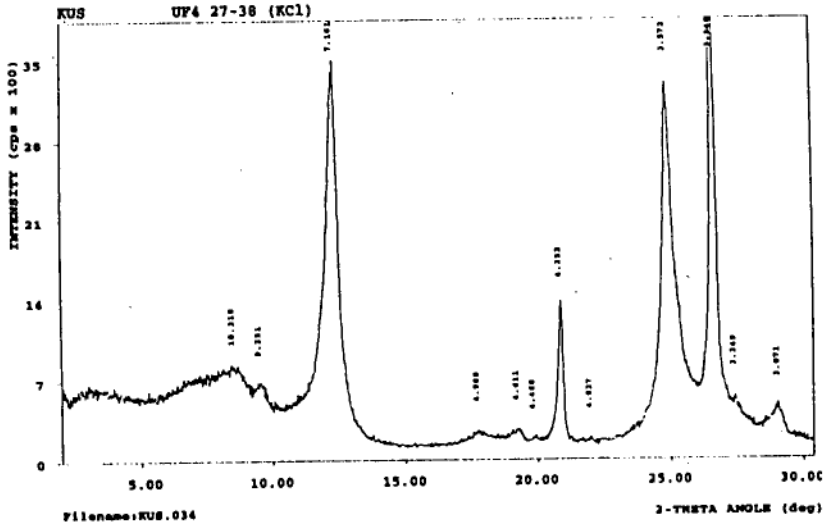
KUS
UF4 27-38 (KCl)
INTENSITY (cps x 100)
2-THETA ANGLE (deg)
Filename:KUS.034

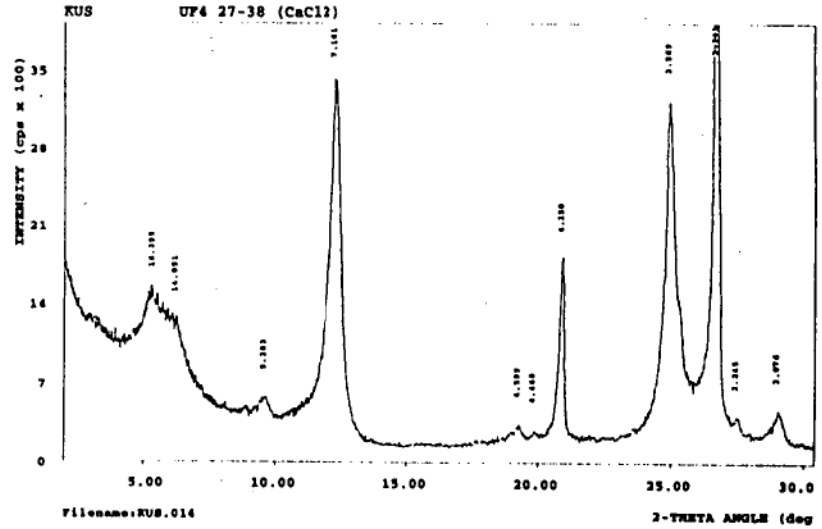
KUS
UF4 27-38 (CaCl2)
INTENSITY (cps x 100)
2-THETA ANGLE (deg
Filename:KUS.014

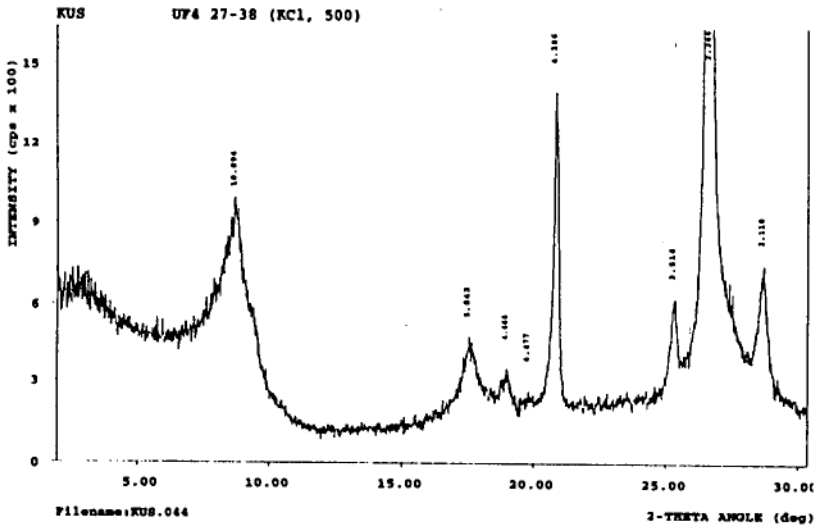
KUS
UF4 27-38 (KCl, 500)
INTENSITY (cps x 100)
2-THETA ANGLE (deg)
Filename:KUS.044

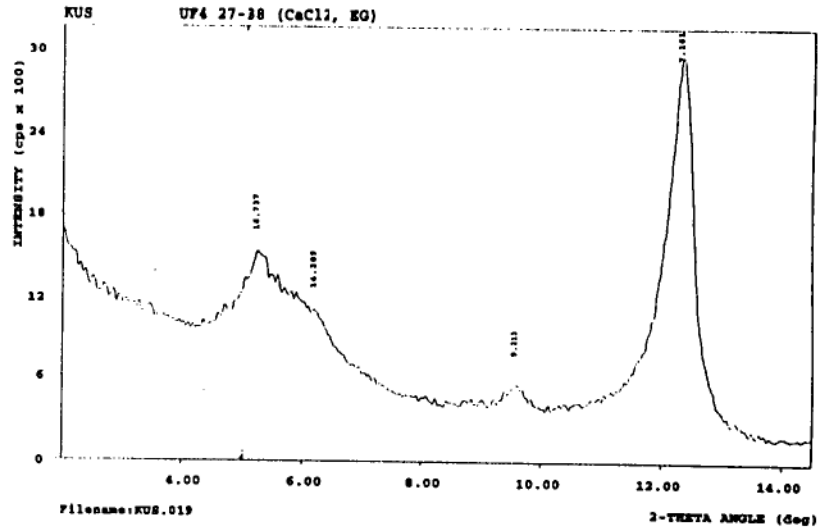
KUS
UF4 27-38 (CaCl2, EG)
INTENSITY (cps x 100)
2-THETA ANGLE (deg)
Filename:KUS.019

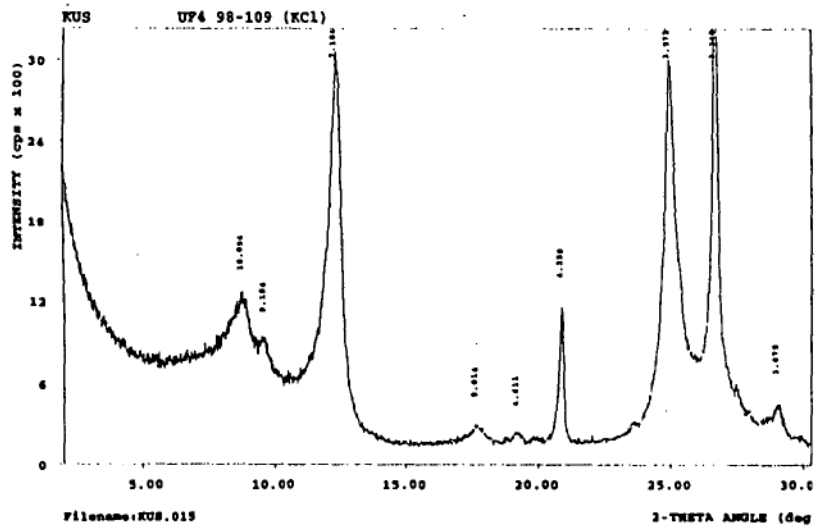
KUS
UF4 98-109 (KCl)
INTENSITY (cps x 100)
2-THETA ANGLE (deg
Filename:KUS.015

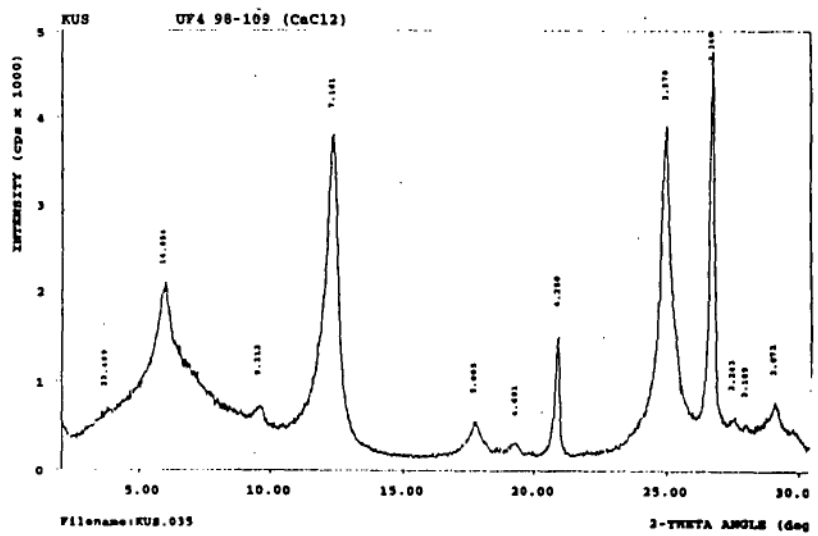
KUS
UF4 98-109 (CaCl2)
INTENSITY (cps x 1000)
2-THETA ANGLE (deg
Filename:KUS.035

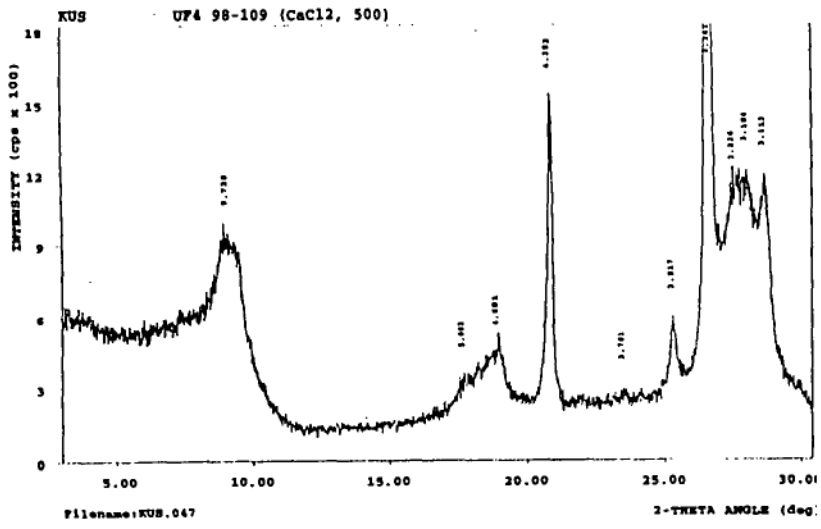
KUS
UF4 98-109 (CaCl2, 500)
INTENSITY (cps x 100)
2-THETA ANGLE (deg
Filename:KUS.047

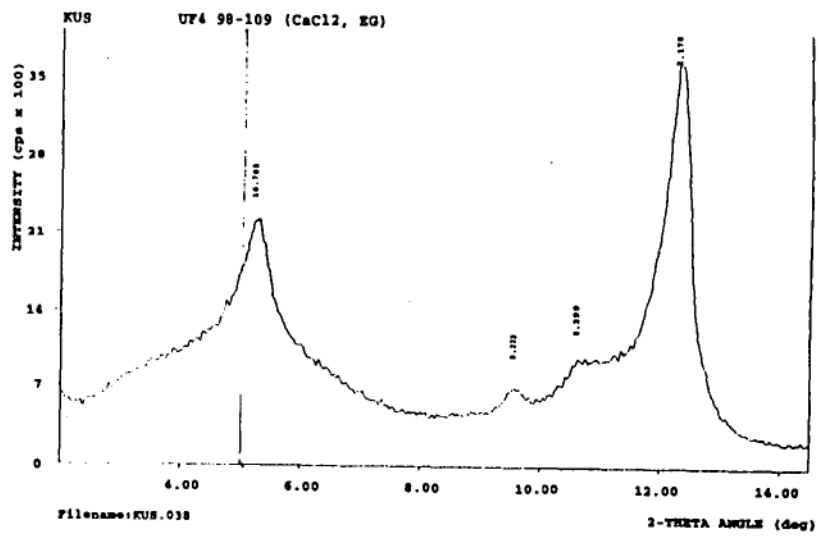
KUS
UF4 98-109 (CaCl2, EG)
INTENSITY (cps x 100)
2-THETA ANGLE (deg)
Filename:KUS.038

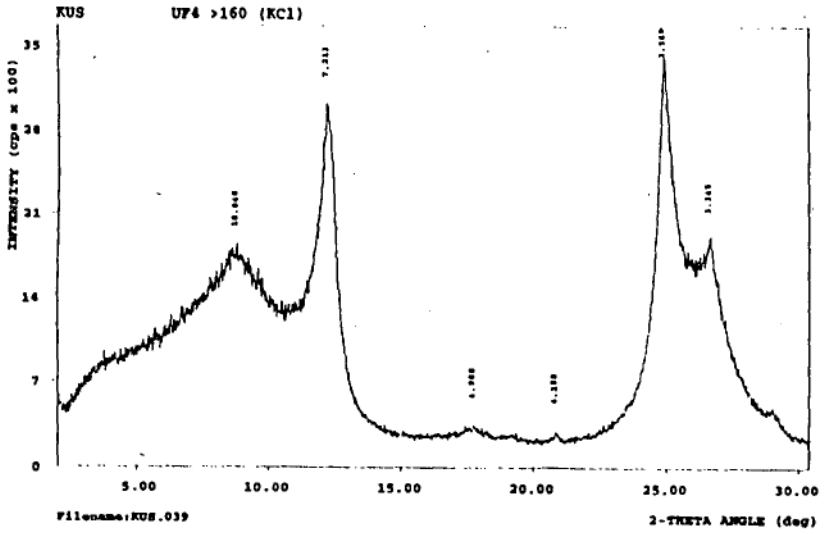
KUS
UF4 >160 (KCl)
INTENSITY (cps x 100)
2-THETA ANGLE (deg)
Filename:KUS.039

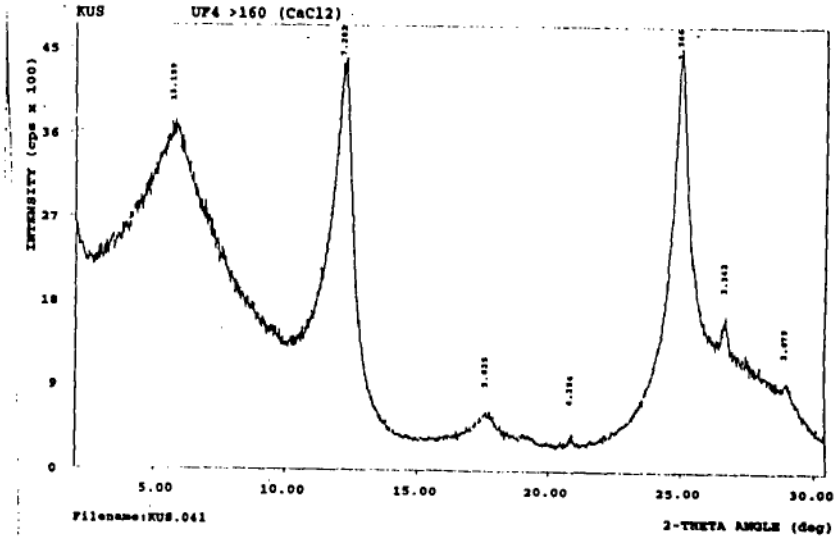
KUS
UF4 >160 (CaCl2)
INTENSITY (cps x 100)
2-THETA ANGLE (deg)
Filename:KUS.041

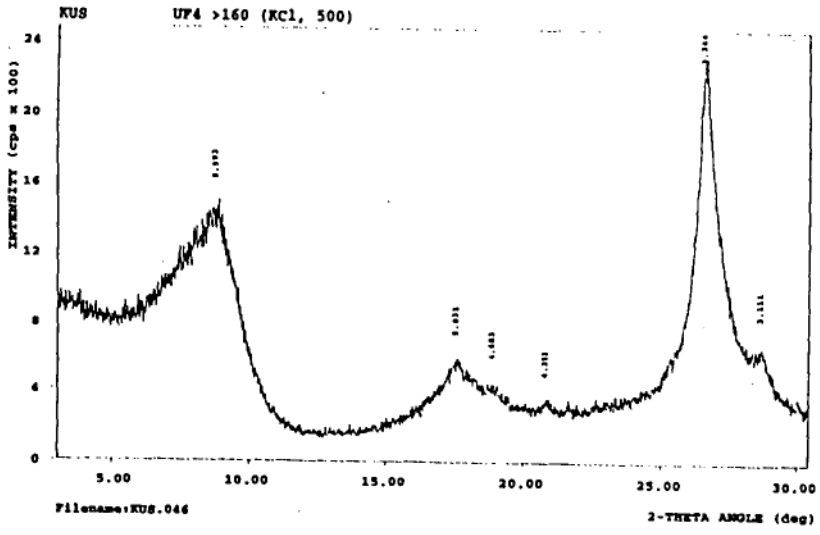
KUS
UF4 >160 (KCl, 500)
INTENSITY (cps x 100)
2-THETA ANGLE (deg)
Filename:KUS.046

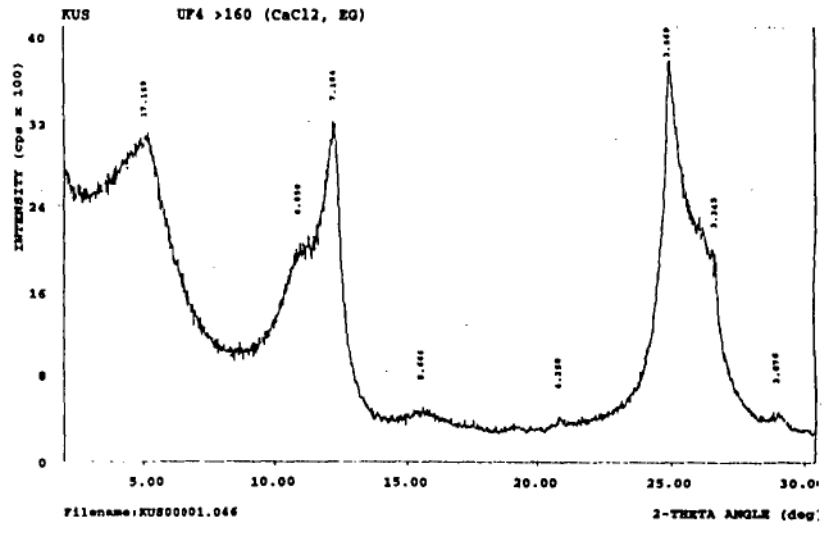
KUS
UF4 >160 (CaCl2, EG)
INTENSITY (cps x 100)
2-THETA ANGLE (deg)
Filename:KUS00001.046

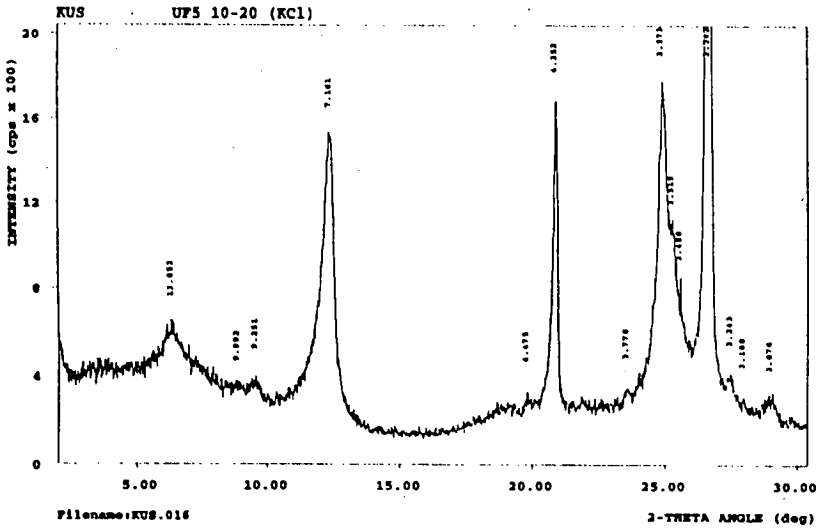
KUS
UF5 10-20 (KCl)
INTENSITY (cps x 100)
2-THETA ANGLE (deg)
Filename:KUS.016

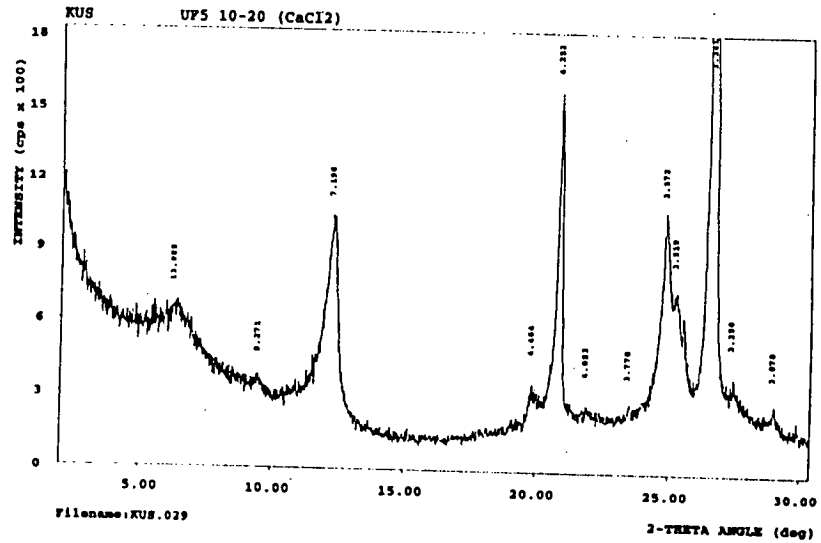
KUS
UF5 10-20 (CaCl2)
INTENSITY (cps x 100)
2-THETA ANGLE (deg)
Filename:KUS.029

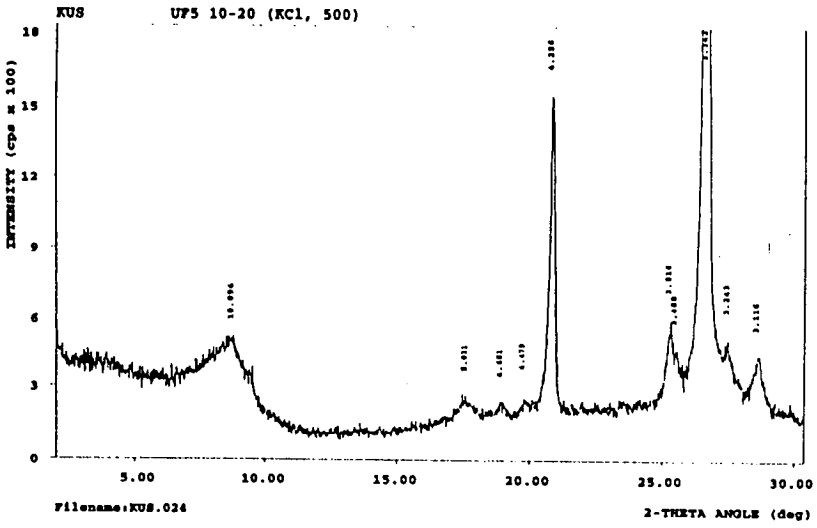
KUS
UF5 10-20 (KCl, 500)
INTENSITY (cps x 100)
2-THETA ANGLE (deg)
Filename:KUS.024

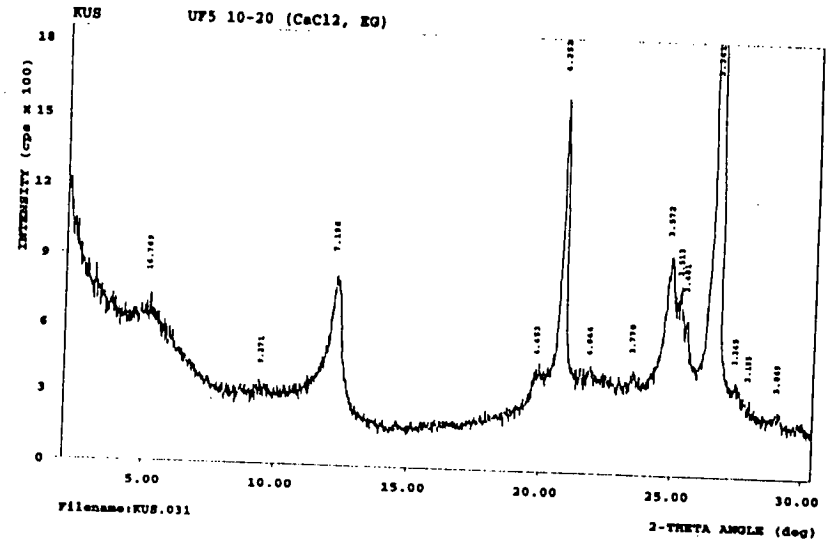
KUS
UF5 10-20 (CaCl2, EG)
INTENSITY (cps x 100)
2-THETA ANGLE (deg)
Filename:KUS.031

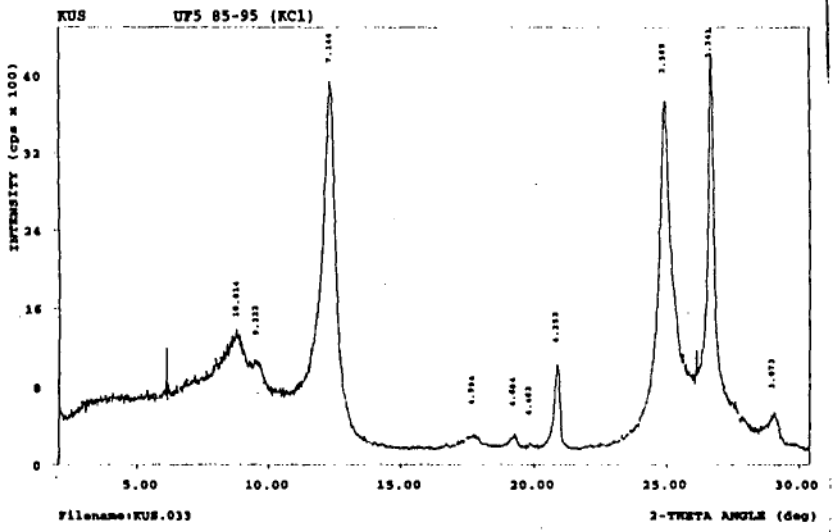
KUS
UF5 85-95 (KCl)
INTENSITY (cps x 100)
2-THETA ANGLE (deg)
Filename:KUS.033

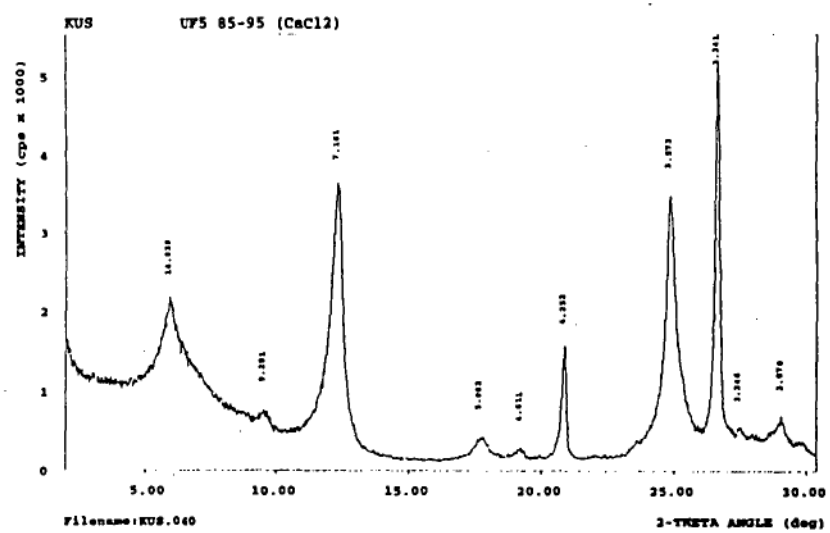
KUS
UF5 85-95 (CaCl2)
INTENSITY (cps x 1000)
2-THETA ANGLE (deg)
Filename:KUS.040

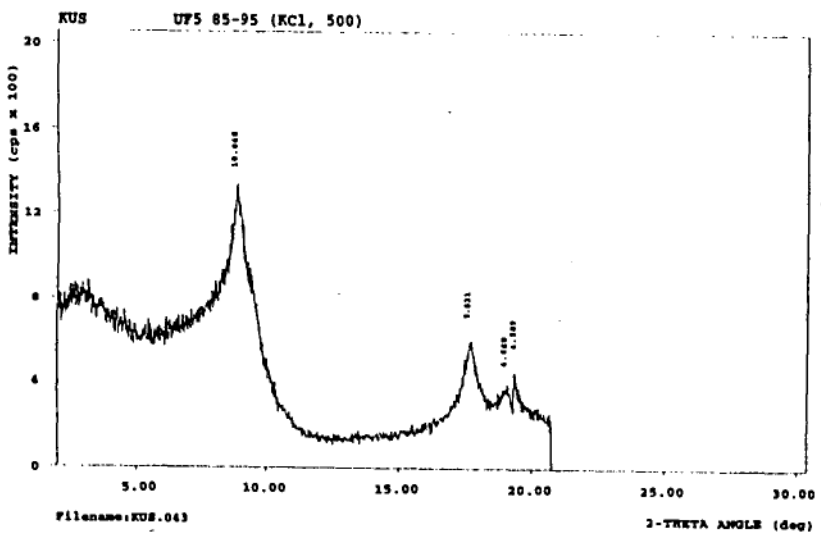
KUS
UF5 85-95 (KCl, 500)
INTENSITY (cps x 100)
2-THETA ANGLE (deg)
Filename:KUS.043

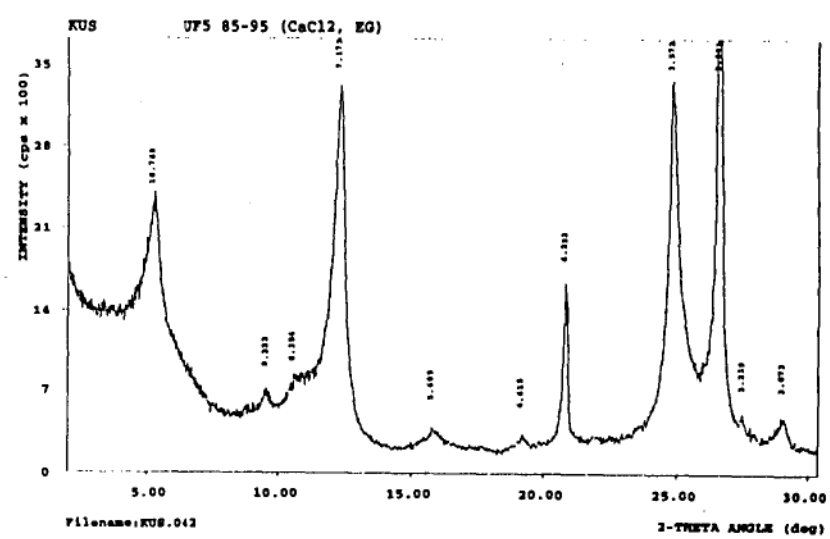
KUS
UF5 85-95 (CaCl2, EG)
INTENSITY (cps x 100)
2-THETA ANGLE (deg)
Filename:KUS.042

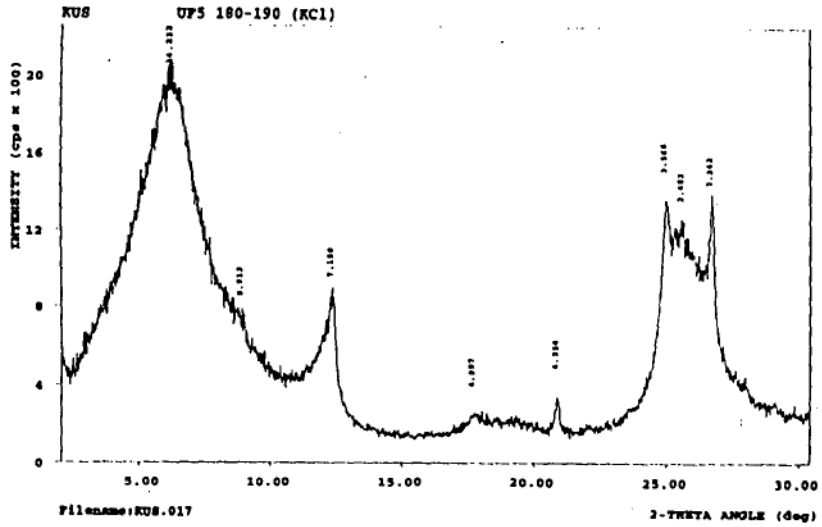
KUS
UF5 180-190 (KC1)
INTENSITY (cps x 100)
0
4
8
12
16
20
5.00
10.00
15.00
20.00
25.00
30.00
Filename:KUS.017
2-THETA ANGLE (deg)

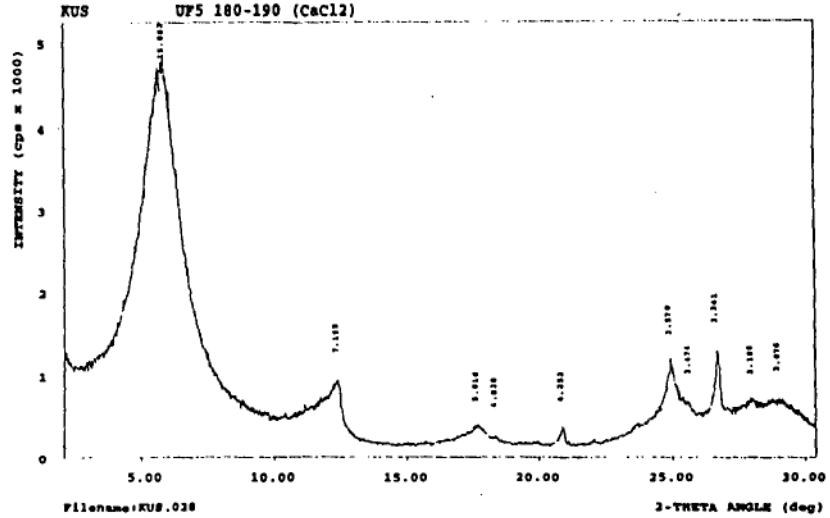
KUS
UF5 180-190 (CaCl2)
INTENSITY (cps x 1000)
0
1
2
3
4
5
5.00
10.00
15.00
20.00
25.00
30.00
Filename:KUS.038
2-THETA ANGLE (deg)

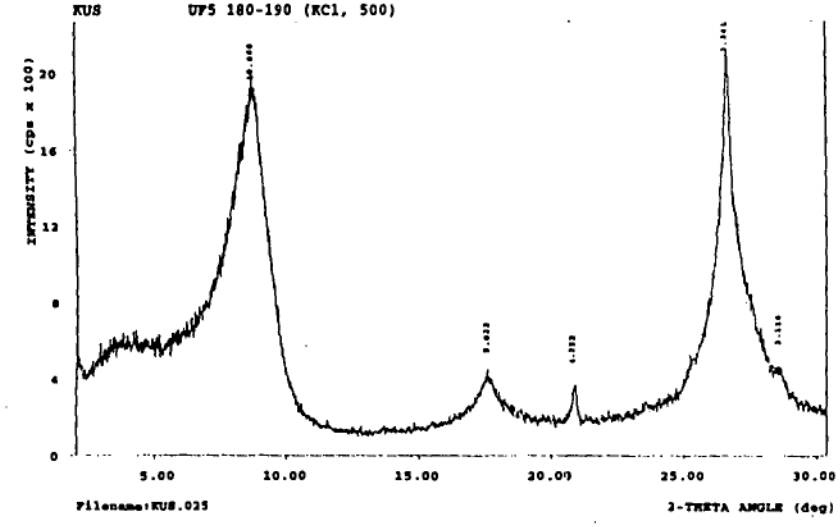
KUS
UF5 180-190 (KC1, 500)
INTENSITY (cps x 100)
0
4
8
12
16
20
5.00
10.00
15.00
20.00
25.00
30.00
Filename:KUS.025
2-THETA ANGLE (deg)

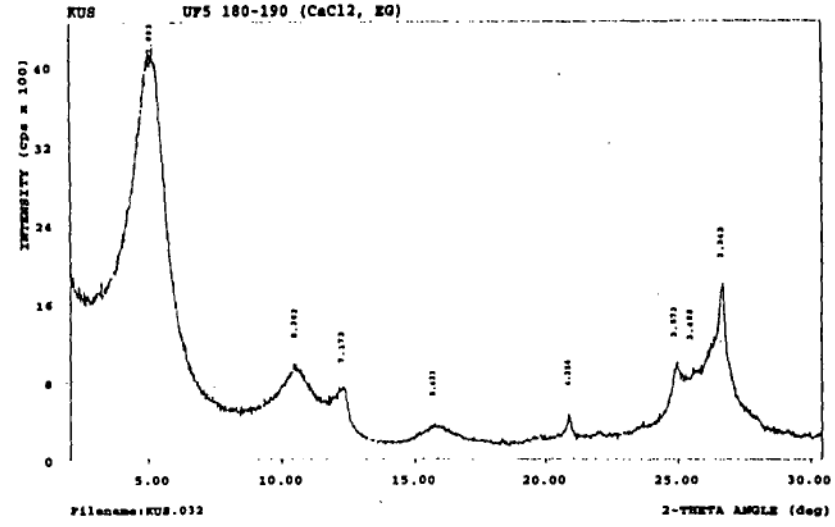
KUS
UF5 180-190 (CaCl2, EG)
INTENSITY (cps x 100)
0
8
16
24
32
40
5.00
10.00
15.00
20.00
25.00
30.00
Filename:KUS.032
2-THETA ANGLE (deg)